DEVELOPMENT OF SITE-INDEPENDENT MODEL AND THE INVESTIGATION OF SPATIAL AND TEMPORAL VARIATIONS OF SOLAR RADIATION CHARACTERISTICS OVER SOME LOCATIONS IN NIGERIA

By

BOLA FATAI AKINWALE
B.Sc. (Hons.) Physics (Ibadan), M.Sc. Physics (OAU)
Matric No: 27087

A Thesis in the Department Physics,

Submitted to the Faculty of Science

In partial fulfilment of the requirements for the Degree of

DOCTOR OF PHILOSOPHY

of the

UNIVERSITY OF IBADAN

APRIL, 2019

CERTIFICATION

I hereby certify that this research work was carried out by Bola Fatai Akinwale under my supervision in the Department of Physics, Faculty of Science, University of Ibadan, Ibadan, Nigeria.

Prof. E.O. Oladiran

B.Sc., Ph.D. (Physics) (Ibadan); M.Sc. (Meteorology)(Reading).

University of Ibadan, Ibadan, Nigeria

DEDICATION

This work is dedicated toGrace and Peace, blessings which are available in abundance in Jesus Christ.

ACKNOWLEDGEMENT

I return all the glory unto my Saviour, Lord Jesus Christ for helping me this far with this research programme.

My special thanks go to my supervisor, Professor E. O. Oladiran for his constructive criticism and guidance in the course of analyzing and reporting this work.

I am very grateful to the Atmospheric Physics group under the able leadership of Prof. E. O. Oladiran and members Dr. (Mrs) M. O. Adeniyi, Dr. E. F. Nymphas, Dr. O. E. Ogunsola and Dr. Otunla for their supports and encouragements.I also appreciate the Tertiary Education Trust Fund (2012 -TETFUND INTERVENTION FUND) for granting me a Ph.D sponsorship award.

I cannot but appreciate Dr. E. O. Joshua of the Department of Physics, University of Ibadan for several invaluable helps rendered to me in the course of this programme. May God bless you and your family.

I must place in record the help rendered to me by Mr. Ogunyemi and other officers at the Nigeria Meteorological Agency (NIMET) Oshodi, in obtaining the required ground data from the agency. I also appreciate the National Aeronautics and Space Administration's (NASA) Atmospheric Science Data Centre for many invaluable helps rendered in the process of acquiring the data used in the work.

Finally, I am grateful to my entire family members, starting from my dear wife to my children for showing understanding and giving me encouragement while on this programme.

ABSTRACT

Accurate information on solar radiation at a specific location on the earth's surface is indispensable for energy applications and atmospheric research. The required data could be obtained from a dense network of solar radiation monitoring stations which is not practicable due to exorbitant costs of equipment and dearth of technical expertise. The available empirical site-independent Hay model, assumed a constant value for clear sky albedo (ρ_a) without taking into account the spatial variation of this parameter. This work was designed to develop a site-independent empirical model which incorporates the parameterisation of the spatial variation of ρ_a.

Monthly averaged daily values of solar radiation ($\overline{H}_e$), relative humidity, sunshine hours ($\overline{n}$), minimum and maximum temperatures, spanning 1984 to 2005, were collected from the National Aeronautics and Space Administration (NASA) and Nigeria Meteorological Agency for eleven locations across Nigeria. Monthly values of ground surface albedo (ρ_g) and surface air pressure were also collected from NASA and optical aerosol thickness at the wavelength of 380 nm from both total ozone mapping spectrometer satellite and Aerosol Robotic Network (AERONET) centre at Ilorin where ground data is available in Nigeria. The $\rho_a$was parameterised using optical aerosol thickness and the average air mass values. The empirical site-independent Hay model was then modified to accommodate the parameterised ρ_a. New empirical coefficients were derived from field data (sunshine hours and global solar radiation) at Ilorin using regression analyses. The spatial and temporal variations of estimated solar radiation over some locations were investigated using descriptive statistics. Solar radiation values were estimated for five locations (Port-Harcourt, Lagos, Ilorin, Maiduguri and Sokoto) where data were homogenous, using the derived-model, Hay model and six site-dependent models (Angstrom-Prescott, Almoroz-Hontoria, Hargreaves-Samani, Bristow-Campbell, Garcia and Chen-Li). These were analysed using correlation coefficient (r), Mean Bias Error (MBE) and Root Mean Square Error (RMSE) statistics at $\alpha_{0.05}$.

Values obtained for ρ_a ranged from 0.09 to 0.12 for the locations as compared to a constant value of 0.25 assumed by Hay. The derived site-independent model was

$\frac{\overline{H}_e}{\overline{H}_o} = \frac{a+b\left(\frac{\overline{n}}{\overline{N}}\right)}{1-\rho_g\left[\rho_a\left(\frac{\overline{n}}{\overline{N}}\right)+0.6\left(1-\frac{\overline{n}}{\overline{N}}\right)\right]}$, where $\overline{H}_o$, $\overline{N}$ and $\overline{n}$ were the monthly averaged daily values of extraterrestrial radiation,day-length and sunshine hours respectively, while a and b were the empirical coefficients with values 0.262 and 0.615, respectively. The r, MBE ($\mathrm{MJm^{-2}}$) and RMSE ($\mathrm{MJm^{-2}}$) obtained with the derived-model were; Port-Harcourt (0.91, -0.99, 1.34), Lagos (0.96, -0.86, 1.03), Ilorin (0.93, -0.01, 0.79), Maiduguri (0.91, 0.99, 1.21) and Sokoto (0.90, 0.58, 0.90) respectively. For Hay model and the six site-dependent models, the range of r, MBE and RMSE were; Port-Harcourt (0.80 – 0.87, -1.53 – 7.87, 2.00 – 7.94), Lagos (0.36 – 0.92, -0.89 – -7.58, 1.69 – -7.64), Ilorin (0.50 – 0.92, -4.44 – 2.68, 1.75 – 4.51), Maiduguri (0.47 – 0.75, -1.80 – 4.11, 1.06 – 4.40) and Sokoto (0.45 – 0.84, -1.26 – 0.71, 0.96 – 2.32) respectively. Values of estimated solar radiation ranged from 16.71 to 23.67$\mathrm{MJm^{-2}day^{-1}}$.

The developed site-independent model improved the estimation of solar radiation values over the selected locations.

Keywords: Solar radiation, Site-independent model, Air mass, Clear sky albedo.

Word count: 483

TABLE OF CONTENTS

LIST OF TABLES

Table

Page

List of Figures

CHAPTER ONE

INTRODUCTION

1.1.Background to Research

1.1.1. Solar Radiation

Solar radiation is the visible and near-visible (ultraviolet and near-infrared) radiation emitted from the solar surface andpropagated from thesun as radiant energy to the earth's surface(Donald, 1982).

The sun shines by radiating its own energy at the rate of 3.9×10^{26} W generated by continuously changing its own mass into energy at the rate of 4.3×10^{9}kg/s.

The radiation emitted by the sun covers a wide range of wavelengths divisible into two major regions according to theionizing strength: ionizing radiation (X-rays and gamma-rays) and non-ionizing radiation (ultra – violet radiation, UVR, visible light and infra-red radiation) (Iqbal, 1983).

About 47% of the incident extraterrestrial solar radiation energy is in the visible wavelengths from 400 nm to 780 nm, the infrared portion with wavelengths greater than 780 nm account for 46% of the incident energy while the ultraviolet portion of the spectrum with wavelengths $\leq$ 400 nm accounts for about 6% of the extraterrestrial solar radiation.The ionizing radiation account for just about 1% of the sun's emitted energy(Drummond and Thekaekara, 1973).

Ultraviolet radiation, UV, is that part of the electromagnetic spectrum with wavelengths between 100 and 400nm. The UV is divided, based on its biological effects, into three major components as shown in Fig 1.1.

(i) UV-A or black light with wavelengths between 320 – 400nm

(ii) UV-B or erythemal radiation with wavelengths between 280 – 320nm, and

(iii) UV-C or germicidal radiation with wavelengths between100 – 280nm.

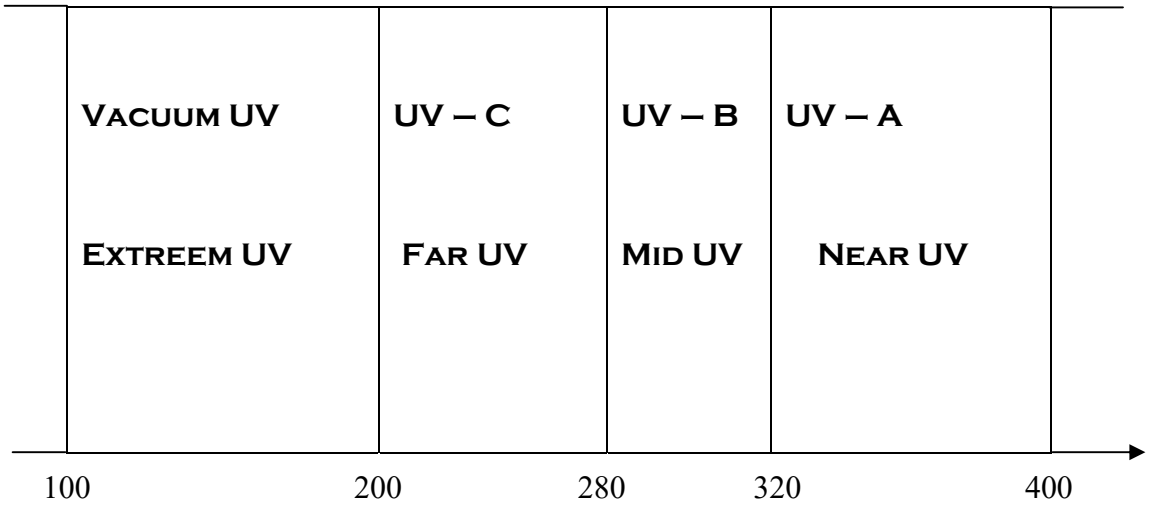

Fig 1.1:UV radiation spectra divisions

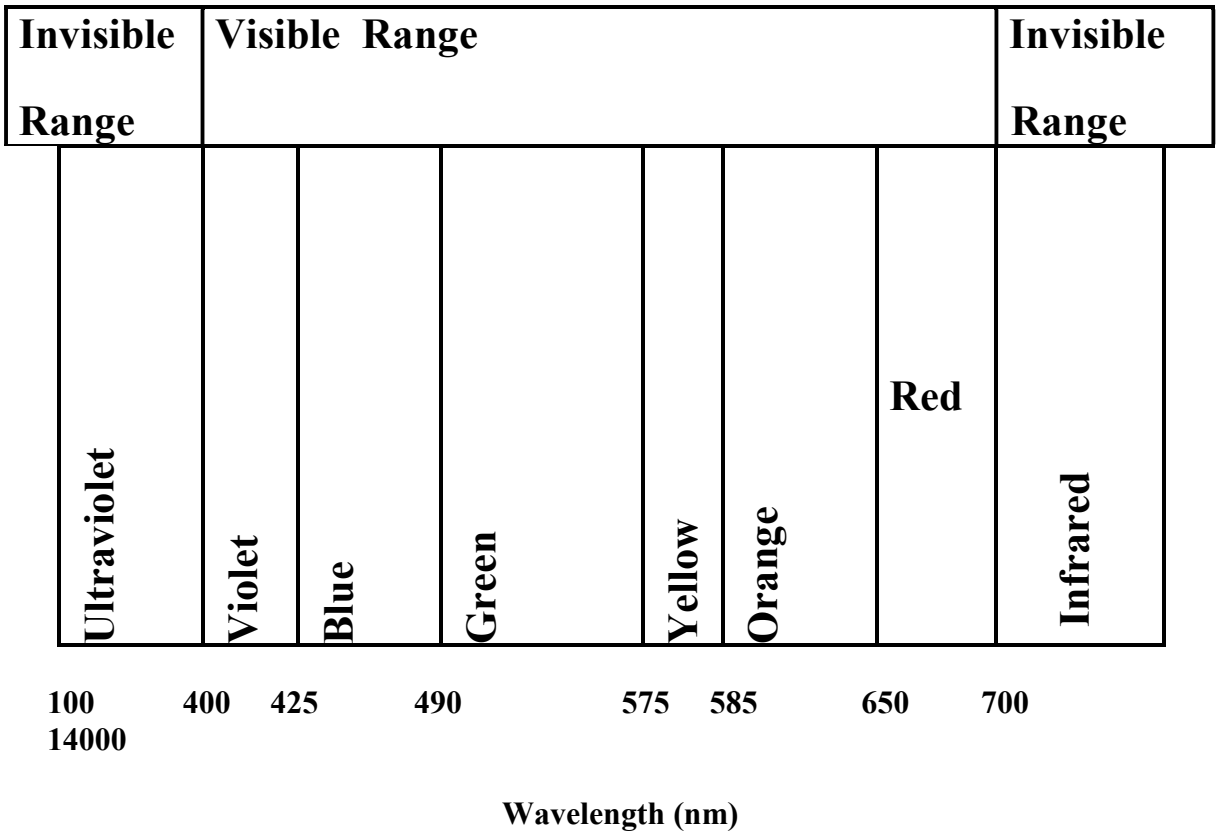

Fig1.2:The Solar Radiation spectrum

Thermal radiation can also be categorized in terms of its nature, either short – wave or long - wave. In solar energy terminology, the major contribution of solar radiation is within the shortwave length while radiation greater than 4μm are classified as longwave radiation. Table 1.1contains the spectral distribution of solar energy.

Table 1:1 Distribution of extraterrestrial solar energy

S/No	Energy from the sun (%)	Wavelength (µm)
1.	95	0.3 – 2.4
2.	1.2	< 0.3
3.	3.6	< 2.4

1.1.2. Variations in incident solar radiation.

Incident solar radiation is unevenly distributed over the earth's surface. Seasonal changes in the sun – earth distance results in the variation of extraterrestrial radiation flux in the range of$\pm 3\%$(Garg and Prakash, 2000). Variation in day length is induced by changes in declination, the angle δ, between the equatorial plane and the plane containing the movement of the earth around the sun. The earth is tilted away from the sun during the northern hemisphere winter, and six months later, it is tilted towards the sun. The time of maximum and minimum declination are known as summer and winter solstices respectively. Declination is determined by using (Iqbal, 1983; Zekai, 2008);

$$\delta = 23.45 \sin\left[\frac{360}{365}(d_n + 284)\right] \text{ in degrees} \quad (1.1)$$

where d_n is the number of day of the year starting 1st of January

This angle varies from +23.45° in summer solstice (21st June) to -23.45° in winter solstice (21st December). Its value is zero at vernal (20th March) and autumnal (22nd September) equinoxes.

The diurnal variation in radiation budget is as a result of the rotation of the earth around its axis. The position of this axis relative to the sun causes seasonal changes in the incident solar radiation.

About 22% (76Wm^{-2}) of the solar radiation reaching the top-of-atmosphere is reflected back, 23% ($79\ \text{Wm}^{-2}$) is absorbed by the clouds, gases and other atmospheric constituents like aerosol while only 54% ($185\ \text{Wm}^{-2}$) is received on the earth's surface (Wild et.al., 2013)

Highest values of insolation received occur in tropical latitudes. Within this zone, there are localized maxima over the tropical oceans and deserts where there is virtually no cloud cover for most of the year. Insolation quantities at the equator over land during the solstices are approximately the same as values found in the middle latitudes during the summer. Outside the tropics, annual receipts of solar radiation generally decrease with increasing latitude. Minimum values occur at the poles.

1.1.3. The Solar constant

The radiation outside the earth's atmosphere is termed the extraterrestrial radiation and this varies for a particular location depending on some solar parameters. The daily extraterrestrial solar radiation falling on a surface parallel to the earth at a point on the earth's surface could be obtained using the expression below (Iqbal, 1983; Zekai, 2008).

$$H_0 = \frac{24}{\pi} S_0 \left[1 + 0.033 \cos\left(\frac{360n}{365}\right)\right]\left(\cos\varphi \cos\delta \sin\omega_s + \frac{2\pi\omega_s}{360} \sin\varphi \sin\delta\right) \quad (1.2)$$

Where S_0 is solar constant, n is the Julian day of the year, δ the declination, $\varphi$the latitude and

$$\omega_s = \cos^{-1}(-\tan\delta \tan\varphi) \quad (1.3)$$

is the sunrise hour angle.

The characteristics of the sun and its spatial relationship to the earth are such that a small range of variation in the intensity of solar radiation outside the earth's atmosphere is always obtained. The solar constant, S_0, the theoretical maximum direct solar radiation input, is the generally accepted value for the flux density of short-wave radiant energyintercepted on a plane perpendicular to the sun's rays at the top of the earth's atmosphere at mean earth-sun distance (Gueymard, 2004).Recent measurements from satellites show that $S_0 \approx 1370$ Wm^{-2}(Hoyt, 1979). This value is known to vary by about 1 Wm^{-2} over a solar cycle that has an average length of 11 years. Angstrom found from some measurements the possibility of a connection between the solar constant S_0 and the sunspot activity through the formula (Saha and Srivastava, 1931).

$$S_0 = 1.903 + 0.011\sqrt{N} - 0.0006N \quad (1.4)$$

Where N is a coefficient characterizing the number and extent of sunspots (called the Wolf and Wolfer's number) and S_0 is given in units of cal/cm^2/min.

The solar energy intercepted by the earth of radius $R_e$equals $S_0 \times \pi R_e^2$; and the average incident solar radiation, H_e, on the earth's surface having a surface area of $4\pi R_e^2$ is therefore (Tompkins, 2010);

$$H_e = \frac{S_0 \pi R_e^2}{4R_e^2} = \frac{S_0}{4} (1.5)$$

This has a value of about $340 Wm^{-2}$

1.1.4. The Clearness Index and Cloudiness Index

The nature and state of the intervening atmosphere is animportant factor in the determination of daily irradiation on the earth surface (Liou, 2002). The intensity of the incoming solar radiation is depleted by the process of scattering, reflection and absorption by air molecules, aerosols suspended in the atmosphere and cloud cover. Because they can reflect a significant part of the incoming radiation, clouds are mostly responsible for the variability in atmospheric Transmissivity.

The part of solar radiation which is neither absorbed nor scattered by the atmospheric constituents, comes directly from the solar disc and reaches the earth's surface as a beam is called the direct solar radiation or direct beam radiation. The scattered part that reaches the earth's surface from all directions from the sky is the diffuse solar radiation. Thus, the global solar radiation, H, received at the earth's surface is composed of direct and diffused components. The diffuse component varies from about 10% of the total on a clear day to about 90% on a very cloudy day (Babatunde and Aro, 1995). The extent of transmission of solar radiation through the atmosphere is called atmospheric transmissivity, atmospheric transmission coefficient or the clearness index;

$$K(t) = \frac{H_e}{H_0} \qquad (1.6)$$

where H_e is the incident solar radiation at the earth's surface, and $H_o$is the extraterrestrial solar radiation measured at the top of the atmosphere.

Equation (1.6) represents the percentage deflection by the sky of the incoming global solar radiation and thus indicates both the level of availability of solar radiation and changes in atmospheric conditions in a given locality (Akpabio et al., 2005).

Similarly, the cloudiness index k(d) is defined as the ratio of diffuse radiation H_d to the global radiation reaching the earth's surface.

$$K(d) = \frac{H_d}{H_e}(1.7)$$

The cloudiness index K(d) monitors the scattering of the incoming extraterrestrial radiation by the sky due to the presence of scattering agents like dusts, clouds, water vapour and so on in the atmosphere. The clearness index and cloudiness index therefore describe different atmospheric conditions related to radiative transfer in the atmosphere. Babatunde and Aro (1995) have studied the characteristics of clearness and cloudiness index by expressing the cloudiness index in terms of clearness index. It was found that they are opposite in characteristics; the higher the clearness index, the more the transparency of the atmosphere and the higher the cloudiness index, the more the turbidity of the atmosphere.

1.1.5. The Relative Optical Air Mass

The extent of absorption and scattering of solar radiation by the atmosphere is a function of the length of the atmospheric path traversed by the sun's beam and the composition of the atmosphere. Solar radiation beam traverses the shortest atmospheric path to reach the earth's surface when the sun is directly overhead (Iqbal, 1983). Generally, solar radiation beam follows an inclined path to reach the earth's surface. To take into account the effect of inclination on the path length traversed by the sun's beam through the atmosphere, a dimensionless quantity, the relative optical air mass m, is made use of. It is defined as the path length which light takes through the atmosphere normalized to the shortest possible path length (that is, when the sun is directly overhead). The air mass quantifies the reduction in the energy of light as it passes through the atmosphere and is absorbed by air dust. It is given as the mass of atmosphere in the actual path of the solar beam divided by the mass of the atmosphere that would be when the sun is directly overhead.

H_0

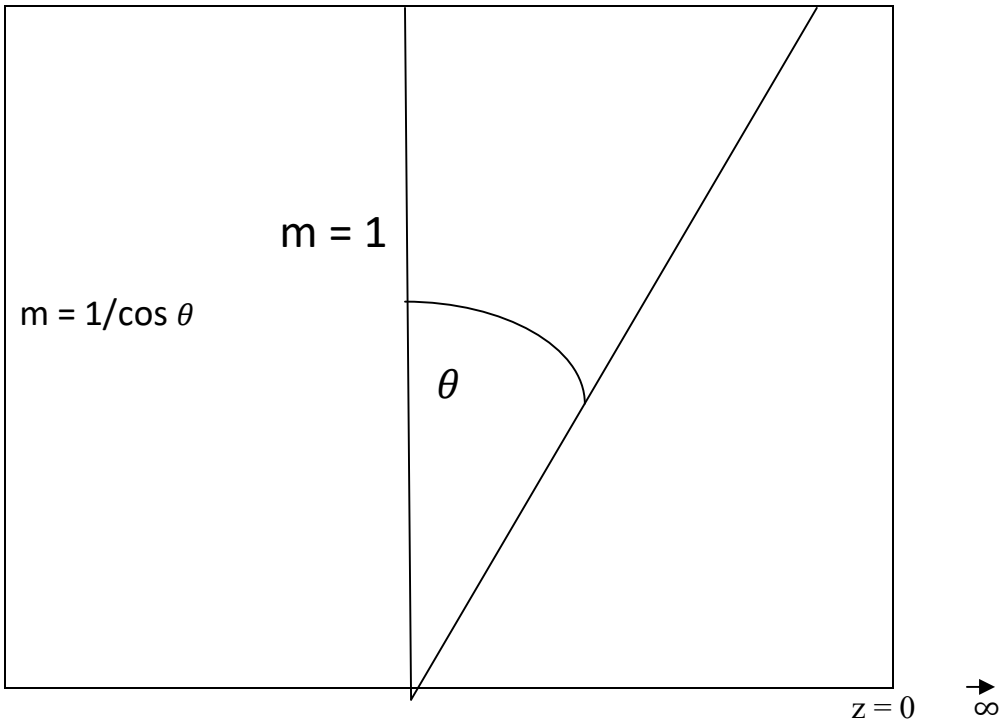

Fig.1.4. Solar radiation and a medium of air mass inclined at an angle $\theta$to the zenith.

From fig 1.4, for a flat earth model, relative optical air mass is given as:

$$m = \frac{1}{\cos\theta} \qquad (1.8)$$

m = 1 corresponds to the case when the sun is directly overhead, and m = 0 when there is no atmosphere. However, the above approximation for a flat earth model is only reasonably accurate for values of θup to around **75°**. And as a result of the neglect of the earth's curvature and the refraction of the real atmosphere in the model, the error inherent in this formula varies between 0.25% at θ= 60° and 10% at θ= 85° (Iqbal, 1983).

A model which takes into consideration the curvature of the earth's surface is (Kasten and Young, 1989);

$$m = \frac{1}{\cos\theta + .050572\,(96.7995 - \theta)} - 1.6364 \qquad (1.9)$$

This model gives an accuracy which is better than 0.1% for $\theta \leq 86^{\circ}$ and 1.25% for $\theta = 89.5^{\circ}$.

Equation (1.9) is applicable for locations at the sea level, that is, at standard pressure of 1013.25 millibars. For locations at an altitude greater than 2000metres, the relative optical air mass is obtained as (Iqbal, 1983);

$$m_a = m\left(\frac{p}{1013.25}\right) \qquad (1.10)$$

where p is local pressure in millibars.

Pressure p above sea level could be obtained from Lunde (1980);

$$p/p_o = \exp^{-0.0001184z} \qquad (1.11)$$

1.1.6. Scattering, Absorption and Reflection of Solar Radiation

Scattering, absorption and reflection are the three methods through which incoming solar radiation is depleted in the atmosphere. Air molecules and other suspended particulate matters in the air are mainly responsible for the scattering, absorption and reflection of incoming shortwave radiation. Scattering make a straight parallel beam of light changes direction either sideways or backwards. The relative intensity of the scattering pattern dependsstrongly on the ratio of particle size to wavelength of the incident wave. If scattering is isotropic, thescattering pattern is symmetric about the direction of the incident wave. A small anisotropic particletends to scatter light equally into the forward and backward directions. For larger particles, the scattered energy is increasingly concentrated in the directions.When particles are much smaller thanthe incident wavelength, the scattering is called Rayleigh scattering. For particles whose sizes arecomparable to or larger than the wavelength, the scattering is customarily referred to as Miescattering. Mie scattering examples include scattering by large water droplets. In such a case, the scattering is said to be neutral to wavelengths. But for larger size droplets or particles, what obtains is more of diffuse reflection or absorption of radiation than true scattering (Saha, 2008).

For Rayleigh scattering, if $I_{0\lambda}$ is the intensity of the light radiation falling on a scattering particle of about the same size, the amount of light scattered I_{λ} is given by the relation:

$$I_{\lambda} = K_{\lambda} I_{0\lambda} / \lambda^4 \quad (1.12)$$

Where K_{λ} is the co-efficient of scattering.

Scattering and reflection by particulate matter thrown up into the atmosphere bymajor volcanic eruptions, which remains suspended in the air for a long time, canmarkedly reduce the intensity of the incoming solar radiation (Wiin-Nielsen, 1967).

Besides scattering, absorption can occur as a parallel beam of radiation of intensity I at wavelength λ passesdownward through a horizontal layer of the atmosphere.Where a fraction dI is absorbed by the mass dm of the layer, then,

$$dI/I = -a_{\lambda} dm \quad (1.13)$$

where a_λ is the co-efficient of mass absorption.

Taking the absorbing gas to be at such a low temperature that its radiation can be ignored, equation (1.13) can be integrated to give,

$$I/I_o = \exp(-\int a_\lambda \, dm) \qquad (1.14)$$

where $I_o$is the intensity of incident radiation.

If the incident beam is inclined to the vertical at an angle θ, (1.11) then takes the form

$$I/I_0 = \exp(-\int \sec\theta \, d\tau) \quad (1.15)$$

where $d\tau = a_\lambda dm$ is called the optical thickness of the atmospheric layer.

Equation (1.15) is the general form of the Beer's law.

Most of the absorption of the incoming radiation energy in the atmosphere takes place in the upper atmosphere. These are those in the ultraviolet and extreme ultraviolet part of the solar spectrum which are absorbed by atmospheric gases such as oxygen, nitrogen and ozone.

The combinations of the parameters mentioned above are responsible for the variability of the surface solar irradiation in space and time.

Presently, there exist two different methods used in determining the amount of incident solar radiation at the earth's surface. It can be measured directly with instrumentation or its values estimated from more readily available meteorological quantities like cloud cover, sunshine duration, surface temperature, etc. The values obtained through one method may then be used to validate the values obtained through the other method (Malinovic *et al*., 2006; Michalsky *et al.,* 2006)

Also, the direct measurement of solar radiation is achieved through two different methods. The values are measured either through ground based instruments or remotely through satellites. Values obtained through the former method are then used to validate

the later (Kimothy *et al.*, 2004; Deneke *et al*., 2005; and Otkin *et al*., 2005). The data obtained through a well maintained ground station usually provide an accurate description of the solar radiation values in the immediate area if readings were obtained for a long period of time to offset local variability.

1.2.Research Problem.

Nearly all atmospheric processes have the sun as their main driving force. The energy of the sun drives physical, chemical and biological processes taking place within the earth-atmosphere system, thus determining the earth's climate (Bonan, 2002) and supporting organic life on the planet (Mavi and Tupper,2004). Solar radiant intensity is the expression of that input upon the earth. The seasonal variation in day length and incident solar radiation along with ambient temperature and precipitation, results in the periodic events in the lives of plant, i.e. plant phenology. The amount of solar radiation is known to determine the upper productivity limit of crops. Thus knowledge about the spatial distribution of solar radiation and its temporal variation is crucial for crop growth monitoring and yield forecasting (Castellvi, 2008; Binghao et al., 2013).

Presently, there is serious concern globally on dwindling and expensive energy supplies for both domestic and industrial use due to over dependence on conventional and non-renewable energy sources. Of similar importance is the environmental degradation associated with the exploitation, exploration and use of fossil fuels. Hence the need to explore and exploit other sources of energy that can serve as alternative to conventional fossil fuels and which are also renewable and environmental friendly. But it is known that time- and space-dependent global solar radiation at the location of interest is the most critical input parameter employed in the design and prediction of the performance of a solar energy devicesince solar radiation reaching the earth's surface depends upon the local meteorological conditions like sunshine duration, cloudiness, ambient temperature, atmospheric turbidity and so on, thus making a study of solar radiation under local climatic condition essential (Journee and Bertrand, 2010; Almorox, 2011; Okogbue and Adedokun, 2009).

In spite of its importance, direct measurements of global radiation are sparse over most of the globe especially in developing countries. The numbers of meteorological stations

measuring daily radiation in most of the developing countries are known to be few (Akpabio et al., 2005). To solve this problem, other approaches for estimating incident solar radiation have been developed. These include the use of empirical models, satellite remote sensing retrieval and so on.

Hence, this work seeks to examine the climatology of solar radiation over eleven locations in Nigeria; Lagos, Benin City, Port Harcourt, Warri, Calabar, Ibadan, Ilorin, Abuja, Maiduguri, Kano and Sokoto representing the climatic zones of the country, using a 22-year satellite data obtained fromthe National Aeronautics and Space Agency's (NASA) Atmospheric Science Data Centre. The satellite data will be compared with 22-year ground data collected for these locations through which algorithms comparing satellite to ground data will be developed.The nature of the relationship which exists between incident solar radiation and air temperature will also beinvestigated over all the locations.

1.3.Justification for the Research.

Provided that the equipment is well maintained and regularly calibrated, direct measurements of solar radiation at weather stations are the most accurate source of solar radiation data. But since this is rarely so, due to the prohibitive costs and difficulty of maintenance, methods have been developed to estimate solar radiation for sites where it is not directly measured. Some of these methods include spatial interpolation (Hay and Suckling, 1979; Rivington et al., 2006), spatial extrapolation (Hunt et al., 1998), empirical modeling (Angstrom, 1924; Prescott, 1940; Hargreaves, 1981; Bamiro, 1983) and so on.

This work will provide a better and precise description of thespatial and temporal distribution of solar radiation over Nigeria. It will also engender a precise information on solar radiation values and related meteorological parameters like air temperature which are crucial for application studies when dealing with exploitation of solar energy, thermal loading on buildings, description of atmospheric phenomena and large-scale weather analysis and prediction (Okogbue and Adedokun, 2002, Almorox, 2011).

Since variations in incident solar radiation is known to have impact on weather and climate (Zurich, 2009), this study will furthermore confirm or otherwise whether or not

the observed decline in surface solar radiation recorded over many places in the world between 1960s and the 1990s and the recovery recorded thereafter were mirrored over Nigeria.

Finally,theempirical models based on correlation equations have been found to perform better when long-term monthly average values of the meteorological parameters rather than when the actual daily data are used (Okogbue and Adedokun, 2009). This work has employed 22-years datato calibrate and validate six existing site-dependent and one site-independent empirical models for five locations which are representative of the climatic zones of the country, anda newsite-independent model proposed.The proposed model will simplify the process of estimation of global solar radiation over locations in Nigeria and elsewhere.

1.4 Objectives of the research work

The objectives of this research work are to:

1. Develop a site-independent empirical model which could be used to predict solar radiation with reasonable accuracy over a widest possible area, validate it with ground data from five locations spread across the country and make comparisons with some of the existing models.
2. Provide a precise description of the spatial and temporal distribution of solar radiation over Nigeria between 1984 and 2005 using satellite data.
3. Investigate the nature of the relationship which exists between incident solar radiation and air temperature.
4. Confirm or otherwise whether or not the observed dimming of surface solar radiation recorded over many places in the world between 1960s and the 1990s and the recovery thereafter were mirrored over Nigeria.
5. Compare satellite data and ground data collected over 11 locations representative of climatic regions of Nigeria and obtain algorithms comparing the two data group.

CHAPTER TWO

LITERATURE REVIEW

2.1. Spatial and Temporal variations of Solar Radiation

The sun is the star closest to the Earth and its radiant energy, termed solar radiation, is the principal energy source forphysical, biological and chemical processes, such as,snow melt, plant photosynthesis, evaporation and cropgrowth.It is an importantparameter for biophysicalmodels to evaluate risk of forest fires, hydrologicalsimulation models and mathematical models of naturalprocesses (Meza and Varas, 2000).Solar radiation data are crucial inputs to regional and global-scale atmospheric models (Yucel et al, 2002). This is especially true in locations within a country like Nigeria where cloud coverage and intensity can change over short time and space as a result of the influence of the inter-tropical discontinuity, a zone where warm, moist air from the Atlantic meets with hot, dry and often dust laden air from the Sahara desert (Falodun and Ogolo, 2007).

The effect of the temporal characteristics of incident solar radiation and air temperature on solar thermal systems is more acute in areas of cloudy climate and those adjacent to coastal areas where variations in local insolation could be large from day to day. These variations are superimposed upon seasonal variations due to the annual cyclic change in solar declination(Adjepong and Okujagu, 1987).

A significant proportion of the incoming solar radiation suffers depletion as it passes through the atmosphere by a combination of processes such as scattering and absorption by clouds, molecular species and aerosols before reaching the ground and, depending on the nature of the surface (i.e. albedo), it is partly reflected and the rest absorbed (Iqbal, 1983; Kyle, 1991).

The solar radiation received from the sun without having undergone scattering through interactions with atmospheric constituents is the direct component, while the part received after it has undergone scattering by interaction with atmosphere is the diffuse radiation. Global solar radiation is the algebraic sum of the direct and diffuse radiations (Trabea and Shaltout, 2000).

Incident solar radiation is unevenly distributed over the earth's surface as a result of such variables as solar altitude, which is associated with latitude and season; and atmospheric conditions, which are determined by cloud cover and degree of pollution (Iqbal, 1983).

In a research carried out in Louisiana, United States, Ye (1996) examined the association between solar radiation and synoptic weather types as well as the spatial and seasonal distribution of solar radiation in Louisiana. In her findings, she noted a minimal degree of spatial variability on an annual basis (but with northern Louisiana displaying the largest range in values), a distinct south-to-north in winter, and a difference across the state in the time of year of peak solar radiation receipt.

Also, Venalainen and Heikinheimo (1997) working on the spatial variation of long-term mean global radiation in Finland discovered that the spatial distribution of global radiation was clearly dependent on latitude during winter, the higher latitudes receiving less radiation than the lower latitudes, while variation of cloudiness determines its variation during summer.

This latitudinal dependence of incident global radiation was also evident in a research conducted in Sweden by Persson (1999). In his result, he found a large difference in the surface solar irradiance for different areas of Sweden, with latitude being the dominant factor. He also observed an increase in the temporal trend of the global radiation of up to 9.3% per decade, of direct normal irradiance and sunshine hours averaging 7.2% per decade over all stations considered. This trend he attributed to decreasing cloudiness.

In a work aimed at determining the extent of attenuation of global radiation by air pollution, Jauregui and Luyando (1999) compared the intensity of observed radiation within the downtown area of Mexico City to those obtained in a cleaner rural environment. Their findings showed that on fine weather days during the dry season, the city receives 21.6% less solar energy than the rural surroundings. Even during the rainy season when aerosol concentration is abated by a wash-out effect, similar values of attenuation were obtained. In a similar research to determine the variation of solar radiation intensities at the surface of the earth in the United States, Hand (1939) found that there was an unprecedented increase in radiation received on a horizontal surface from the sun at various places within the United States in 1932 and linked this with the

business depression of that year which culminated in less industrial activities and hence a reduction in effluent gases released into the atmosphere.

Liepert (2002) observed a 19W/m^2 decline in surface solar radiation in the United States from 1961 to 1990. This decline is found to be strong when compared to sites in other regions of the globe which had a 7W/m^2 decline within those three decades. He gave the combination of green-house gas and aerosol forcing as a possible explanation for this observation. This interpretation is in line with Tselioudis and Rossow's (1994) suggestion that greenhouse gas warming leads to increasing cloud optical thickness at overcast conditions (through increasing cloud height and liquid water content). An increase in optical thickness reduces surface solar radiation and surface temperature.

Falodun and Ogolo (2007) studied the diurnal and seasonal variations of mean global radiation in Akure by analyzing a two year data (August 2003 to July 2005) measured at the ground surface. Their results showed that the maximum mean global solar radiation (occurring at about 14.00 LT) varies in the course of the year from 512Wm^{-2} during the rainy season (i.e. April – October) to 543Wm^{-2} during the dry season (i.e. November – March). They attributed the low values (and large fluctuations) of the hourly mean values recorded during the wet season to the important roles that the convective clouds and water vapour play in the atmospheric radiation budget which is very pronounced in the tropical areas of West Africa. They finally observed that the daily amplitude of the global radiation is larger for the dry season (maximum in November) than it is for the wet season (maximum in July), and that a time – lag of about 2h is noted between the times when the air temperature maxima and the mean global radiation courses occur over the area. This period coincides with the harmattan period.

Adeniyi et al. (2012) noted a variation in the values of global solar radiation and mean surface temperature in Ibadan during the dry and rainy seasons. They observed that the dry months have larger values (642.5 ± 10.8 Wm^{-2}) of total radiation than wet months (584.3 ± 10.9 Wm^{-2}). The variations were attributed to the effects of clouds, dust haze and harmattan.

2.2. Remote sensing of the Earth's Insolation

Remote sensingis an expression referring to any technique for making measurements without the use of in-situ instruments. Instruments for remote sensing may be ground-based, airborne or mounted on space platforms. The availability of space platforms or artificial satellites over the last 30 years has stimulated the development of new techniques for making measurements and for analyzing the data (Olatona, 2009). Whilst in-situ measured data is considered to be an important feature in solar energy applications, its availability has proven to be spatially and temporally inadequate for many applications (Journee and Bertrand, 2010).The major reason being the high costs of running surface networks which therefore limits their use to selected locations. Thus, the alternative method of obtaining long term surface solar radiation data involves retrieving surface flux from satellite measurements and validation for each locality by the use of ground data. The geostationary satellites used for this purpose offer broad spatial coverage and high temporal resolution (Sengupta, 2010).

The data for solar radiation at the earth's surface is derived from satellite measurements in two ways. The empirical methods involve forming empirical relationships between multi-spectral satellite radiances and surface radiation as measured from terrestrial-based instrumentation (Perez et al., 2002). These empirical relationships are used to compute surface flux directly from satellite measurements.

The physical methods use a two stage process. The first stage involves the creation of a cloudy/clear-sky mask and cloud type (e.g., cirrus, cumulus, stratocumulus) from multi-spectral satellite measurements (Stowe, et al., 1999; Heidinger, 2003; Pavlonis et al., 2005). The second stage involved the use of the cloud information in a radiative transfer model to compute the down-welling surface flux properties while physically accounting for cloud transmittance (Pinker et al., 2002; Laszlo et al., 2008).

Whereas the empirical method is attractive because of its speed, there is the potential for large inaccuracies because of the non-linear relationships that exists between the satellite-measured radiance fields, the cloud properties, and the surface solar radiation. The physical method is expected to produce more accurate results as the two-stage process deals explicitlywith these non-linear interactions between clouds and radiation (Sengupta, 2010).

Vignola et al (2007) noted that ground based measurements and satellite-derived solar radiation data complement each other and are necessary to build a comprehensive solar radiation database. They argued that it is impractical to have a high density ground-based solar radiation monitoring network that would match the coverage capability of a satellite-derived solar radiation database.

Because satellite images cover large areas (about 100km^2 once an hour), while ground-based measurements look at a small portion of the sky, averages and statistics are the instruments usually employed to compare and contrast these two diverse databases (Zelenka, et al., 1999).

2.3.Surface Solar Radiation and Atmospheric Temperature

The radiation coming from the sun to the earth is the only form of incoming radiant energy which determines the heat balance and the thermal regime of the earth (Borzenkova, 1992). The solar radiation that reaches the surface has a part of it absorbed as heat energy and a part reflected back to space. The portion absorbed raises the temperature of the earth's surface which then emits its own radiation in the longwave spectrum with maximum emissions at wavelengths between 10μ and 15μ. A fraction of this infrared radiation is absorbed by greenhouse gases which results in the increase in the ambient temperature at the earth's surface (Saha, 2008).

There exists therefore a strong correlation between surface solar radiation and daily temperature range (Makowski, 2009). Variations in solar radiation have impact on weather and climate (Zurich, 2009).

2.4. Estimating Global Solar Radiation from other meteorological parameters.

Despite the importance of global solar radiation data, its measurements are not frequently available especially in developing countries. This is because the meteorological stations measuring solar radiation data are few (Akpabio, et al., 2005). In Nigeria for example, there are presently about 44 weather stations that routinely measure weather variables like sunshine hours, surface temperature etc. But there are only about 16 weather stations where surface solar radiation is measured. To overcome this problem therefore, methods

have been developedto model the global solar radiation. The two categories of solar radiation models available in the literature are described below.

2.4.1. Parametric models

Parametric models usually involve detailed information of atmospheric conditions. Examples of the meteorological parameters frequently used as predictors are the type, quantity and distribution of clouds or other observations, such as the fractional sunshine, atmospheric turbidity and precipitable water amount (Wong and Chow, 2001).

2.4.2. Empirical models

These models are based on empirical correlations between solar radiation and other more readily measured meteorological quantities like bright sunshine hours, air temperature and other climatic variables of the environments of the locality where the study is being carried out.

Angstrom (1924) originally suggested a simple linear relationship to estimate global solar radiation. Prescott (1940) later put the correlation in a convenient form as:

$$\frac{H_e}{H_o} = a + b\ n/N \quad (2.1)$$

whereH_e is the global solar radiation ($MJm^{-2}day^{--1}$), H_o is the top of the atmosphere (extraterrestrial radiation)($MJm^{-2}day^{-1}$), n, the monthly average daily bright sunshine hour; N, the maximum possible monthly average daily sunshine hour otherwise called the day length; a and b are the site-specific regression coefficients. The values of 0.25 and 0.50 fora andbrespectively are recommended in the absence of locally calibrated values (Allen, et al, 1998).

The day-length N is calculated as follows;

$$N = \frac{\omega_s 24}{\pi} \quad (2.2)$$

where ω_s, the sunrise hour angle is calculated as in equation (1.3).

Different models based on this equation employ different approaches to estimate the coefficients a and b (Rietveld, 1978; Neuwirth, 1980).

Besides the Angstrom-Prescott model, other models, linear and non-linear, employing sunshine hours to estimate solar radiation at the surface have been proposed by several workers in the field (Glover and McCulloch, 1958; Garg and Garg, 1982; Hussain, 1984; Newland, 1988; Akinoglu and Ecevit, 1990; Samuel, 1991; Tamm and Thormalla, 1992, Almorox and Hontoria (2004), etc.

Hargreaves and Samani (1982) proposed (and later used by Allen, 1997) an empirical equation expressed in the form of a linear regression between the clearness index and the square root of the monthly mean of the daily temperature range ΔT as:

$$\frac{H_e}{H_o} = k_r \Delta T^{0.5} \quad (2.3)$$

where, ΔT, is the difference between the monthly average of daily values of the maximum and minimum temperatures; and k_r, empirical coefficient. Hargreaves (1994) recommended the values of $k_r = 0.16$ interior regions and $k_r = 0.19$ for coastal locations.

Equation (2.3) is based on the assumption that the difference betweendaily maximum and minimumtemperature provides ageneral indication of cloudiness. Compared to clear skies,cloud cover usually decreases maximum air temperatures dueto lower solar radiation levels, and usually increases minimumair temperatures due to increased downward emission and reflectionof long wave radiation by clouds at night. It is a fact that many other factors besides incident solar radiation H_e,and cloudiness affect levels ofmaximum and minimum air temperature, especially on a dailybasis. Other factors include wind speed, air-vapor content,availability of soil water for evaporation, elevation, precipitation,and frontal weather systems. However, over periods ofas long as one month, many of these weather variables tendto follow long term averages, resulting in a fairly consistentrelationship between $\Delta T$and $\frac{H_e}{H_o}$. The coefficient $k_r$varies somewhatwith time, location, and climate. The equation is thus primarily intended for application on monthly daily averages (Allen, 1997)

To account for the altitude of a particular location, Allen (1995a), modified (2.3) by estimating k_r as a function of elevation as;

$$k_r = k_{ra}\left(\frac{P}{P_o}\right)^{0.5} \quad (2.4)$$

where P = mean atmospheric pressure at the location;

P_o = mean atmospheric pressure at sea level and;

k_{ra}, the empirical coefficient given as 0.17 for inland locations and 0.20 for coastal locations.

The introduction of $\frac{P}{P_o}$ was to account for elevation effects on the volumetric heat capacity of the atmosphere.

It has been shown in equation (1.11) that Lunde (1980) obtained the hypsometric equation as;

$$\frac{P}{P_o} = \exp(-0.0001184z) \quad (2.5)$$

Annandale, et al (2002) obtained the correction to the altitude to be;

$$2 \times 10^{-5}z \quad (2.6)$$

where z = altitude of the location in meters.

Dividing eq. (2.5) by 0.75, the maximum clear sky transmissivity of the atmosphere gives (Duffie and Beckman, 1985);

$$2.7 \times 10^{-5}z, \quad (2.7)$$

Either of the equations (2.5) or (2.7) providesthe coefficient to correct the effects of altitude on the incident solar radiation, H_e. This coefficient is a modification to the recommendation in FAO-56 for predicting incident solar radiation and its presence is important to account for effects of reduced atmospheric thickness on H_e (Allen, et al. 1998).

Annandale, et al (2002) rewrote Hargreaves equation (2.3)to include Allen's correction for altitudeas;

$$\frac{H_e}{H_o} = k_{ra}(1 + 2.7 \times 10^{-5}z)\sqrt{\Delta T}(2.8)$$

where z is the altitude in meters. This model was subsequently calibrated in three locations, Stellenbosch, Pietermaritzburg and Kakamas in South Africa.

Sanusi and Abisoye (2011) working in Ibadan, southwest Nigeria, proposed a power regression form of the Hargreaves model;

$$\frac{H_e}{H_o} = a_1\sqrt{(\Delta T)^{b_1}}(2.9)$$

Garcia (1994) model is a variant of the Angstrom-Prescott model having a slight modification with ΔT replacing n:

$$\frac{H_e}{H_o} = a_2 + b_2\frac{\Delta T}{N}(2.10)$$

wherea_2 and b_2 are empirical coefficients. Using monthly average daily estimates, Garcia (1994) proposed the following values:

a_2= 0.060 and b_2= 0.640 for the central coast;a_2= 0.360 and b_2= 0.211 for the northern coasta_2= 0.457 and b_2= 0.207 for the central highlands;a_2= 0.230 and b_2= 0.380 for the southern highlands of Peru.

Bristow and Campbell (1984), using the argument that since sensible heat is responsible for temperature variations, it is possible to obtain a relationship between temperature differences and solar radiation, temperature being a signature of radiation balance, obtained the relationship between clearness index and ΔT:

$$\frac{H_e}{H_o} = a_3[1 - \exp(-b_3\Delta T^{c_3})](2.11)$$

where, a_3, b_3 and c_3 are empirical coefficients. Values for these coefficients are 0.7 for a_3, 0.004 – 0.01 for b_3 and 2.4 for c_3.

The coefficients have some physical meanings. $a_i$represents the maximum radiation that can be expected on a clear day while b_3 and c_3 control the rate at which a_3 is approached as the temperature difference increases.

Panday and Katiyar (2010) working over five different locations across India proposed this model;

$$\frac{H_e}{H_o} = a_4 + b_4 T_r (2.12)$$

where $T_r = \frac{T_{max}}{T_{min}}$

Okogbue and Adedokun (2009) proposed the following models and applied them to a 5-year (1986-1990) meteorological data for Ondo, Southwest Nigeria.

$$\frac{H_e}{H_o} = a_5 + b_5(\Delta T) + c_5(T_r) (2.13)$$

$$\frac{H_e}{H_o} = a_6 + b_6(\Delta T) + c_6(T_{ave}) (2.14)$$

$$\frac{H_e}{H_o} = a_7 + b_7(T_{ave}) + c_7(T_r) (2.15)$$

where $T_{ave} = {(T_{max} + T_{min})}/{2}$

Water vapour affects atmospheric transmissivity through refraction effects (Tamm and Thormalla, 1992). Thus atmospheric water content in the form of absolute or relative humidity should be accommodated in any attempt to estimate incident solar radiation (Garg and Garg, 1982; Hussain, 1984). Chen and Li (2012) working in China proposed models which have other routinely measured parameters like relative humidity and surface pressure included in equation (2.3);

$$\frac{H_e}{H_o} = a_8 + b_8 \Delta T^{0.5} + c_8 RH (2.16)$$

Burari and Sambo (2001) correlated solar radiation with relative humidity over Bauchi, Northern Nigeria, through the relation;

$$\frac{H_e}{H_o} = a_9 + b_9 \frac{RH}{100} \quad (2.17)$$

The empirical models described in equation (2.3) to (2.16) are temperature based as they employ minimum and maximum temperatures as the required meteorological data. In equations (2.1) to (2.17), the top of the atmosphere radiation (extraterrestrial radiation) was calculated using equations (1.2)and(1.3).

Almost all the models described so far has varying empirical coefficients for different locations, that is, they are site–specific. Hay (1979) incorporated the effects of Optical properties of the cloud cover, ground reflectivity and average air mass in his site-independent model;

$$\frac{\bar{H}_e}{\bar{H}_o} = \frac{0.1572 + 0.5566\left(\frac{\bar{n}}{\bar{N}_m}\right)}{1 - \rho_g\left[\rho_a\left(\frac{\bar{n}}{\bar{N}_m}\right) + \rho_c\left(1 - \frac{\bar{n}}{\bar{N}_m}\right)\right]} \quad (2.18)$$

Whereρ_a, is the clear sky albedo, ρ_c is the cloud base albedo, ρ_g is the ground albedo and$\bar{N}_m$ is the modified day–length for a solar zenith angle θ_z greater than 85° and is given by;

$$\bar{N}_m = \frac{1}{7.5}\cos^{-1}\left(\frac{\cos 85 - \sin\varphi \sin \quad _c}{\cos\varphi\cos\delta_c}\right) \quad (2.19)$$

Where δ_c (degree) is the characteristic declination, i.e. the declination at which the extraterrestrial irradiation is equivalent to its monthly average value.

With this model, he obtained values of solar radiation for locations in Canada without changing the coefficients. Iqbal (1983) however noted that the value of cloudless clear sky albedo ρ_a (0.25) assumed by Hay (1979) in obtaining his coefficients (therefore, model) is too high compared to values obtained for some locations in parts of the globe which varies from 0.07 to 0.15. Using the value of 0.25 will therefore have an effect on the coefficients a and b of his model. He also observed that $\bar{N}_m$ is only relevant in obtaining the coefficients and should not have been part of the final model equation.

Korachagaon and Bapat (2012) proposed 2 multi-parameter site–independent models in India;

$$\frac{H_e}{H_o} = a(T_{max}) + b(\Delta T) + c(RH) + d(T_{min}) + e(\text{moisture}) + f(\text{longitude}) + g(\text{altitude}) + h(\text{windspd}) + i\left(\frac{T_{min}}{T_{max}}\right) + j(\text{latitude}) + K \quad (2.20)$$

$$\frac{H_e}{H_o} = a + b(T_{max}) + c(T_{max})^2 + d(T_{max})^3 + e(T_{max})^4 + f(T_{max})^5 + g(RH) + h(RH)^2 + i(RH)^3 + j(RH)^4 + k(RH)^5 \quad (2.21)$$

Korachagoan and Bapat model has the deficiency of requiring too many parameters with the attendant difficulty of availability, rather low correlation coefficients and each of the two models is onlyapplicable to specified parts of theglobe

This work aims at employing a 22–year data for elevenstations spread over Nigeria to establish spatial and temporal patterns for global radiation and the associated meteorological parameters along the coastal, N-S and W-E transientswithin the country for the same period. This study is also aimedat developing a site-independent empirical model to predict incident solar radiation with reasonable accuracy over a widest possible area. Finally, the relationship between surface temperatures (maximum and minimum) and global radiation will be examined.

CHAPTER THREE

METHODOLOGY

3:1. The Study Area

Nigeria shares land borders with the Republic of Benin in the west, Republics of Chad and Cameroon in the east and Niger Republic in the north. Its southern boundary lies on the Gulf of Guinea.It bordersLake Chad in the northeast. Nigeria's total land area is 923,768km^2, where 910,768km^2 of it is land, and with water surfaces accounting for 13,000km^2. In perimeter, Nigeria's total boundaries are 4,047km; 3,194km of this on land while the coastline is 853km (Areola et. al., 2014)

Four different climate zones exist in Nigeria from the south to the north. The southern part of the country has an equatorial monsoon climate influenced by the south-east monsoonal winds carrying maritime tropical(MT) airmass coming from the Atlantic Ocean.

Along the coast, precipitation is heavy, between 1824mm to over 4000mm. Rain falls most of the year with a short break in August and a longer break between December and January. Next to this is the central region which has a tropical humid climate. This region has a marked rainy season which lasts from March to October and a pronounced dry season lasting from November to March. The Northern part exhibitsdrier climate where rainfall is recorded for only three to four months (June-September). The rest of the year is dry and hot with temperature going up to 40°C. Finally, the mountain or highland climate is found on different highland regions scattered across the country. Most highlands in Nigeria are over 1000 metres high which forces temperature to remain cool throughout the year (Iloeje, 1981).

The main influence on weather in Nigeria are the trade winds, the south-east trade wind from the southern part of the country originating from the Atlantic ocean and is responsible for the rainy season, and the north-east trade winds from the north blowing over the Sahara desertand is responsible for the Harmattan, adry dusty wind that blows across the country from November to March. Thus, the climate of Nigeria is marked by

two seasons, dry and rainy. These two seasons are influenced by two different air masses, the tropical maritime (MT) airmass from the South Atlantic Ocean and the tropical continental (CT) airmass. The MT airmass as a result of its instability is easily forced to rise when it encounters highlands, resulting in the formation of orographic clouds,usuallybringing down heavy rainfall. Some of the places which experience this type of rainfall include Jos plateau, Mambilla Plateau, Obudu plateau in Cross-River state, Shebshi Mountains in Adamawa State, Western highlands in South-Western Nigeria and central highlands in Kaduna state (Iloeje, 1980).

Temperatures throughout Nigeria are generally high; diurnal variations are more pronounced than seasonal ones. Highest temperatures occur during the dry season; and moderate afternoon highs during the wet season. Average highs and lows in Lagos,for example, are 31℃ and 23℃ in January and 28℃ and 23℃ in June. Although average temperatures vary little from coastal to inland areas,they have greater extremes especially in the northeast. There, temperatures reach as high as 44℃ before the onset of the rains and drop as low as 6℃ during theharmattan seasonbetween December and February.

Sunshine hours average from six hours a day during the rainy season to as high as ten hours in the dry season in the northern part of the country. In the south, they average about four hours in the wettest months to eight hours during the driest period of the year. Thus, significant variability exists in the amount of solar radiation reaching the surface within the country (Areola et. al., 2014).

3:2. Data and Methods.

The satellite data used in this study were extracts from the surface meteorology and solar energy data archive of the National Aeronautics and Space Administration, (NASA) Atmospheric Science Data Centre (ASDC). The data, spanning 22-years (January, 1984 to December, 2005), were archived through NASA Science Mission Directorate's satellite and re-analysis research programmes. The daily average data weregenerated using the Pinker/Laszlo shortwave algorithm and made available in a 1-degree latitude by 1-degree longitude grid covering the entire globe (64,800 regions).The data were validated with ground data obtained from National Climatic Data Center (NCDC) and

Baseline Surface Radiation Network (BSRN) of the United States of America before they were made available for public use. They displayed a high correlation with coefficient of determination, $r^2 = 0.95$. The data obtained consist of daily averages of global radiation, relative humidity, sunshine hours, maximum and minimum temperatures.

The ground dataset consisting of global radiation, relative humidity, sunshine hours,minimum and maximum temperatures for the eleven locations were obtained from the Nigeria Meteorological Agency Oshodi, Lagos. The calibration of Gunn-Bellani readings with Pyranometer readings was done using the method ofFolayan (1988) as 1 millimetre of Gunn-Bellani distillate being equivalent to 1.357 ± 0.176 MJm^{-2}.

The study was carried out forelevenlocations which are representative of all the climatic regions in Nigeria.Figure 2:1 depicts the nine locations, while Table 3 gives theirgeographical coordinates(in increasing latitude).

Fig3.1: The elevenlocations on the Nigerian map
(www.mapsofworld.com)

Table 3.1:The geographical coordinates and altitudes of the locations.
(www.mapsofworld.com)

S/N	Location	Longitude	Latitude	Altitude (metres above sea level)
1.	Port Harcourt	7.17E	4.67N	16.0
2.	Calabar	8.33E	4.95N	94.0
3.	Warri	5.68E	5.50N	15.0
4.	Benin City	5.52E	6.33N	78.0
5.	Lagos	3.24E	6.27 N	34.0
6.	Ibadan	3.97E	7.37N	237.0
7.	Ilorin	4.58E	8.5N	289.0
8.	Abuja	7.52E	9.08 N	777.0
9.	Maiduguri	13.33E	12.0N	299.0
10.	Kano	8.5E	12.03N	476.0
11.	Sokoto	5.27E	13.07N	272.0

3.3. Trend Analysis

Trend analysis is a statistical procedure performed to evaluate hypothesized linear and nonlinear relationships between two quantitative variables. Typically, it is implemented either as an analysis of variance for quantitative variables or as a regression analysis. It is commonly used in situations when data have been collected over time or at different levels of a variable; especially when a single independent variable, or factor, has been manipulated to observe its effects on a dependent variable, or response variable.

Series patterns usually are described in terms of two basic classes of components; trend and seasonality. Trend represents a general systematic linear or nonlinear component that changes over time and does not repeat itself within the time range captured by our data (e.g. a plateau followed by a period of exponential growth). Seasonality may have a similar nature as the former; however it repeats itself in systematic intervals over time. These two general classes of time series components may coexist within the same data.A simple description of thesetechniques istrend estimation, which can be undertakenwithinaformal regressionanalysis (Brockwell and Davis, 1991).

The seasonal trends of the variations for each of the eleven locations were determined.

3.3.1 Time Series

This is an ordered sequence of values of a variable $x_t$obtained at equally spaced time intervals,Δt.The observations are usually plotted against time on annual or seasonal basis. Time series forecasting is the process of using a model to generate predictions (forecasts) for future events based on known past events.A mathematical model for the time variations of data set can allow compact representation of characteristics of that data in terms of few parameters (Wilks, 2006). The two basic approaches in time series analysis are the frequency domain and time domain analyses. While time-domain methods characterize data series in the time scale of measurement, frequency-domain analysis represents data series in their characteristic frequencies.

3.3.2 Moving Average

Data in the form of time series usually consist of other systematic pattern and random fluctuations which mask the overall trend, hence the concept of moving average smoothing was usually employed.

Given a sequence$\{a_i\}_{i=1}^{N}$, an n-moving average is a new sequence $\{S_i\}_{i=1}^{N-n+1}$defined from the $a_i$by taking the averageof sequences of n-terms,

$$S_i = \frac{1}{n}\sum_{j=i}^{i+n-1} a_j \quad (3.1)$$

So the sequences $S_n$giving 6 months-moving averages is

$S_6 = 1/6\ (a_1 + a_2 + a_3 + a_4 + a_5 + a_6, a_2 + a_3 + a_4 + a_5 + a_6 + a_7, a_3 + \ldots + a_{n-2}, + a_{n-1}, + a_n)$ (3.2)

Moving average is used to smoothing out the seasonal fluctuations of climatic components so as to make the trends within the data become apparent.

3.3.3Regression Analyses

Correlation and regression analyses are statistical techniques used extensively to examine causal relationships between variables. Both of them measure the degree of relationshipbetween two or more variables in two different but related ways.

Correlation analysis is a tool employed to determine the strength of linear relationships between two variables. Correlation coefficient ranges from –1.0 through 0.0 to +1.0. A correlation coefficient of -1.0 indicates a perfect but negative correlation between the variables being compared. A correlation of 0.00 means there is no linear association between the variables, while a correlation of +1.0 indicates a perfect and positive correlation between the variables.Regression analysis, however, goes a step further to give the actual rate of change of one variable when the other is increased or decreased at a given rate.

Utilization of correlation analysis on dependent and independent variables produces a statistical parameter called the correlation coefficient (r). The square of correlation coefficient, r, is the coefficient of determination or r^2 which describes what proportion of

the variation in the dependent variable is associated with the regression of an independent variable.

In a simple regression analysis, one dependent variable is examined in relation to only one independent variable. The analysis is designed to derive an equation for the line that best models the relationship between the dependent and independent variables. This equation has the mathematical form:

$$y = a + bx + \varepsilon \qquad (3.3)$$

where, y is the value of the dependent variable, x is the value of the independent variable, a is the intercept of the regression line on the y axis when x = 0,b is the slope of the regression linerepresenting the amount of change in y that corresponds to a change of 1 unit in xand εis error term of prediction (y-$\hat{y}$), showing the difference between observed y and predicted y.Least-square technique is usually employed in obtaining the regression line since it ensures that the sum of the square of the differences of the individual observed values from the regression line, $\sum_{i=1}^{n}(y_i - \hat{y}_i)^2$, is at an absolute minimum (Gregory, 1980).

If $(x_i, y_i), (x_2, y_2), \ldots., (x_n, y_n)$represent a pair of random variables, to predicty, parameters a andb in equation (3.3) must be estimated such that the sum of the square of the differences between the observations y_i and the straight line is minimum.The interpolating straight line is;

$$y_i = a + bx_i + \varepsilon_i , \quad i = 1,2, \ldots..n \qquad (3.4)$$

The coefficients that minimize the square of the distance between the line and the points are;

$$a = \bar{y} - b\bar{x} \qquad (3.5)$$

$$b = \frac{\sum_{i=1}^{n} y_i x_i - \frac{\left(\sum_{i=1}^{n} y_i\right)\left(\sum_{i=1}^{n} x_i\right)}{n}}{\sum_{i=1}^{n} x_i^2 - \frac{\left(\sum_{i=1}^{n} x_i\right)^2}{n}} \quad (3.6)$$

where;

$$\bar{y} = \frac{1}{n}\sum_{i=1}^{n} y_i \,, \quad (3.7)$$

and

$$\bar{x} = \frac{1}{n}\sum_{i=1}^{n} x_i \quad (3.8)$$

are the averages of y_i and x_i respectively. Thus a andb are the least squares estimators of the intercept and slope. The fitted simple linear regression model is given as

$$\hat{y}_{LS} = \hat{a} + \hat{b}x_i \quad (3.9)$$

In situations where the dependent variable y is explained by more than a single variable x_i, equation (3.9) becomes;

$$\hat{y} = a + \sum_{i=1}^{n} b_i x_i + \varepsilon \quad (3.10)$$

where$\hat{y}$ is the parameter to be estimated, a is a constant, the intercept of the regression plane, x_i are the predictor variables and ε the stochastic error term. The $b_i$are the partial regression coefficients. This is a multiple linear regression equation.

Equation (3.10) could be expanded to accommodate n number of independent variables. For example, a two-variable multiple regression equation is given as;

$$\hat{y} = a + b_1 x_1 + b_2 x_2 + \varepsilon \quad (3.11)$$

To obtain the values of a, b_1 and b_2, equation (3.11) is multiplied by 1,x_1 and $x_2$successively and summing both sides to obtain a set of simultaneous equations;

$$\sum y = na + b_1 \sum x_1 + b_2 \sum x_2 \quad (3.12)$$

$$\sum yx_1 = a\sum x_1 + b_1\sum x_1^2 + b_2\sum x_2x_1 (3.13)$$

$$\sum yx_2 = a\sum x_2 + b_1\sum x_1x_2 + b_2\sum x_2^2 (3.14)$$

3.3.4Standard Deviation and Standard Error

In statistics, the standard deviation (SD) is a measure of the amount of variation or dispersion from the mean. A large standard deviation indicates that the data points can spread far from the mean and a small standard deviation indicates that they are clustered closely around the mean.If all the data values are equal, then the standard deviation will be zero. It is also the root mean square deviation of the measurement which is calculated by summing the square of the deviation of each value from the mean, dividing by the number of cases and then taking the square root.

$$SD = \sqrt{\frac{\sum(x_i - \bar{x})^2}{N}} (3.15)$$

Wherex_i is the ith sample, $\bar{x}$, the sample mean and N, the number of scores in the sample. Variance is the square of standard deviation, i.e.,

$$SD^2 = \frac{(x_i - \bar{x})^2}{N} (3.16)$$

Both variance and standard deviation measure variability (Dodge, 2003).

The standard error (SE),also called the standard deviation of the mean of the sampling distribution of a sample is expressed as(Everitt, 2003);

$$SE = \frac{SD}{\sqrt{N}} (3.17)$$

Standard error was used to indicate anomalies in this work.

3.3.5Fast Fourier Transform

Periodic signals in the time domain are made up of many discrete sinusoidal frequency components. The process of obtaining the spectrum of frequencies H(f) comprising a time-dependent signal h(t) is called Fourier Analysis and it is realized by the Fourier Transform (FT).H(f) can be derived from h(t) by employing the Fourier Integral:

$$H(f) = \int_{-\infty}^{\infty} h(t)e^{2\pi ift}dt \quad (3.18)$$

This is the (forward) Fourier Transform (FT). The inverse Fourier Transform (FT^{-1}) is given by the expression;

$$h(t) = \int_{-\infty}^{+\infty} H(f)e^{-2\pi ift}df \quad (3.19)$$

When t is in seconds, f the frequency is in cycles per second or Hertz. Fourier transformation is a linear operation. Thus the transform of the sum of two functions equals the sum of the transforms.

In the most common situations, function h(t) is sampled (i.e., its value is recorded) atevenly spaced intervals in time. IfΔdenote the time interval between consecutive samples, so that the sequence of sampled values is

$$h_n = h(n\Delta), \ n = \ldots., -3, -2, -1, 0, 1, 2, 3, \ldots\ldots \quad (3.20)$$

The reciprocal of the time interval $\Delta$is the sampling rate;if $\Delta$is measuredin seconds, for example, then the sampling rate is the number of samples recorded per second. Assuming we have N consecutive sampled values

$$h_k \equiv h(t_k), \qquad t_k \equiv k\Delta, \qquad k = 0,1,2, \ldots\ldots, N-1 \quad (3.21)$$

makingΔ the sampling interval. With N inputs, it is evident that the numbers of independent outputs will not be more than N. Thus instead of estimating the Fourier transform H(f) at all values of f in the range $-f_c$ to f_c, we can estimate only at the discrete values

$$f_n \equiv \frac{n}{N\Delta}, \qquad n = -\frac{N}{2}, \ldots\ldots\ldots, \frac{N}{2} \quad (3.22)$$

The extreme values of n in equation (3.22) correspond exactly to the lower and upper limits of the Nyquist critical frequency range, making the total counts to reduce to N. Using equations (3.21) and (3.22), equation (3.18) can then be approximated by a discrete sum as;

$$H(f_n) = \int_{-\infty}^{\infty} h(t)e^{2\pi i f_n t}dt \approx \sum_{k=0}^{N-1} h_k e^{2\pi i f_n t_k}\Delta = \Delta \sum_{k=0}^{N-1} h_k e^{2\pi ikn/N} \quad (3.23)$$

The final summation of equation (3.23) called the discrete Fourier transform of the N points denoted by H_n is written as;

$$H_n \equiv \sum_{k=0}^{N-1} h_k e^{2\pi ikn/N} \quad (3.24)$$

Its inverse is written as

$$h_k = \frac{1}{N}\sum_{n=0}^{N-1} H_n e^{-2\pi ik\ /N} \quad (3.25)$$

Cooley and Tukey (1965) showed that a discrete Fourier transform of length N can be rewritten as the sum of two discrete Fourier transforms, each of length N/2, where one is formed from the even-numbered points of the original N and the other from the odd-numbered points, i.e.,

$$F_k = F_k^{even} + W^k F_k^{odd} \quad (3.26)$$

Where $W^k = e^{2\pi i/N}$, is the complex number, and F_k^{even} denotes the k_{th} component of the Fourier transform of length N = 2 formed from the even components of the original f_j's while F_k^{odd} is the corresponding transform of length N = 2 formed from the odd components. K in eq. (3.26) also varies from 0 to N. It is noteworthy that equation (3.26) can be used recursively.

Based on equations (3.24), (3.25) and (3.26), the incident solar radiation and the surface temperature (minimum and maximum) data were subjected to Fast Fourier Transform

(FFT) smoothing. This was done so as to obtain the required information on the general trends of the data.

3.4 Modified-Hay-Model (MHM) Description

Angstrom proposed the correlation between duration of sunshine and insolation as;

$$\frac{\bar{H}}{H_c} = a_1 + (1 - a_1)S = a_1 + b_1 S \quad (3.27)$$

Where, H_c is the perfectly clear day horizontal insolation and S the monthly mean daily fraction of possible sunshine. Sis obtained as;

$$S = \frac{\bar{n}}{\bar{N}_d} \quad (3.28)$$

where $\bar{n}$ is the monthly average number of bright sunshine hours per day as recorded by the instrument, and $\bar{N}_d$ is the average day length.

$$\bar{N}_d = \frac{\omega_s 24}{\pi} \quad (3.29)$$

ω_s, the sunrise hour angle is given by;

$$\omega_s = \cos^{-1}(-\tan\delta \tan\varphi) \quad (3.30)$$

where δ is the declination and $\varphi$the latitude.

a_1 and b_1 are empirical coefficients. Angstrom recommended values of 0.25 and 0.75 respectively for these constants.

Prescott later modified eq. (3.27), basing it on the extraterrestrial radiation, a quantity that can be readily computed;

$$\frac{\bar{H}_e}{\bar{H}_o} = a + b\,\bar{n}/\bar{N} \quad (3.31)$$

Different values of the coefficients a and bhave been obtained for different parts of the world. Such coefficients may be used to compute $\bar{H}$ for nearby locations having similar climatic conditions. Allen (1997) suggested that such coefficients could be used to compute $\bar{H}$ for stations within about 400 km.

The coefficients are generally site dependent as presented in equation (3.31). This is because they are affected by (Iqbal, 1983);

i. Optical properties of the cloud cover,

ii. Ground reflectivity, and

iii. Average air mass above the location.

To make the coefficients site independent requires taking these effects into account as was done by Hay (1979) with data collected in Western Canada.

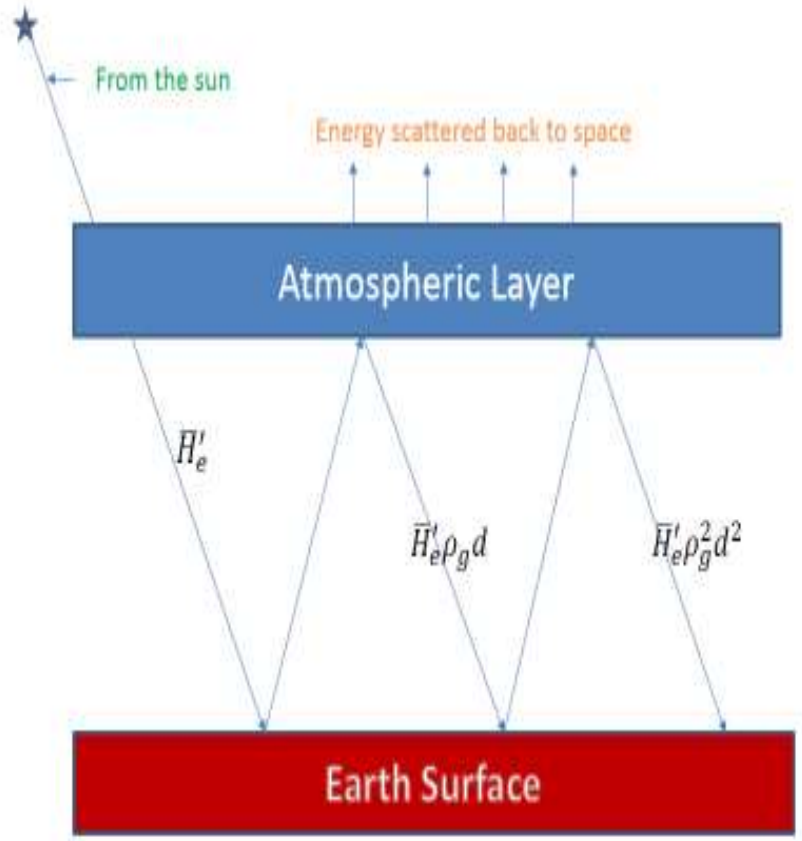

Fig 3.2. A Multiple reflection model between the Earth and the Atmosphere

Fig. (3.2) illustrates the process of multiple reflections between the ground and the atmosphere. The diffuse radiation arriving on the ground surface after the first pass through the atmosphere and direct radiation are in part reflected by the ground. This upwelling radiation is partly reflected back to the ground by the atmosphere. This process continues ad infinitum. These multiple reflections between the ground and the atmosphere add to the diffuse radiation reaching the ground after the first pass through the atmosphere and thus increasing the amount of the global radiation observed at the surface by the measuring instrument (Hay, 1970). Multiple reflection is a function of both surface albedo and the atmospheric back scattering (Moller, 1965).

Expressing the short wave radiation fluxes (before multiple reflection) in terms of the observed radiation fluxes (which includes the effects of multiple reflections);

$$\bar{H}_e = \bar{H}'_e + \bar{H}'_e\rho_g d + \bar{H}'_e\rho_g^2 d^2 + \ldots + \bar{H}'_e\rho_g^n d^n \quad (3.32)$$

This is a geometric progression S_n with 1st term a = 1 and common ratio $r = \rho_g d$

$$\lim_{n\to\infty} S_n = \frac{1}{1-\rho_g d} \quad (3.33)$$

Using eq. (3.33) in eq. (3.32);

$$\bar{H}_e = \frac{\bar{H}'_e}{(1-\rho_g d)} \quad (3.34)$$

$$\bar{H}'_e = \bar{H}_e(1-\rho_g d) \quad (3.35)$$

Where ρ_g is the ground albedo andd is the atmospheric back – scatterance.

The true transmissivity is given by;

$$\frac{\bar{H}'_e}{\bar{H}_o} = \frac{\bar{H}_e(1-\rho_g d)}{\bar{H}_o} \quad (3.36)$$

The atmospheric back–scatterance dis expressed in terms of the cloudless clear sky albedo ρ_a and cloud base albedo ρ_c, weighted by the proportion of the sky hemisphere which is clear $\left(1-\bar{n}/\bar{N}\right)$ and covered by cloud $\left(\bar{n}/\bar{N}\right)$ respectively.

Substituting for d in eq. (3.35);

$$\bar{H}_e' = \bar{H}_e\left[1-\rho_g\left(\frac{\bar{n}}{\bar{N}}\rho_a+\left(1-\frac{\bar{n}}{\bar{N}}\right)\rho_c\right)\right] \quad (3.37)$$

From equations (3.31), (3.36) and (3.37);

$$\frac{\bar{H}_e}{\bar{H}_o} = \frac{a+b\left(\frac{\bar{n}}{\bar{N}}\right)}{1-\rho_g\left[\rho_a\left(\frac{\bar{n}}{\bar{N}}\right)+\rho_c\left(1-\frac{\bar{n}}{\bar{N}}\right)\right]} \quad (3.38)$$

Hay (1979) assumed a constant clear sky albedo ρ_a= 0.25 and cloud base albedo ρ_c=0.6 to obtain his model as;

$$\frac{\bar{H}_e}{\bar{H}_o} = \frac{0.157 \quad .5566\left(\frac{\bar{n}}{\bar{N}_m}\right)}{1-\rho_g\left[\rho_a\left(\frac{\bar{n}}{\bar{N}_m}\right)+\rho_c\left(1-\frac{\bar{n}}{\bar{N}_m}\right)\right]} \quad (3.39).$$

where $\bar{N}_m$ is the modified day – length for a solar zenith angle θ_z greater than 85° given by;

$$\bar{N}_m = \frac{1}{7.5}\cos^{-1}\left(\frac{\cos 85-\sin\varphi\sin\delta_c}{\cos\varphi\cos\delta_c}\right) \quad (3.40)$$

Where δ_c (degree) is the characteristic declination, i.e. the declination at which the extraterrestrial irradiation is equivalent to its monthly average value.

As noted by Iqbal (1983), the constant value of clear sky albedo ρ_a (0.25) assumed by Hay (1979) in obtaining his coefficients (therefore, model) is too high compared to values obtained for some locations around the world which varies from 0.07 to 0.15. Using the value of 0.25 will therefore have an effect on the empirical coefficients a and bof his

model. Also the retention of $\overline{N}_m$as part of the model equation has a negative impact on the model results.

3.4.1 Determination of the clear sky albedoρ_a

The albedo of the atmosphere $\rho_a$is the diffuse component of incident radiation which is reflected back to space. This consists of the albedo of the Rayleigh atmosphere and that of aerosols (the first and second terms respectively on the right hand side of equation (3.41) and is given by Iqbal (1983) as;

$$\rho_a = \tau_{ma}[0.5(1-\tau_r)\tau_a + (1-F_c)\omega_o(1-\tau_a)\tau_r] \quad (3.41)$$

Where τ_{ma} is the total transmittance due to molecular absorbers given by eq. (3.46);
τ_r is the transmittance by Rayleigh scattering given by;

$$\tau_r = e^{-0.0903 \ \ {}^{0.84}_{a}(1+m_a-m_a^{1.01})} \quad (3.42)$$

τ_a is the aerosol transmittance given by;

$$\tau_a = \exp[-k_a^{0.873}(1+k_a-k_a^{0.7808})m_a^{0.9108}] \quad (3.43)$$

$$k_a = 0.2758k_{a_{\lambda=0.38\mu m}} + 0.35k_{a_{\lambda=0.5\mu m}} \quad (3.44)$$

is the aerosol optical thickness and λ (μm) is the wavelength.
F_c is the is the ratio of the energy scattered in the forward direction to the total energy scattered called the forward scatterance usually taken as 0.84 ($1-F_c$ is the backscatterance) andω_o is the single scattering albedo, that is the ratio of energy scattered by aerosols to total attenuation under the first impingement by direct radiation. This is usually taken as 0.9 for rural areas and 0.6 for urban industrial areas.

$$m_a = m_r\left(\frac{P}{1013.25}\right) \quad (3.45)$$

is air mass at actual pressure.

m_r is the air mass at standard pressure and P is the local air pressure.

$\tau_{ma} = \tau_o \tau_g \tau_w$(3.46)

Where τ_o, τ_g and τ_w are ozone, gas and water scaterring-transmittances respectively. They are given by;

$$\tau_o = 1 - [0.1611U_3(1 + 139.48U_3)^{-0.3035} - 0.002715U_3(1 + 0.044U_3 + 0.0003U_3^2)^{-1}]$$

(3.47)

$\tau_g = e^{-0.0127 m_a^{0.26}}$(3.48)

$\tau_w = 1 - 2.4959U_1[(1 + 79.034U_1)^{0.6828} + 6.385U_1]^{-1}$(3.49)

U_3 (cm) is the ozone's relative optical-path length under the normal temperature and surface pressure (NTP) given as

$U_3 = k_{oz} m_r$(3.50)

Where k_{oz} (cm) is the vertical ozone-layer thickness.

U_1 (cm) is the pressure-corrected relative optical-path length of precipitable water given by;

$U_1 = w m_r$(3.51)

Where w (cm) is the precipitable water-vapour thickness reduced to the standard pressure (1013.25 mbar) and at the temperature T of 273 K. w is obtained with the precipitable water-vapour thickness under the actual condition w'(cm) by;

$w = w' \left(\frac{p}{1013.25}\right)^{\frac{3}{4}} \left(\frac{273}{T}\right)^{\frac{1}{2}}$(3.52)

Putting the values of the different constants in equation (3.41) gives;

$$\rho_a = 0.0685 + 0.16(1 - \tau_a)\omega_o \quad (3.53)$$

The 1st and 2nd terms in eq. (3.53) are the Rayleigh atmosphere and aerosol transmittances respectively. The clear sky albedo ρ_a for the locations were calculated using equation (3.53). the values of theρ_a so obtained were used in eq. (3.38) along with other constants and variables to obtain the empirical model termed the Modified-Hay-Model (MHM);

$$\frac{\bar{H}_e}{\bar{H}_o} = \frac{0.262+0.615\left(\frac{\bar{n}}{\bar{N}}\right)}{1-\rho_g\left[\rho_a\left(\frac{\bar{n}}{\bar{N}}\right)+\rho_c\left(1-\frac{\bar{n}}{\bar{N}}\right)\right]} (3.54)$$

3.5 Performance Indicators

The calculated values of H_e are compared with the measured data utilizing statistical methods. The Pearson correlation coefficient (r) between the observed and estimated values was obtained. The prediction capability of the model was analyzed by determining the Mean Bias Error (MBE) and Root Mean Square Error (RMSE) defined respectively (Iqbal, 1983) as;

$$\text{MBE} = \sum_{i=1}^{n} \frac{\bar{H}_i(\text{Predicted} - \text{O} \quad)}{n} (3.55)$$

$$\text{RMSE} = \sum_{i=1}^{n} \frac{\bar{H}_i(\text{Observed} - \text{Predicted})^2}{n} (3.56)$$

Where $\bar{H}_{i(\text{predicted})}$ and $\bar{H}_{i(\text{observed})}$ is respectively, the i_{th} predicted and observed value and n the number of observations

$$r = \frac{\sum_{n=1}^{n}(x_i - \bar{x})(y_i - \bar{y})}{\sqrt{\sum_{n=1}^{n}(x_i - \bar{x})^2 \sum_{n=1}^{n}(y_i - \bar{y})^2}} (3.57)$$

where $\bar{x}$ is the mean of the x values, $\bar{y}$ is the mean of the y values, x_i is the i_{th} value of the x variable and y_i the i_{th} value of the y variable.

The RMSE allows a term by term comparison of the actual deviation between the calculated value and the measured value and therefore provides information on the short-term performance of the model. It is always positive; however a zero value is ideal. On the other hand, the test on MBE provides information on the long-term performance of the model. A positive MBE value gives the average amount of overestimation in the calculated values and vice versa. In general, a low MBE is desirable (El-Sebaii and Trabea, 2005).

CHAPTER FOUR

RESULTS AND DISCUSSION

4.1. Spatial Distribution of global solar radiation

4.1.1.The Daily Frequency of occurrence

The eleven locations were grouped into the four main climatic zones of Nigeria namely Mangrove Swamp, Tropical Rain Forest, Guinea Savannah and Sudan/Sahel Savannah.Also, the daily global solar irradiance was grouped into seven classes using interval of 5. The classes are (in MJm^{-2}/day) 0.0-5.0, 5.0-10.0, 10.0-15.0, 15.0-20.0, 25.0-25.0, 25.0-30.0 and 30.0-35.0.

The frequency of occurrence of global solar irradiance in percentageover the four climatic zones are presented in Figs. 4.1. to 4.4.

For the Mangrove Swamp and the Tropical regions, the daily global irradiance is fairly even in distribution with peaks at the interval of 15-20 MJ/m^2/day. On the average, 37.11% of the total number of days over 22 years (8044 days) have total irradiation within the range of 15-20 MJ/m^2/day for theMangrove Swamp region. Within this modal group, Port Harcourt has the highest frequency of 40.49% while Calabar has the lowest 30.54% number of days falling within the irradiation interval. The low frequency observed for Calabar within this interval is compensated for in other irradiation intervals like 20-25 MJ/m^2/day and 5-10 MJ/m^2/day.For the tropical rain forest region which has an average of 48.18% of the total number of days receiving total irradiation within this range (15-20 MJ/m^2/day), Benin City has the highest frequency of 49.87% and Ibadan has the lowest frequency of 47.24%. It isnoteworthy that within this modal group, Ibadan has the highest frequency of 30.03% and Benin City the lowest frequency of 21.95% of the total number of days in the interval 20-25 MJ/m^2/day. The frequency distribution shows that the occurrence of irradiationat the intervals of 0-5 MJ/m^2/day, 5-10 MJ/m^2/day and 10-15 MJ/m^2/day respectively for the mangrove swamp region is generally higherthan that of the tropical rain forest, whereas the reverse is the case at the intervals 20-25 MJ/m^2/day and 25-30 MJ/m^2/day respectively. For these two climatic regions, no irradiance data is observed within the radiation data interval 30-35MJ/m^2/day.

Over the Guinea savannah and Sahel savannah regions, the frequency of occurrence showed an average of total irradiation of 46.89% and 49.59% respectively and which now peaked at 20-25 MJ/m^2/day modal interval. Abuja has the higher frequency of 52.17% in the Guinea Savannah and Kano has 53.14% in the Sudan/Sahel Savannah regions respectively. The lower frequency of occurrence for Ilorin within this modal distribution range is compensated for in the 15-20MJ/m^2/day interval. Sokoto which has the lowest frequency of 46.06% in the Sudan/Sahel Savannah region is seen to enjoy the highest frequency in the 25-30MJ/m^2/day irradiation interval. The irradiance data within the interval 30-35MJ/m^2/day is observed only for the Sudan/Sahel Savannah region, notably over Kano and Sokoto. Kano and Sokoto also posted the highest frequencies of the irradiance interval of 25-30MJ/m^2/day.

From Figs 4.1–4.4., it is seen that amount of global irradiance received on the surface has a zonalsymmetry, increasing in the northward direction. This is as a result of decreasing cloudiness in the northward direction (Persson, 1999).

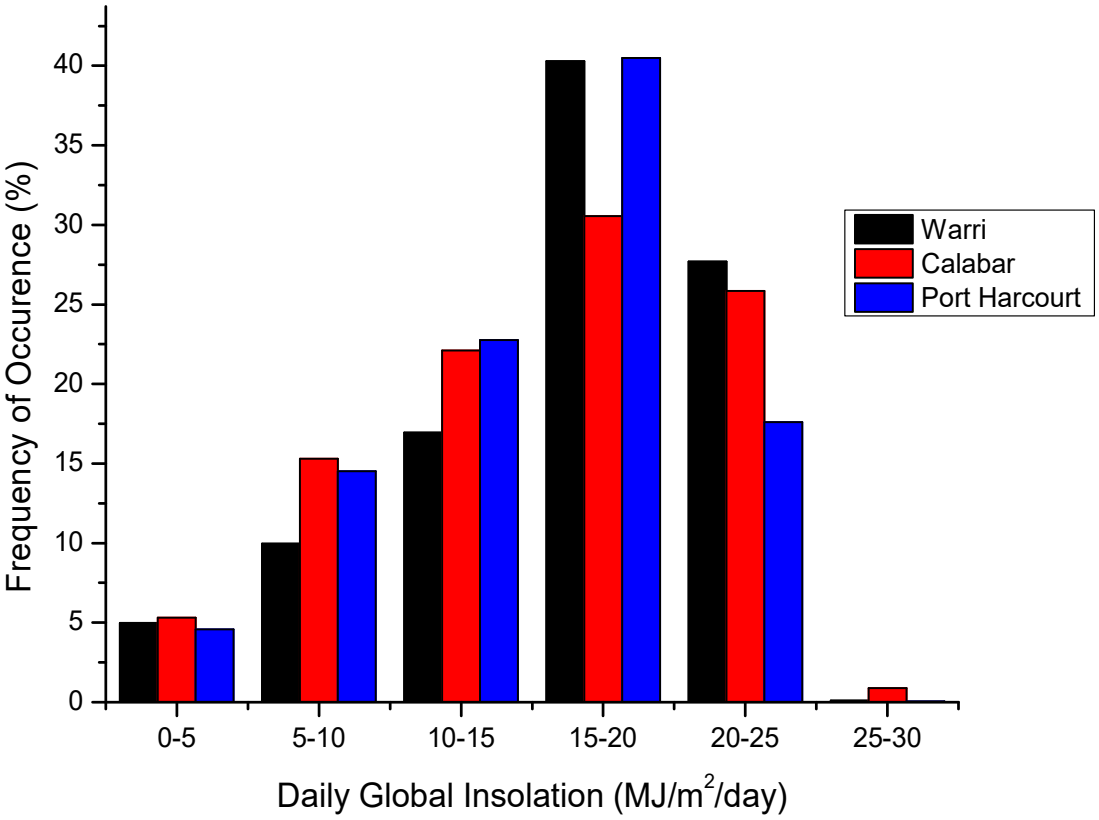

Fig. 4.1: Percentage Frequency Distribution of Daily Global Solar Irradiance over the Mangrove Swampregion

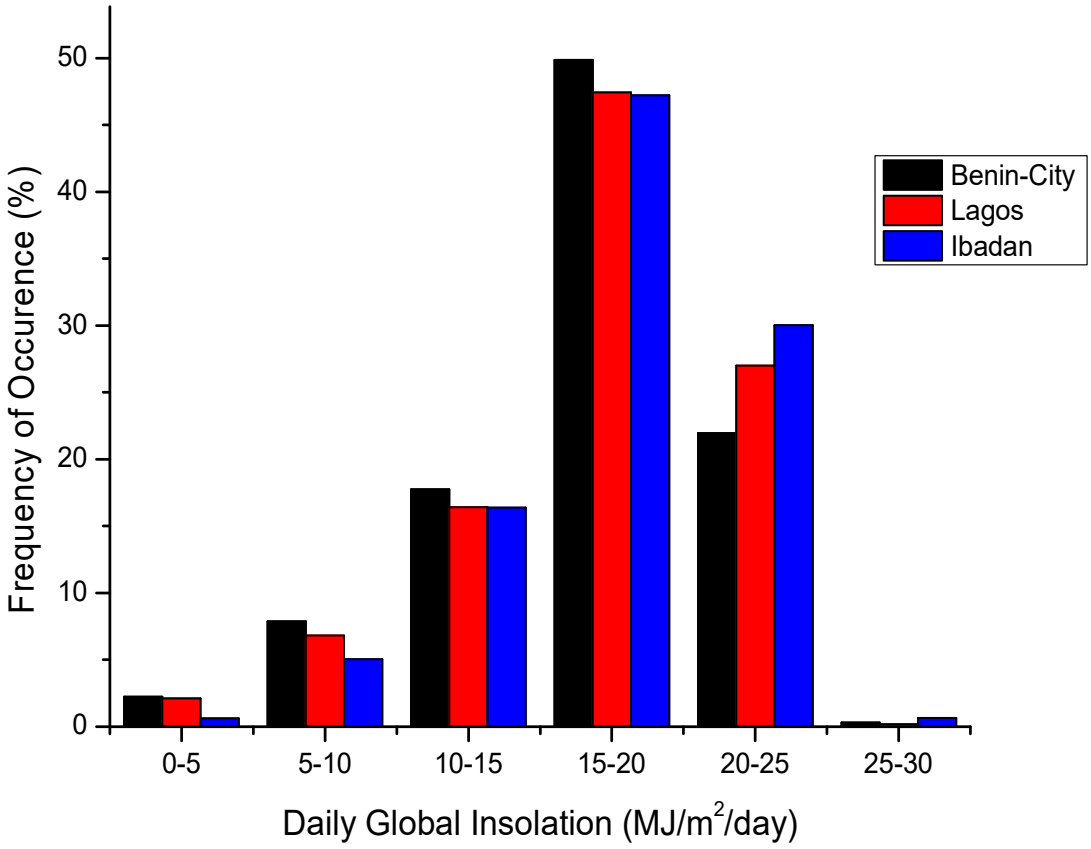

Fig. 4.2: Percentage Frequency Distribution of Daily Global Solar Irradiance over the Tropical RainForest region

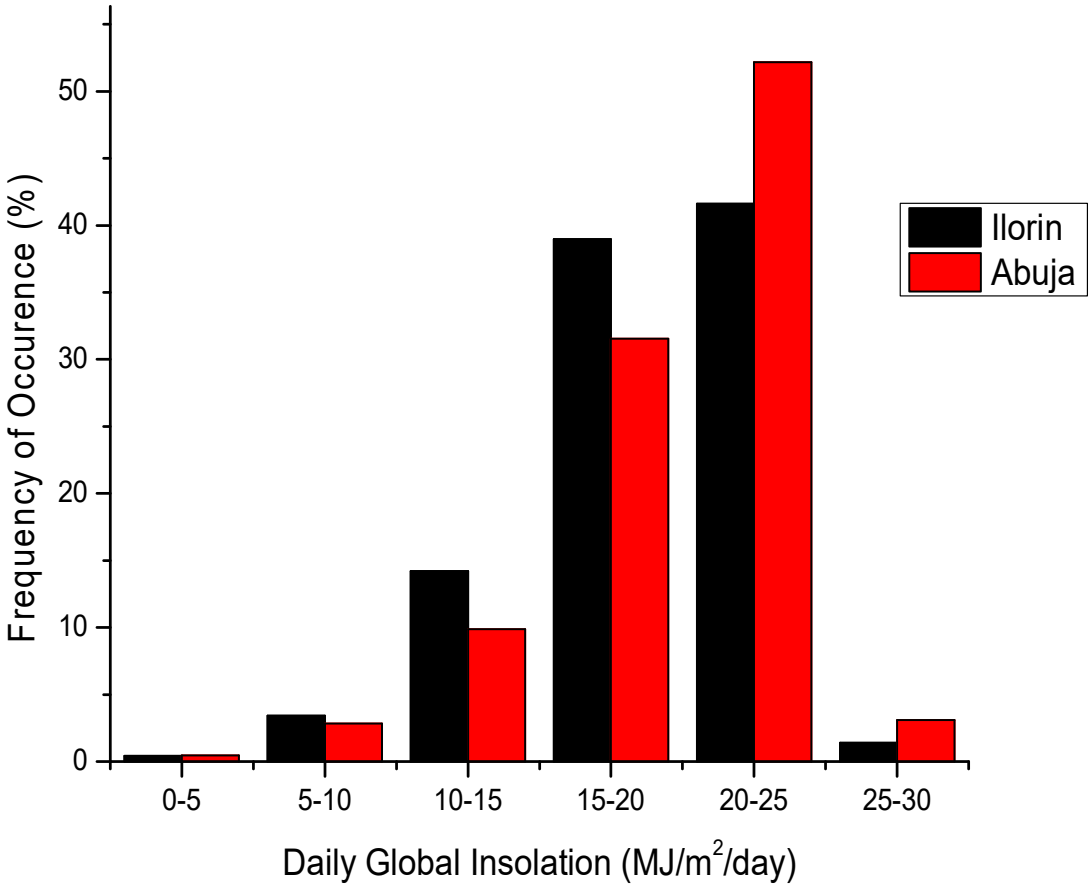

Fig. 4.3: Percentage Frequency Distribution of Daily Global Solar Irradiance over the Guinea Savannah region

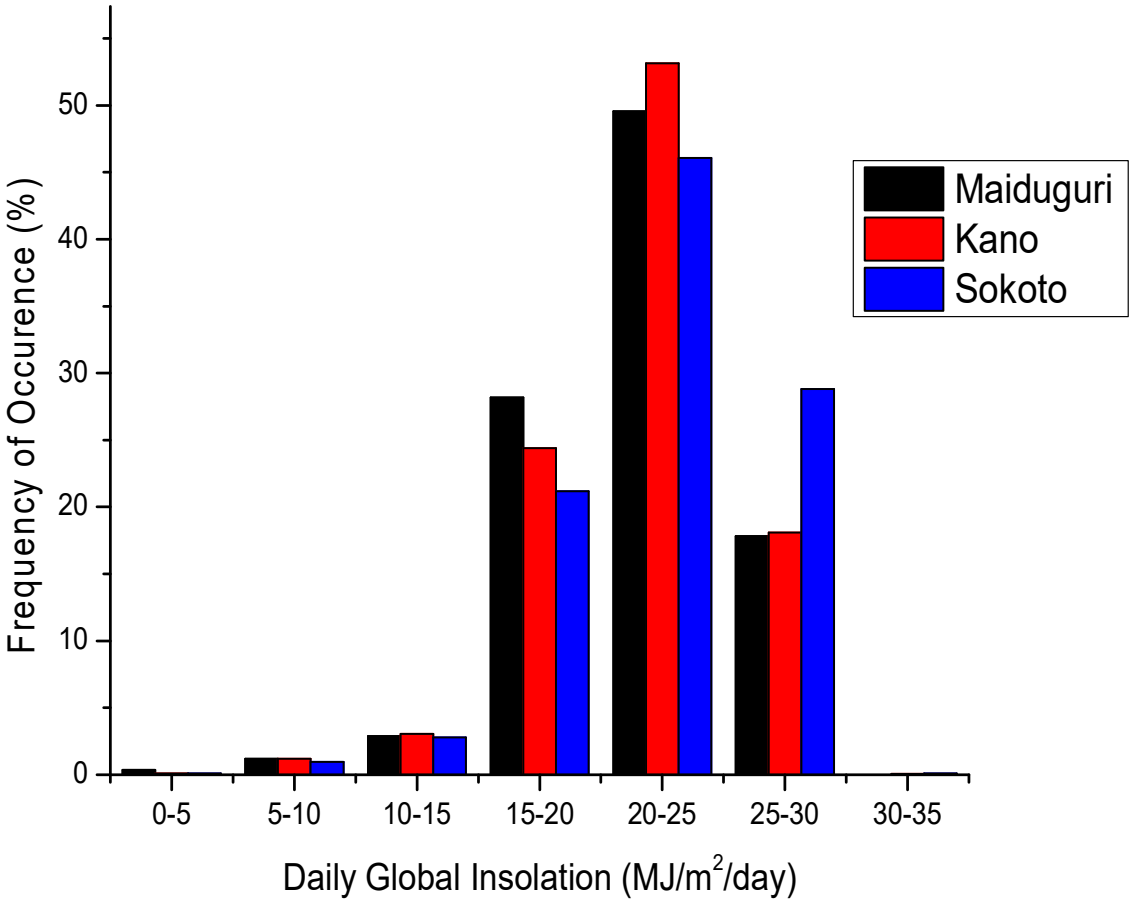

Fig. 4.4: Percentage Frequency Distribution of Daily Global Solar Irradiance over the Sudan/Sahel Savannah region

4.1.2. The Solar Radiation Maps

In Figs 4.5 - 4.7, plots of the extraterrestrial radiation, transmissivity and global radiation are respectively presented as a function of time (months) and the latitude over the locations. From Fig 4.5, it is obvious that solar movement dictates the amount of the extraterrestrial radiation available over a location at a particular time of the year. This is evident from the contour lines. Between the December solstice and March equinox, the value of extraterrestrial radiation over the locations reduces with increasing latitudewhile it increases with latitude between June solstice and September equinox.Atmospheric transmissivity from Fig 4.6 also displayed a latitudinal and time depedence. It displayed a generalincrease with latitude over the entire region. The value of transmissity over the region of investigationranged between a minimum of 0.36 in Julyanda maximum of 0.66 in February,while averageddaily global irradiance varied between a maximum of 24.5MJ/m^2/day in March and a minimum of 13.0 MJ/m^2/day in July.

The contour maps of the 22-year mean annualtotal extraterrestrial radiation, atmospheric transmissivity and global radiation over Nigeria are presented in Figs 4.8, 4.9 and 4.10 respectively. The mean yearly total extraterrestrial radiation varied between a maximum of 13,110 MJ/m^2/year (35.92 MJ/m^2/day) in Port Harcourt and a minimum of 12,850 MJ/m^2/year(35.21 MJ/m^2/day) in Sokoto. Atmospheric transmissivity also demonstrated a spatial variation with maximum of 230 (0.63) over Sokoto in the north and a minimum of 155 (0.42) in Calabar and Port Harcourt, the two southernmost stations. Thereis a zonal symmetry in the spatial distribution of incident global radiation with an increase in the northward direction. Sokoto, the nothernmost station, has the maximum receipt of 8,150 MJ/m^2/year (22.33 MJ/m^2/day), while Port Harcourt, the southernmost station has the minimum of 5,550 MJ/m^2/year (15.21 MJ/m^2/day). Comparing the spatial distributions of extraterrestrial radiation, atmospheric transmissivity and global radiation over the locations, it is evident that cloudiness is the major determinant factor of incident solar radiation over the region.

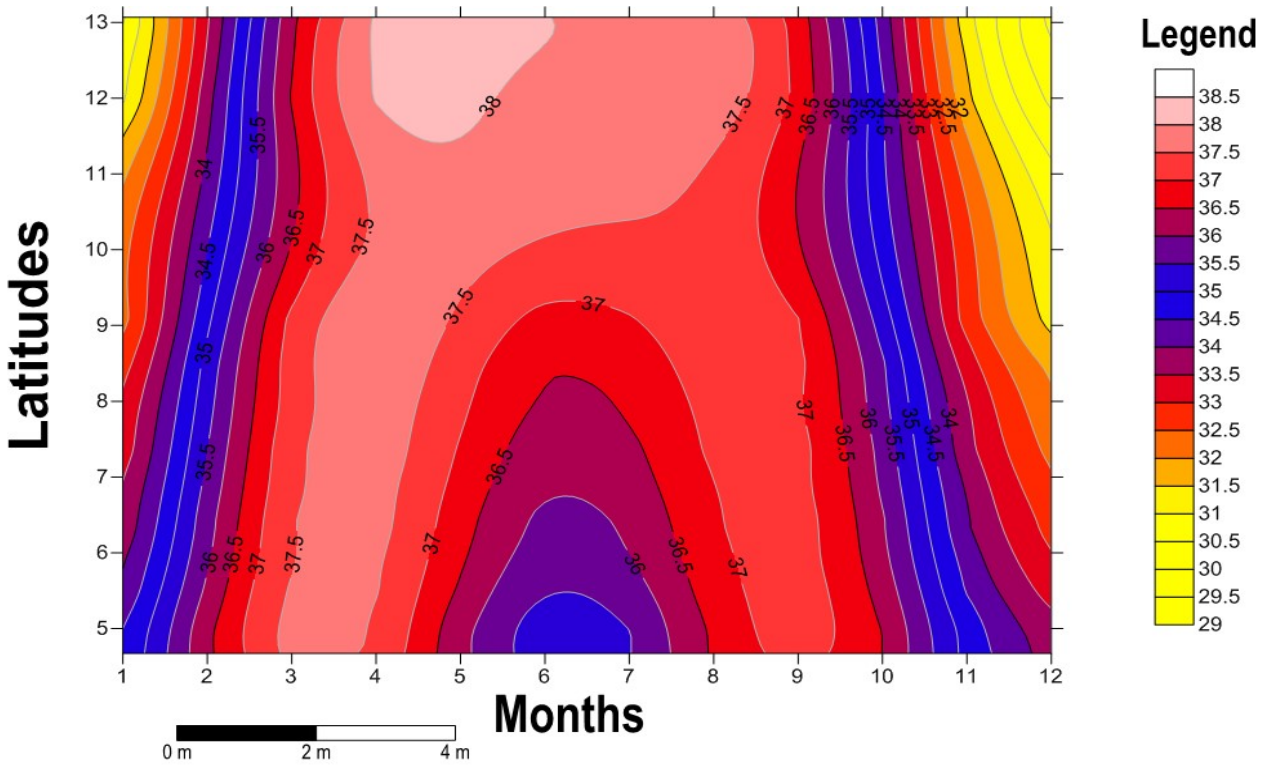

Fig. 4.5:Mean monthly daily variation of extraterrestrial solar radiationH_o over the region

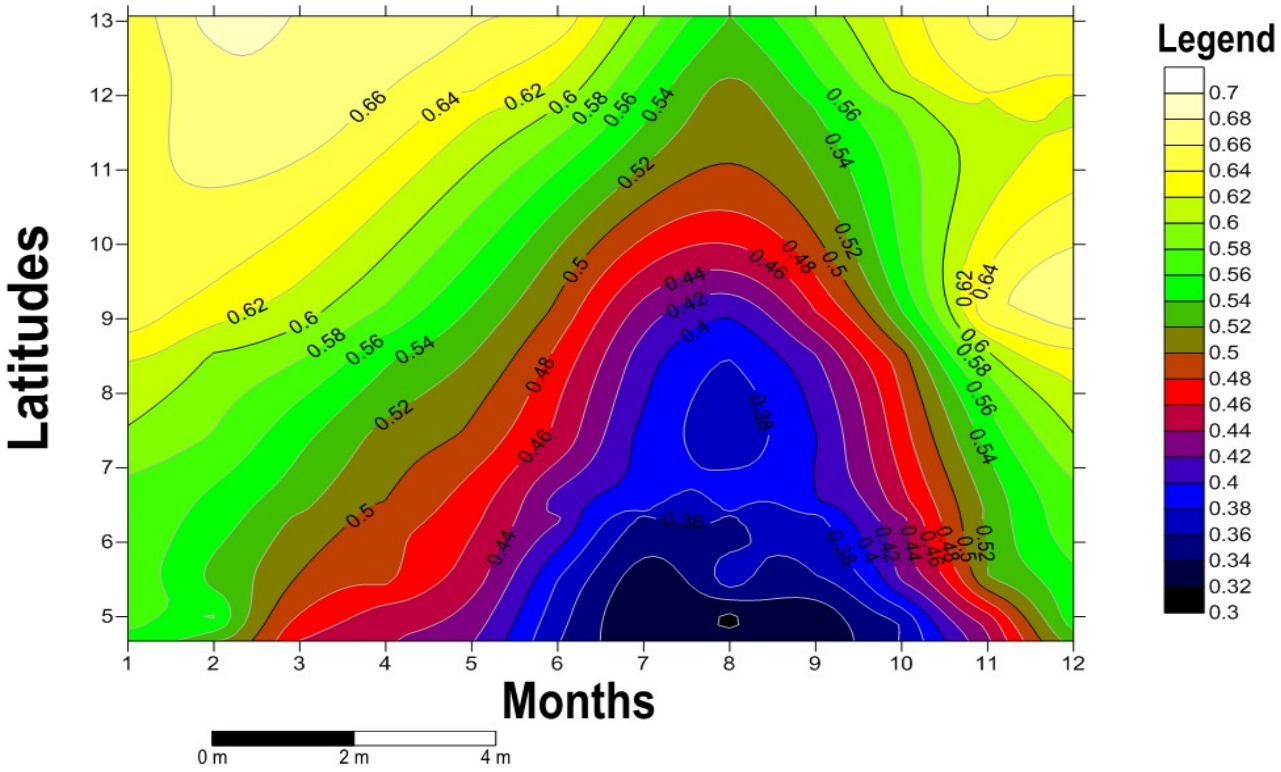

Fig. 4.6:Mean monthly dailyvariation of Transmissivitty over the region

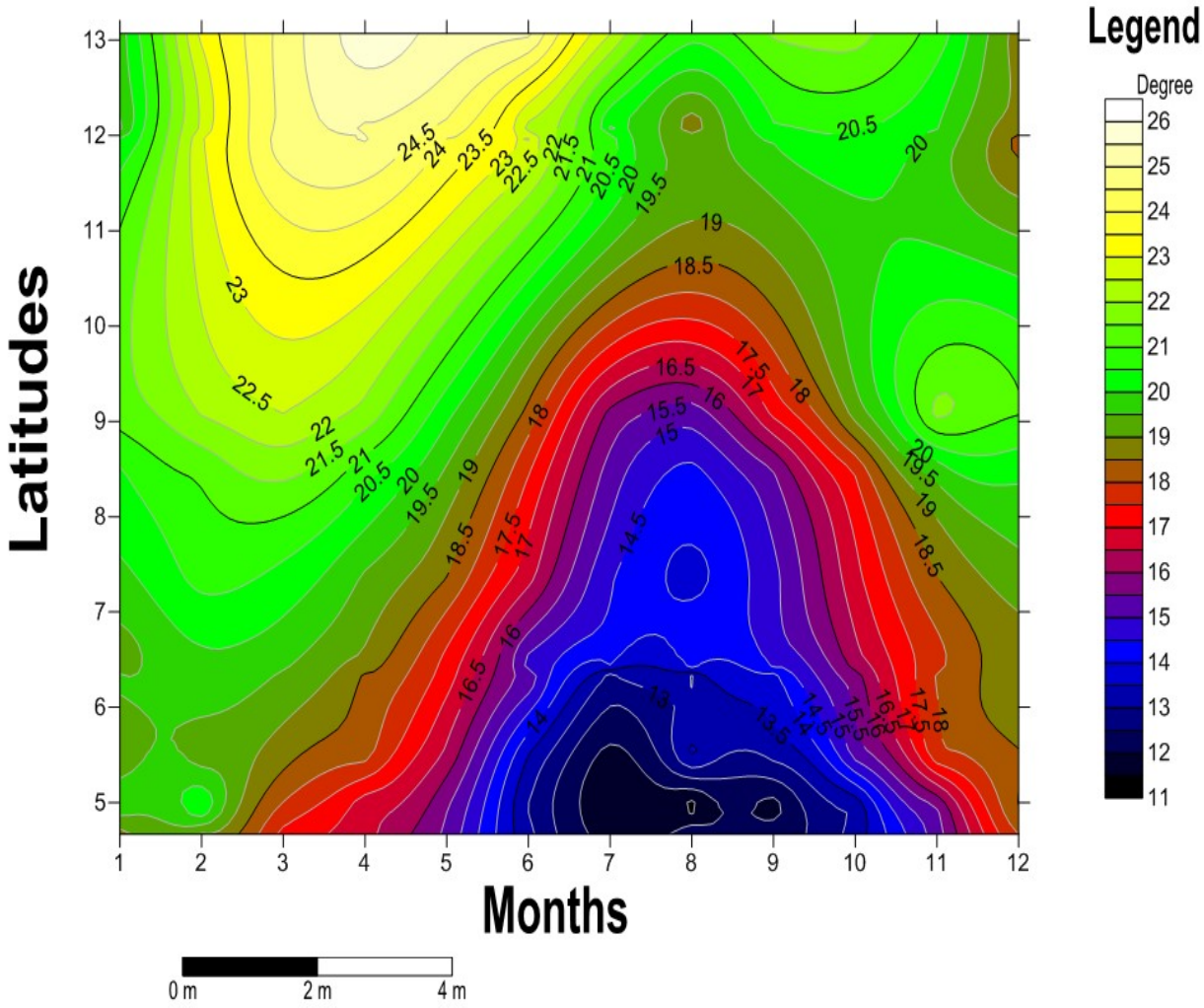

Fig. 4.7:Mean monthly daily variation of global solar radiation H_e over the region

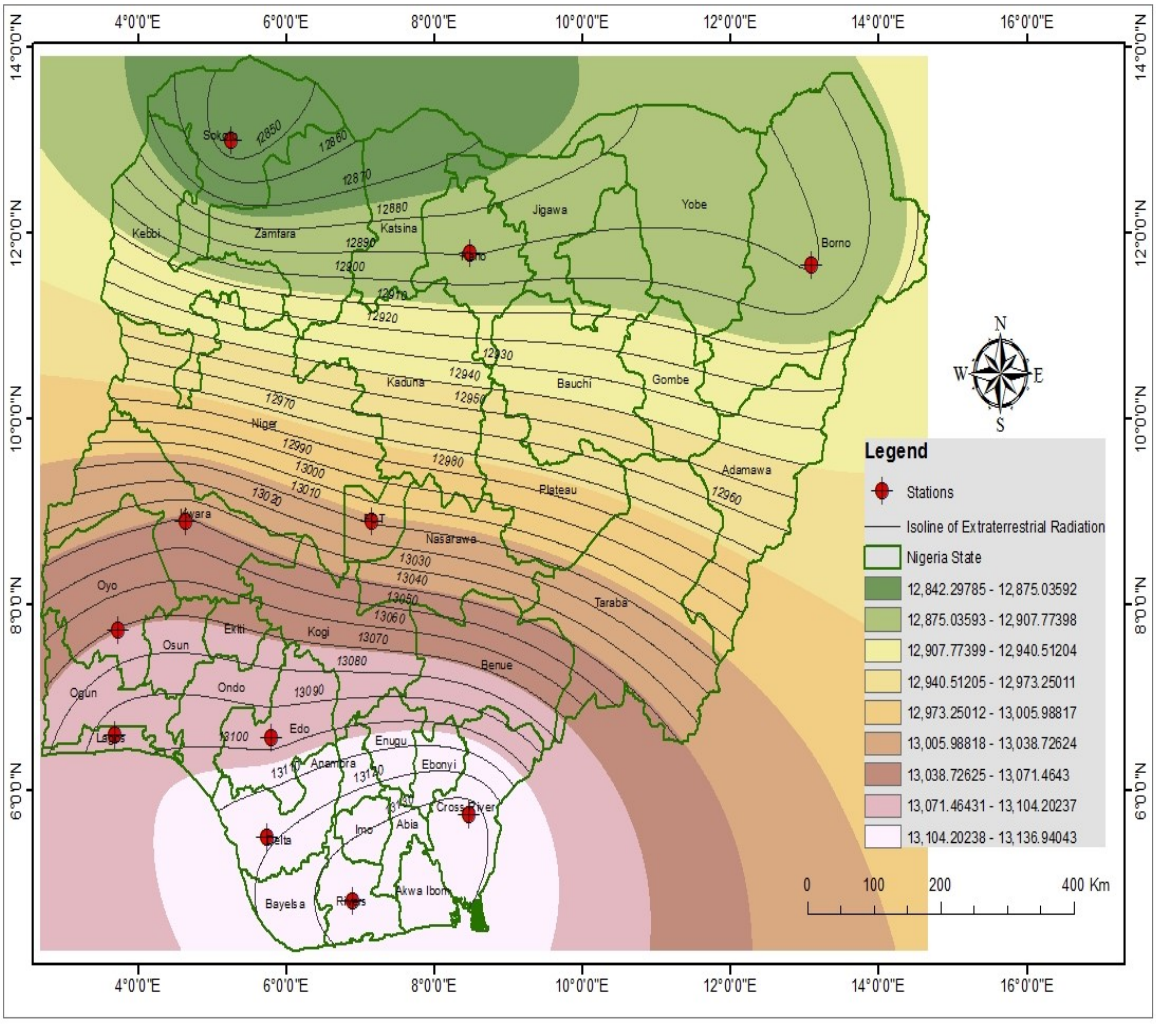

Fig. 4.8:Contour Map of mean annual Extraterrestrial Radiation over Nigeria over 22 years

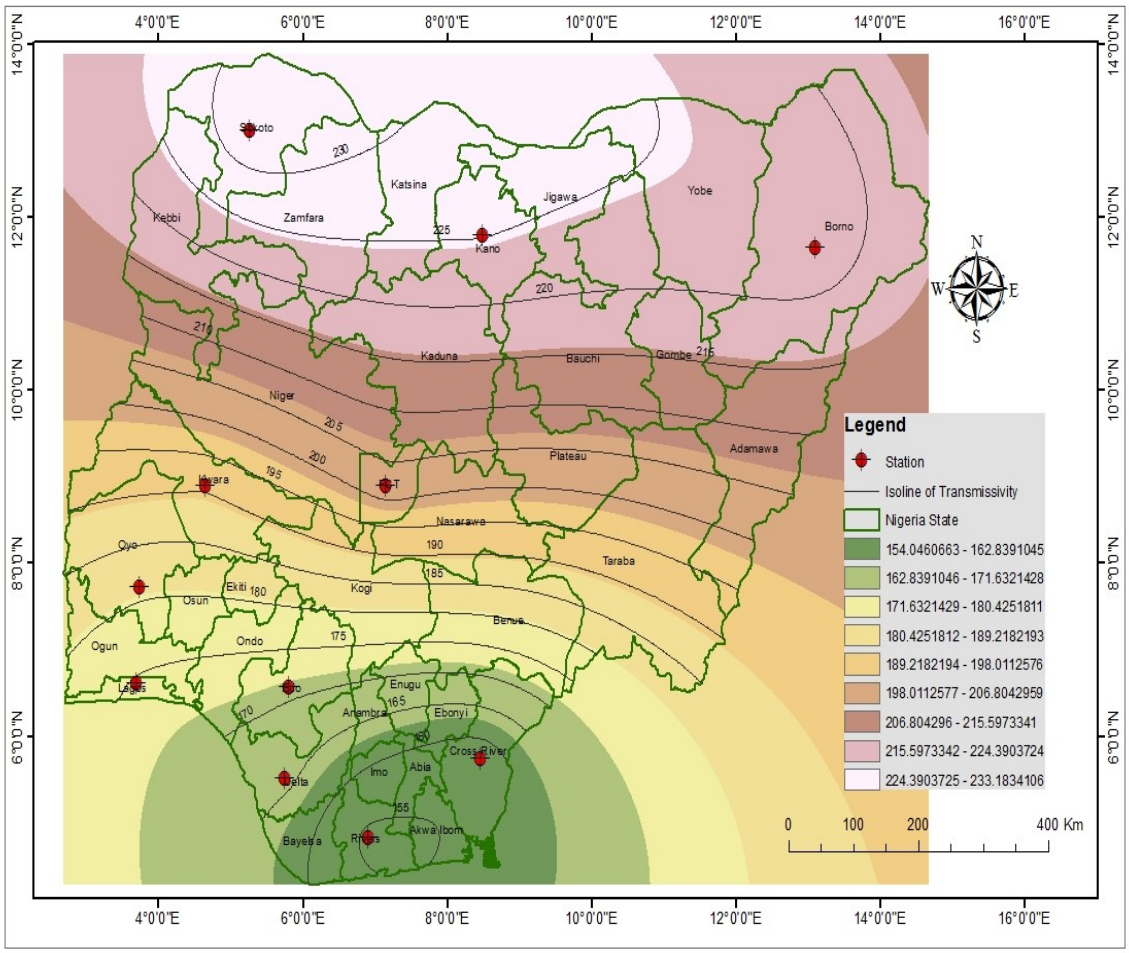

Fig. 4.9:Contour Map of meanannual Atmospheric Transmissivity over Nigeria in 22 years

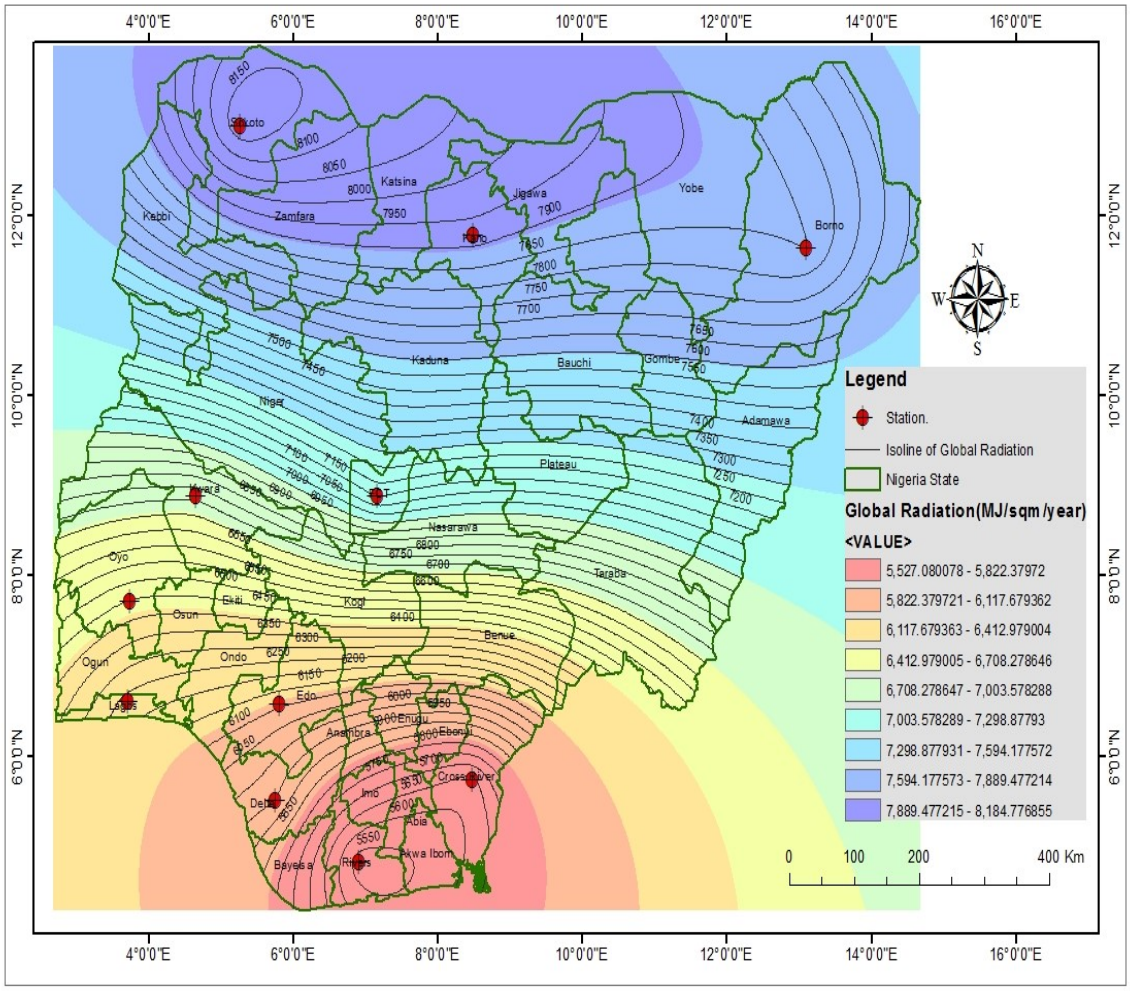

Fig. 4.10:Contour map of the meanannual global solar irradiance over 22 years

4.2Time Series Analysis

In order to have a good understanding of the temporal trends of the incident solar radiation over the nine locations, annual means were aggregated from the daily values. These yearly values were then plotted sequentially against time for each station. For each station, the regression line was found as well as the fast Fourier transform (FFT) drawn to indicate the trend. From Figs 4.11 to Figs 4:21, a dip in the amount of incident global radiation was noted over all the stations between 1984 and 1995 after which there occurred a recovery. The noted decline over some of the stations like Ibadan, Abuja and Ilorin continued till about 1999.From Figs 4:22 to 4:32, there was a generally downward trend in the value of the atmospheric transmissivitysignifying an increase in cloudiness and atmospheric turbidity.This resulted in attenuation in the passage of global radiation to the surface.Persson (1999), observed a similar increase in the incident global solar radiation trend over some locations in Sweden during the years 1983-1996. This he adduced to a decrease in mean annual total cloudiness.

Another factor which could have been responsible is the dust laden North-East trade wind blowing from the Saharadesert. Any increase in the quantity of the dust in the wind results in an increase in the atmospheric turbidity. Atmospheric transmissivity is an expression of the combination of the effects of cloudiness and atmospheric turbidity. This, from Figs 4:22 to 4.32, showed a generally downward trend over the entire region during the period 1984-2005. And this naturally explains the general decreasing trend of solar radiation receipt at the surface over the region during the period. However, Falodun and Ogolo(2007), in a study of the diurnal and seasonal variation of solar radiation carried out in Akure observed that incident solar radiation is more affected by clouds than by the hazy conditions of the harmattan dust spells. Thus the generally observed decrease in the passage of global radiation to the surface can be adduced more to an increase the atmospheric cloudiness over the entire region during the years of investigation rather than to the atmospheric turbidity alone.

Table 4.2 shows the summary of the linear equations for the trendswhile table 4.3 shows the percentage change in the values of the quantities over 22-years and 10-years respectively.

(a)

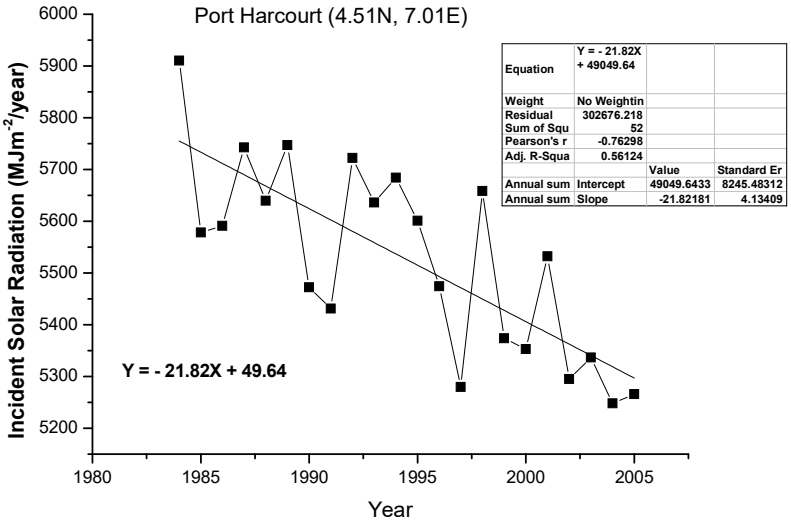

(b)

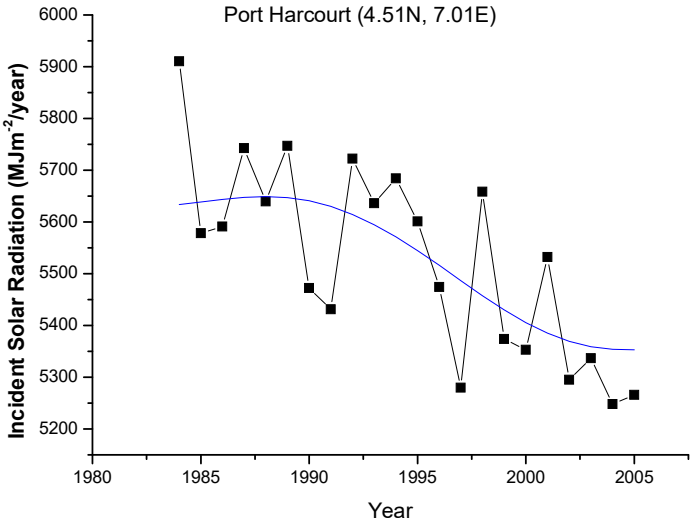

Fig 4.11 (a):Time series and Linear trend of annual mean of global solar radiation(Port Harcourt)

(b)Fast Fourier Transform smoothing of the Time series of global Solar Radiation.

(a)

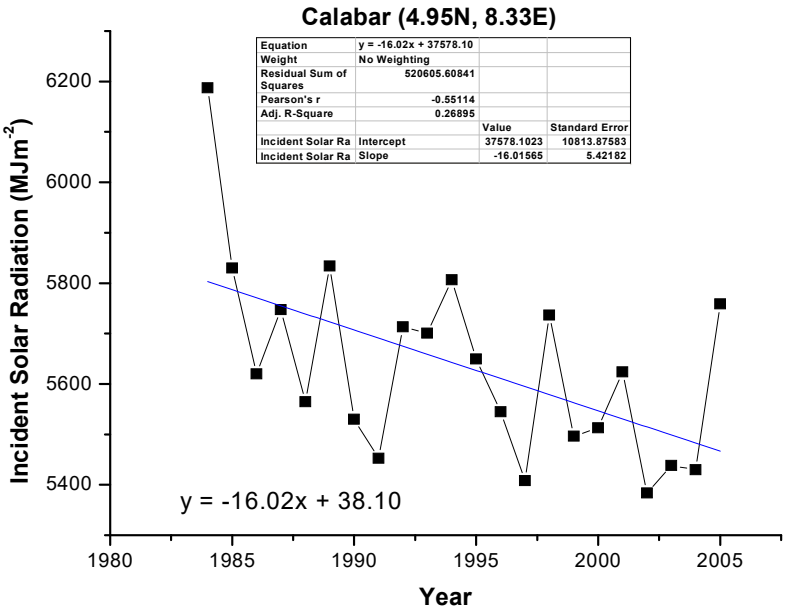

(b)

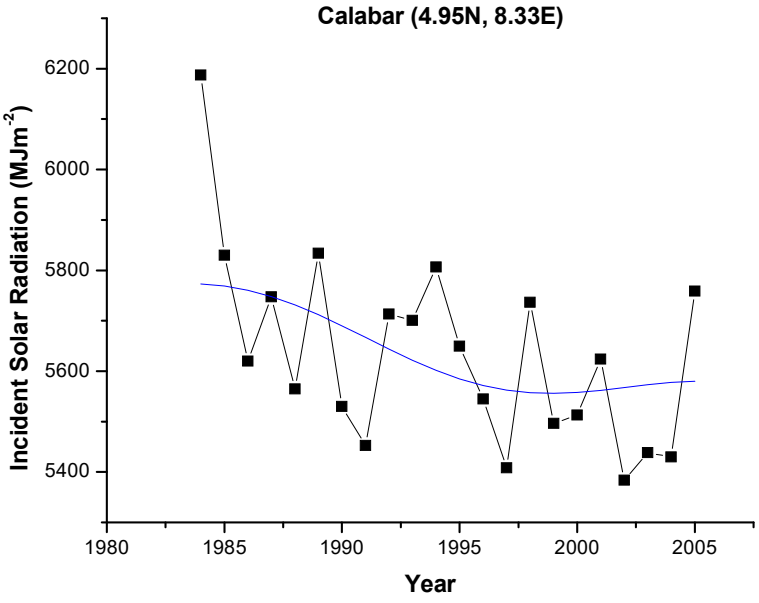

Fig 4.12 (a)**:** Time series and Linear trend of annual mean of global solar radiation (Calabar)

(b)Fast Fourier Transform smoothing of the Time series of global Solar Radiation.

(a)

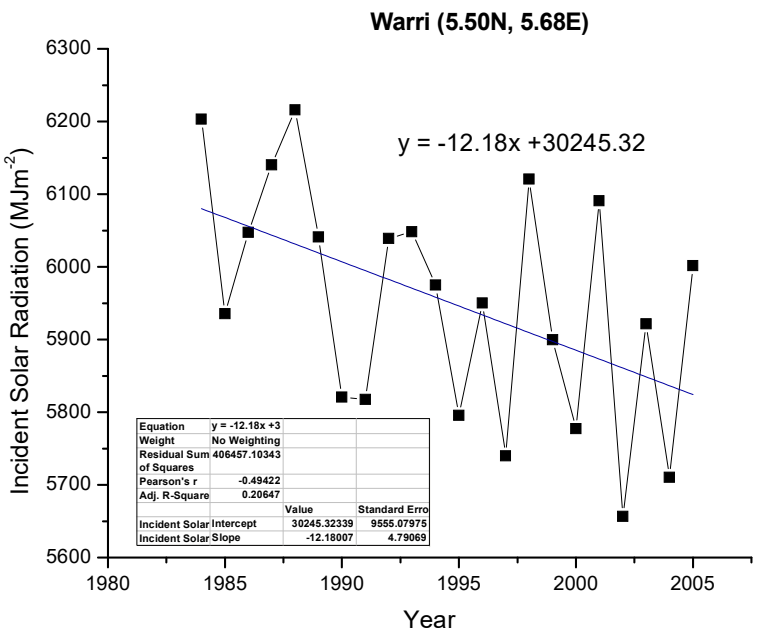

(b)

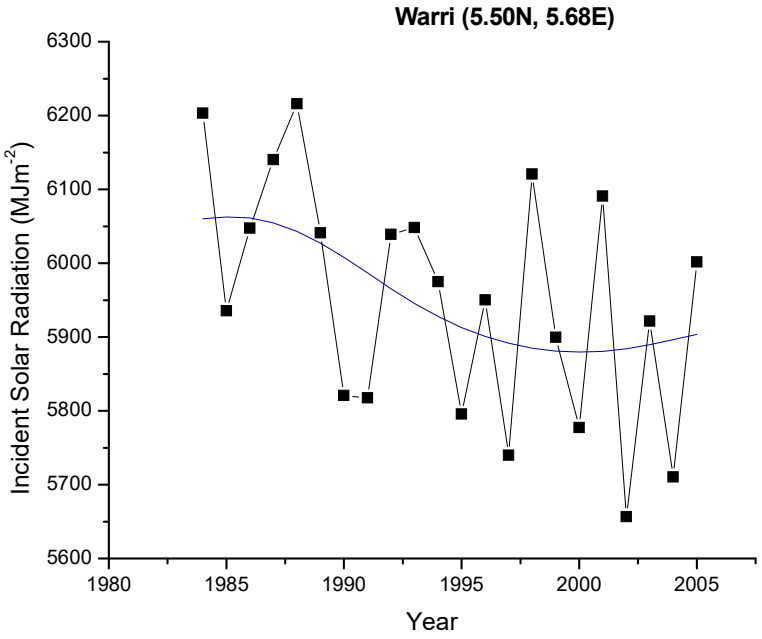

Fig 4.13: (a)Time series and Linear trend of annual mean of global solar radiation (Warri)

(b) Fast Fourier Transform smoothing of the Time series of global Solar Radiation.

(a)

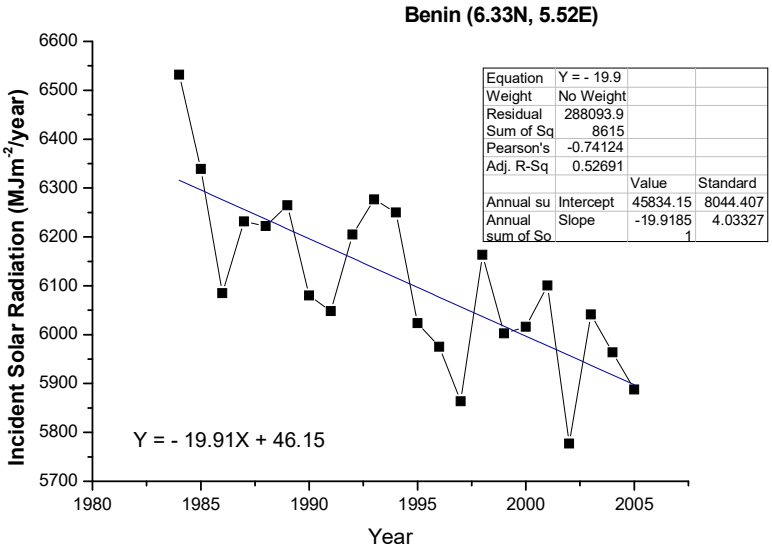

(b)

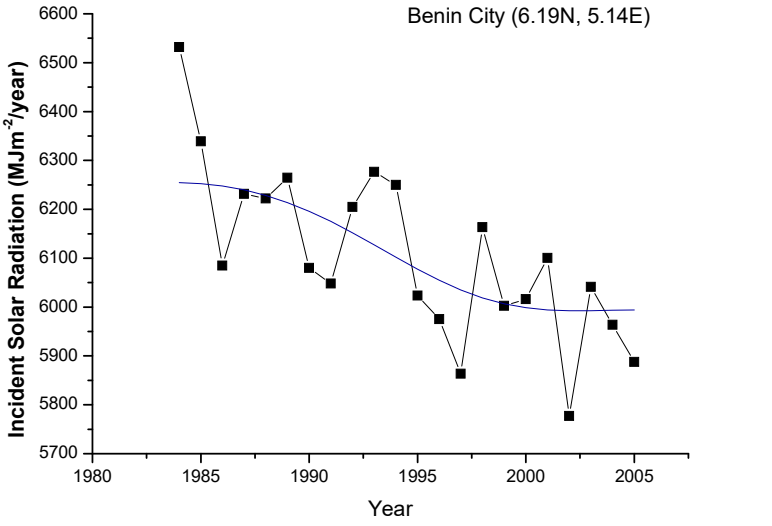

Fig 4.14**:** (a)Time series and Linear trend of annual mean of global solar radiation(Benin City)

(b)Fast Fourier Transform smoothing of the Time series of global Solar Radiation

(a)

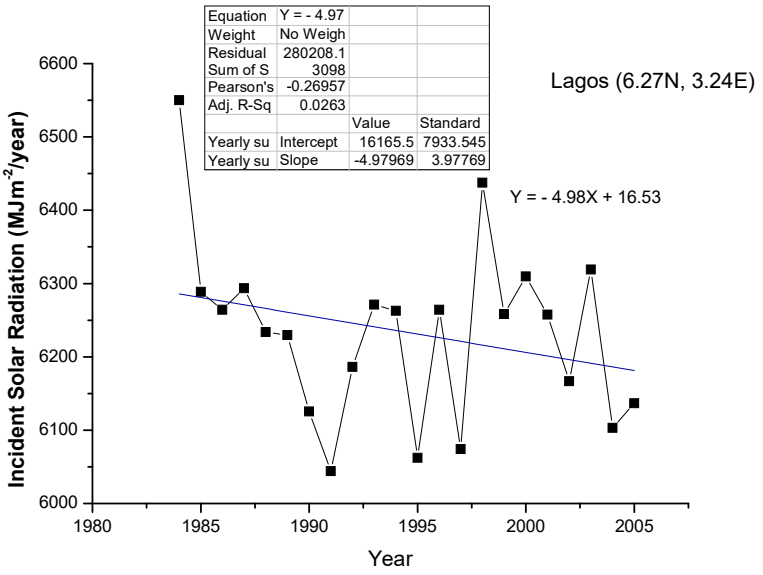

(b)

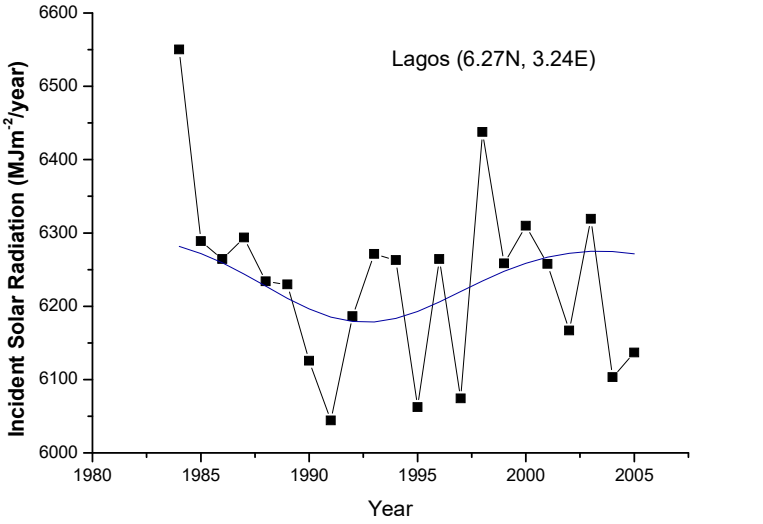

Fig 4.15: (a) Time series and Linear trend of annual mean of global solar radiation (Lagos)

(b)Fast Fourier Transform smoothing of the Time series of globalSolar Radiation

(a)

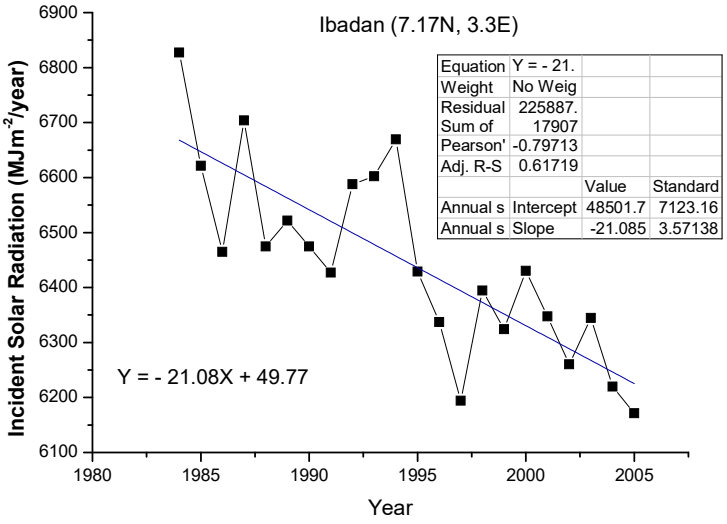

(b)

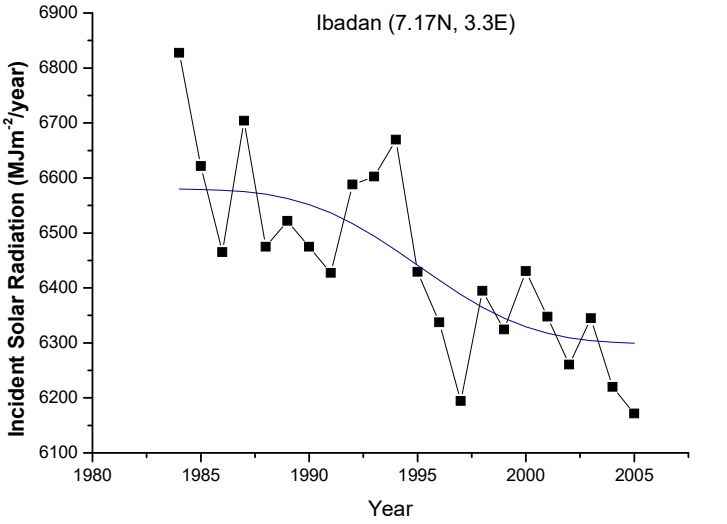

Fig 4.16:(a) Time series and Linear trend of annual mean of global solar radiation (Ibadan)

(b) Fast Fourier Transform smoothing of the Time series of globalSolar Radiation

(a)

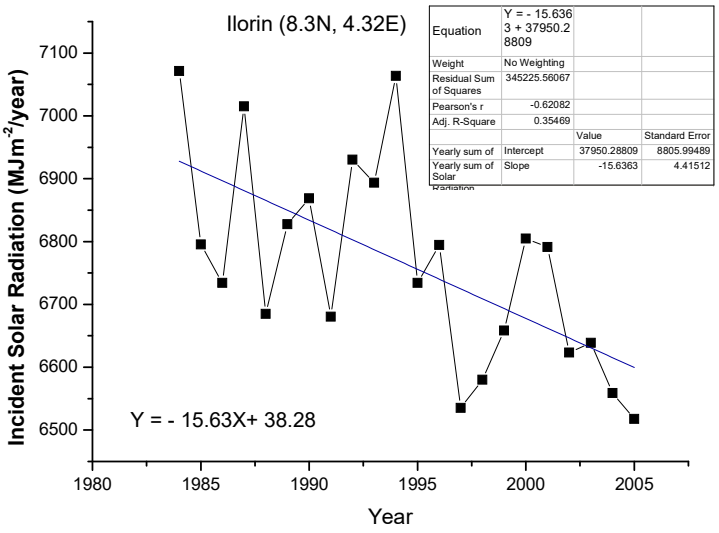

(b)

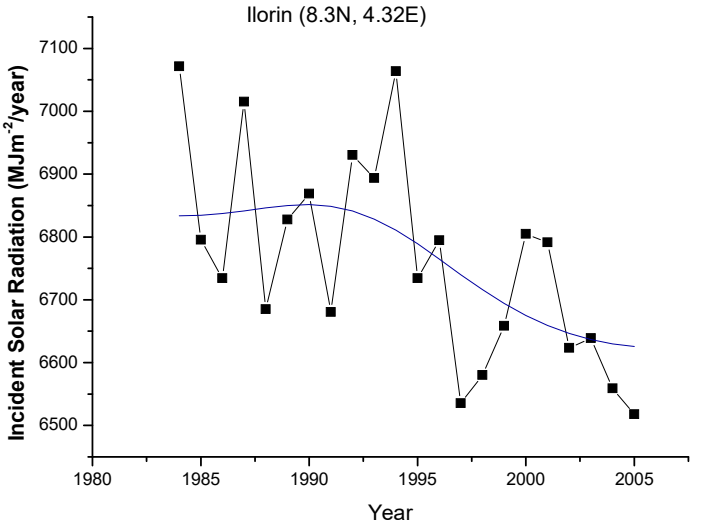

Fig 4.17:(a) Time series and Linear trend of annual mean of global solar radiation(Ilorin)
(b) Fast Fourier Transform smoothing of the Time series of global Solar Radiation

(a)

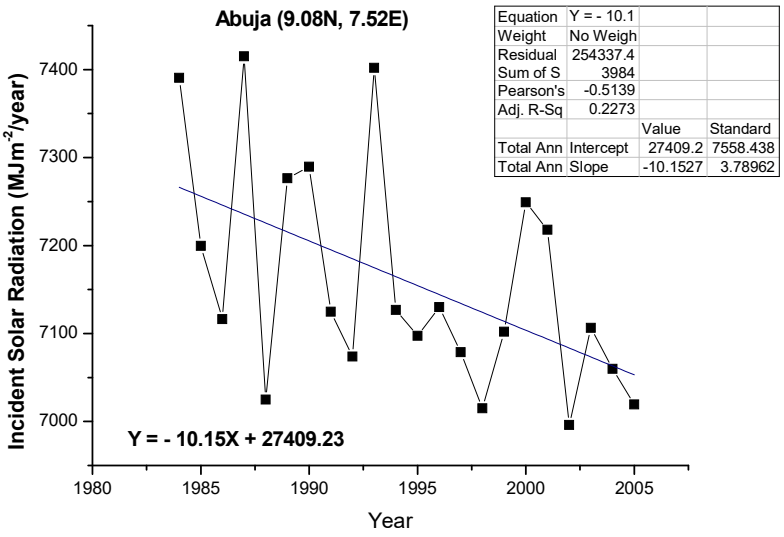

(b)

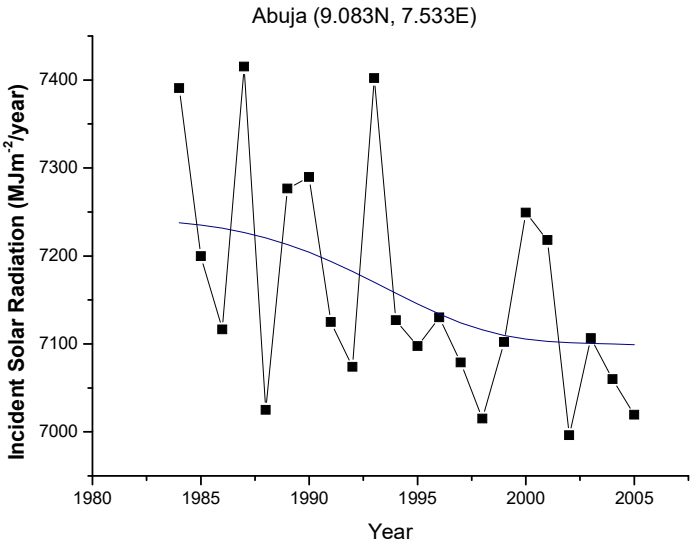

Fig 4.18: (a) Time series and linear trend of annual mean of global solar radiation(Abuja) (b)Fast Fourier Transform smoothing of the Time series of global Solar Radiation

(a)

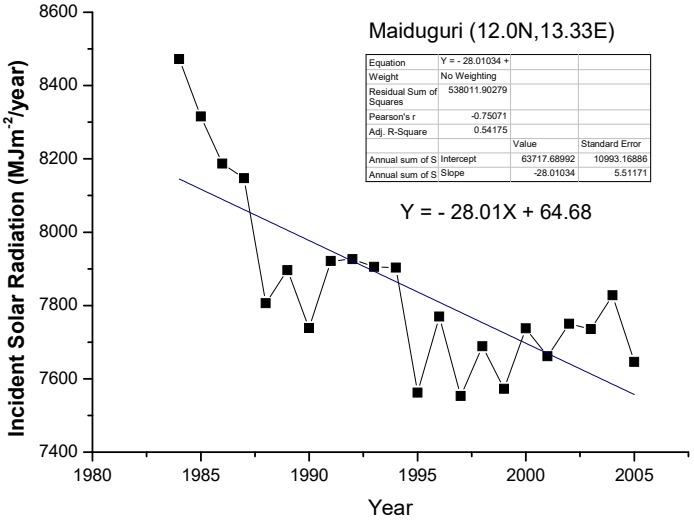

(b)

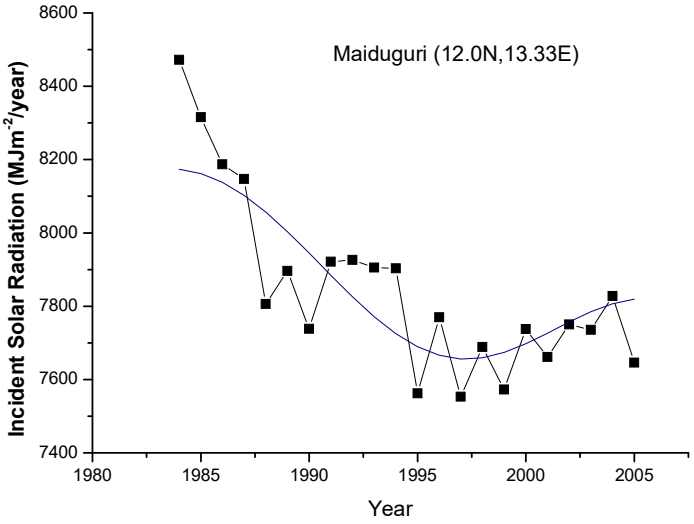

Fig 4.19: (a) Time series and linear trend of annual mean of global solar radiation (Maiduguri)

(b) Fast Fourier Transform smoothing of the Time series of global Solar Radiation

(a)

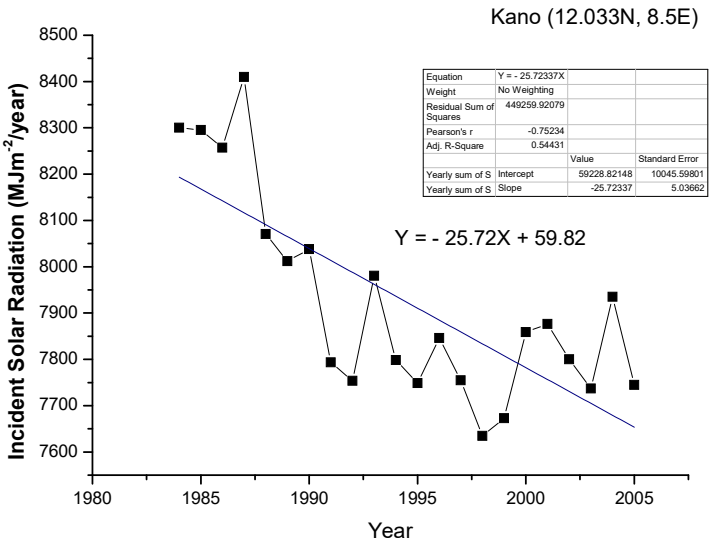

(b)

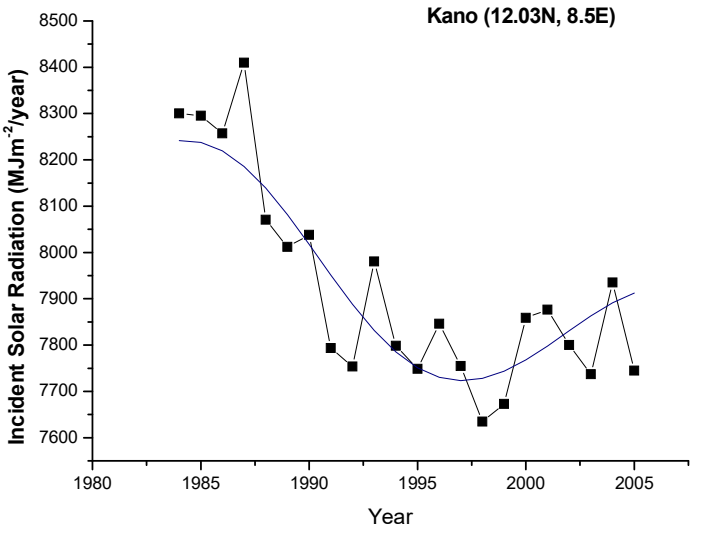

Fig 4.20: (a) Time series and linear trend of annual mean of global solar radiation (Kano)

(b) Fast Fourier Transform smoothing of the Time series of global Solar Radiation

(a)

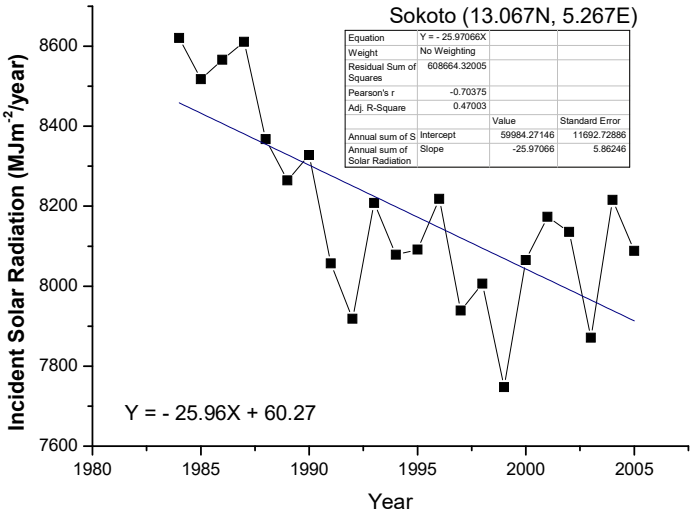

(b)

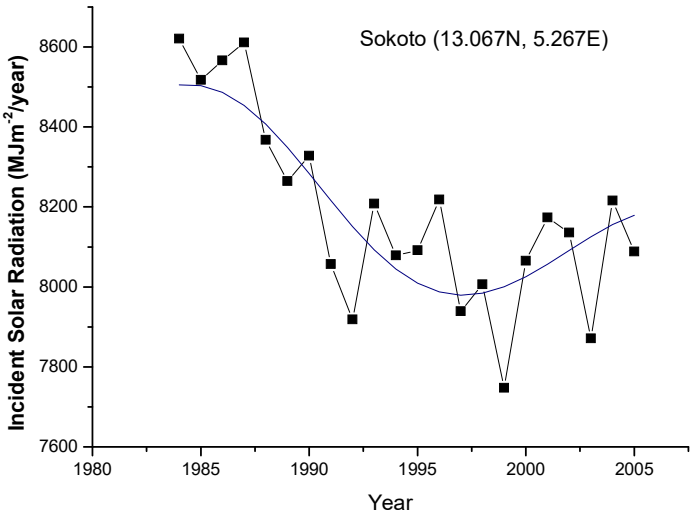

Fig 4.21: (a) Time series and linear trend of annual mean of global solar radiation (Sokoto)

(b)Fast Fourier Transform smoothing of the Time series of global Solar Radiation

(a)

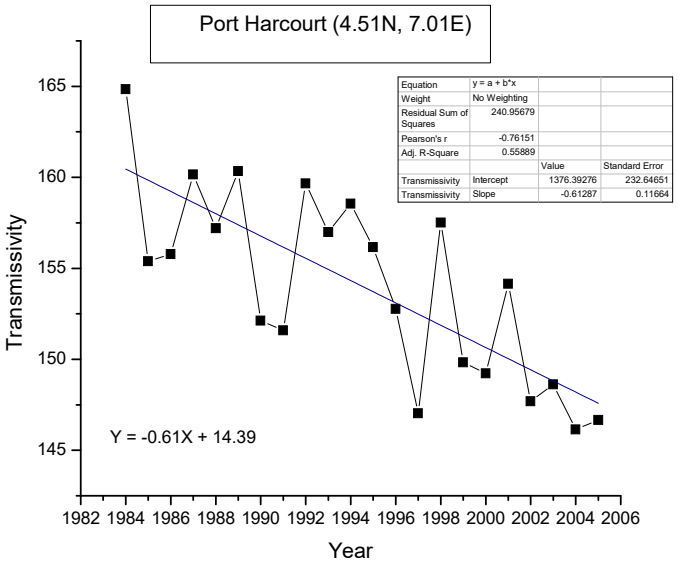

(b)

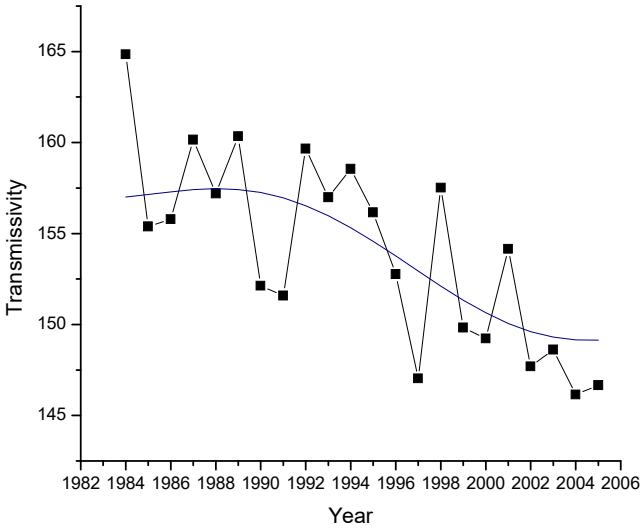

Fig 4.22: (a) Time series and linear trend of Transmissivity (Port Harcourt)

(b)Fast Fourier Transform smoothing of the Time series of Transmissivity

(a)

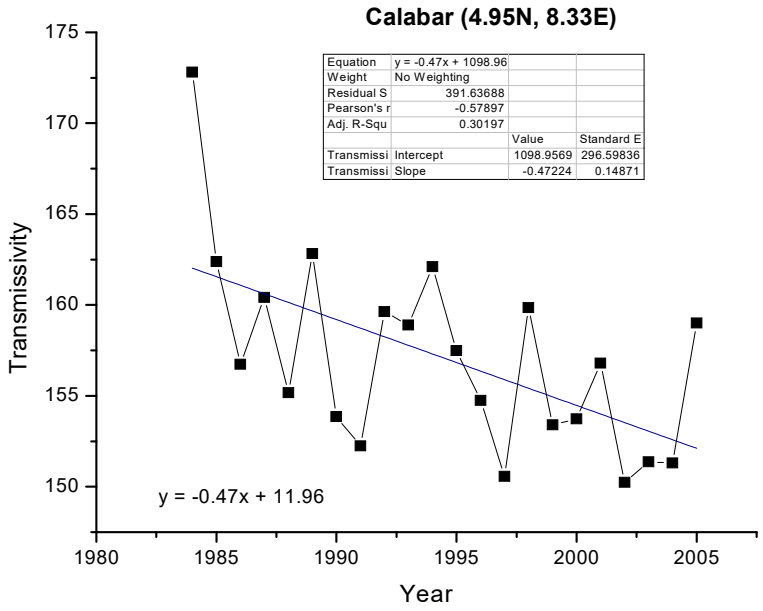

(b)

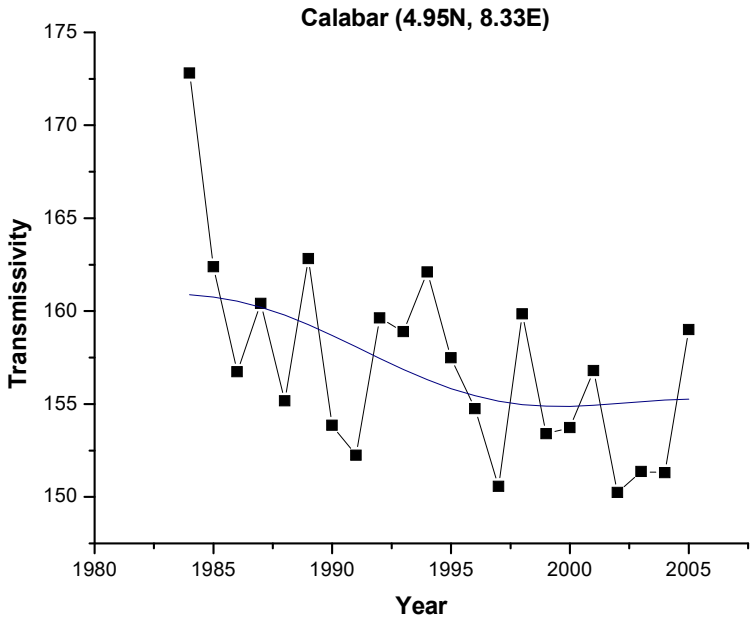

Fig 4.23: (a) Time series and linear trend of Transmissivity (Calabar)

(b)Fast Fourier Transform smoothing of the Time series of Transmissivity

(a)

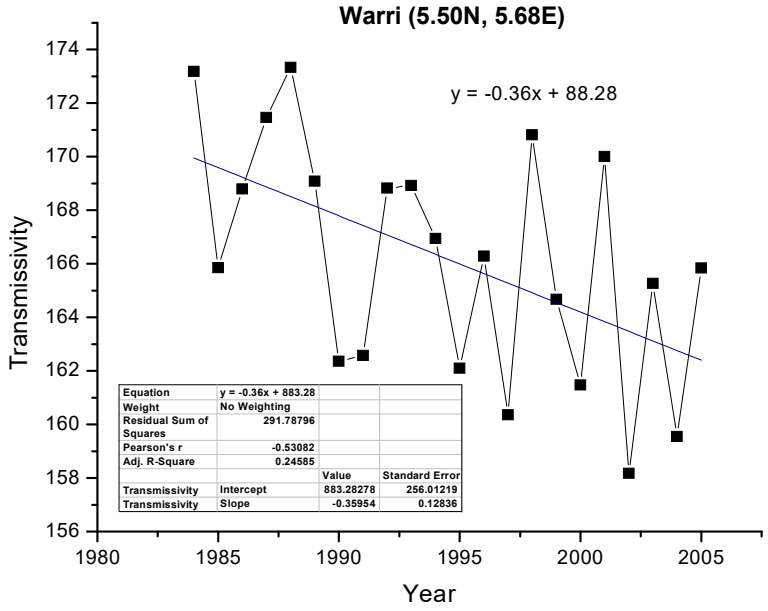

(b)

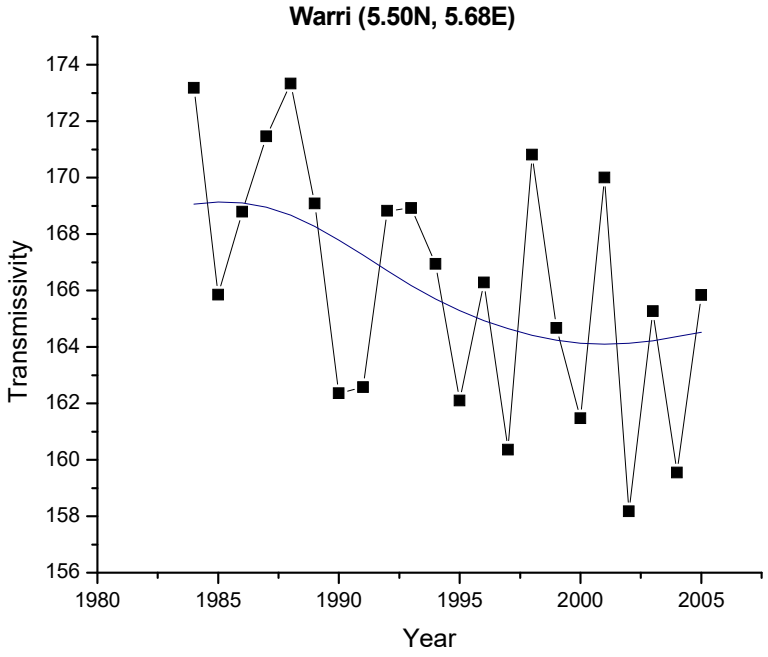

Fig 4.24: (a) Time series and linear trend of Transmissivity (Warri)

(b) Fast Fourier Transform smoothing of the Time series of Transmissivity

(a)

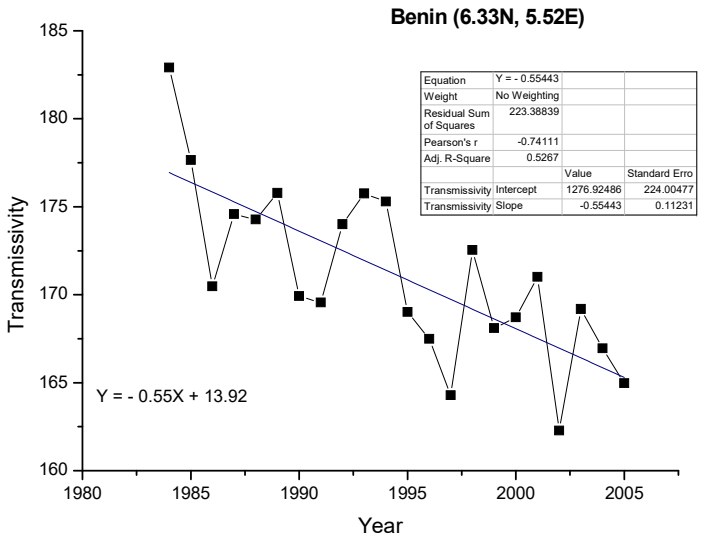

(b)

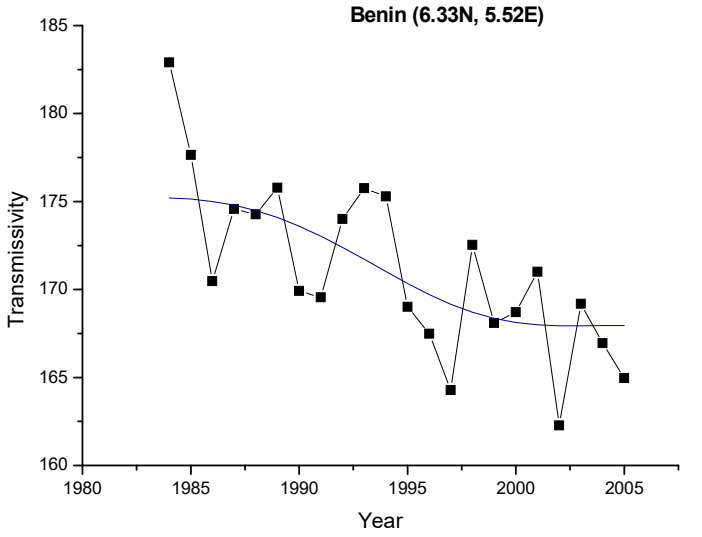

Fig 4.25: (a) Time series and linear trend of Transmissivity (Benin City)

(b) Fast Fourier Transform smoothing of the Time series of Transmissivity

(a)

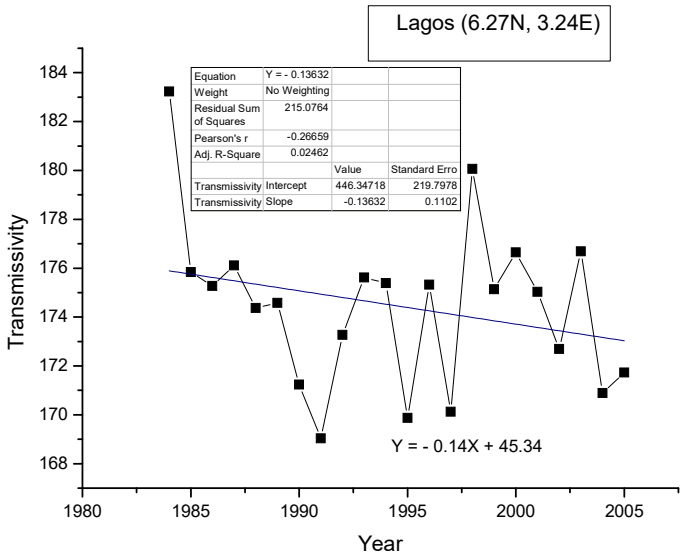

(b)

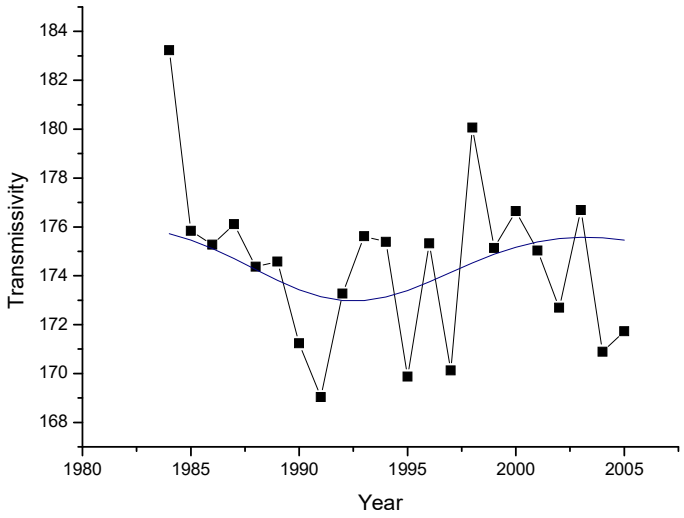

Fig 4.26: (a) Time series and linear trend of Transmissivity (Lagos)

(b) Fast Fourier Transform smoothing of the Time series of Transmissivity

(a)

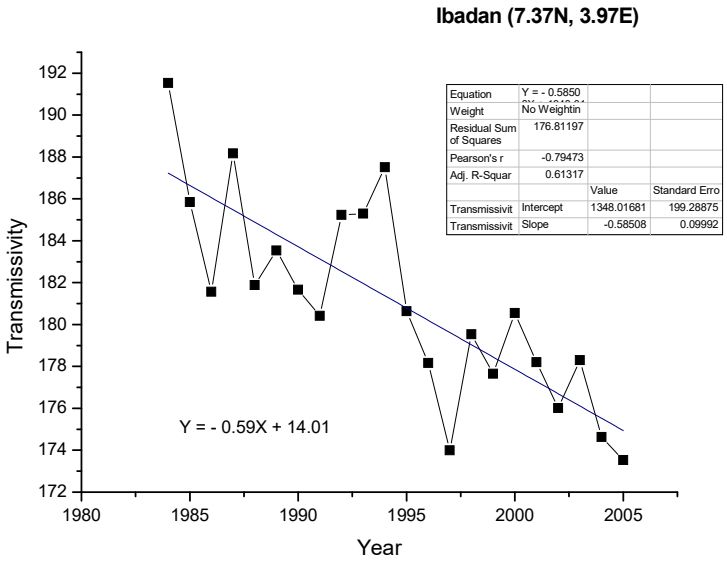

(b)

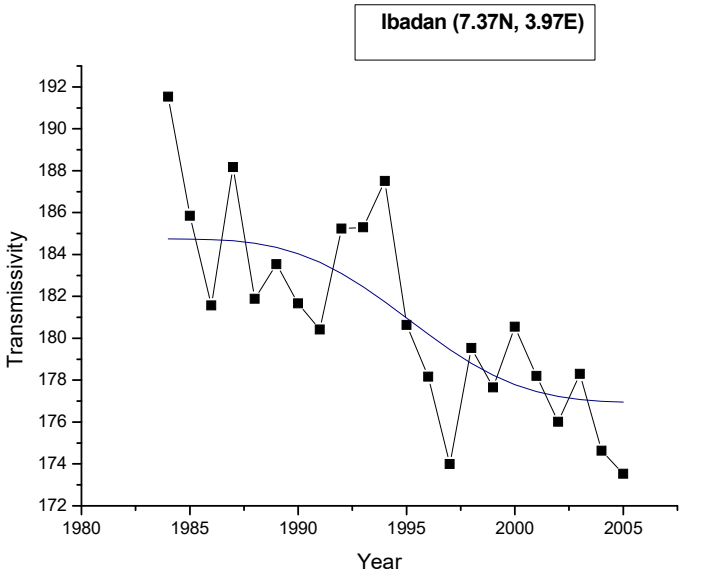

Fig 4.27: (a) Time series and linear trend of Transmissivity (Ibadan)

(b)Fast Fourier Transform smoothing of the Time series of Transmissivity

(a)

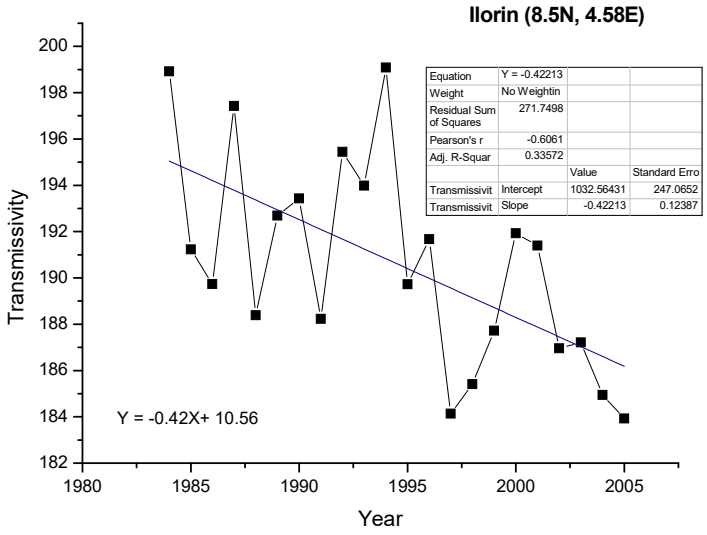

(b)

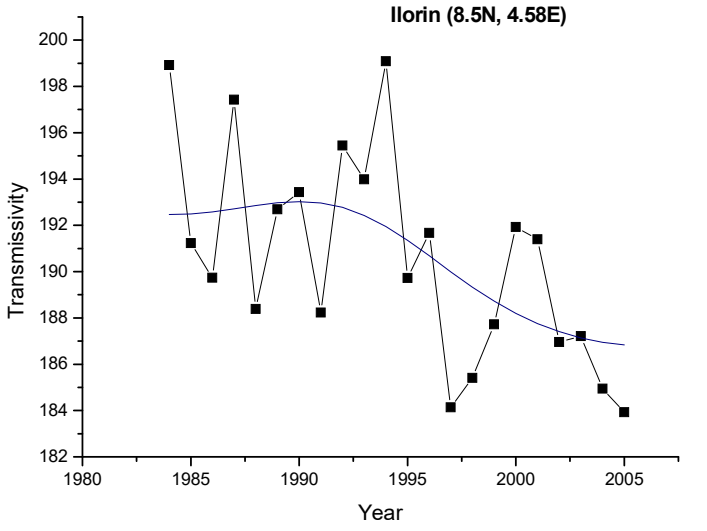

Fig 4.28: (a) Time series and linear trend of Transmissivity (Ilorin)

(b) Fast Fourier Transform smoothing of the Time series of Transmissivity

(a)

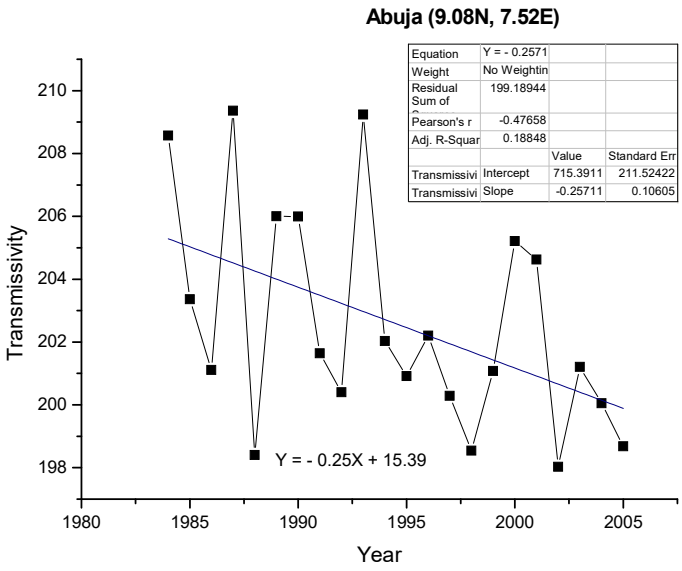

(b)

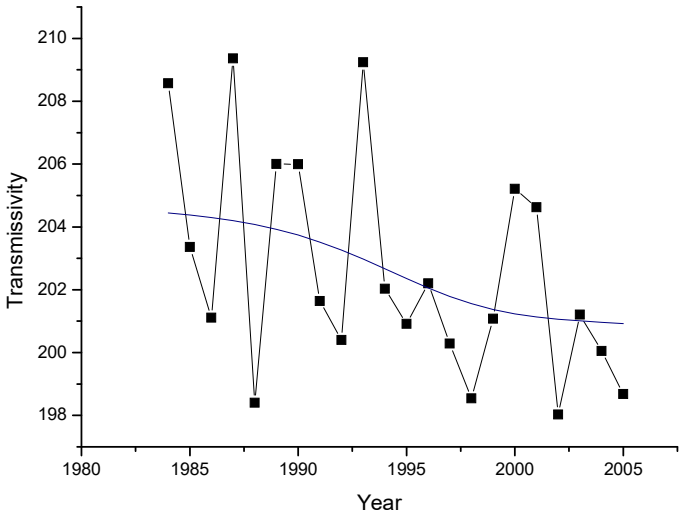

Fig 4.29: (a) Time series and linear trend of Transmissivity (Abuja)

(b) Fast Fourier Transform smoothing of the Time series of Transmissivity

(a)

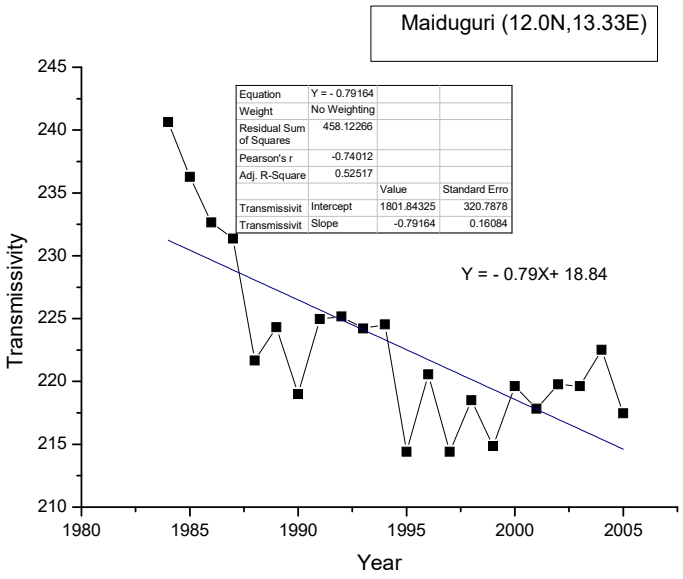

(b)

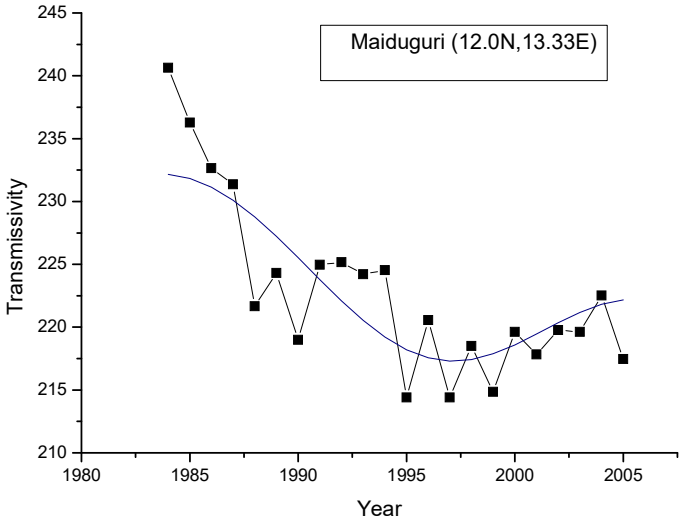

Fig 4.30: (a) Time series and linear trend of Transmissivity (Maiduguri)

(b) Fast Fourier Transform smoothing of the Time series of Transmissivity

(a)

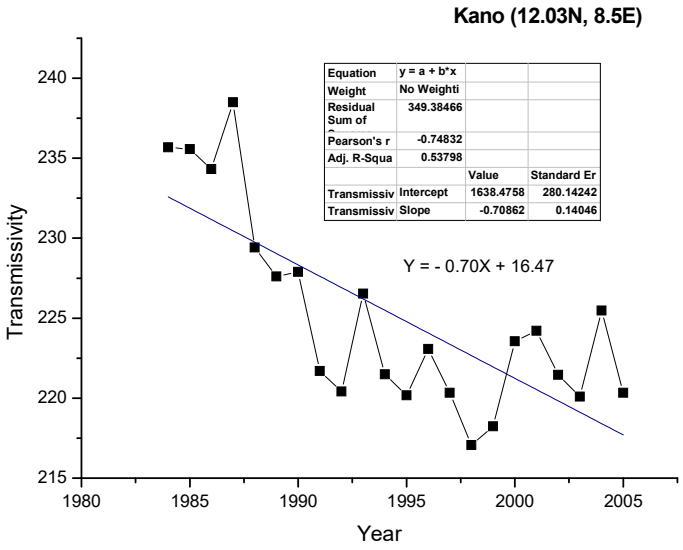

(b)

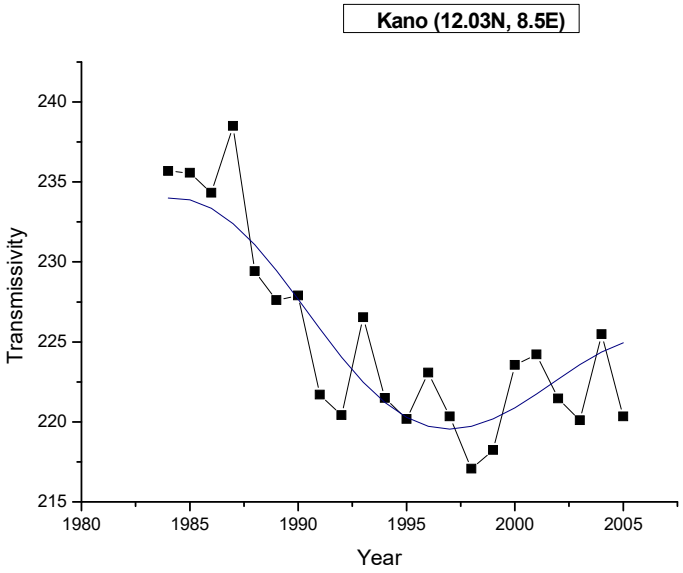

Fig4.31: (a) Time series and linear trend of Transmissivity (Kano)

(b) Fast Fourier Transform smoothing of the Time series of Transmissivity

(a)

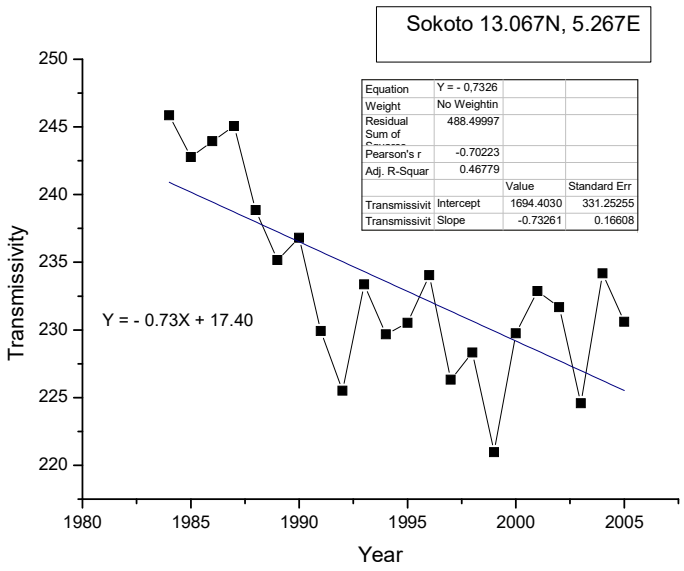

(b)

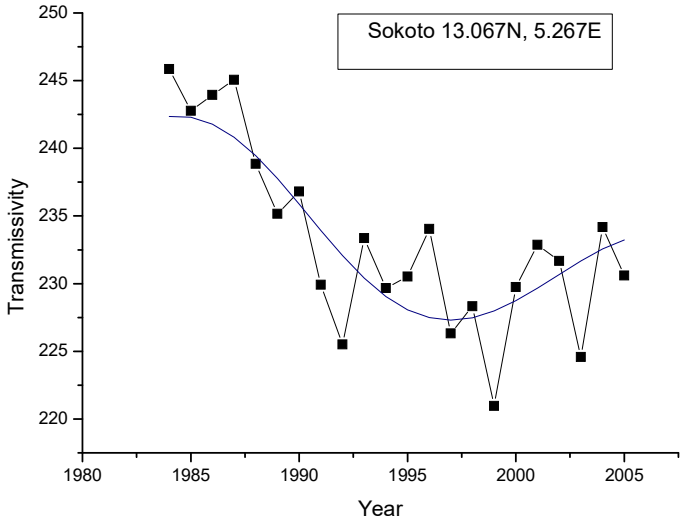

Fig4.32: (a) Time series and linear trend of Transmissivity (Sokoto)

(b) Fast Fourier Transform smoothing of the Time series of Transmissivity

Table 4.1: Summary of the linear trend equations

	Trend equations	
Location	Incident solar radiation	Transmissivity
Port Harcourt	Y = - 21.82X + 49.64	Y = -0.61X + 14.39
Calabar	Y = -16.02X + 38.10	Y = -0.47X + 11.96
Warri	Y = -12.18X +30.32	Y = -0.36X + 88.28
Benin – City	Y = - 19.92X + 46.16	Y = - 0.55X + 13.92
Lagos	Y = - 4.98X + 16.53	Y = - 0.14X + 45.35
Ibadan	Y = - 21.09X + 49.78	Y = - 0.59X + 14.02
Ilorin	Y = - 15.64 + 38.29	Y = -0.42X + 10.56
Abuja	Y = - 10.15X + 27.24	Y = - 0.26X + 72.39
Maiduguri	Y = - 28.01 + 64.69	Y = - 0.79 + 18.84
Kano	Y = - 25.72X + 59.82	Y = - 0.71X + 16.47
Sokoto	Y = - 25.97X + 60.27	Y = - 0.73X + 17.40

Table 4.2. Changes in the values of the quantities

Location	% ofchangesin the values of the quantities			
	Solar Radiation (MJm^{-1})		Transmissivity	
	% ofchangeinvalue/22years	% ofchangeinvalue/decade	% of change in value/22years	% of change in value/decade
Port Harcourt	- 7.96	-3.61	- 8.02	-3.65
Calabar	- 5.80	-2.64	- 6.12	-2.78
Warri	- 4.21	-1.91	- 4.44	-2.02
Benin – City	- 6.62	-3.01	- 6.58	-2.99
Lagos	- 1.66	-0.75	- 1.63	-0.74
Ibadan	- 6.85	-3.11	- 6.56	-2.98
Ilorin	- 4.74	-2.15	- 4.54	-2.06
Abuja	- 2.93	-1.33	- 2.63	-1.20
Maiduguri	- 7.22	-3.28	- 7.19	-3.27
Kano	- 6.59	-3.00	- 6.40	-2.91
Sokoto	- 6.45	-2.93	- 6.39	-2.90

4.3 Relationship between Incident Solar Radiation and Atmospheric Temperature

Daily data of global solar radiation averaged over 22–years for incident solar radiation for each of the eleven locations was plotted against the corresponding maximum and minimum temperatures respectively.

The results, as depicted in the graphs in Figs 4.33 to 4.54,showed a generally good positive correlation between the amounts of solar radiation incident on the earth's surface and the maximum temperature, whilst the correlation between incident solar radiation and the minimum temperature is generally poor. In fact, it showed negative correlation in Abuja. The correlation is poor in all other locations except Sokoto, where solar radiation exhibits a better correlation with the minimum temperature than maximum temperature. The correlation between incident solar radiation and maximum temperature displays a general reduction going from the south towards north.

Now, the solar radiation incident on the surface at a particular location is known to be dependent on the day of the year, the latitude of the location and the atmospheric transmissivity. On reaching the surface, the incoming radiation is partly reflected and partly absorbed. Net radiation, corresponding to the overall balance of absorbed solar radiation and longwave exchange, is converted to the sum of sensible heat, latent heat and ground heat fluxes. During the day, the earth's surface receives radiative energy which results in an increase in the ambient air and soil temperatures. But at night, the surface loses energy by emitting radiation. Thus, a non-cloudy day will be characterized by an increased difference between minimum and maximum temperatures. For low transmissivity days, cloudiness reduces the incoming radiation during daytime and also traps the outgoing radiation at night. Thus the diurnal temperature range, DTR, will thus be reduced (Miglietta, 1991;Kemp,2007). These are complex negative feedback mechanisms which complement one another.

The summary of the correlation coefficients between incident solar radiation and atmospheric temperatures for the locations are shown in table. 4.4.

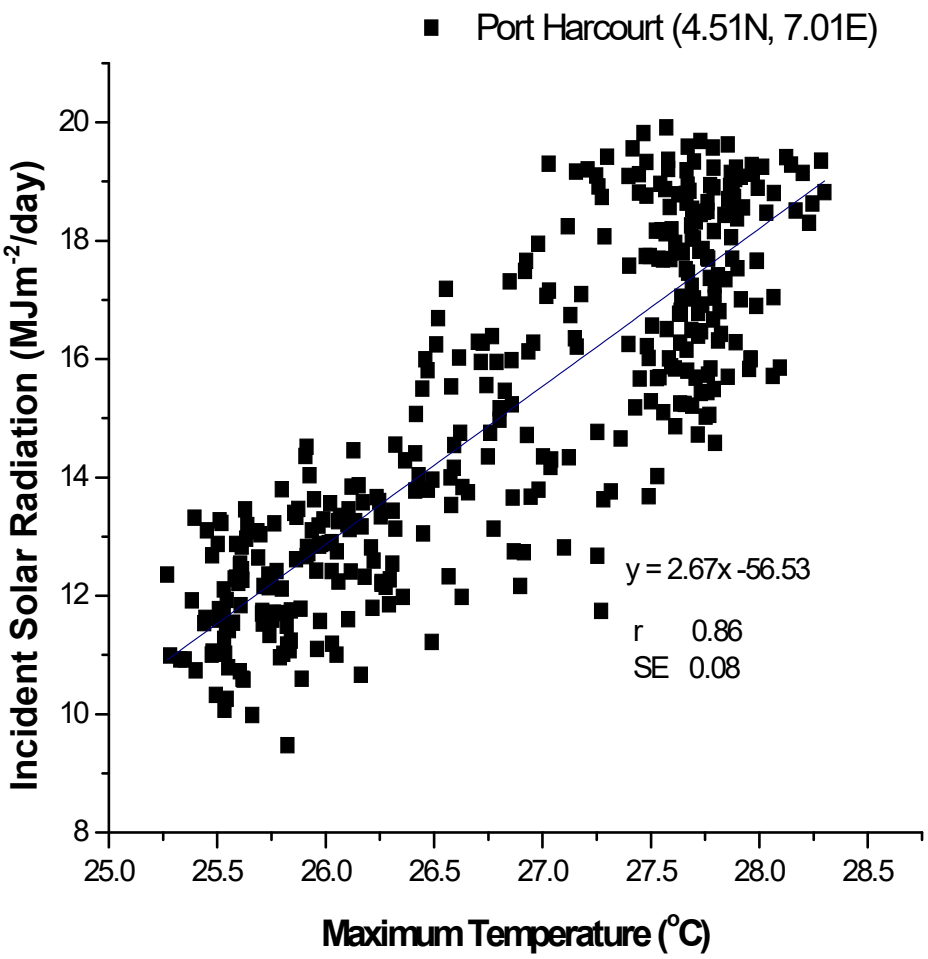

Fig 4.33:**C**orrelationof Incident SolarRadiation and Maximum Temperature for Port Harcourt

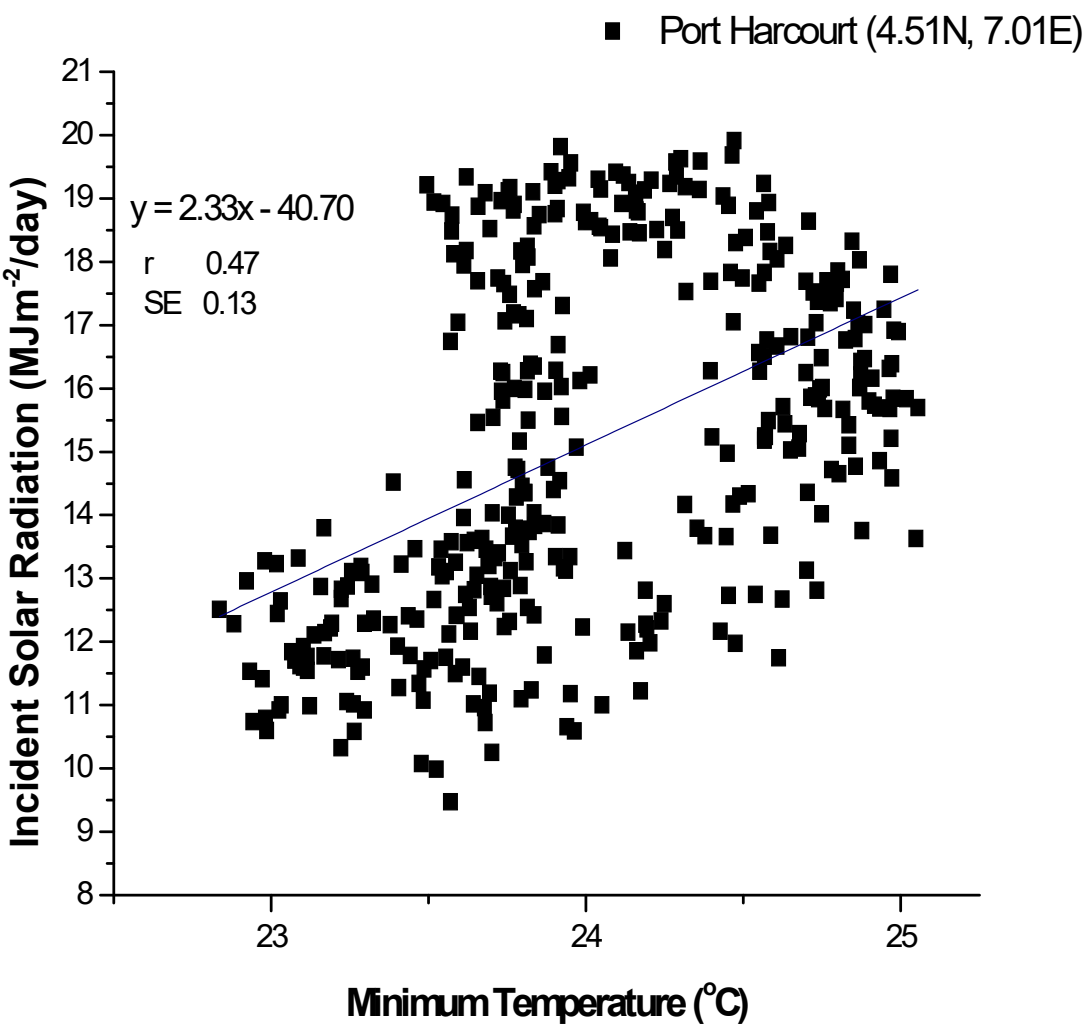

Fig 4.34:**C**orrelation ofIncident Solar Radiation and Minimum Temperature for Port Harcourt

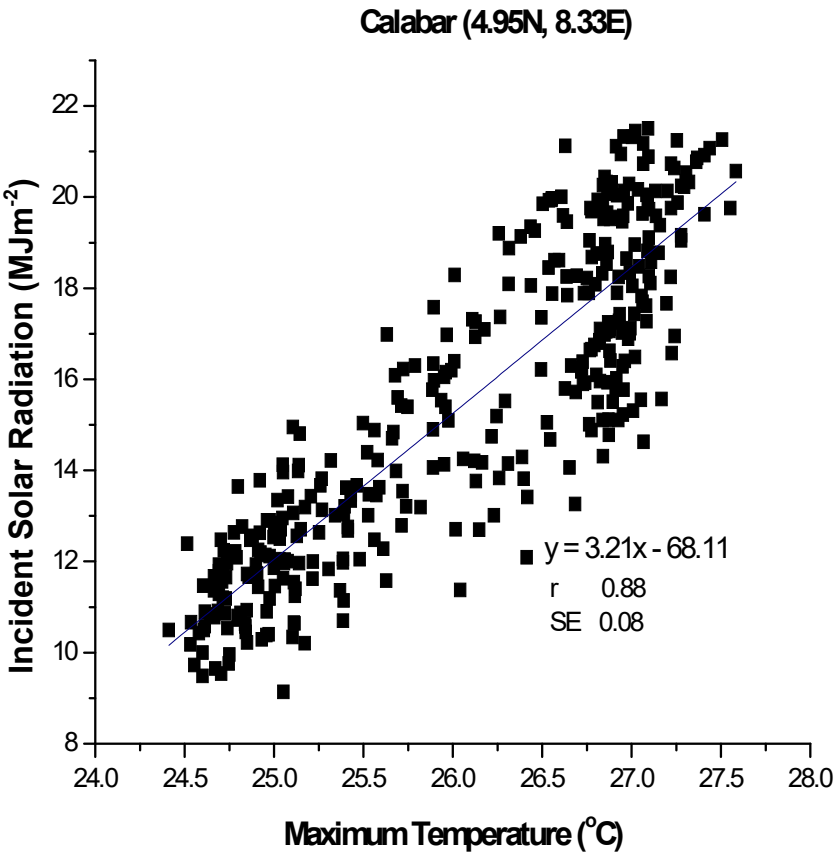

Fig 4.35:**C**orrelation ofIncident Solar Radiation and Maximum Temperature forCalabar

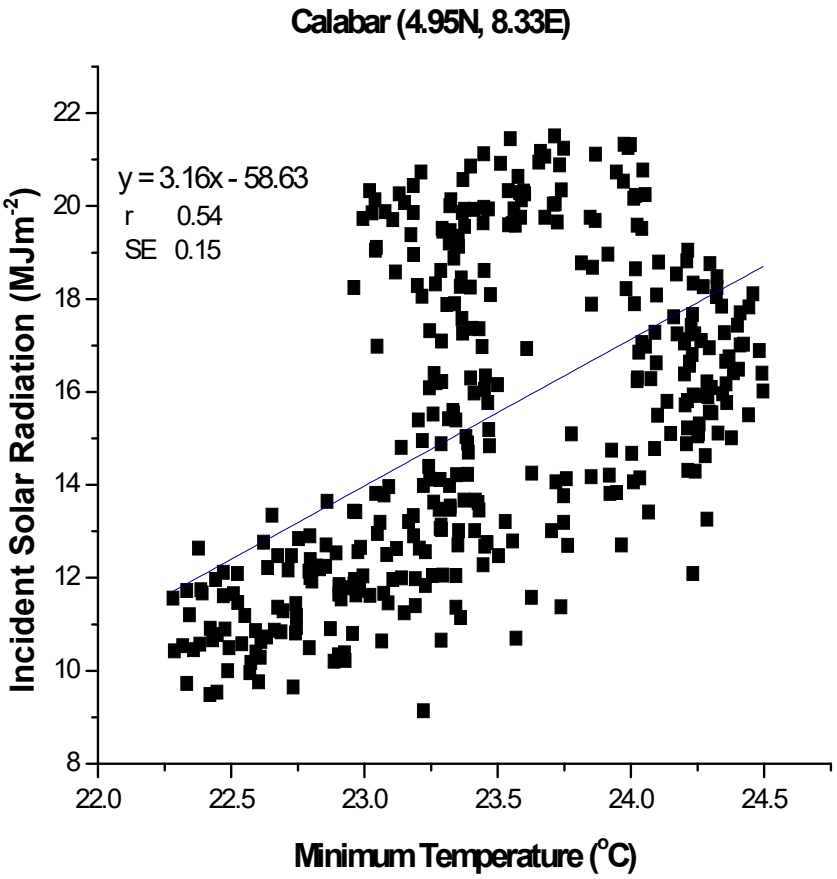

Fig 4.36:Correlation ofIncident Solar Radiation and Minimum Temperature forCalabar

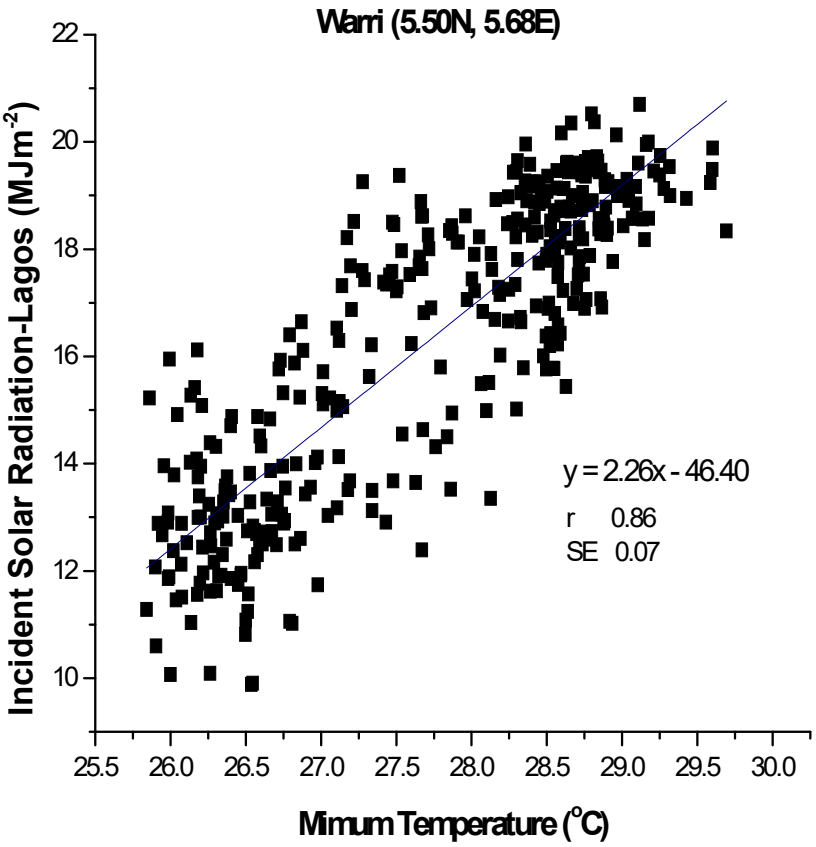

Fig 4.37: Correlation ofIncident Solar Radiation and Maximum Temperature for Warri

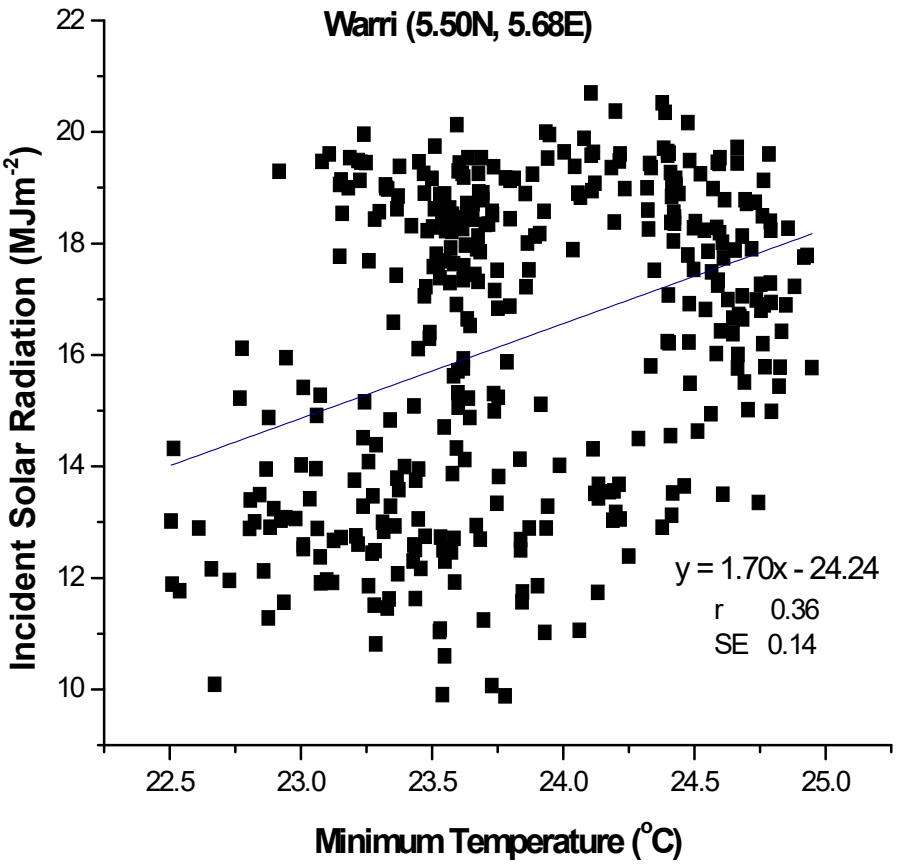

Fig 4.38: Correlation ofIncident Solar Radiation and Minimum Temperature for Warri

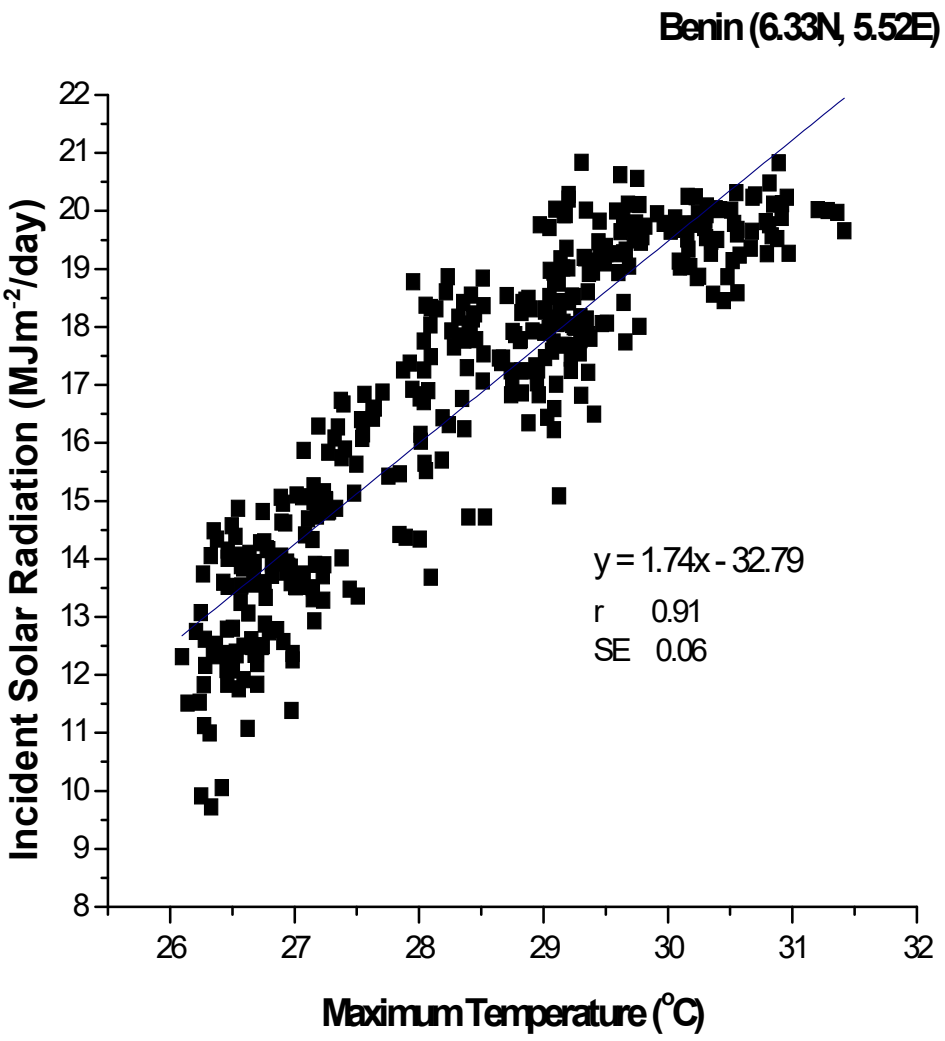

Fig 4.39: Correlation ofIncident Solar Radiation and Maximum Temperature for Benin City

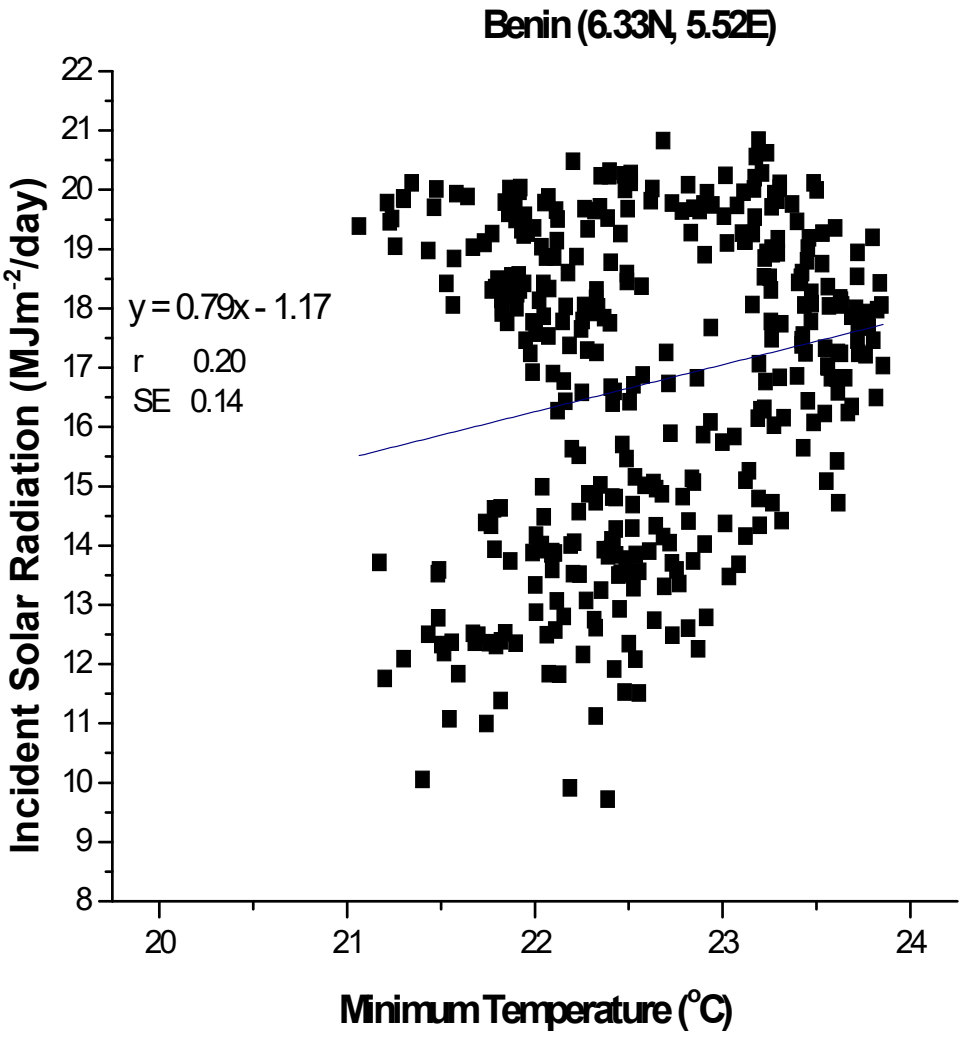

Fig 4.40:Correlation ofIncident Solar Radiation and Minimum Temperature forBenin-City

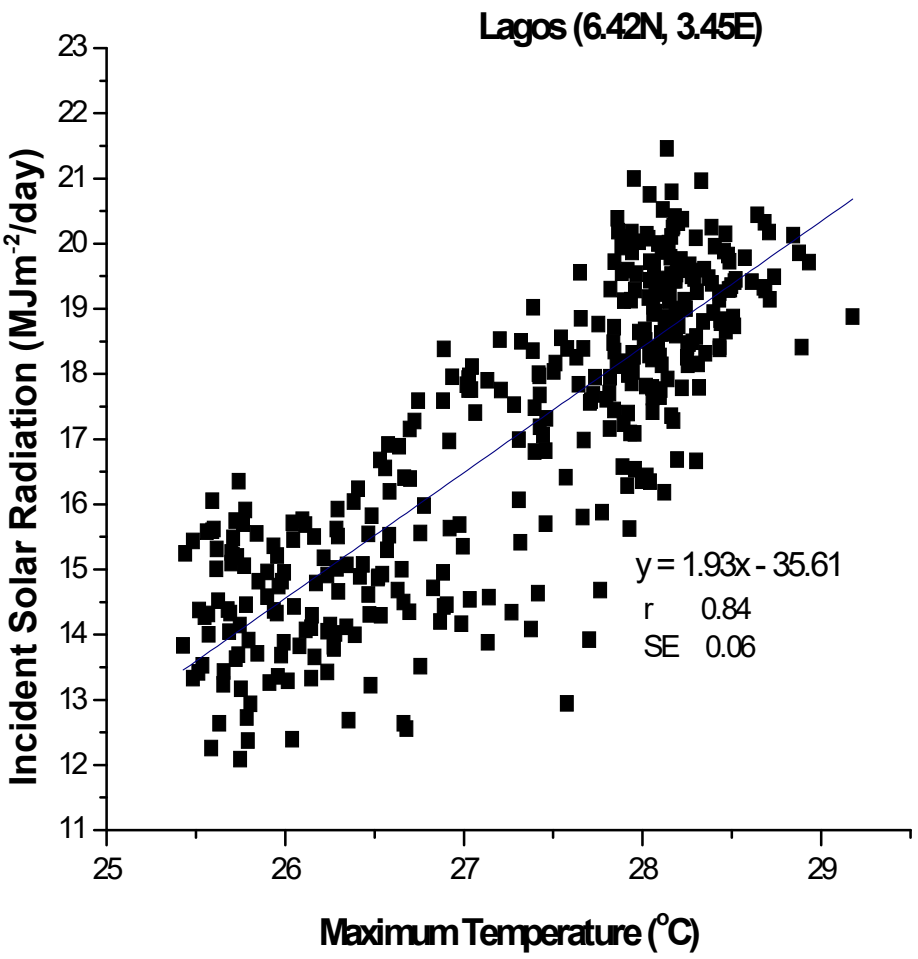

Fig 4.41:Correlation ofIncident Solar Radiation and Maximum Temperature forLagos

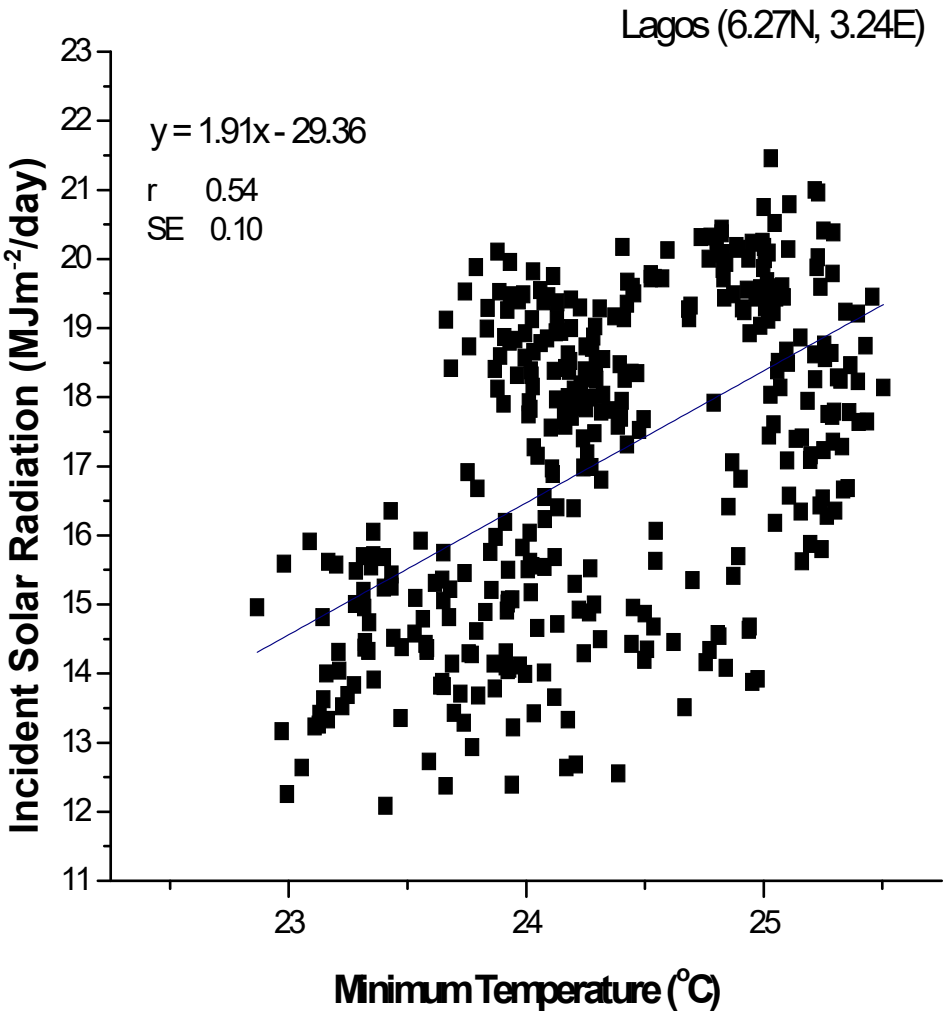

Fig 4.42:Correlation ofIncident Solar Radiation and Minimum Temperature for Lagos

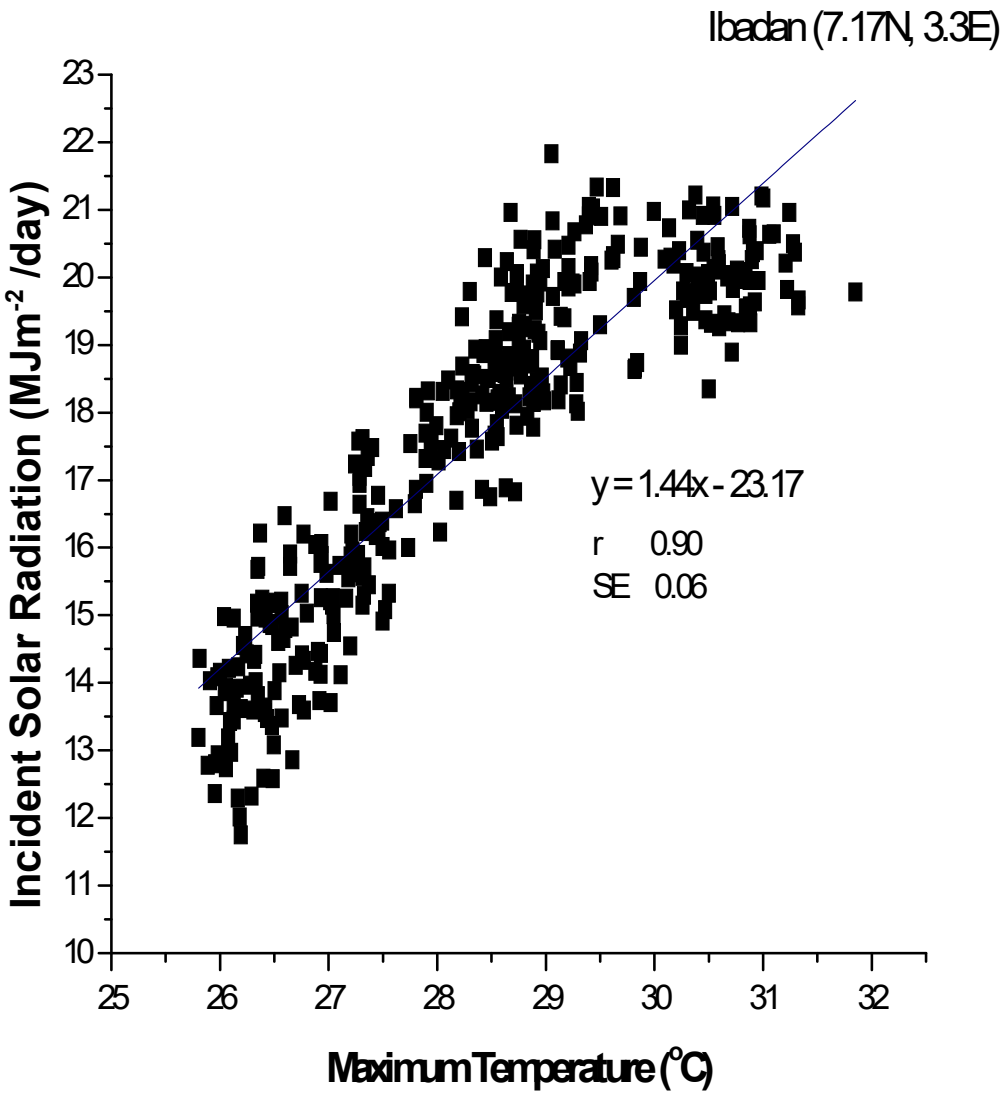

Fig 4.43:Correlation ofIncident Solar Radiation and Maximum Temperature forIbadan

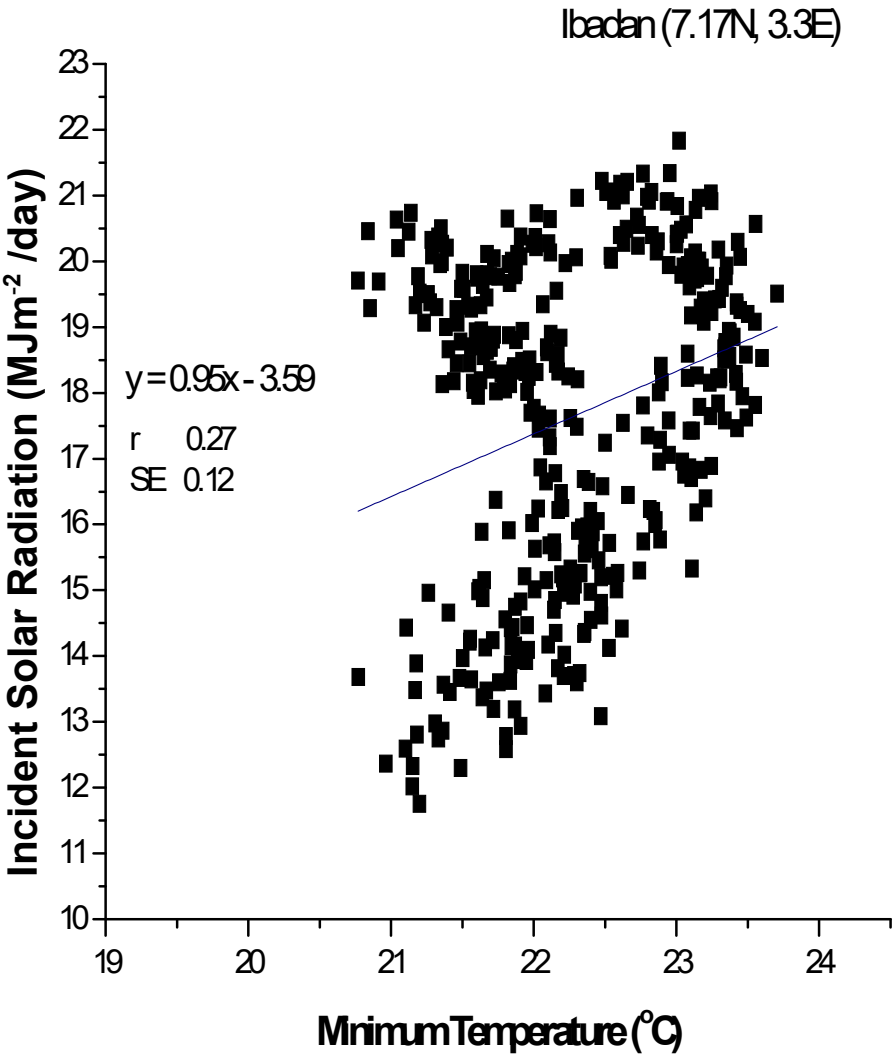

Fig 4.44 Correlation ofIncident SolarRadiation and Minimum Temperature for Ibadan

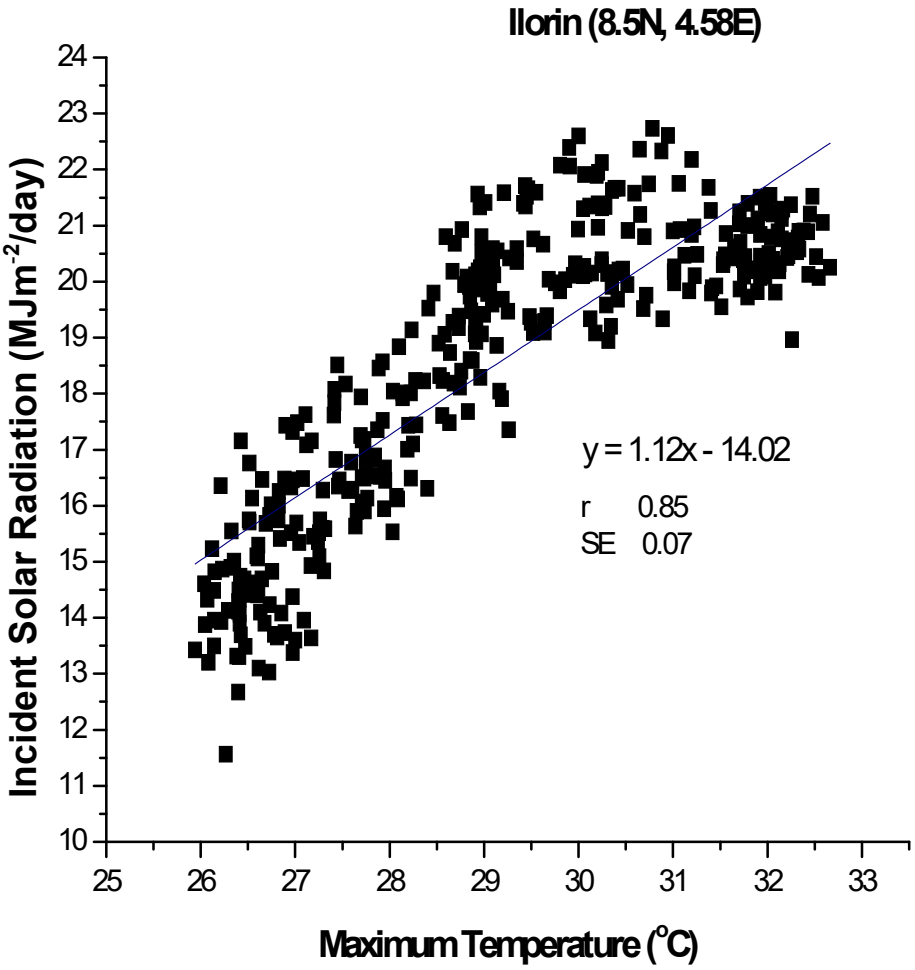

Fig 4.45 Correlation ofIncident SolarRadiation and Maximum Temperaturefor Ilorin

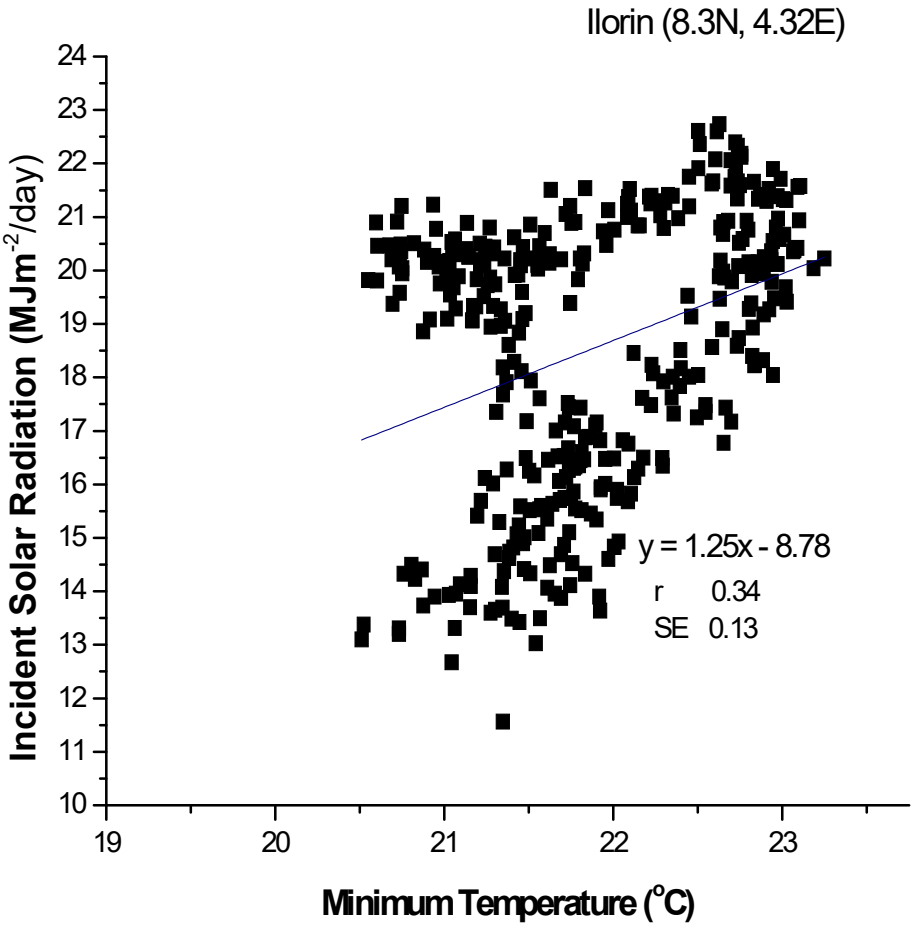

Fig 4.46 Correlation ofIncident SolarRadiation and Minimum Temperature for Ilorin

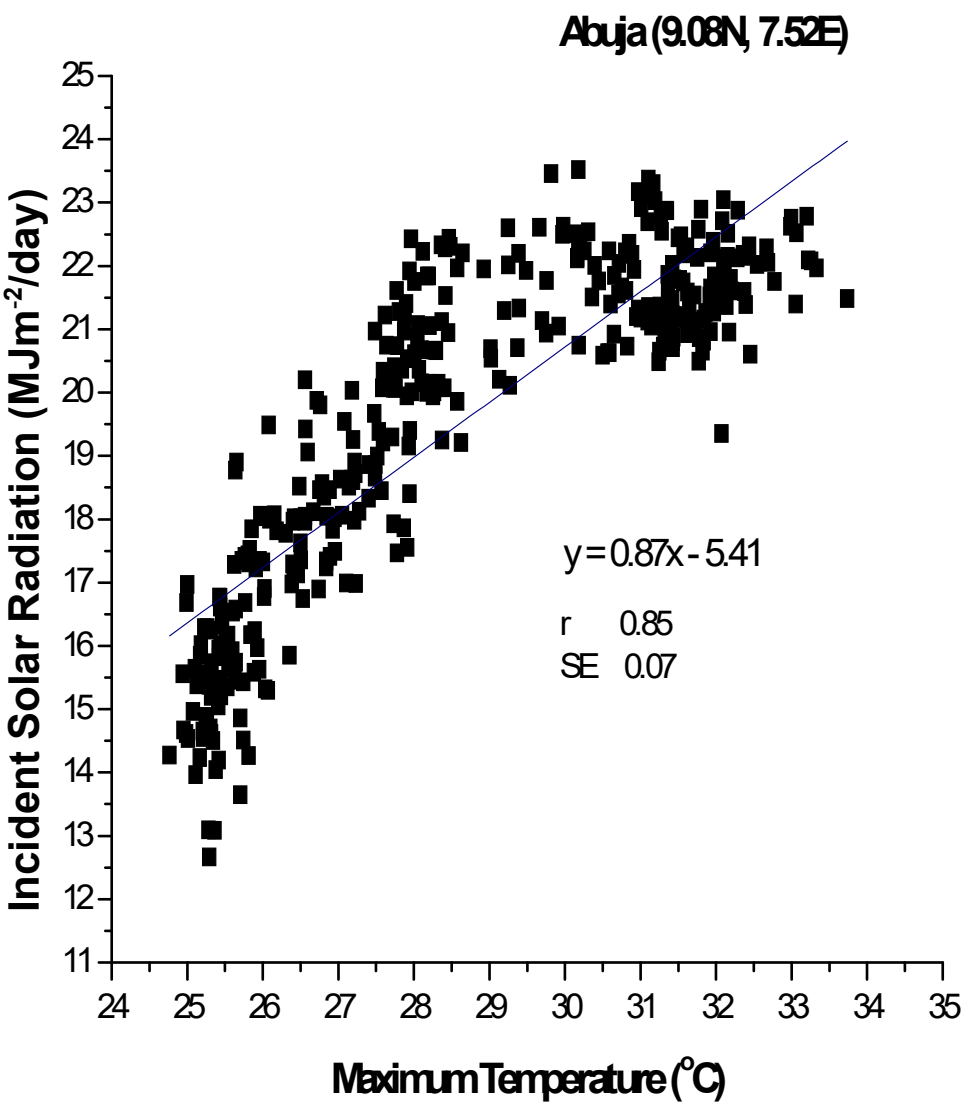

Fig 4.47: Correlation ofIncident Solar Radiation and MaximumTemperature for Abuja

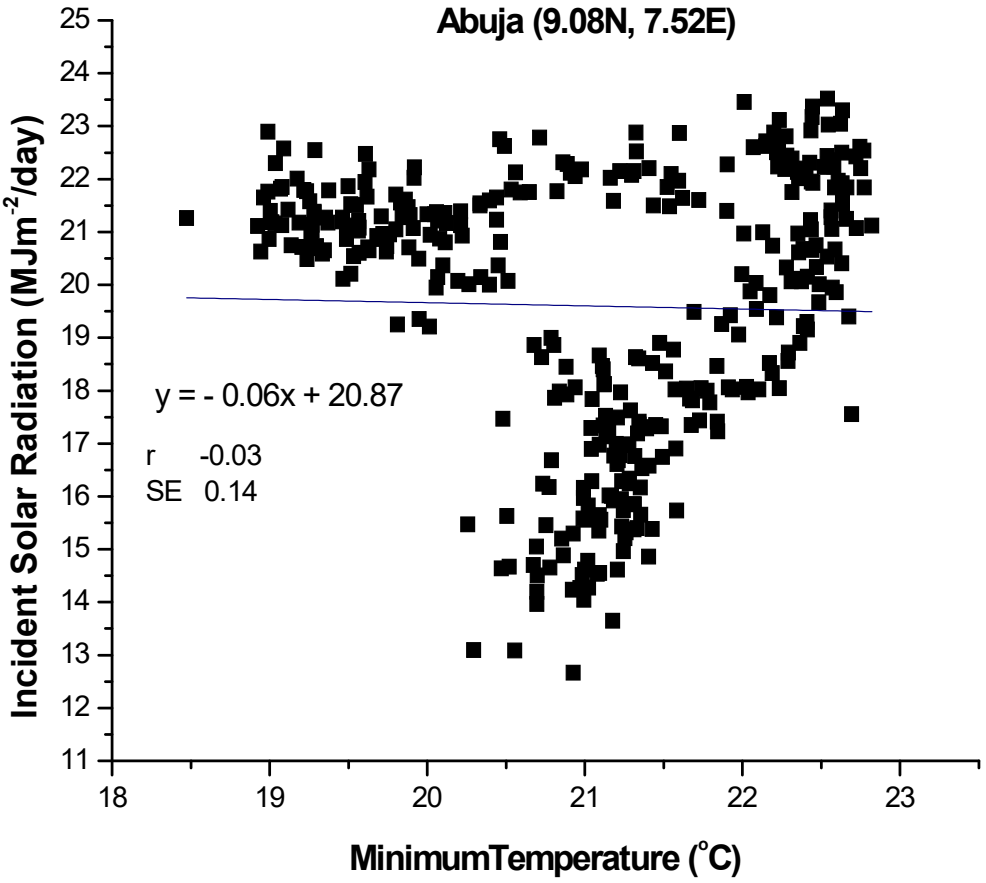

Fig 4.48 Correlation ofIncident Solar Radiation and MinimumTemperaturefor Abuja

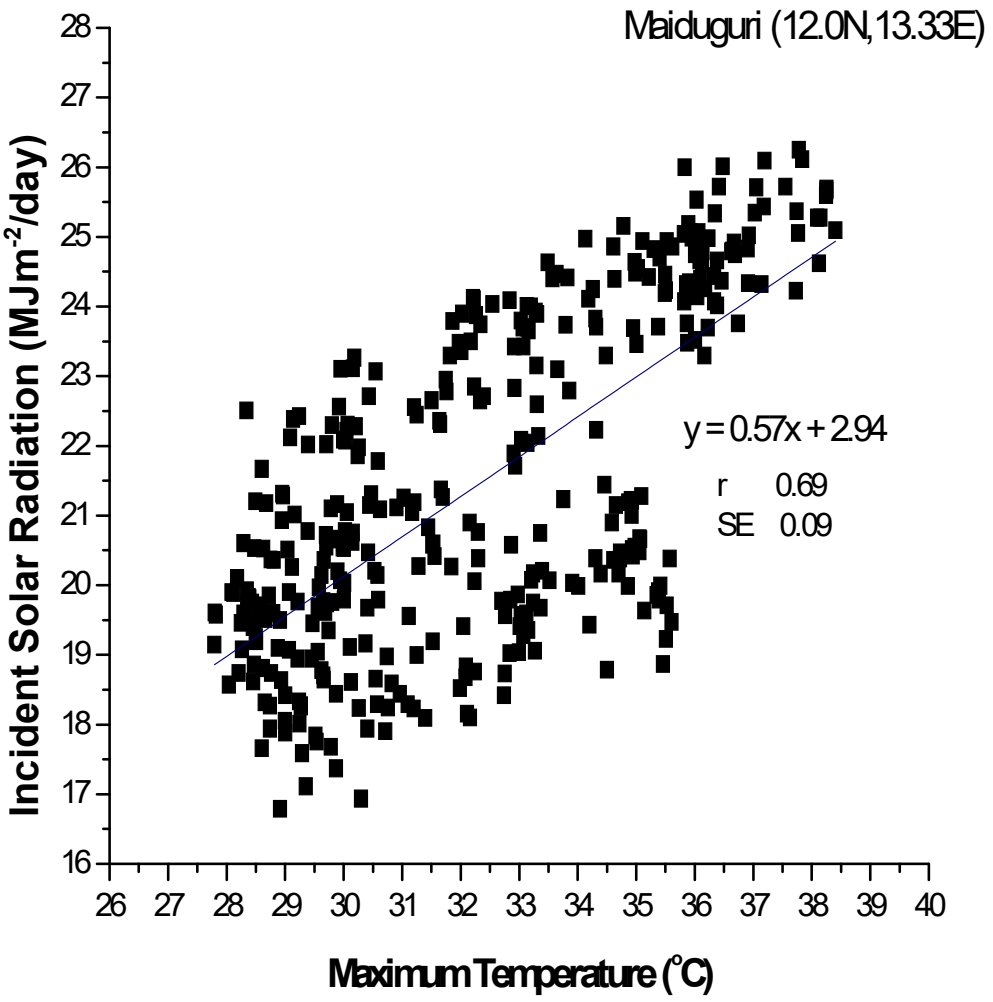

Fig 4.49 Correlation of Incident Solar Radiation and Maximum Temperaturefor Maiduguri

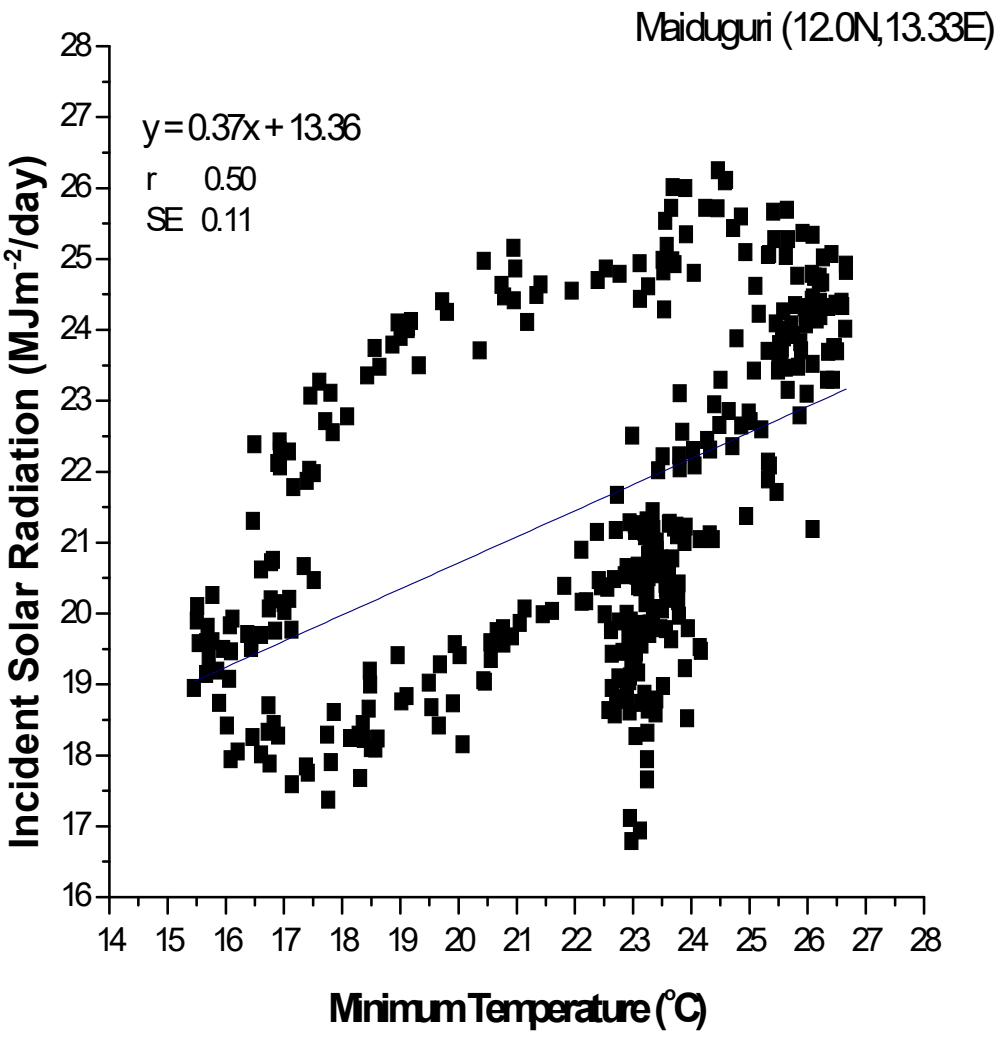

Fig 4.50 Correlation of Incident Solar Radiation and Minimum Temperaturefor Maiduguri

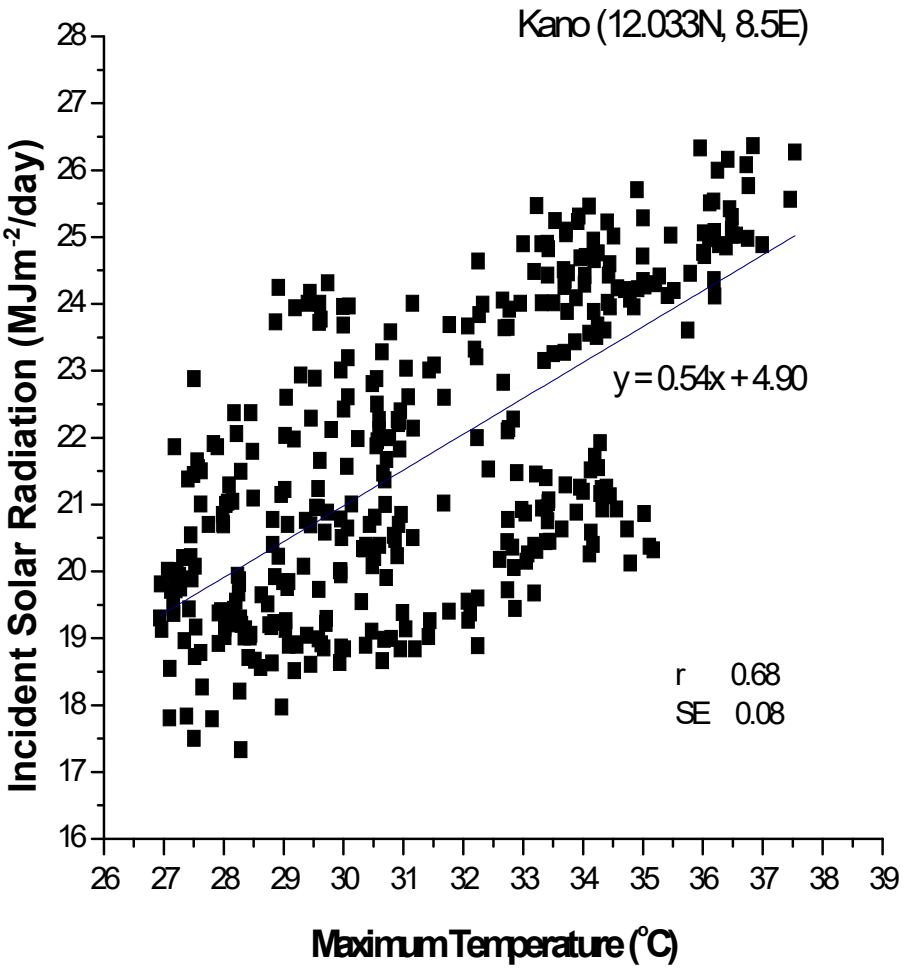

Fig 4.51 Correlation of Incident Solar Radiation and Maximum Temperaturefor Kano

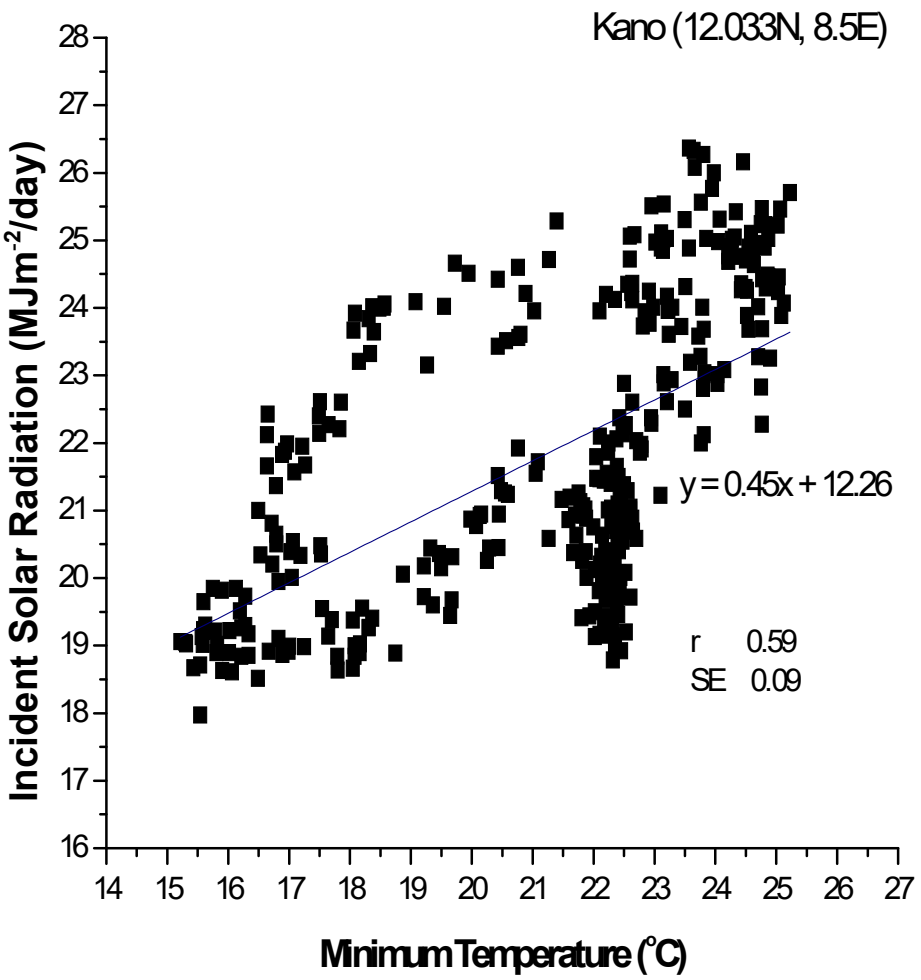

Fig 4.52 Correlation of Incident Solar Radiation and Minimum TemperatureforKano

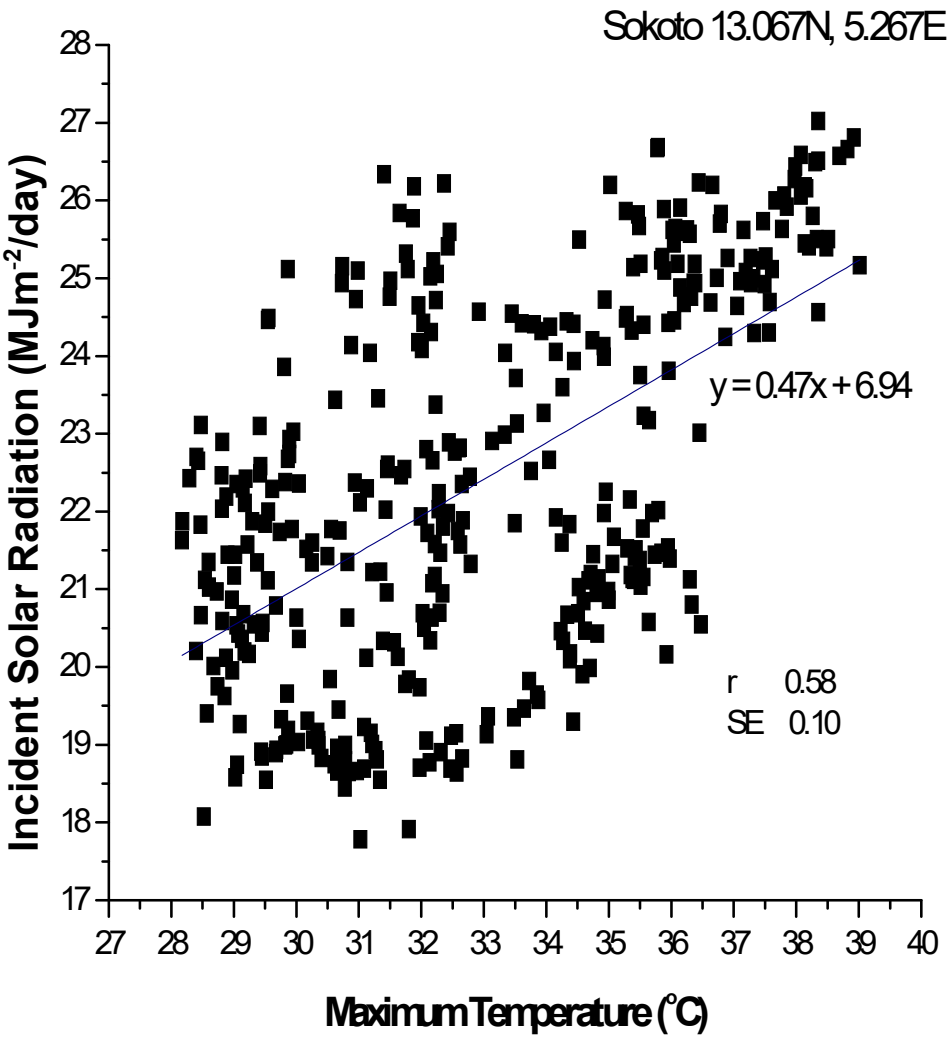

Fig 4.53 Correlation of Incident Solar Radiation and Maximum Temperaturefor Sokoto

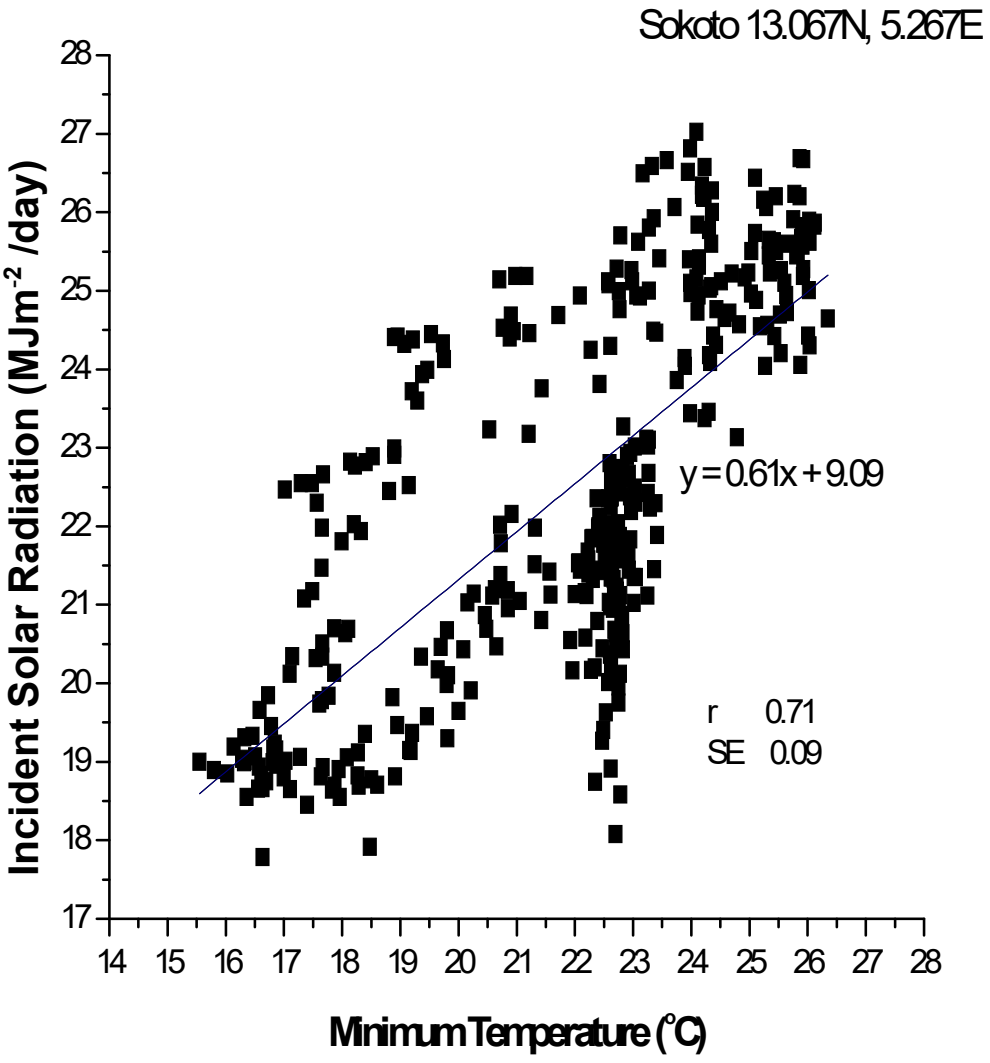

Fig 4.54 Correlation of Incident SolarRadiation and Minimum Temperature forSokoto

Table 4.3:Summary of the correlation coefficients betweenincident solarradiation and airtemperatures for the locations.

	Pearson's correlation coefficient, R			
Location	Minimum Temperature	SE	Maximum Temperature	SE
Port Harcourt	0.47	0.13	0.86	0.08
Calabar	0.54	0.15	0.88	0.08
Warri	0.36	0.14	0.86	0.07
Benin city	0.20	0.14	0.91	0.06
Lagos	0.54	0.10	0.84	0.06
Ibadan	0.27	0.12	0.90	0.06
Ilorin	0.34	0.13	0.85	0.07
Abuja	-0.03	0.14	0.85	0.07
Maiduguri	0.50	0.11	0.69	0.09
Kano	0.59	0.09	0.68	0.08
Sokoto	0.71	0.09	0.58	0.10

4.4.Temporal Trends of Maximum and Minimum Temperatures over the regionduring 1984 – 2005

Annual means were aggregated from the daily values of both the maximum and minimum temperatures. These yearly values were then plotted sequentially against time for each station. For each station, the regression line was found as well as the fast Fourier transform (FFT) drawn to indicate the general direction of the trend.Comparing the trends of solar radiation (Figs 4.11 to 4.21) to those of minimum and maximum temperatures (Figs 4.55 to fig 4.76), the nine locations could be separated roughly into twodifferent regimes in terms of the similarities between the maximum temperature and solar radiation.

Over Port Harcourt, Calabar, Warri, Benin City, Lagos Ibadan, Ilorin and Abuja, incident solar radiation showed positive correlation with the maximum temperature and a generally negative correlation with the minimum temperature. That is, as solar radiation trends upward over time, maximum temperature also trend upward while minimum temperature trend downward. This is also true in reverse order. Benin City produced the best positive relationship between solar radiation and maximum temperature while Abuja gave the smallest slope. Actually, there exists a gradual decline in positive correlation between these two quantities with increasing latitude.

The next three locations of Maiduguri, Kano and Sokoto provide a different relationship between solar radiation and maximum and minimum temperatures respectively (Figs 4.63 to 4.65 and 4.74 to 4.76).At these stations, there was a sharp decrease in the values of the incident solar radiation between 1984 and 1992 and thereafter the rate of the decrease became lower. During this time, minimum temperature increased with time only slightly while maximum temperature increased steeply. The increase in the maximum temperature with time is seen to increase with latitude.

As noted in section 4.3., the decrease in the trend of the maximum temperature and increase in the minimum temperature trend in the southern locations could be attributed to the abundance ofatmospheric water vapour within this region.This encourages formation of clouds. And as explained, it results in increased reflection of incoming shortwave radiation and absorption of outgoing longwave radiation resulting indecreasing daytime and rising nighttime temperatures respectively. These results as depicted for all

the locations below latitude 9.0^0indicatethat cloudiness has been on the increase during the years under investigation. This might be part of the manifestation of global warming.

The northern locations of Maiduguri, Kano and Sokoto depicted a different scenario. Here, daytime have been getting hotter while nighttime have been getting cooler. From the explanation given above, only a continued decrease in cloudiness could be responsible for this. This is because such a situation will encourage the passage of short wave radiation through the atmosphere and therefore heating up the surface during the daytime and the escape of longwave radiation during the nighttimeresulting in nocturnal cooling.

Tables 4.5 and 4.6 respectively are the summary of the linear trend equations and the percentage change in the values of the quantities.

(a)

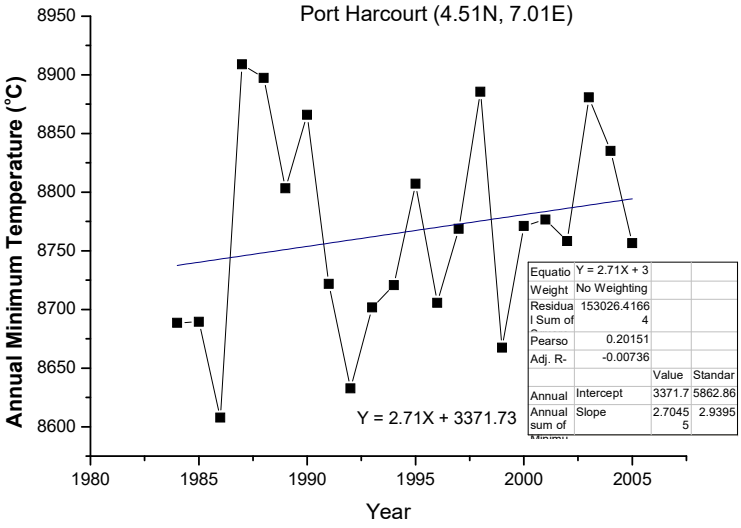

(b)

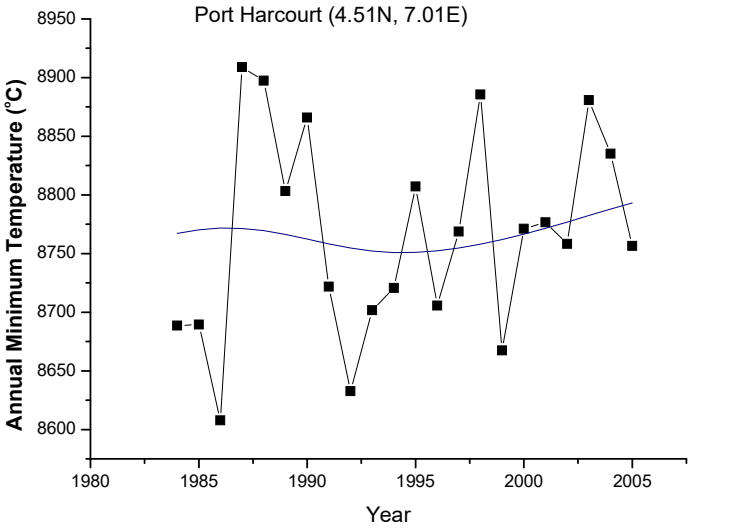

Fig4.55: (a) Linear trend of Minimum Temperature (Port Harcourt)

(b)Fast Fourier Transform smoothing of the Time series of Minimum Temperature

(a)

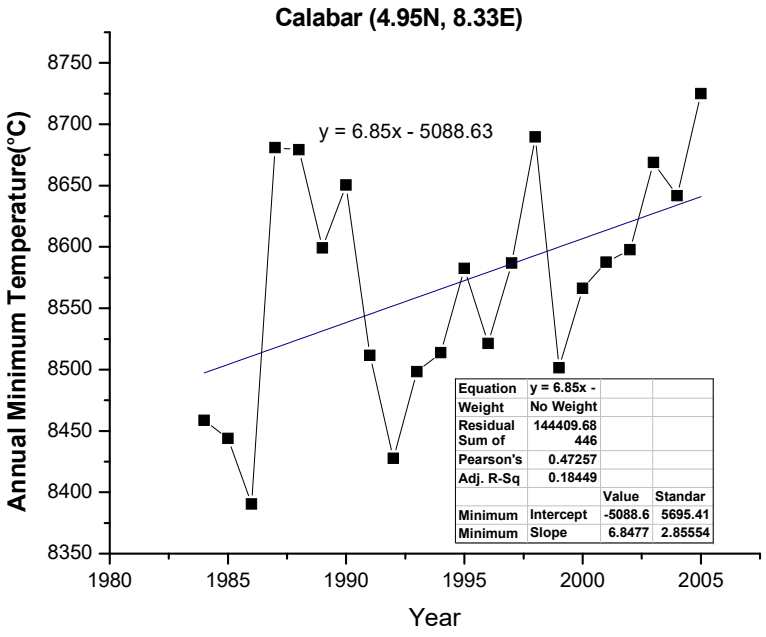

(b)

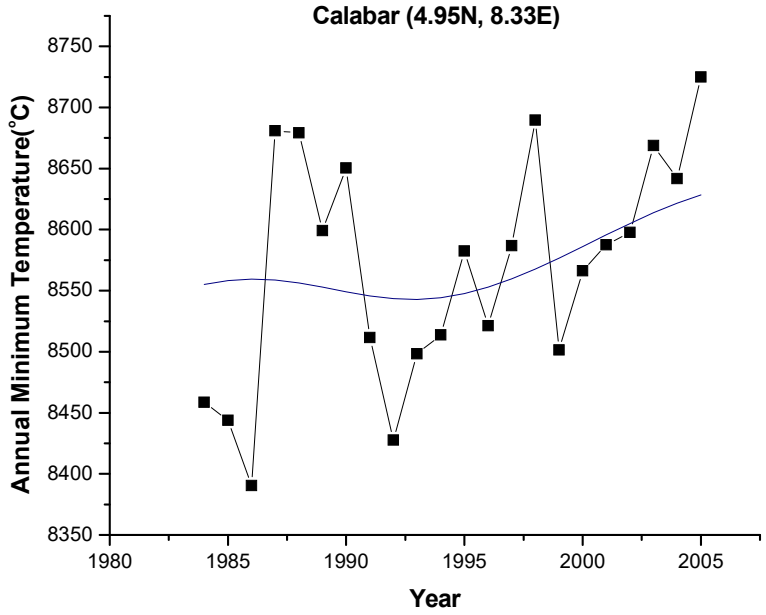

Fig 4.56: (a) Linear trend of Minimum Temperature (Calabar)

(b)Fast Fourier Transform smoothing of the Time series of Minimum Temperature

(a)

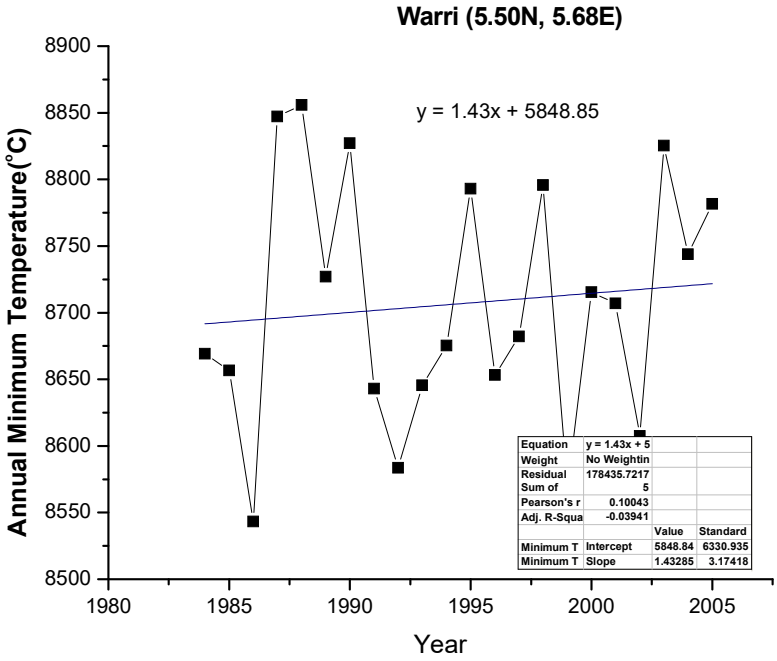

(b)

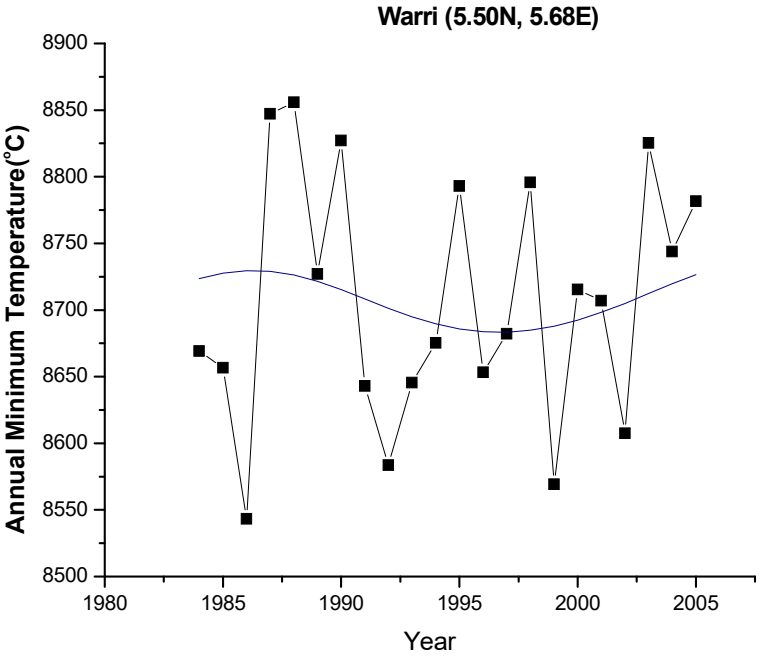

Fig 4.57: (a) Linear trend of Minimum Temperature (Warri)

(b)Fast Fourier Transform smoothing of the Time series of Minimum Temperature

(a)

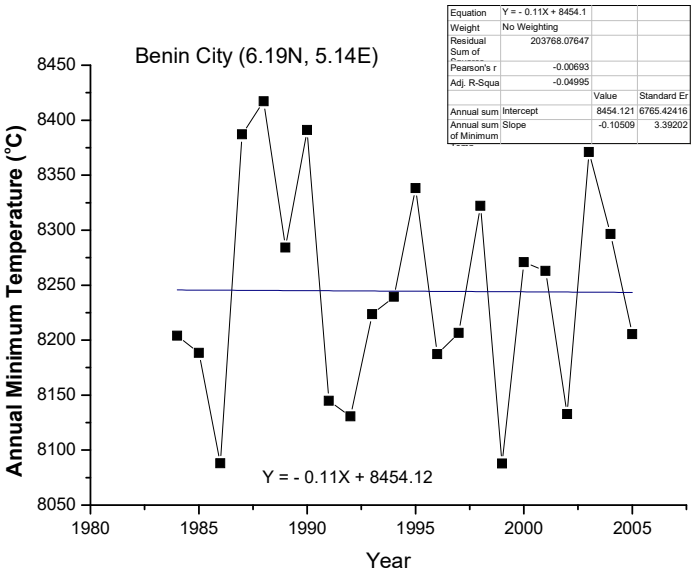

(b)

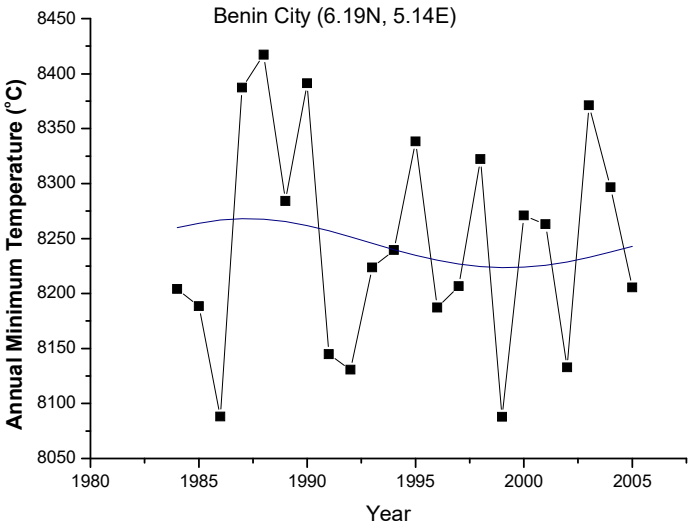

Fig4.58: (a) Linear trend of Minimum Temperature (Benin City)

(b) Fast Fourier Transform smoothing of the Time series of Minimum Temperature

(a)

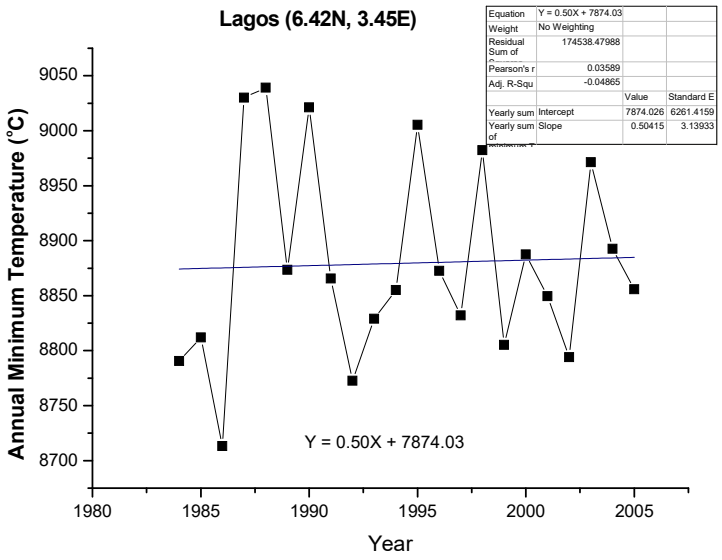

(b)

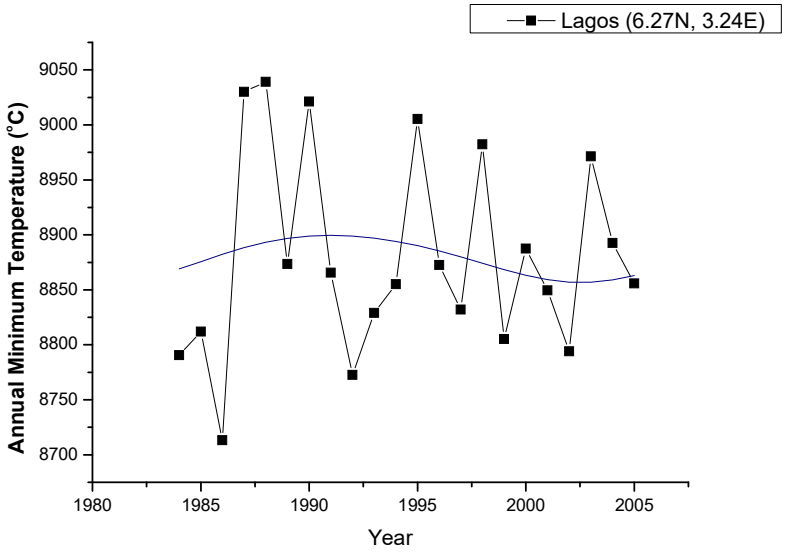

Fig4.59**:** (a)Linear trend of Minimum Temperature (Lagos)

(b) Fast Fourier Transform smoothing of the Time series of Minimum Temperature

(a)

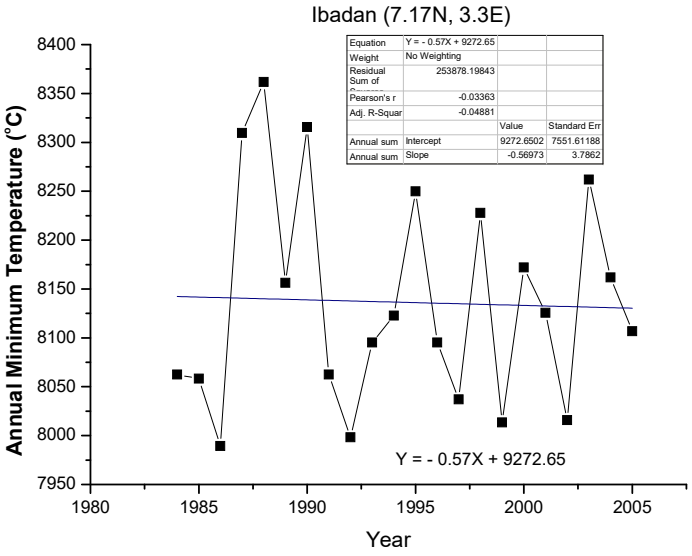

(b)

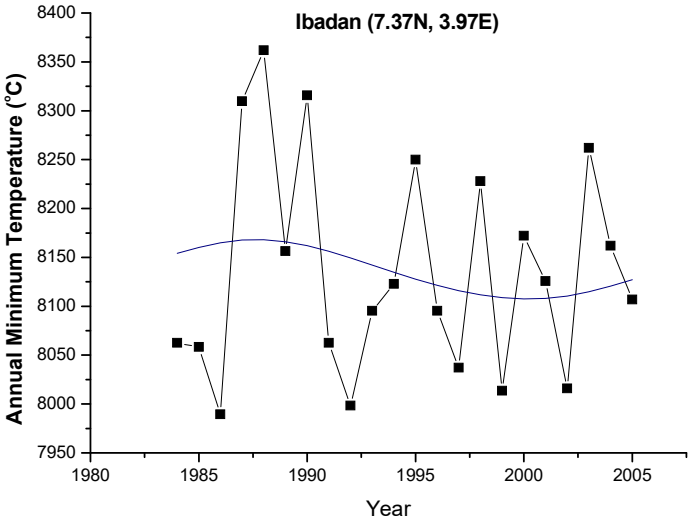

Fig4.60: (a) Linear trend of Minimum Temperature (Ibadan)

(b)Fast Fourier Transform smoothing of the Time series of Minimum Temperature

(a)

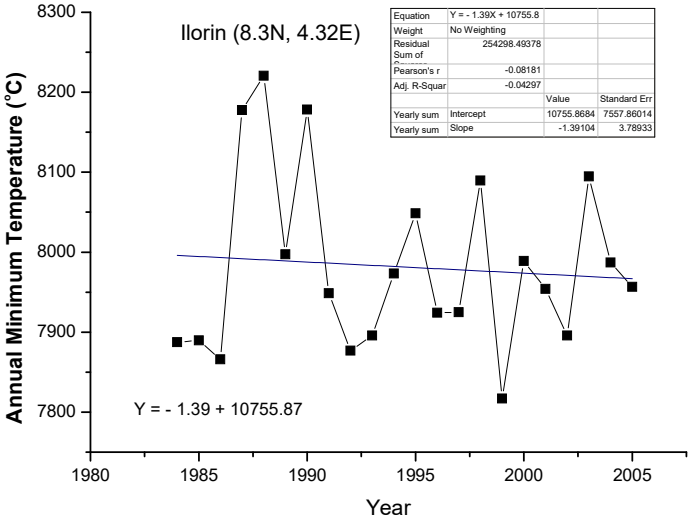

(b)

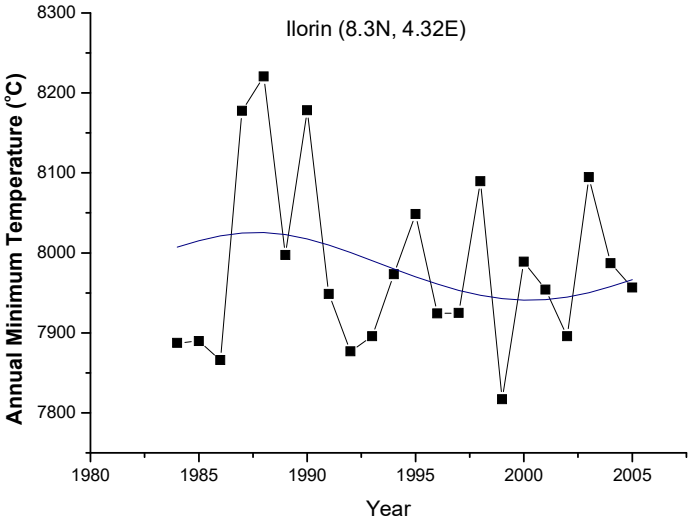

Fig4.61: (a) Linear trend of Minimum Temperature (Ilorin)

(b)Fast Fourier Transform smoothing of the Time series of Minimum Temperature

(a)

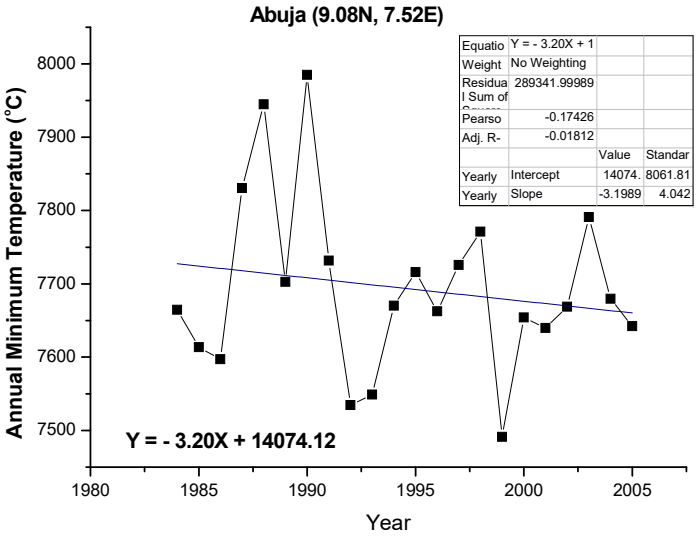

(b)

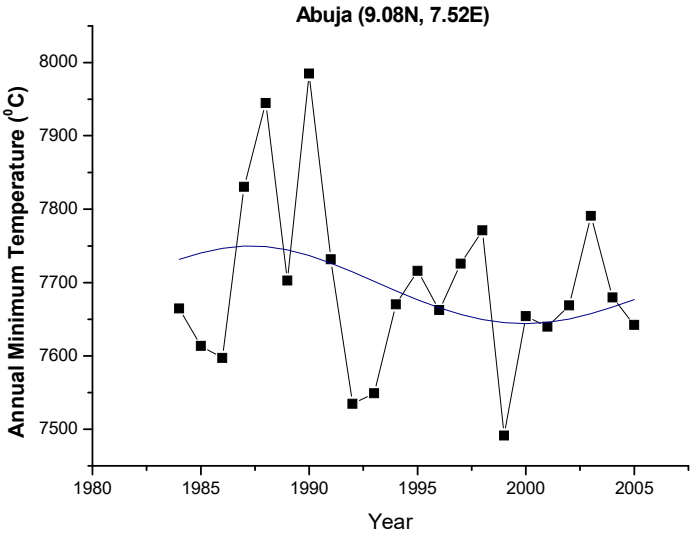

Fig4.62: (a) Linear trend of Minimum Temperature (Abuja)

(b)Fast Fourier Transform smoothing of the Time series of Minimum Temperature

(a)

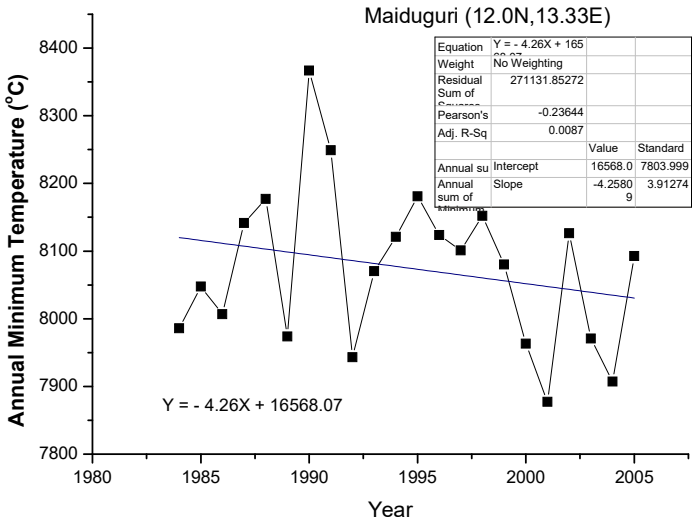

(a)

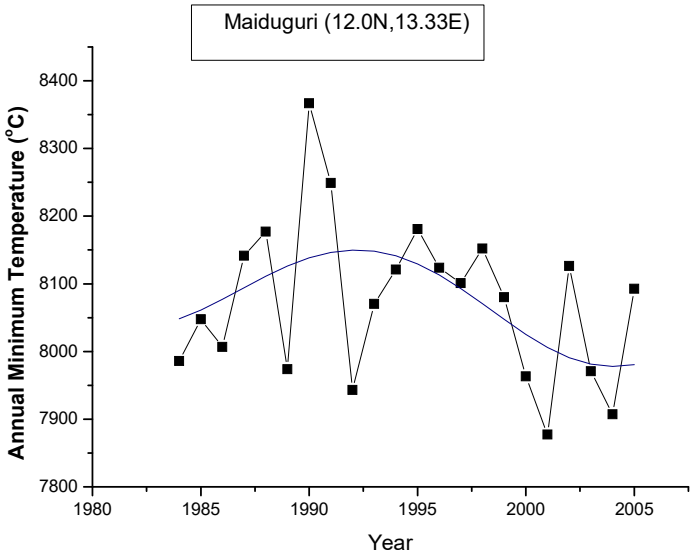

Fig4.63: (a) Linear trend of Minimum Temperature (Maiduguri)

(b)Fast Fourier Transform smoothing of the Time series of Minimum Temperature

(a)

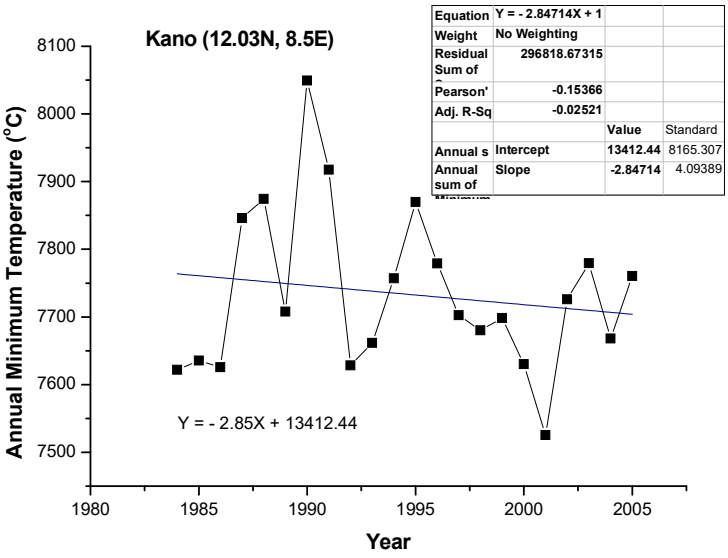

(b)

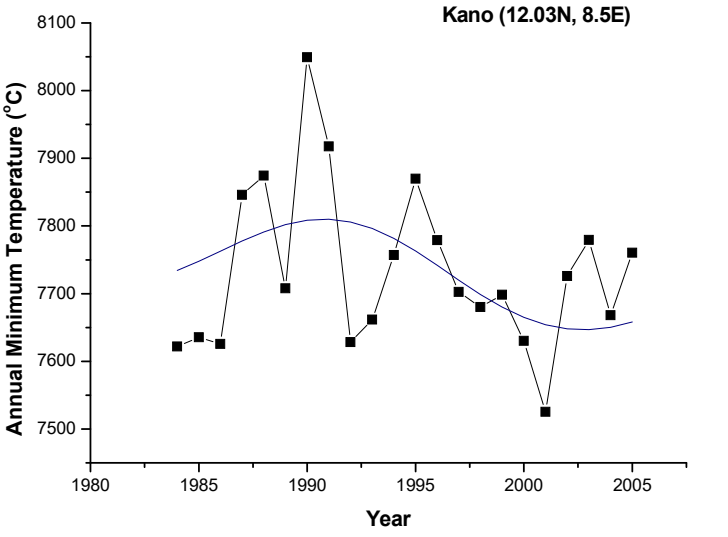

Fig4.64: (a) Linear trend of Minimum Temperature (Kano)

(b)Fast Fourier Transform smoothing of the Time series of Minimum Temperature

(a)

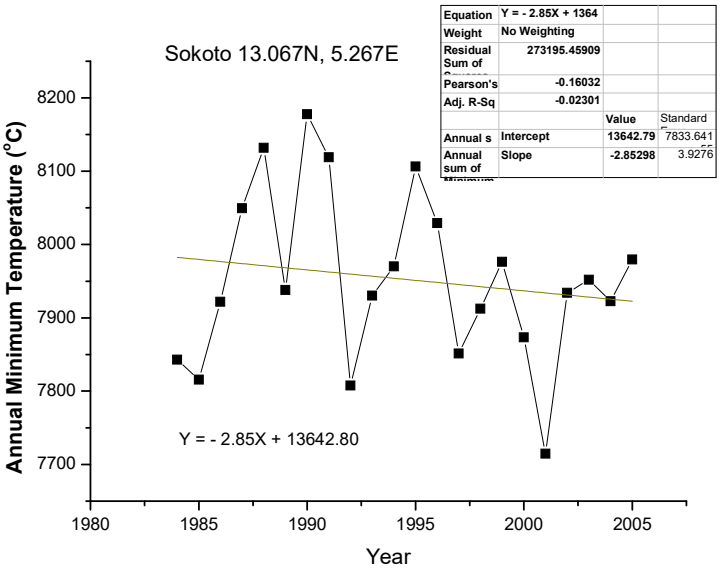

(b)

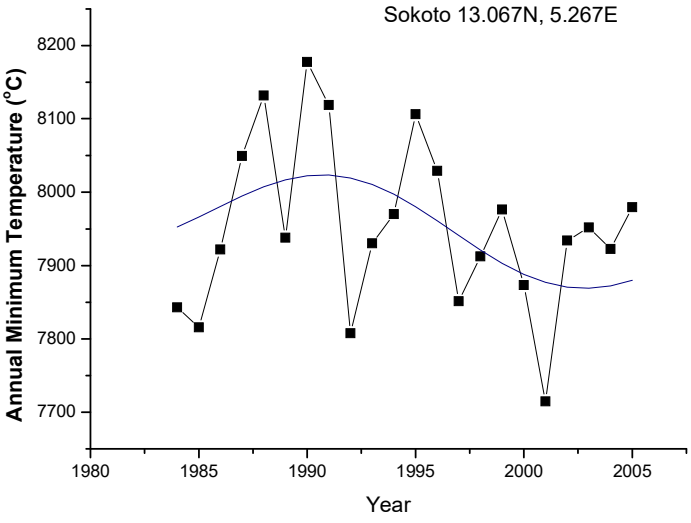

Fig4.65: (a) Linear trend of Minimum Temperature (Sokoto)

(b)Fast Fourier Transform smoothing of the Time series of Minimum Temperature

(a)

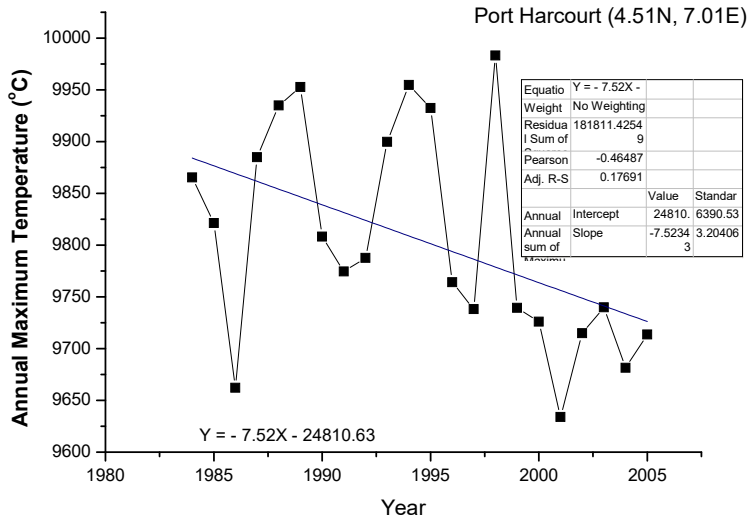

(b)

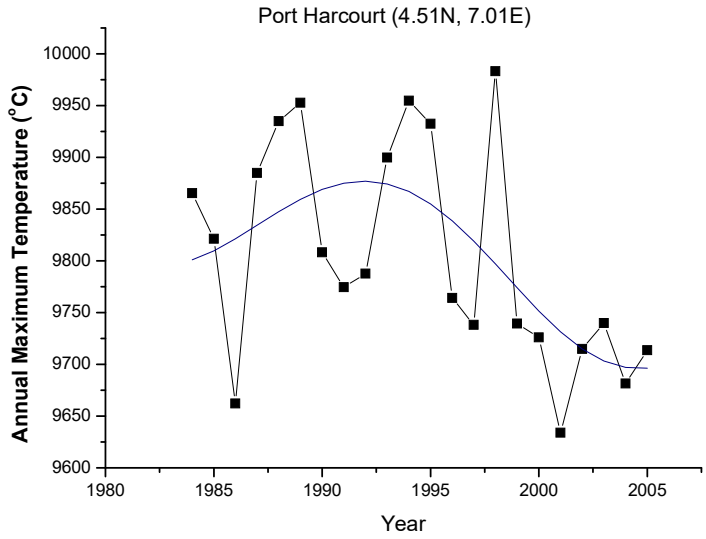

Fig4.66: (a) Linear trend of Maximum Temperature (Port Harcourt)

(b)Fast Fourier Transform smoothing of the Time series of Maximum Temperature

(a)

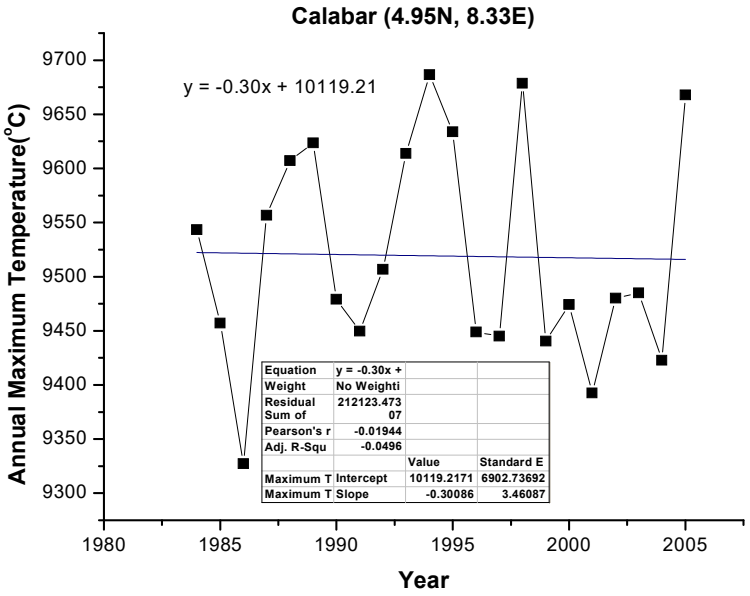

(b)

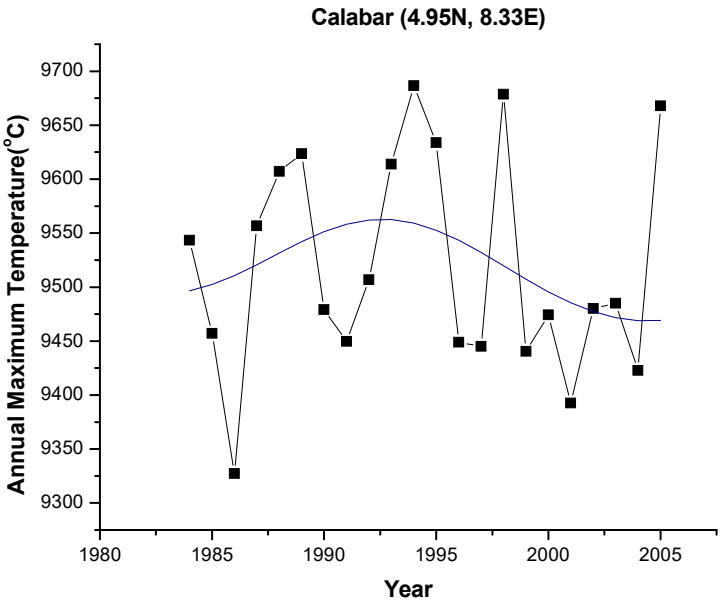

Fig 4.67: (a) Linear trend of Maximum Temperature (Calabar)

(b)Fast Fourier Transform smoothing of the Time series of Maximum Temperature

(a)

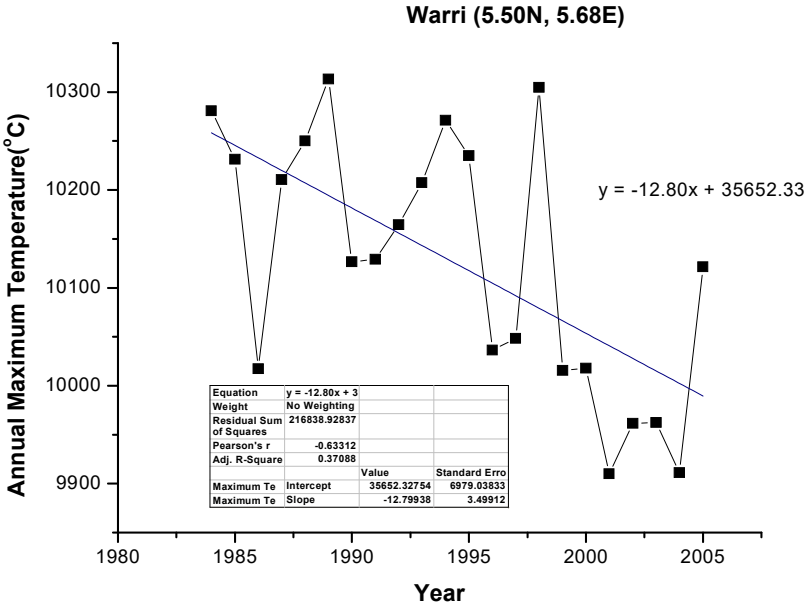

(b)

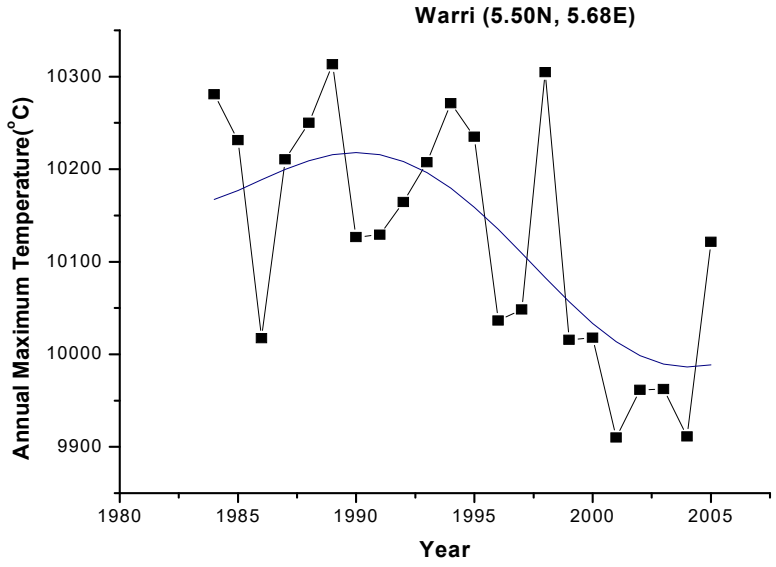

Fig 4.68: (a) Linear trend of Maximum Temperature (Warri)

(b)Fast Fourier Transform smoothing of the Time series of Maximum Temperature

(a)

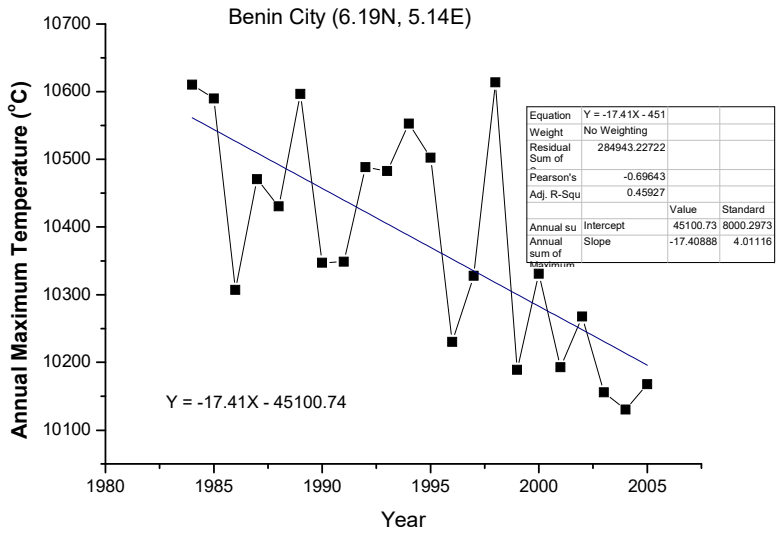

(b)

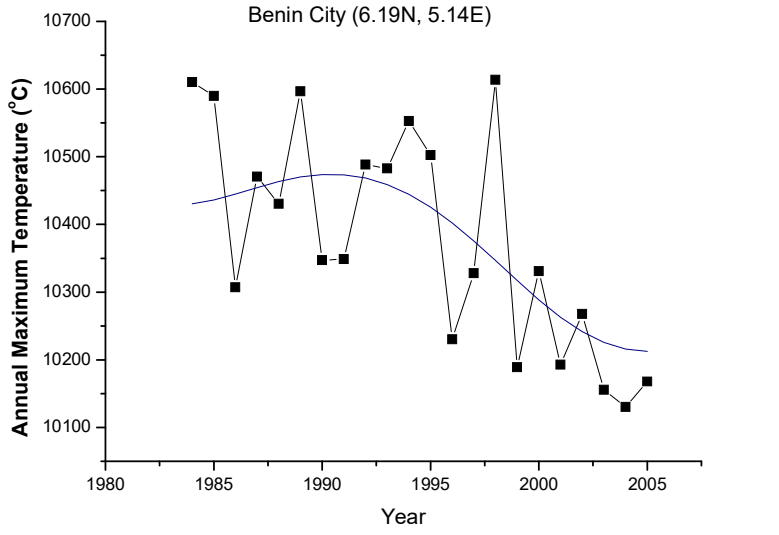

Fig4.69: (a) Linear trend of Maximum Temperature (Benin City)

(b)Fast Fourier Transform smoothing of the Time series of Maximum Temperature

(a)

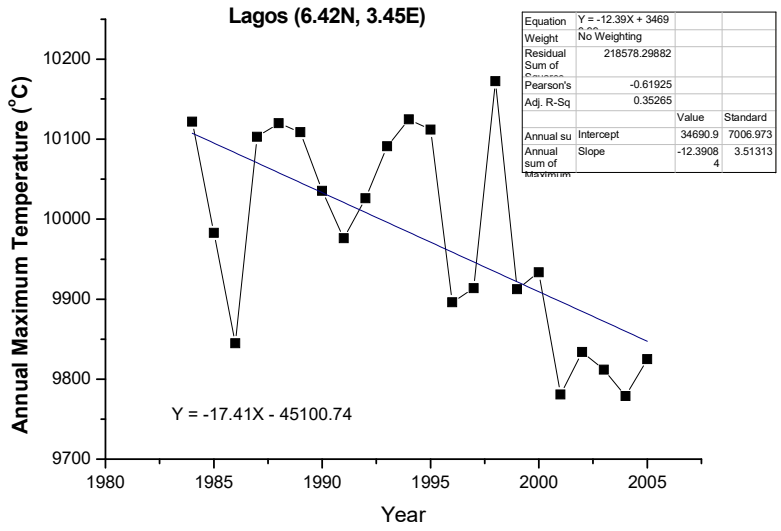

(b)

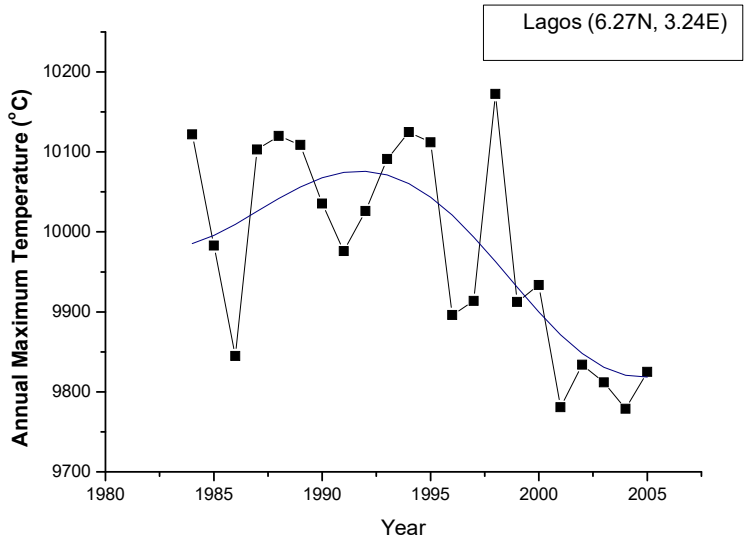

Fig4.70: (a) Linear trend of Maximum Temperature (Lagos)

(b)Fast Fourier Transform smoothing of the Time series of Maximum Temperature

(a)

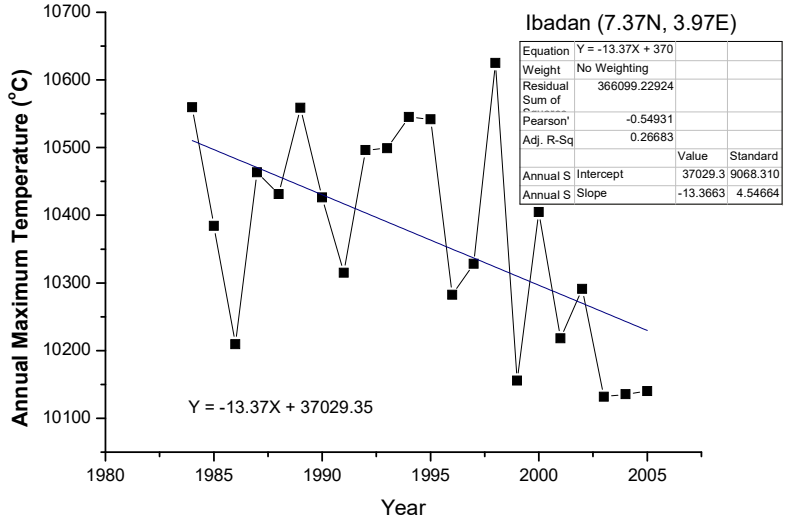

(b)

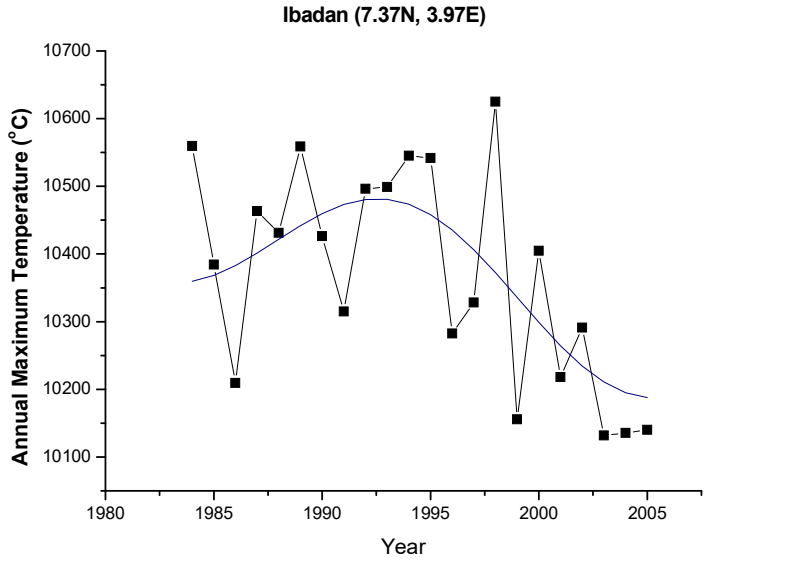

Fig4.71: (a) Linear trend of Maximum Temperature (Ibadan)

(b)Fast Fourier Transform smoothing of the Time series of Maximum Temperature

(a)

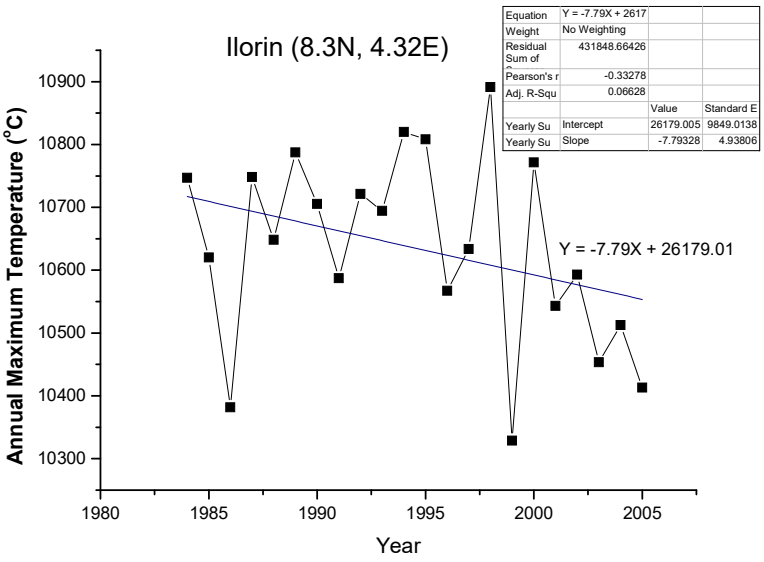

(b)

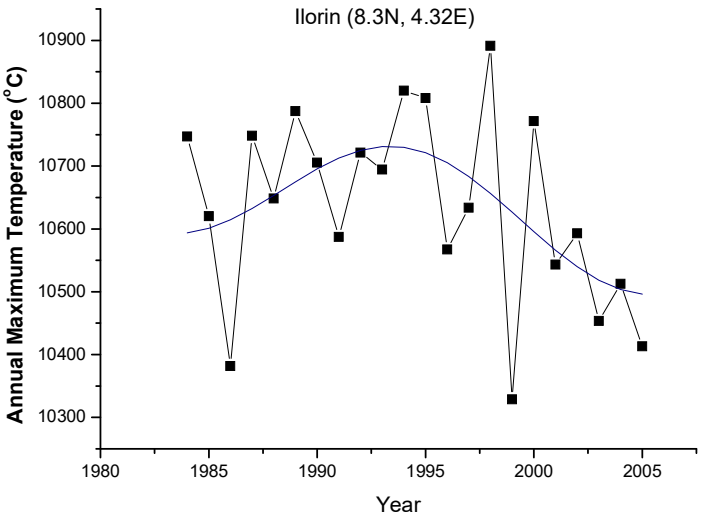

Fig4.72: (a) Linear trend of Maximum Temperature (Ilorin)

(b)Fast Fourier Transform smoothing of the Time series of Maximum Temperature

(a)

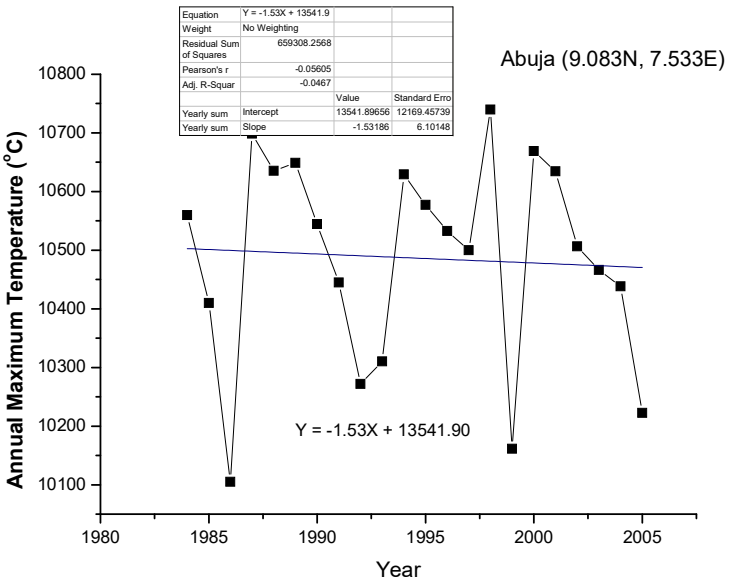

(b)

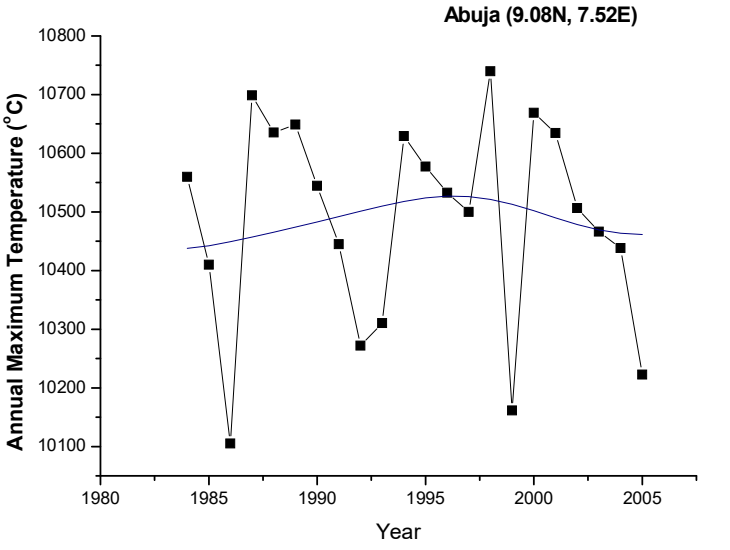

Fig4. 73: (a) Linear trend of Maximum Temperature (Abuja)

(b)Fast Fourier Transform smoothing of the Time series of Maximum Temperature

(a)

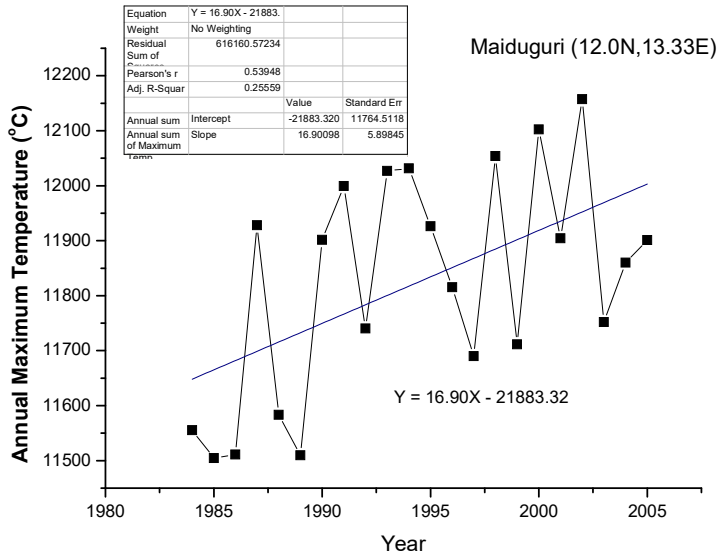

(b)

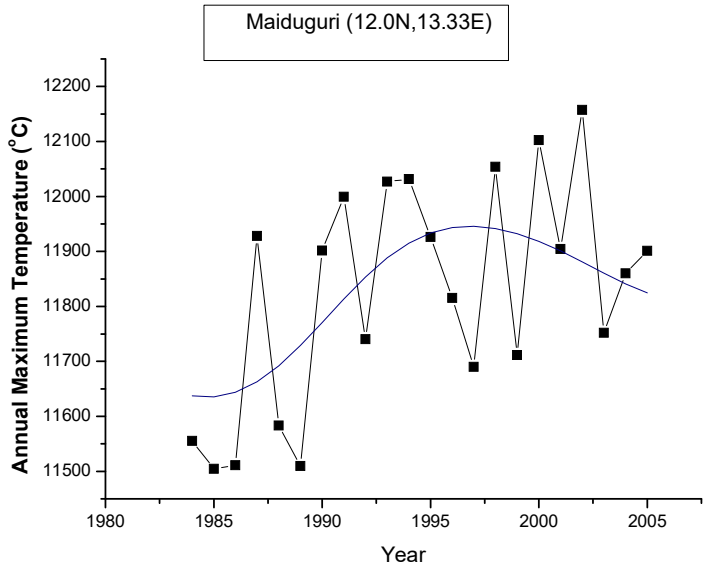

Fig4.74**:** (a)Linear trend of Maximum Temperature (Maiduguri)

(b)Fast Fourier Transform smoothing of the Time series of Maximum Temperature

(a)

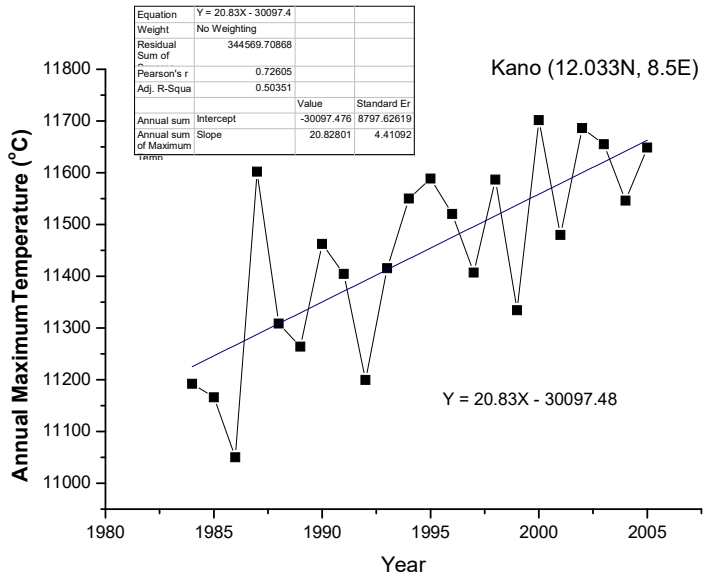

(b)

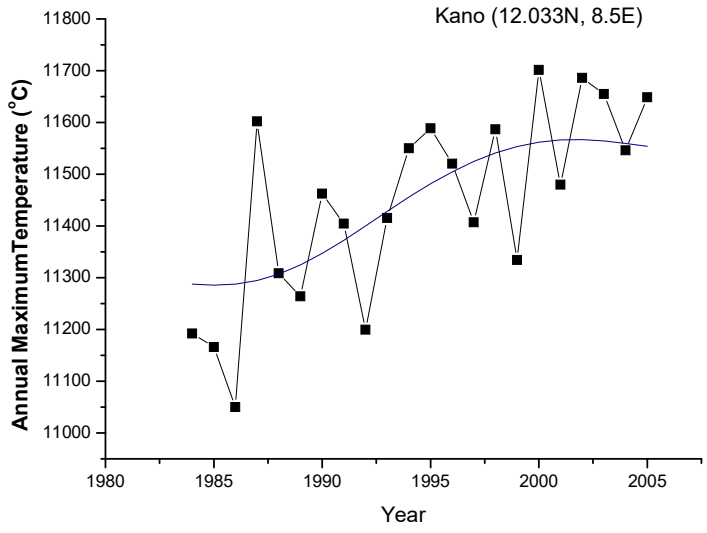

Fig4.75: (a) Linear trend of Maximum Temperature (Kano)

(b)Fast Fourier Transform smoothing of the Time series of Maximum Temperature

(a)

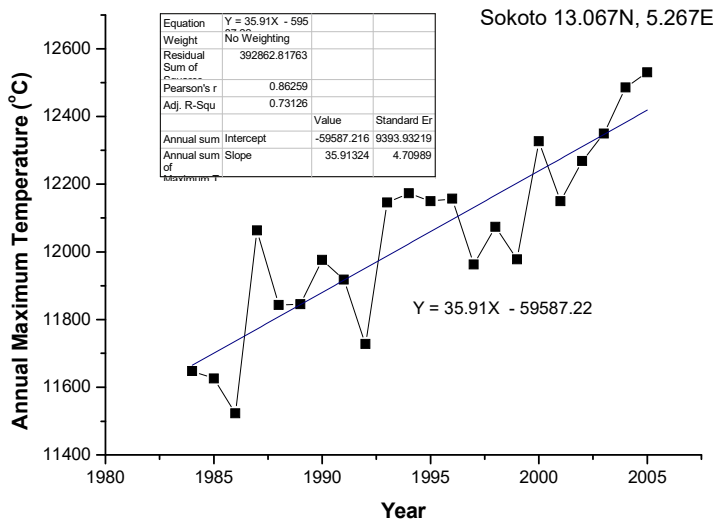

(b)

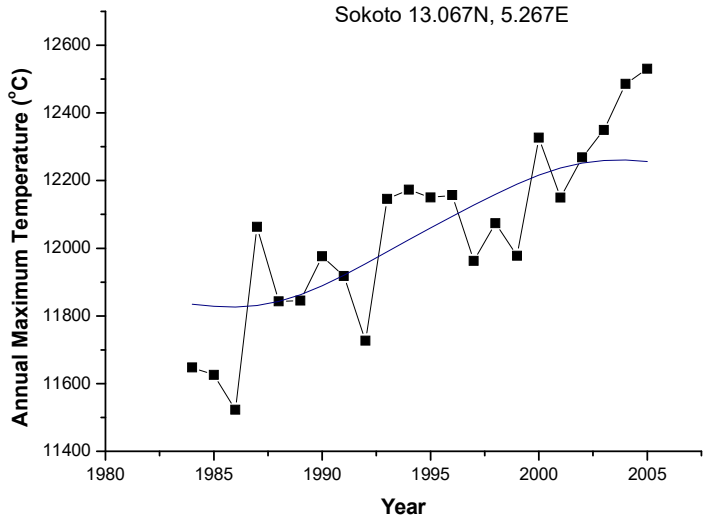

Fig4.76: (a) Linear trend of Maximum Temperature (Sokoto)

(b)Fast Fourier Transform smoothing of the Time series of Maximum Temperature

Table 4.4:Summary of the equations of linear trends

Location	Trend equations	
	Minimum Temperature	Maximum temperature
Port Harcourt	Y = 2.70X + 3371.73	Y = - 7.52X - 24810.63
Calabar	Y = 6.85X - 5088.63	Y = -0.30X + 10119.21
Warri	Y = 1.43X + 5848.85	Y = -12.80X + 35652.33
Benin – City	Y = - 0.11X + 8454.12	Y = -17.41X - 45100.74
Lagos	Y = 0.50X + 7874.03	Y = -12.39X + 34690.99
Ibadan	Y = - 0.57X + 9272.65	Y = -13.37X + 37029.35
Ilorin	Y = - 1.39X + 10755.87	Y = -7.79X + 26179.01
Abuja	Y = - 3.20X + 14074.12	Y = -1.53X + 13541.90
Maiduguri	Y = - 4.26X + 16568.07	Y = 16.90X - 21883.32
Kano	Y = - 2.85X + 13412.44	Y = 20.83X - 30097.48
Sokoto	Y = - 2.85X + 13642.80	Y = 35.91X - 59587.22

Table 4.5: Change in the values of quantities

Location	% ofchangesin thevaluesof the quantities			
	Minimum Temperature (℃)		Maximum Temperature (℃)	
	% of change in values/22Yrs	% of change in values/decade	% of change in values/22Yrs	Of change in values/decade
Port Harcourt	0.65	0.30	- 1.60	-0.73
Calabar	1.69	0.77	- 0.07	-0.03
Warri	0.35	0.16	- 2.62	-1.19
Benin – City	- 0.03	-0.01	- 3.46	-1.57
Lagos	0.12	0.05	- 2.57	-1.17
Ibadan	- 0.34	-0.15	- 2.90	-1.32
Ilorin	- 0.37	-0.17	- 1.53	-0.70
Abuja	-3.50	-1.59	-0.52	-0.24
Maiduguri	- 1.10	-0.50	3.05	1.39
Kano	- 0.77	-0.35	3.89	1.77
Sokoto	- 0.75	-0.34	6.47	2.94

4.5Seasonal Variations of Solar Radiation, Air Temperature and Atmospheric Transmissivity over the region.

In this section, the rainy and dry seasons variation trends of incident solar radiation, minimum and maximum temperatures were computed and the daily means over 22-years plotted against time for all the locations.For the locations below latitude 9.0°N (i.e. Port Harcourt, Calabar, Warri, Benin-City, Lagos, Ibadan and Ilorin), the months of April to October and November to March were taken as rainy and dry seasons respectively, while for locations above 9.0°N (i.e. Abuja. Maiduguri, Kano and Sokoto), May to October and November to April were taken as the rainy and dry seasons respectively. The intention is to examine the seasonal contributions of each of the three parameters to the trend during the years of investigation.

The results showed that over all the stations, the dry season showed a better solar radiation receipt. The rainy season depicted a downward trend in incident solar radiation for all the locations. The poor solar radiation receipt of solar radiation during rainy season is as a result of the increased cloudiness during this period which reflects and absorbs incoming shortwave radiation. During the dry season, Lagos (Fig 4.89a) and Abuja (Fig 4.98a) showed an upward trend in the incident solar radiation, while Maiduguri, Kano and Sokoto (Figs 101a, 104a and 107a) all depicted a downward trend between 1984 to the mid-nineties and then an upward trend to 2005.

From Table.4.7, a notable difference is seen in the rates of change of the minimum temperatures between the dry and the rainy seasons. In Lagos, Ibadan, Ilorin, Maiduguri and Sokoto, nights have been progressively getting warmer during the raining season, and progressively getting cooler during the dry seasons over the years of investigation. As stated earlier, this observed increase in the minimum temperature could only be due to the absorption of the longwave radiation by the cloud which is much abundant during the raining season. Minimum temperature in Port Harcourt showed an upward trend during both dry and rainy seasons. However, the rate of the increase during the rainy season is much larger than that of the dry season. Nighttime temperatures trends depict a gradual decrease of similar magnitude in Abuja and Kano during the two seasons.

The rate of change of the maximum temperature during the years of investigation exhibitsa little variation between the two seasons for most of the locations.For Port

Harcourt, Calabar, Warri, Benin-city, Lagos, Ibadan and Ilorin, the trends depict a larger decrease during the dry season than rainy season. The magnitudes of the decrease in the trends for Abuja for the two seasons are about equal. Maiduguri, Kano and Sokoto experienced an increasing trend in maximum temperature for the two seasons, with rainy season having a higher magnitude than the dry season throughout the years of investigation.

(a)

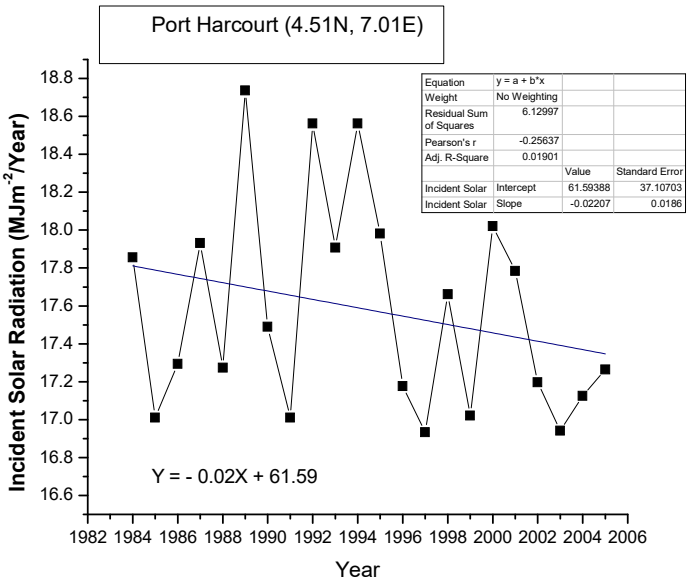

(b)

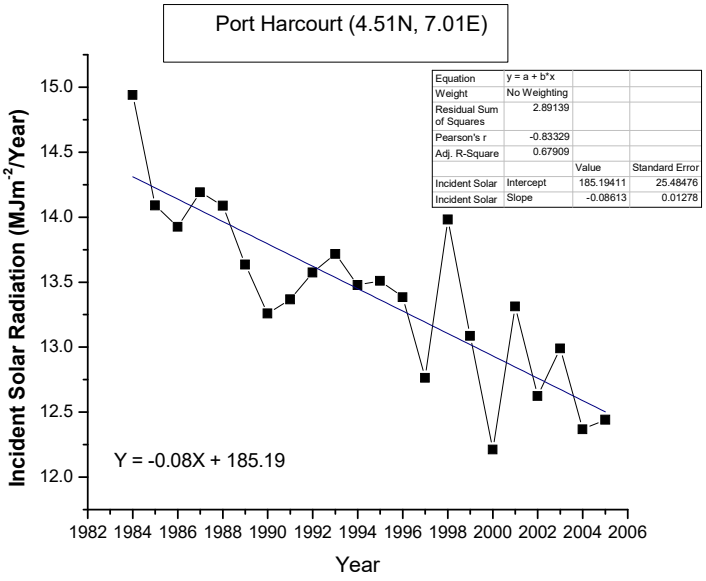

Fig 4.77: (a) Dry Season Trend of Solar Radiation

(b) Rainy Season Trend of Solar Radiation

(a)

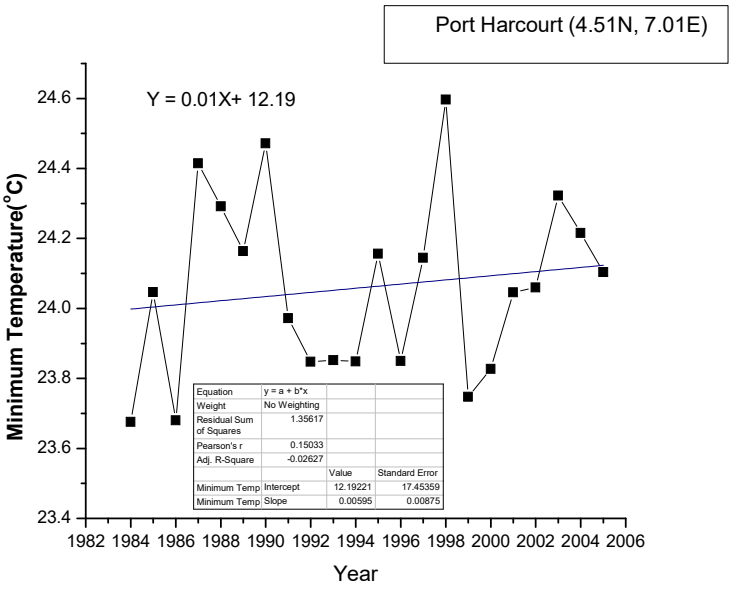

(b)

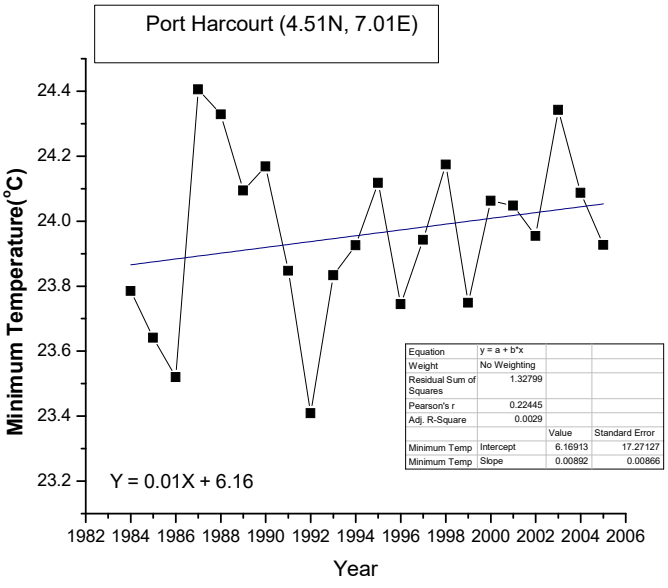

Fig 4.78: (a) Dry Season Trend of Minimum Temperature

(b)Rainy Season Trend of Minimum Temperature

(a)

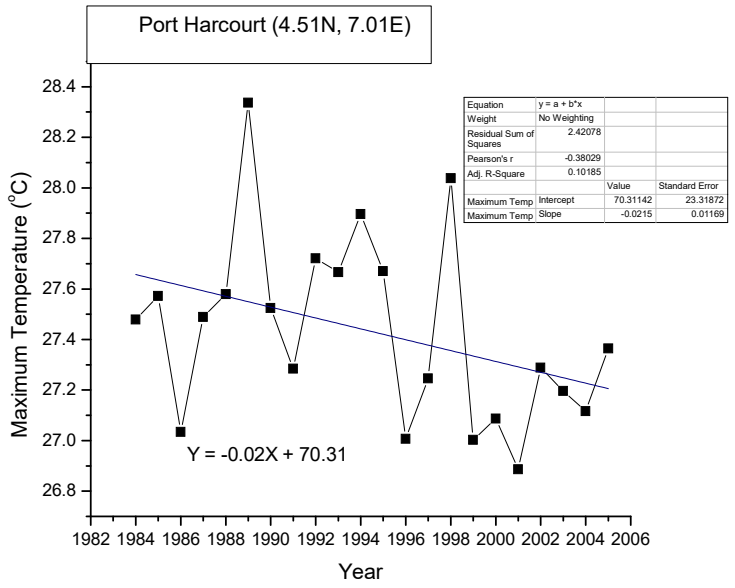

(b)

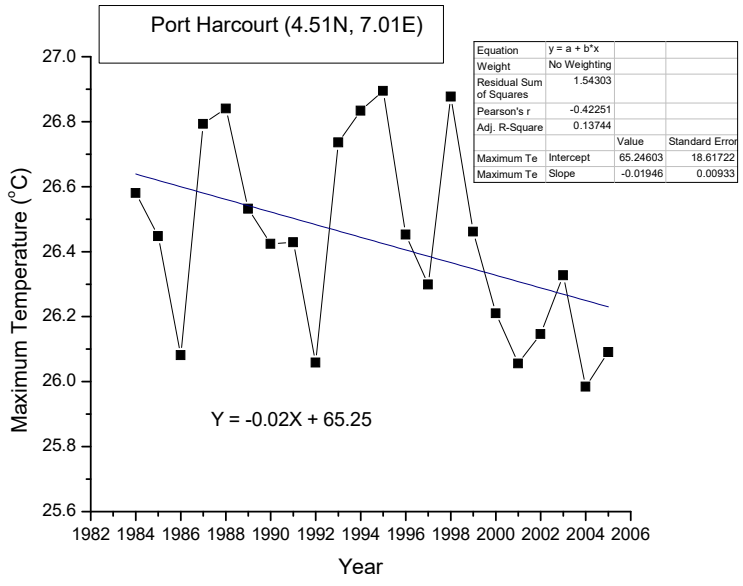

Fig 4.79: (a) Dry Season Trend of Maximum Temperature

(b)Rainy Season trend of Maximum Temperature

(a)

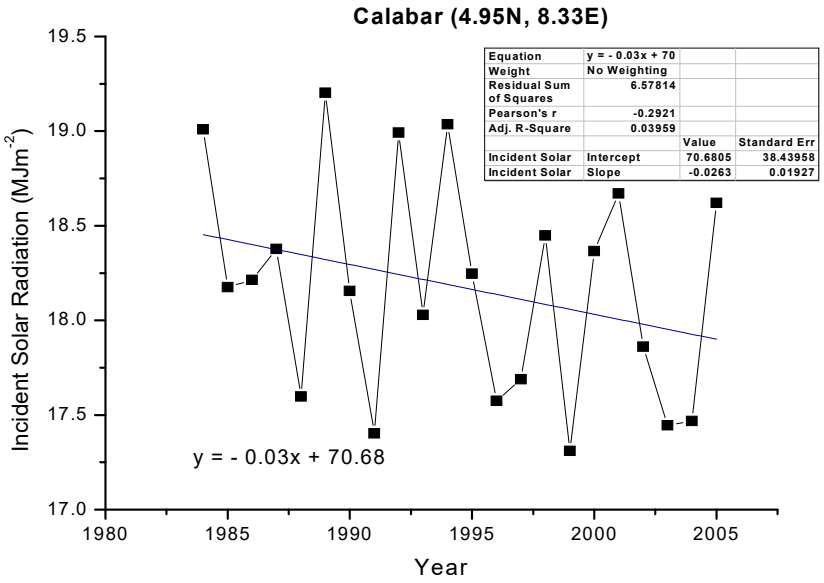

(b)

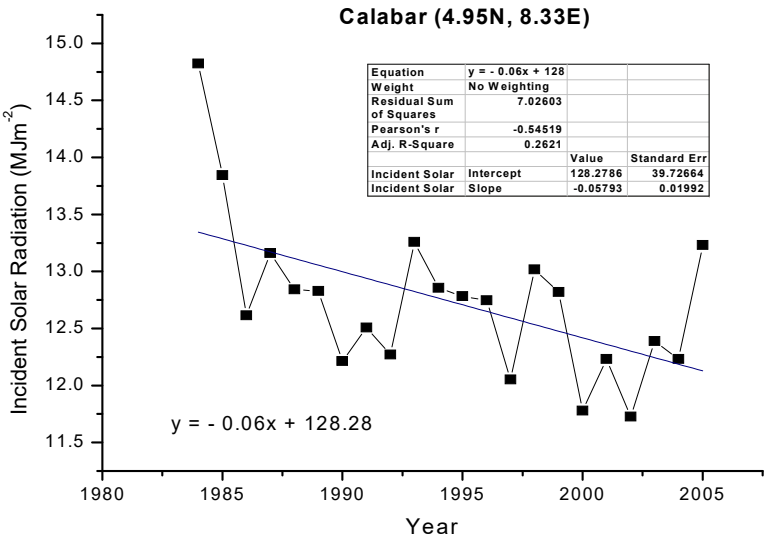

Fig 4.80: (a) Dry Season Trend of Solar Radiation

(b) Rainy Season Trend of Solar Radiation

(a)

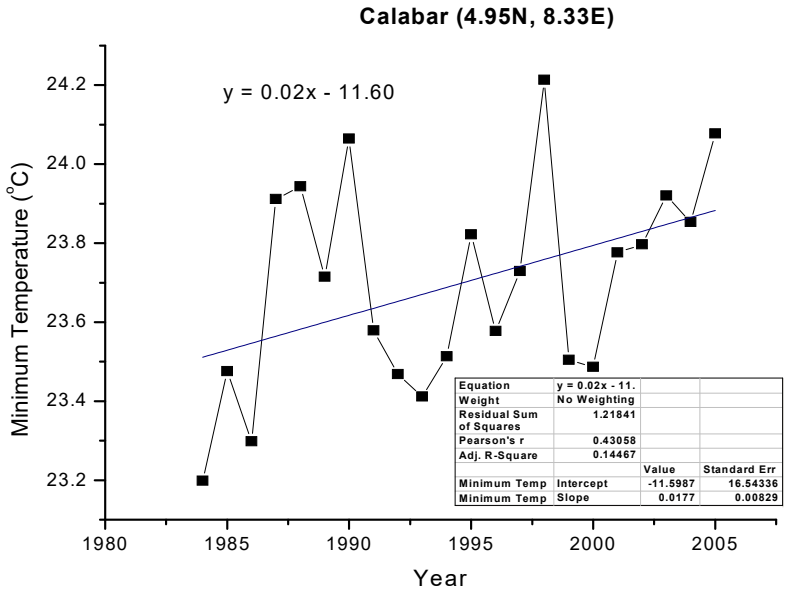

(b)

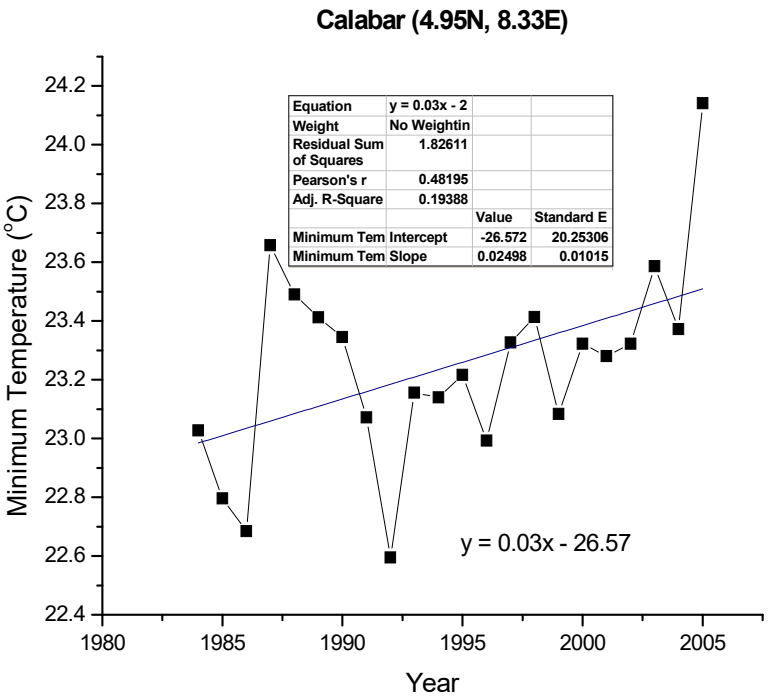

Fig 4.81:(a) Dry Season Trend of Minimum Temperature

(b) Rainy Season Trend of Minimum Temperature

(a)

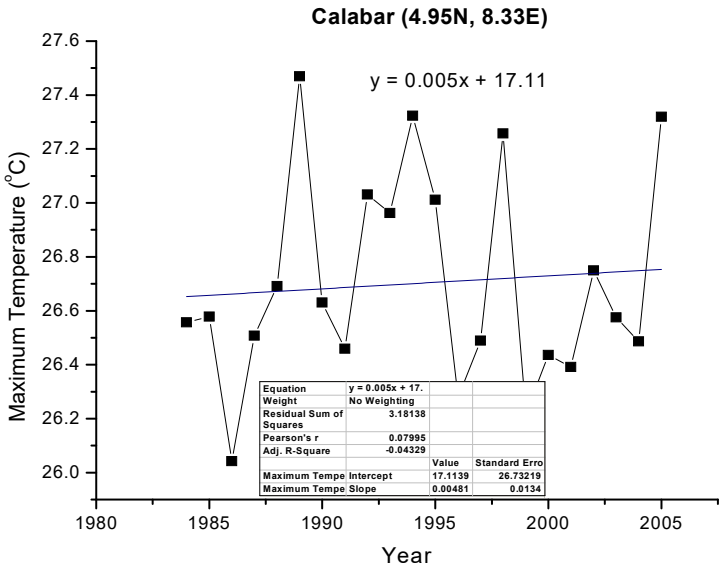

(b)

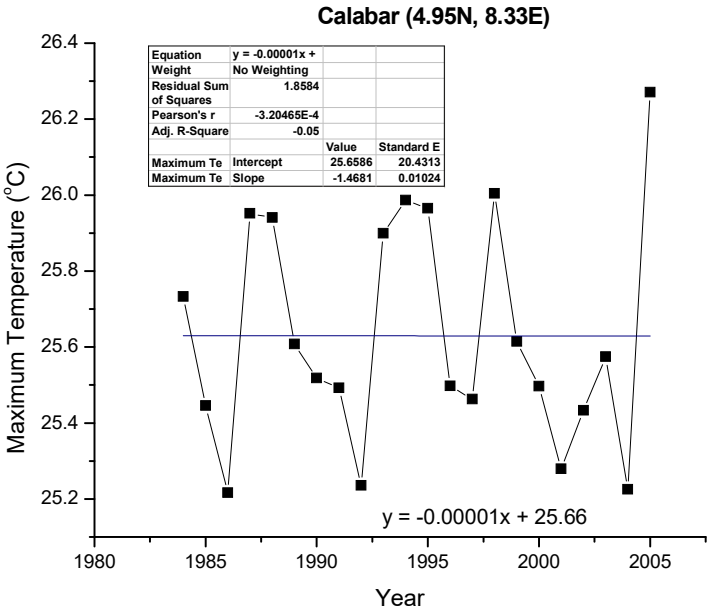

Fig 4.82: (a) Dry Season Trend of Maximum Temperature

(b) Rainy Season Trend of Maximum Temperature

(a)

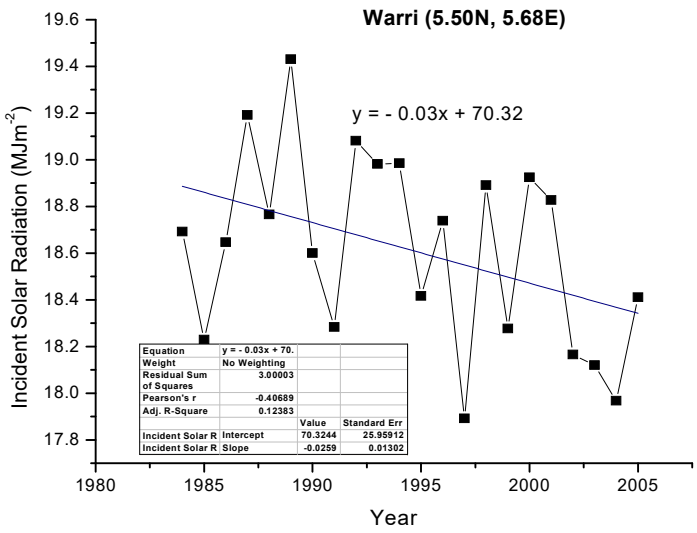

(b)

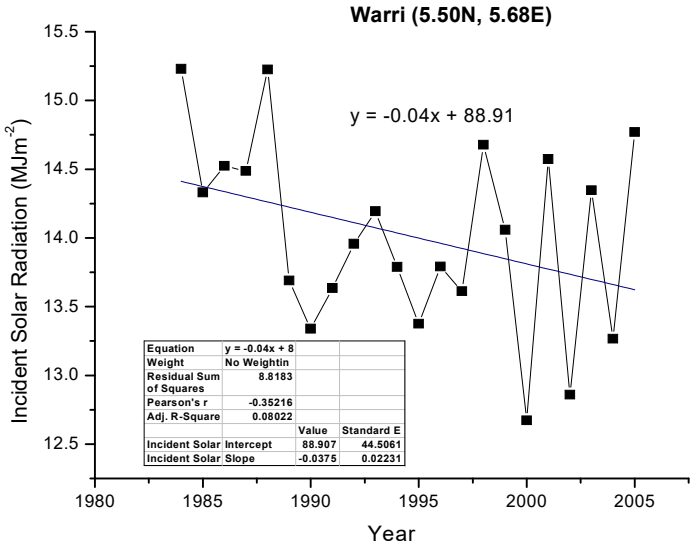

Fig 4.83: (a) Dry Season Trend of Solar Radiation

(b) Rainy Season Trend of Solar Radiation

(a)

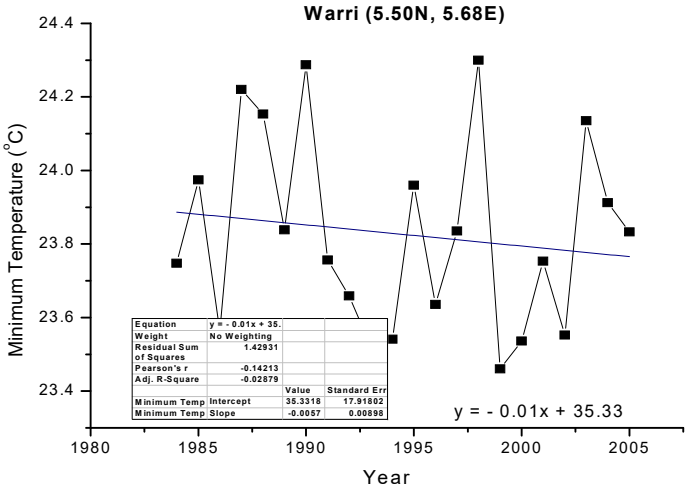

(b)

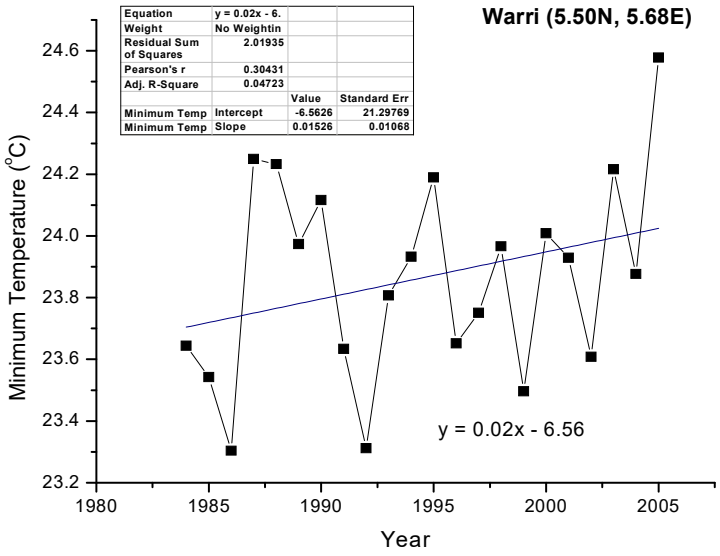

Fig 4.84: (a) Dry Season Trend of Minimum Temperature

(b) Rainy Season Trend of Minimum Temperature

(a)

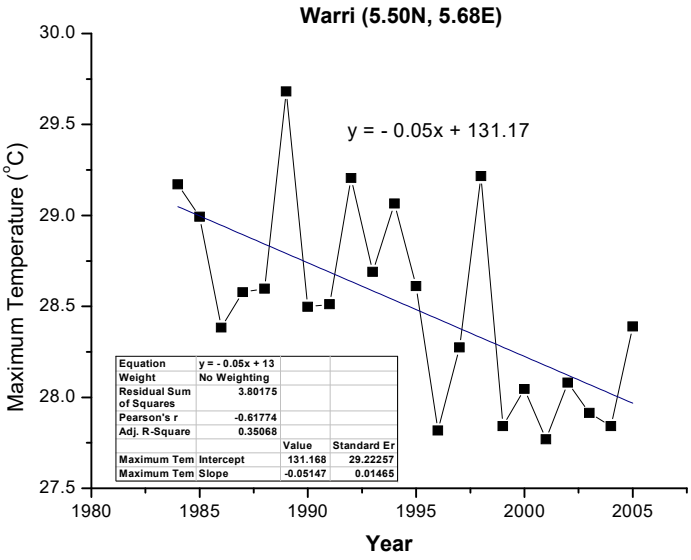

(b)

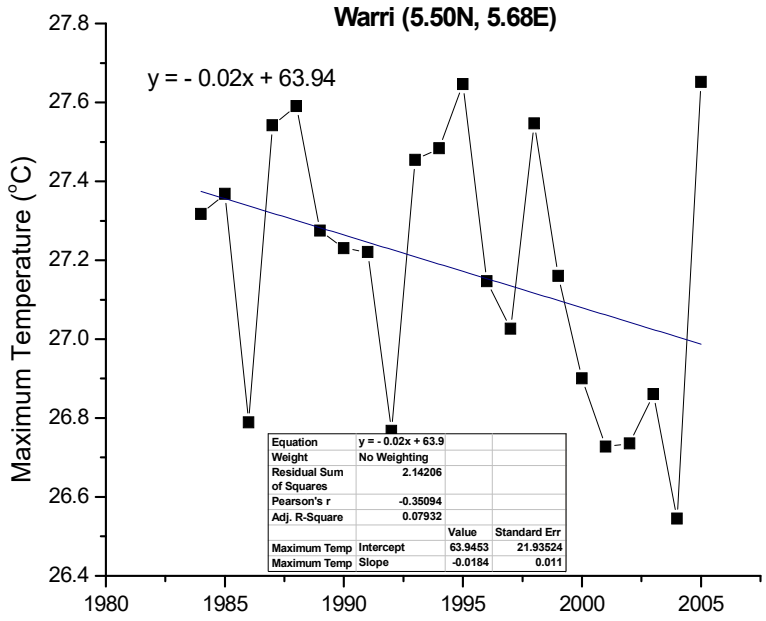

Fig 4.85: (a) Dry Season Trend of Maximum Temperature

(b) Rainy Season Trend of Maximum Temperature

(a)

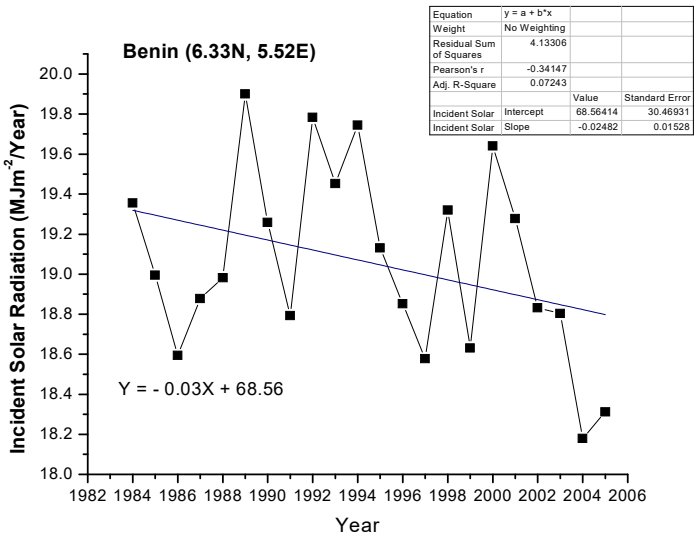

(b)

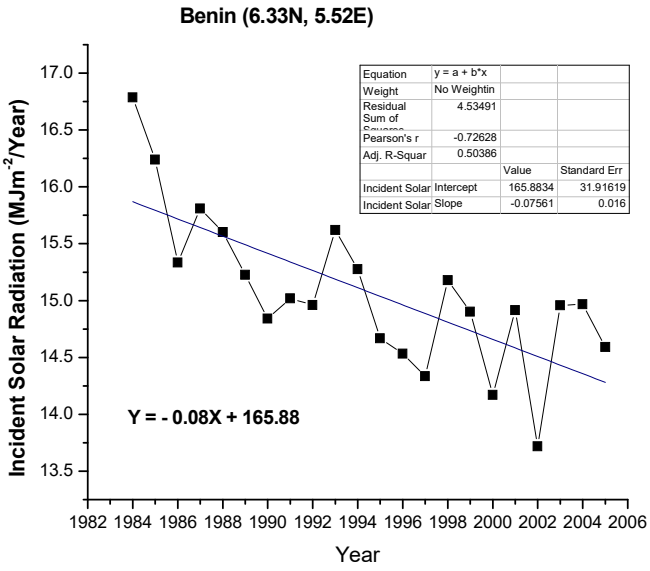

Fig 4.86: (a) Dry Season Trend of Solar Radiation

(b) Rainy Season Trend of Solar Radiation

(a)

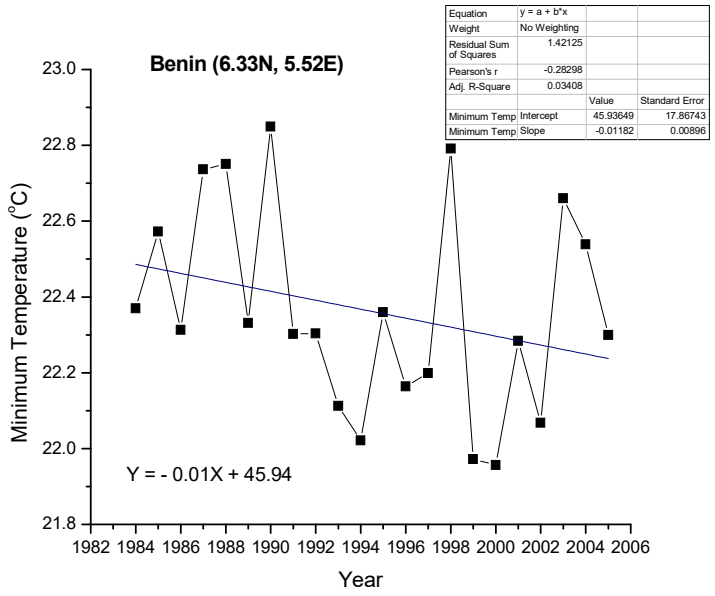

(b)

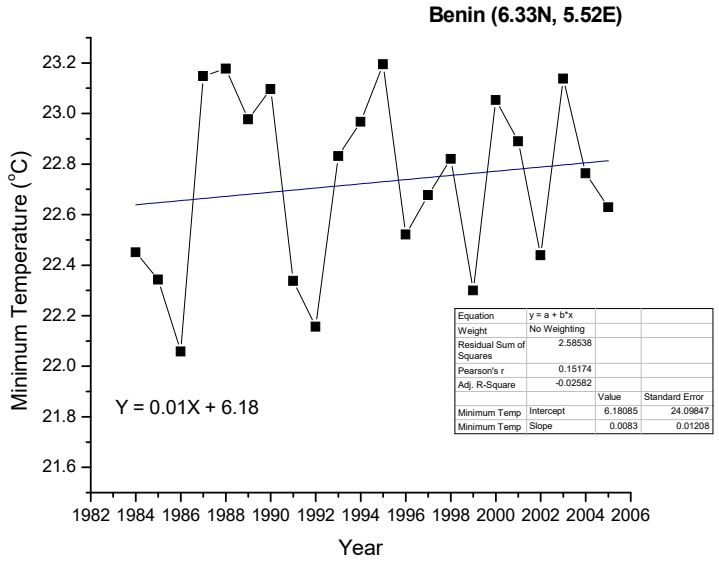

Fig 4.87: (a) Dry Season Trend of Minimum Temperature

(b)Rainy Season Trend of Minimum temperature

(a)

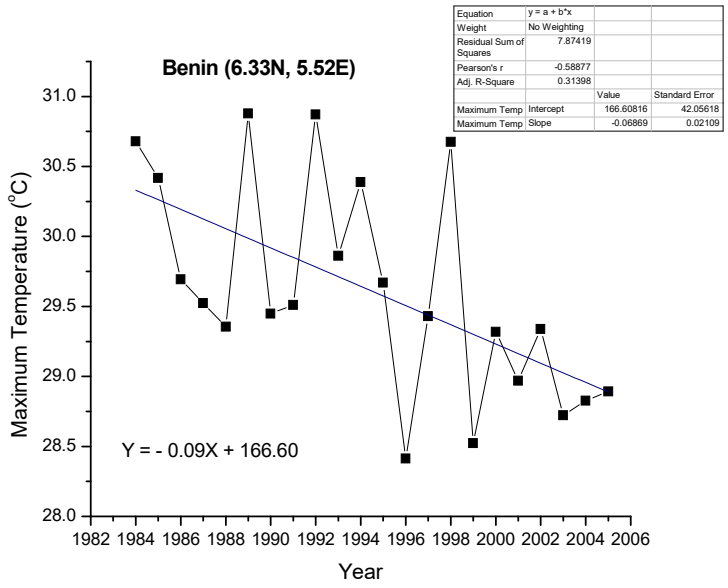

(b)

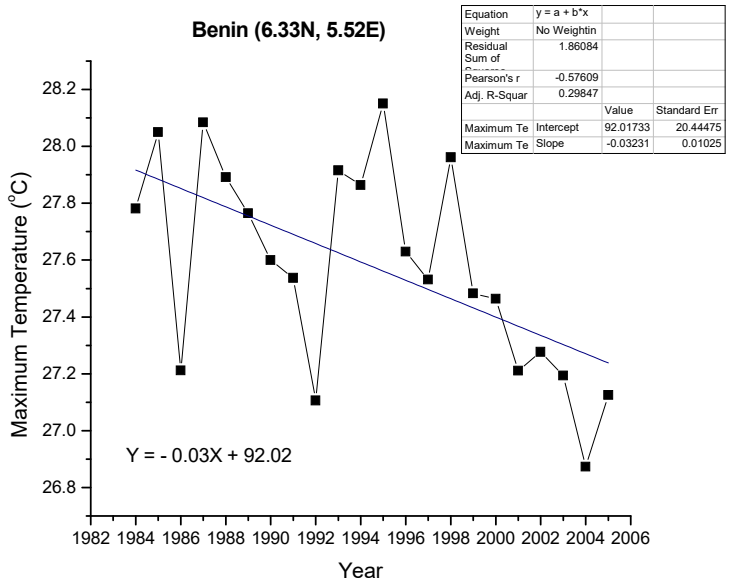

Fig 4.88: (a) Dry Season Trend of Maximum Temperature

(b)Rainy Season Trend of Maximum Temperature

(a)

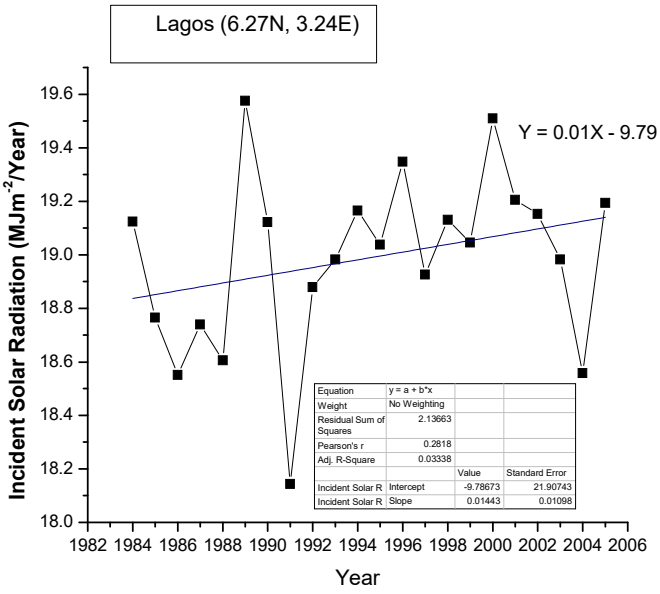

(b)

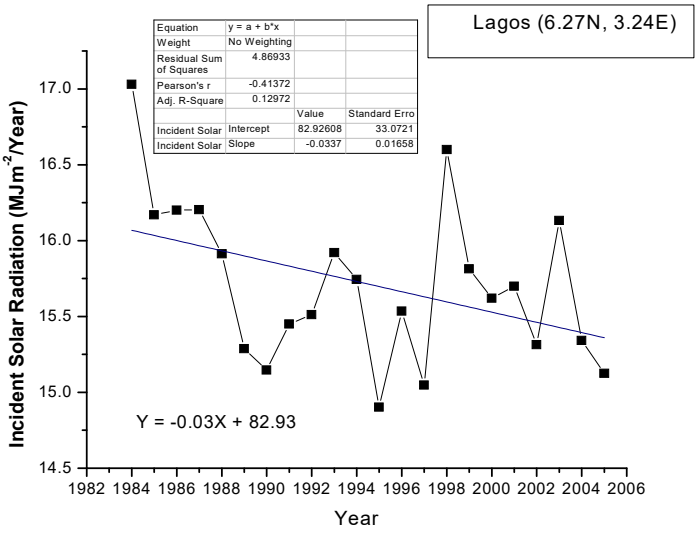

Fig 4.89: (a) Dry Season Trend of Solar Radiation

(b)Rainy Season Trend of Solar Radiation

(a)

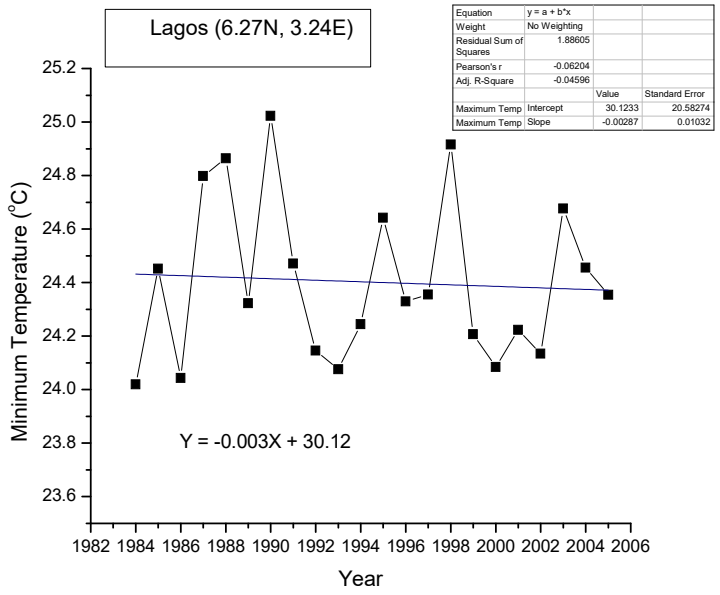

(b)

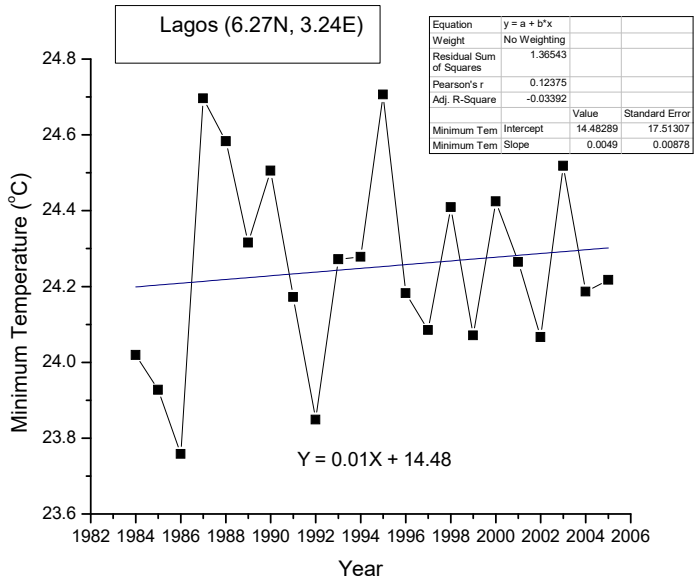

Fig 4.90: (a) Dry Season Trend of Minimum Temperature

(b)Rainy Season Trend of Minimum Temperature

(a)

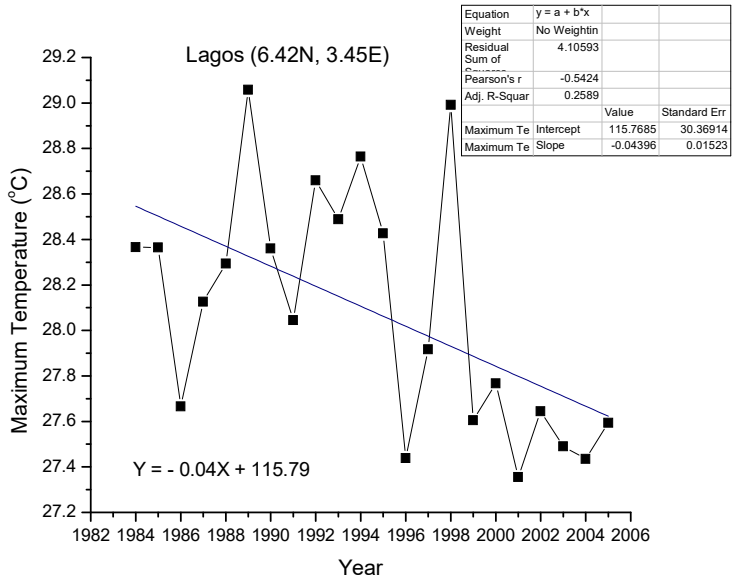

(b)

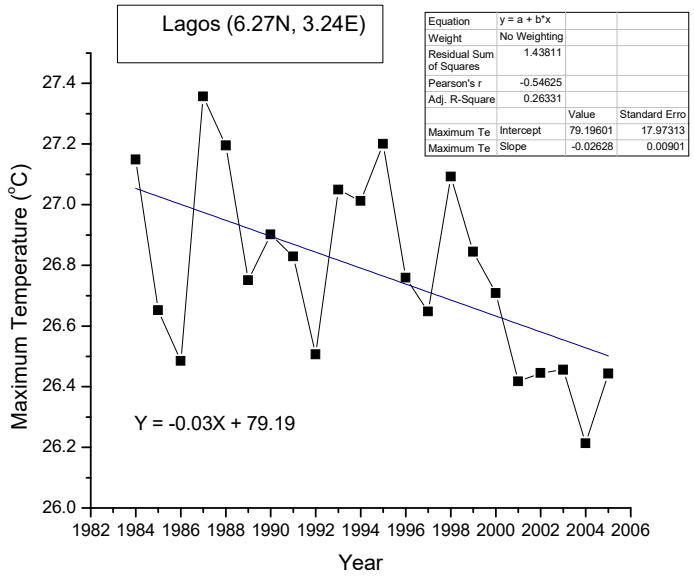

Fig 4.91: (a) Dry Season Trend of Maximum Temperature

(b)Rainy Season Trend of Maximum Temperature

(a)

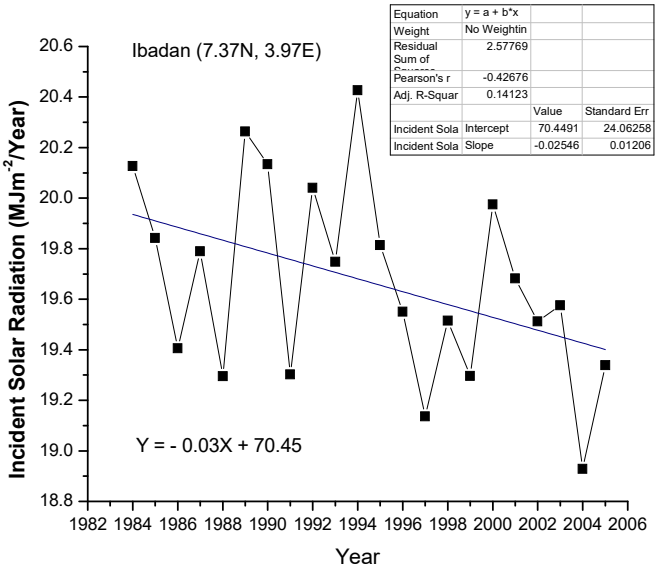

(b)

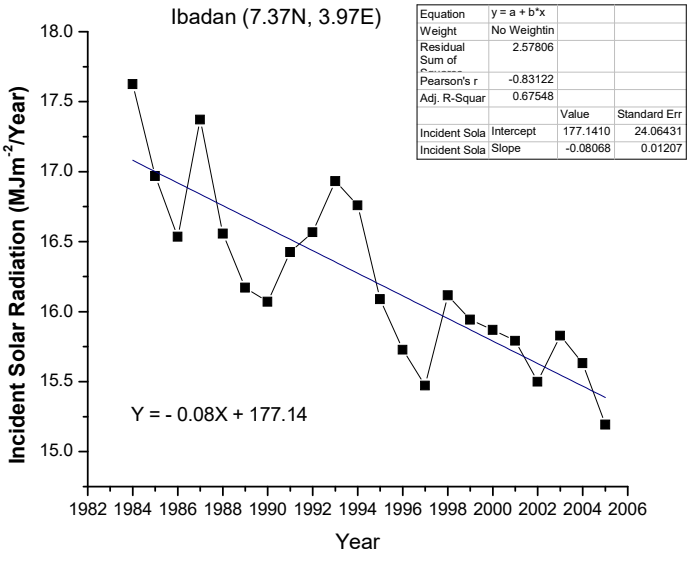

Fig 4.92: (a) Dry Season Trend of Solar Radiation

(b)Rainy Season Trend of Solar Radiation

(a)

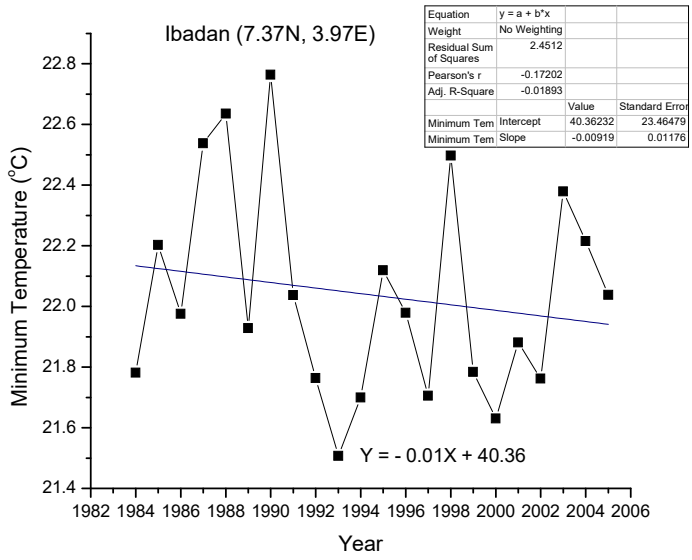

(b)

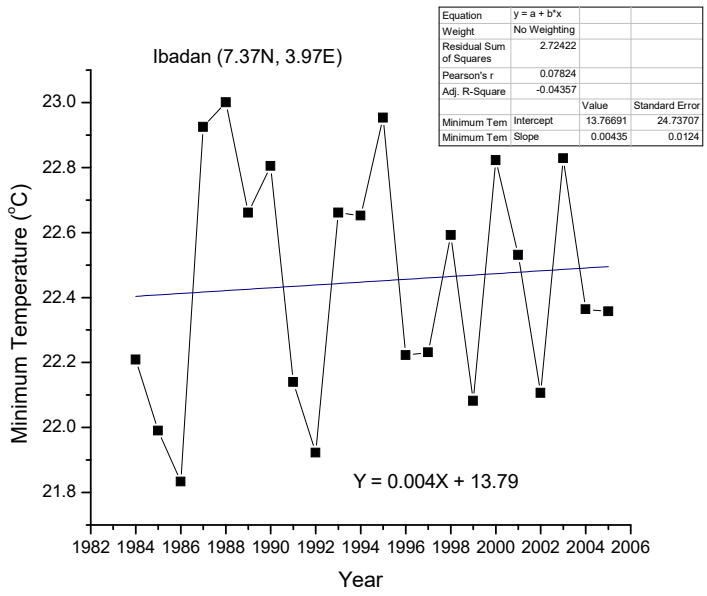

Fig 4.93: (a) Dry Season Trend of Minimum Temperature

(b) Rainy Season Trend of Minimum Temperature

(a)

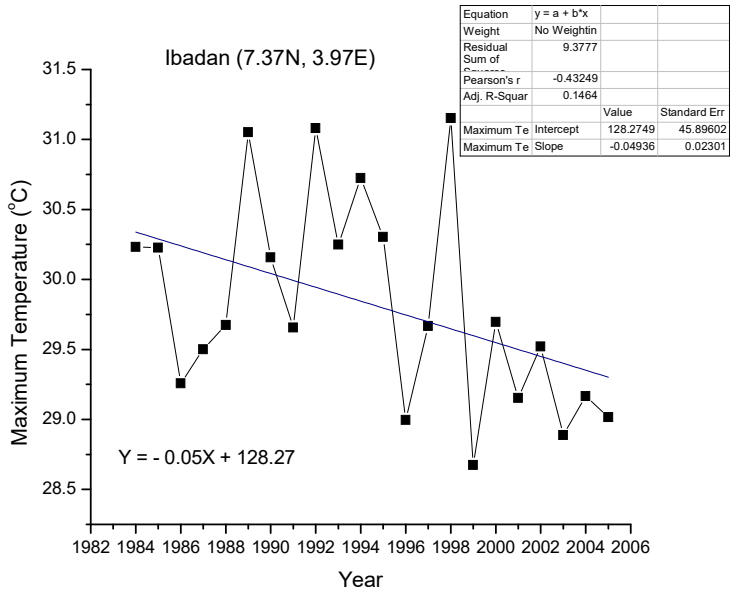

(b)

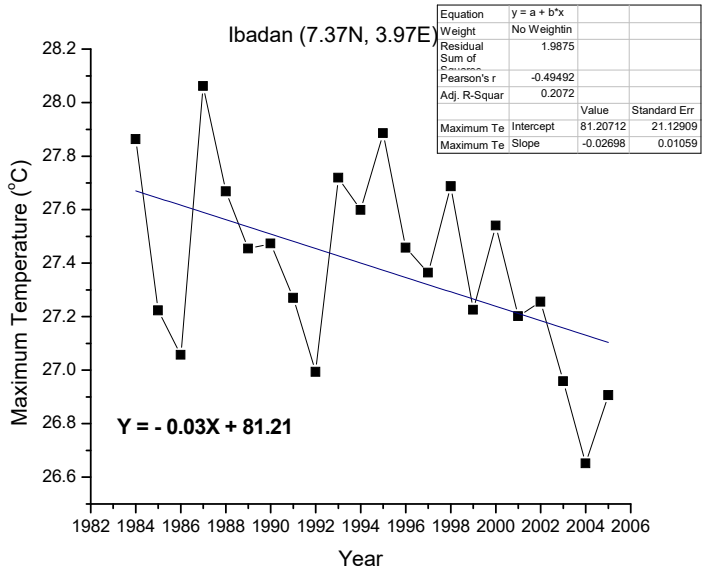

Fig 4.94: (a) Dry Season Trend of Maximum Temperature

(b)Rainy Season Trend of Maximum Temperature

(a)

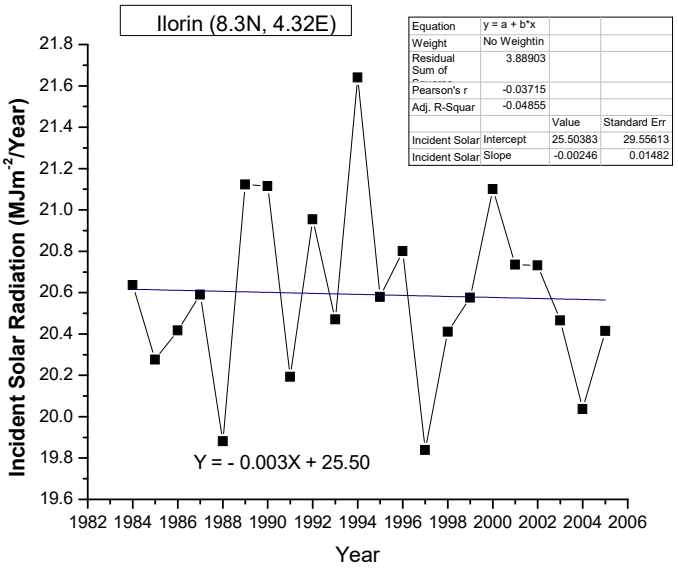

(b)

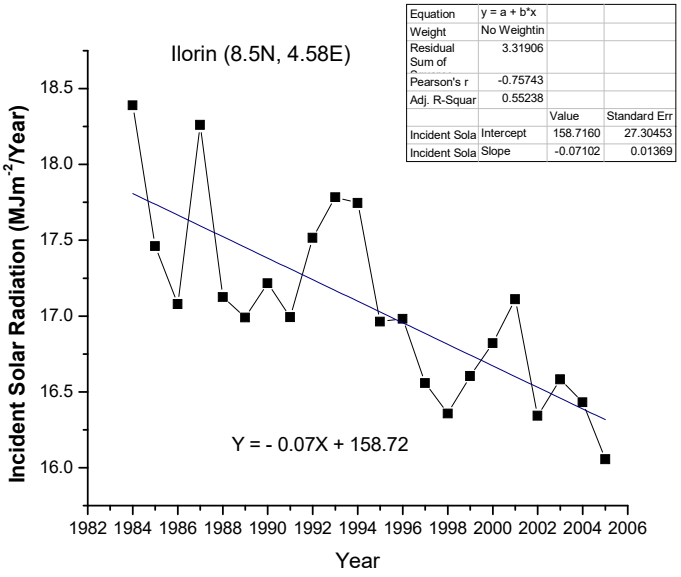

Fig 4.95: (a) Dry Season Trend of Solar Radiation

(b)Rainy Season Trend of Solar Radiation

(a)

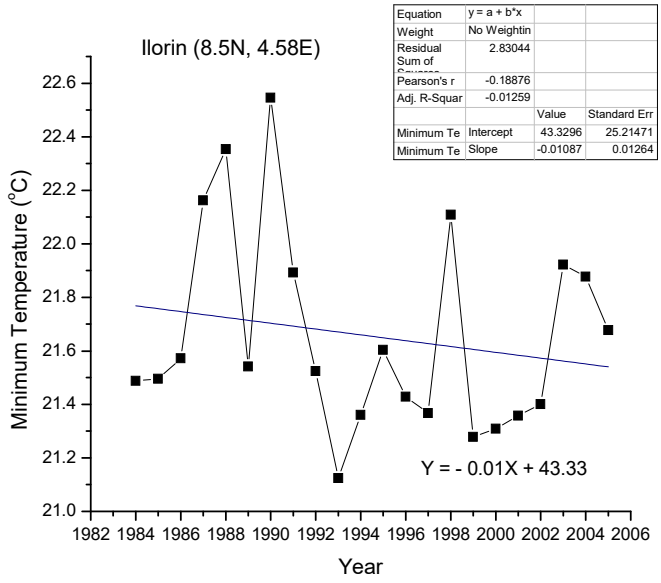

(b)

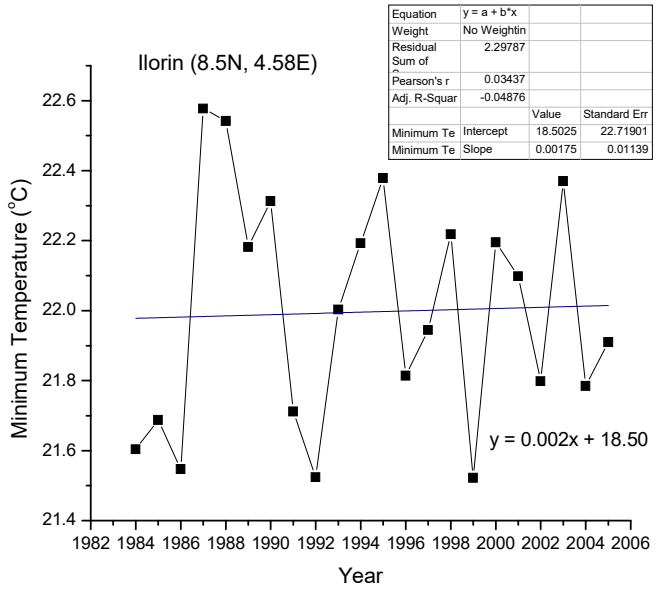

Fig 4.96: (a) Dry Season Trend of Minimum Temperature
(b)Rainy Season Trend of Minimum Temperature

(a)

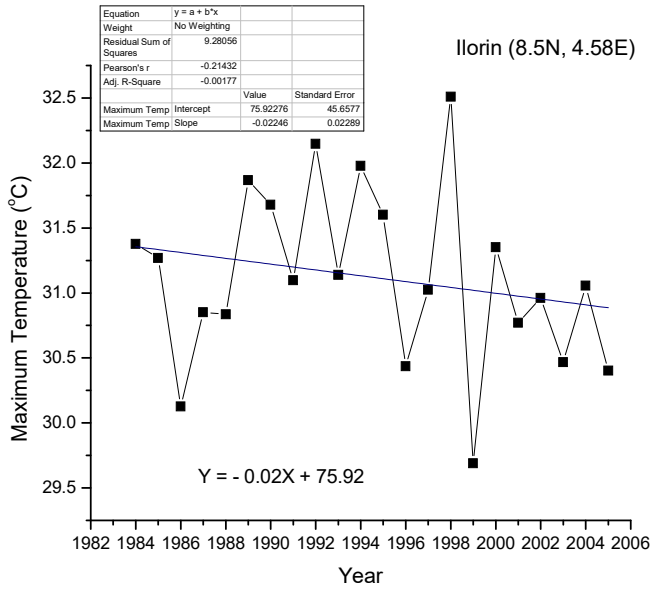

(b)

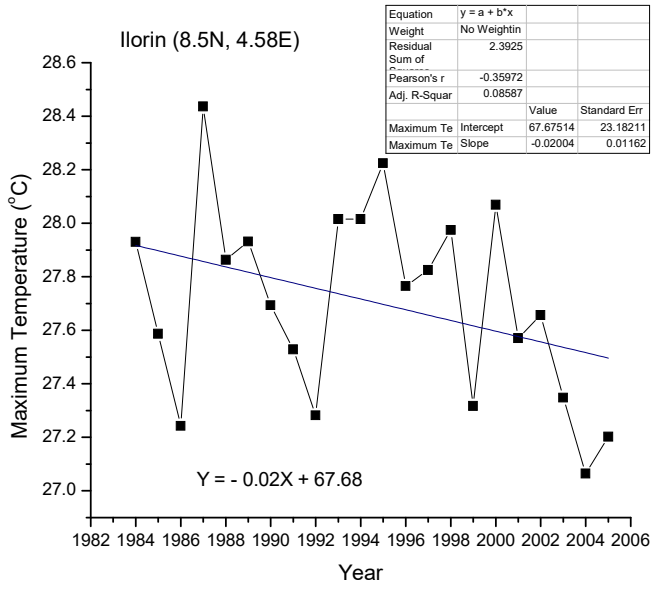

Fig 4.97: (a) Dry Season Trend of Maximum Temperature

(b)Rainy Season Trend of Maximum Temperature

(a)

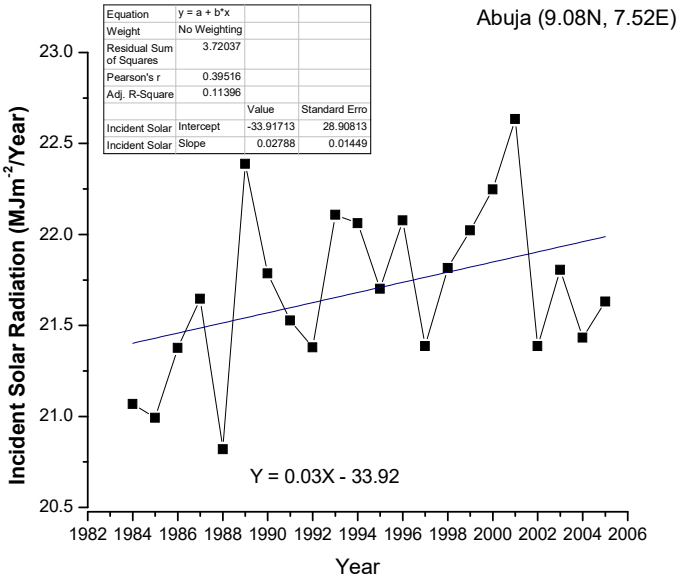

(b)

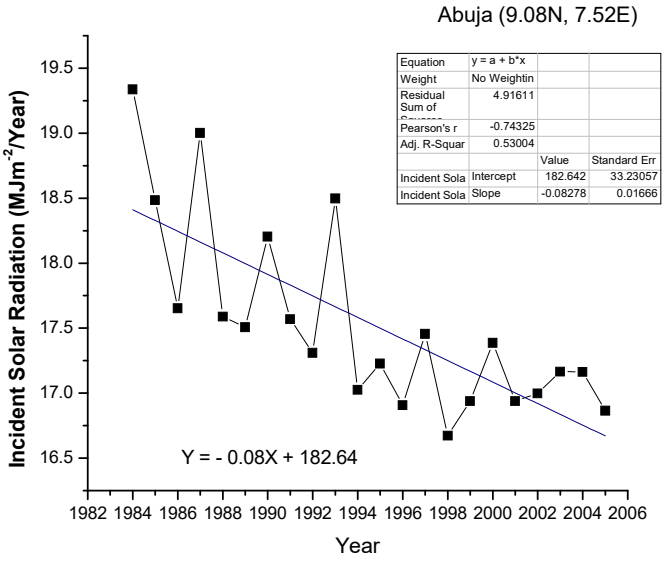

Fig 4.98: (a) Dry Season Trend of Solar Radiation

(b)Rainy Season Trend of Solar Radiation

(a)

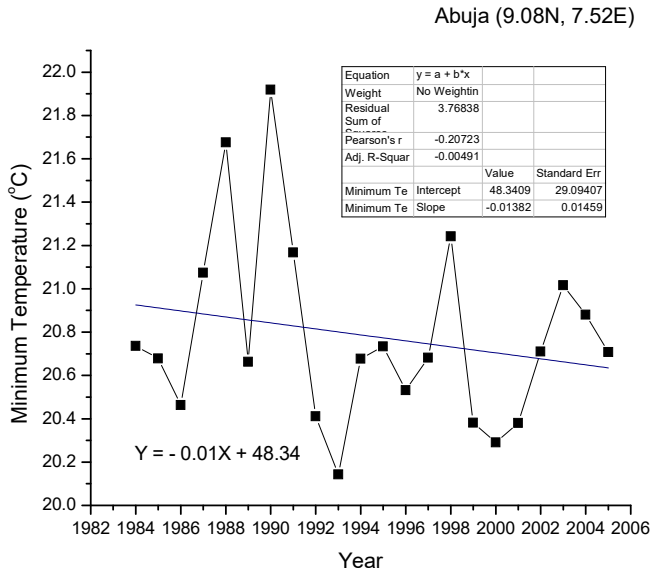

(b)

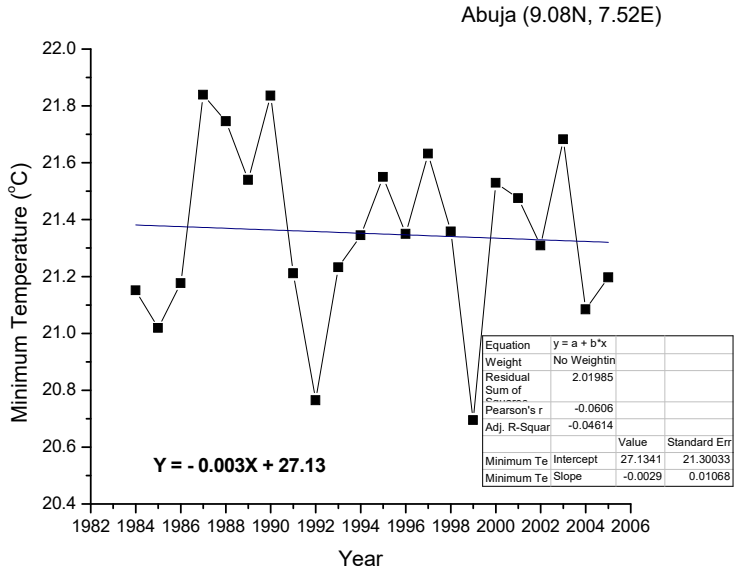

Fig 4.99: (a) Dry Season Trend of Minimum Temperature

(b)Rainy Season Trend of Minimum Temperature

(a)

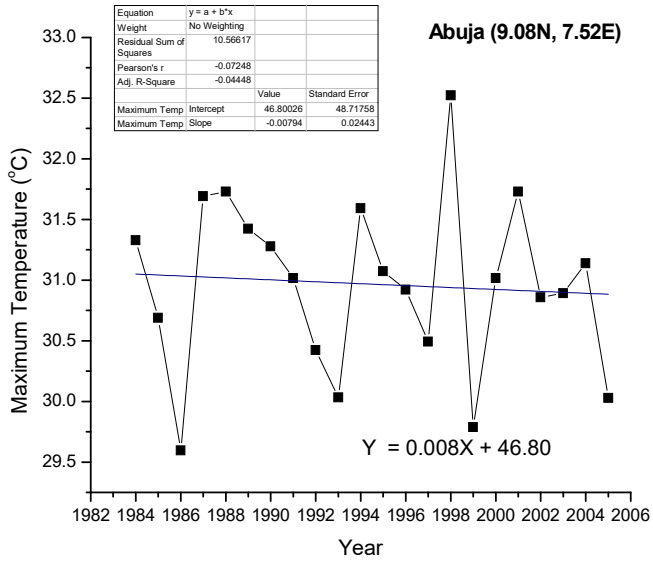

(b)

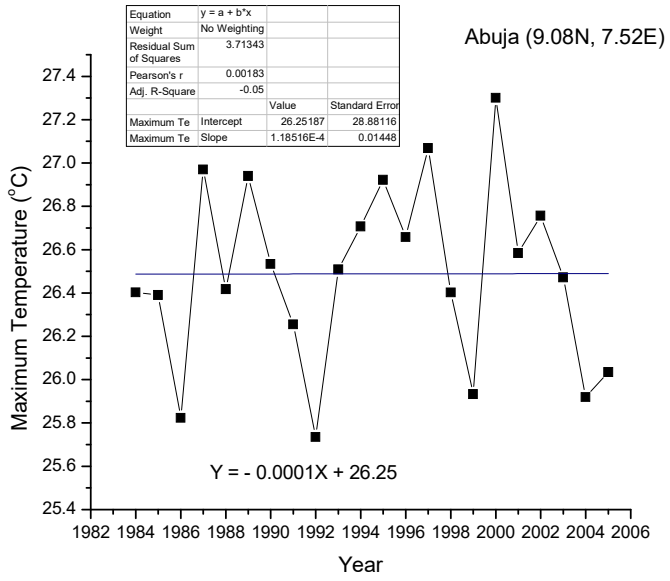

Fig 4.100: (a) Dry Season Trend of Maximum Temperature

(b)Rainy Season Trend of Maximum Temperature

(a)

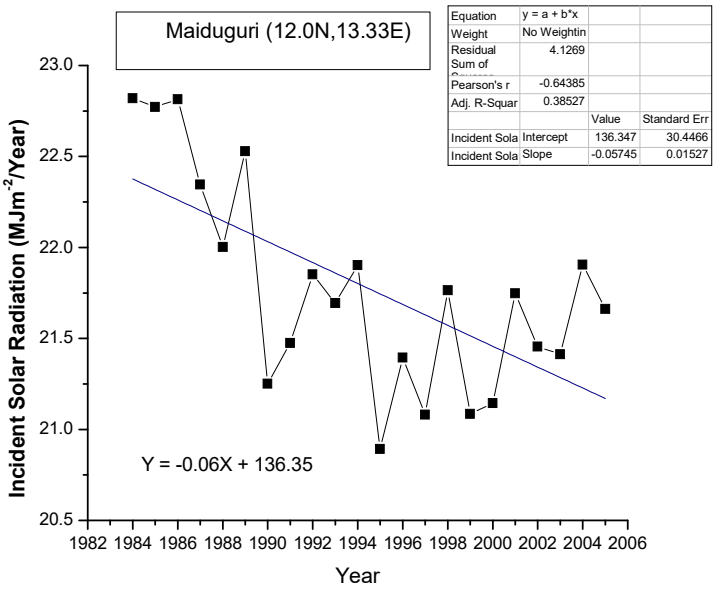

(b)

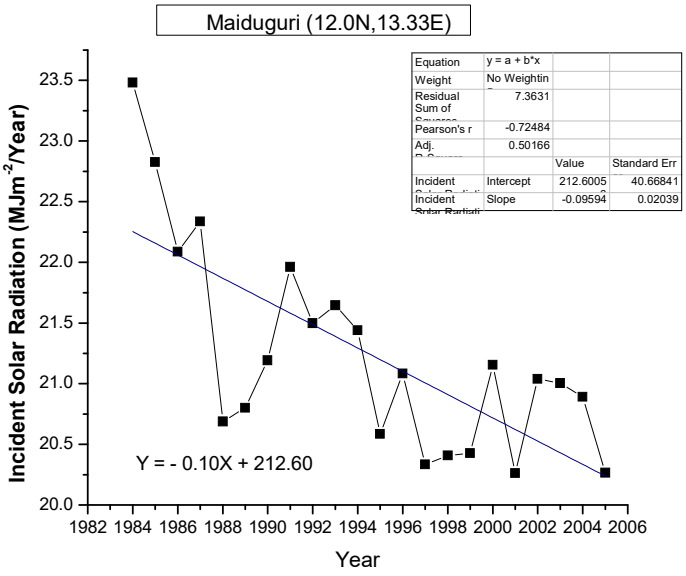

Fig 4.101: (a) Dry Season Trend of Solar Radiation

(b)Rainy Season Trend of Solar Radiation

(a)

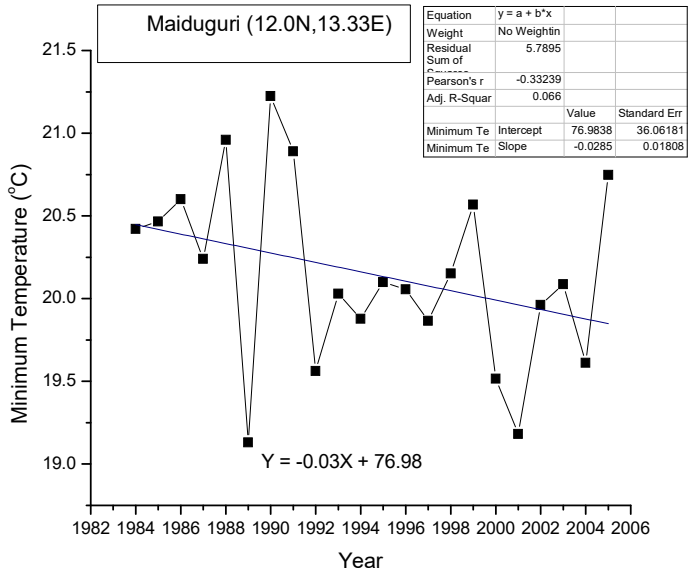

(b)

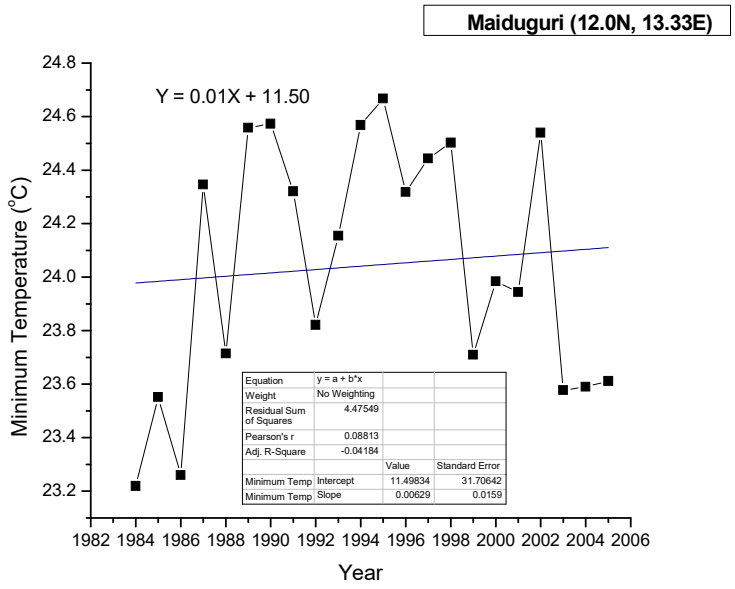

Fig 4.102: (a) Dry Season Trend of Minimum Temperature

(b)Rainy Season Trend of Minimum Temperature

(a)

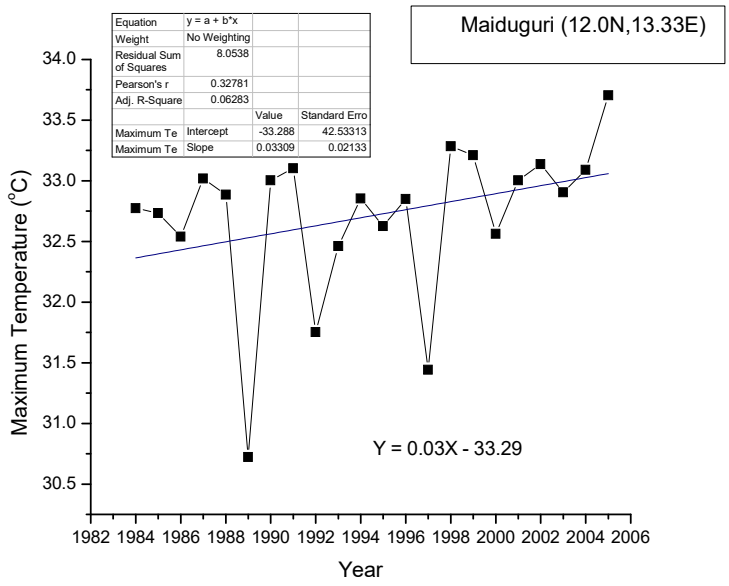

(b)

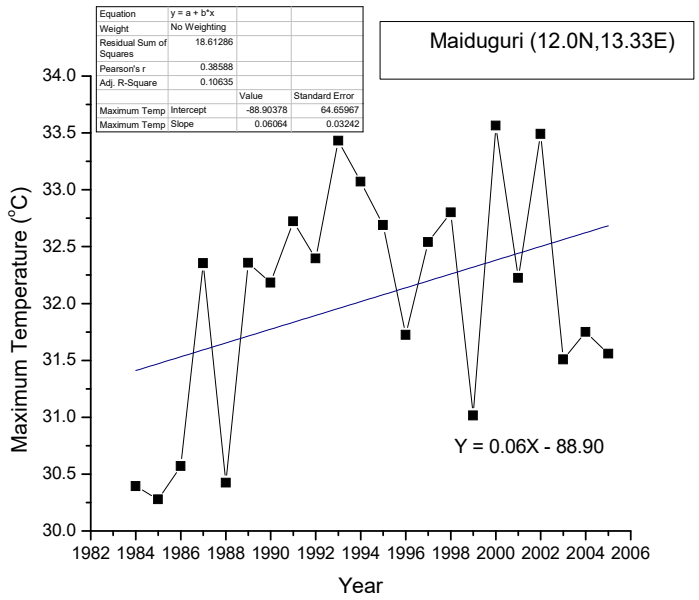

Fig 4.103: (a) Dry Season Trend of Maximum Temperature

(b)Rainy Season Trend of Maximum Temperature

(a)

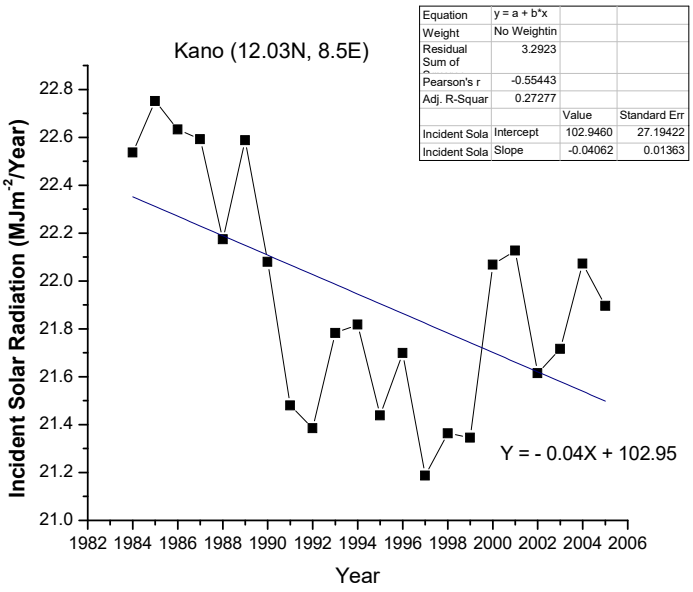

(b)

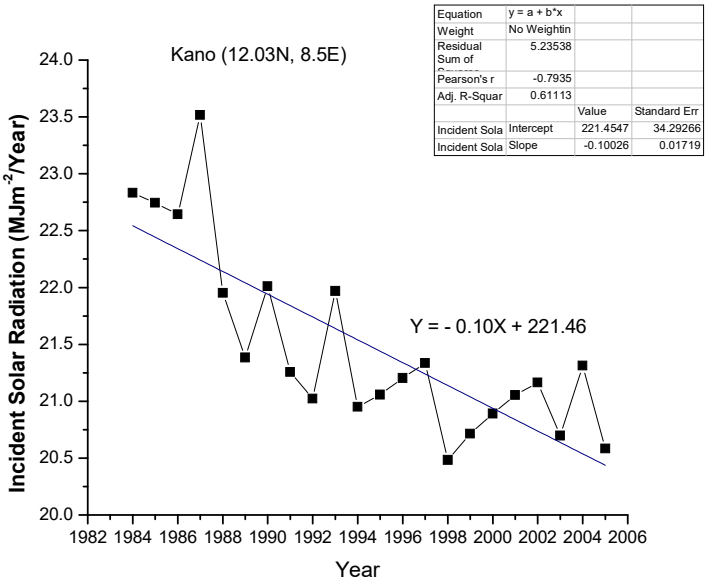

Fig 4.104: (a) Dry Season Trend of Solar Radiation

(b)Rainy Season Trend of Solar Radiation

(a)

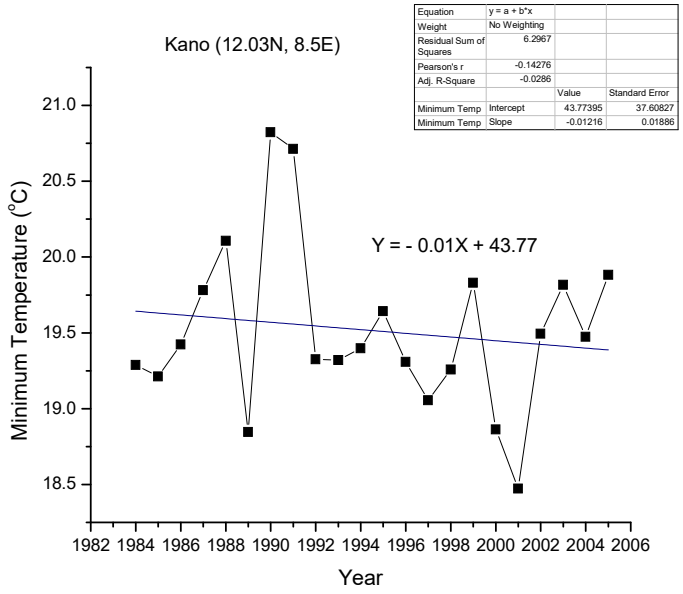

(b)

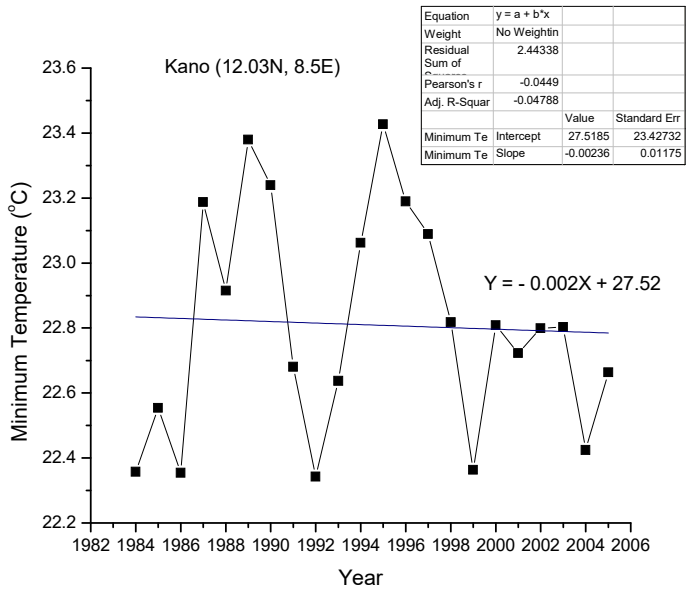

Fig 4.105: (a) Dry Season Trend of Minimum Temperature

(b)Rainy Season Trend of Minimum Temperature

(a)

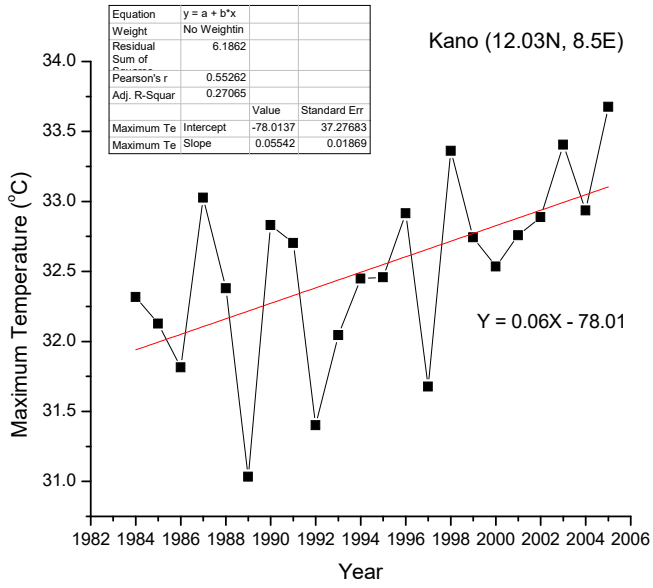

(b)

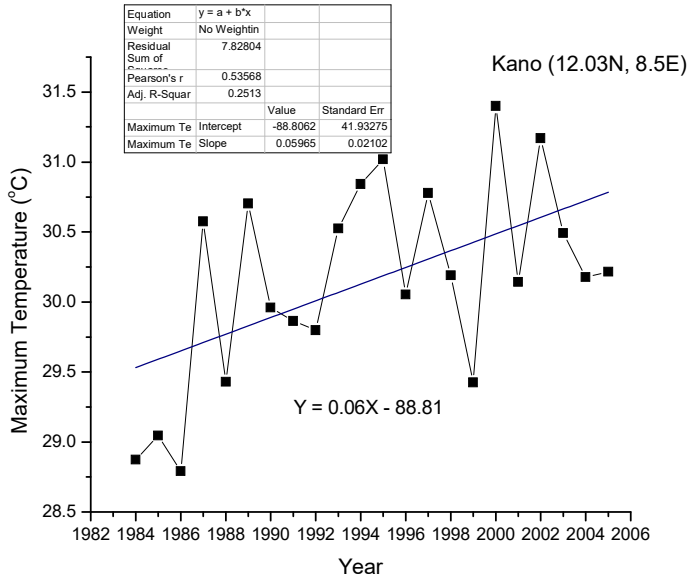

Fig 4.106: (a) Dry Season Trend of Maximum Temperature

(b)Rainy Season Trend of Maximum Temperature

(a)

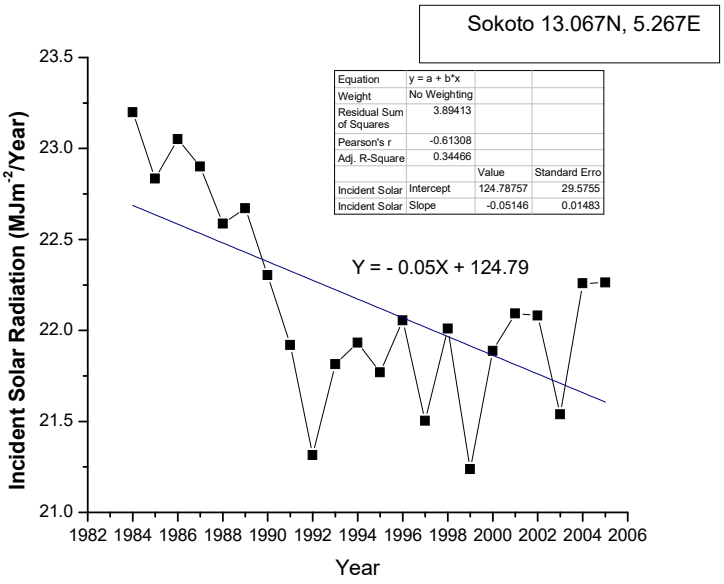

(b)

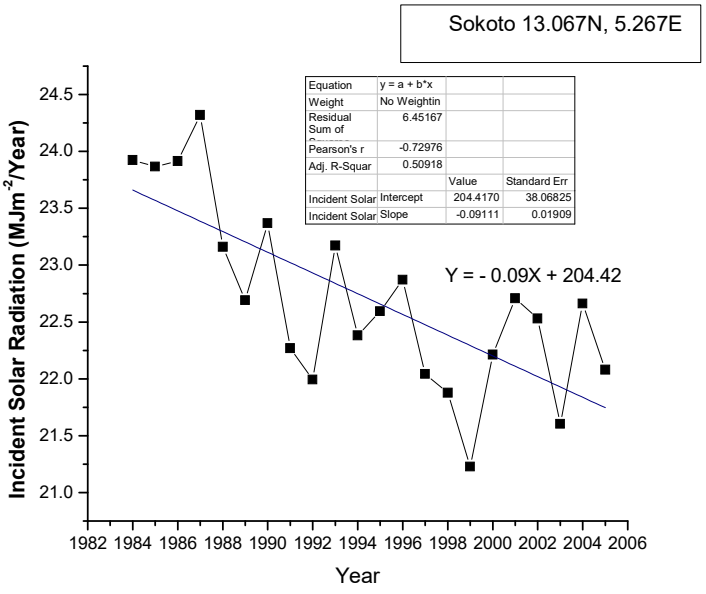

Fig 4.107: (a) Dry Season Trend of Solar Radiation
(b)Rainy Season Trend of Solar Radiation

(a)

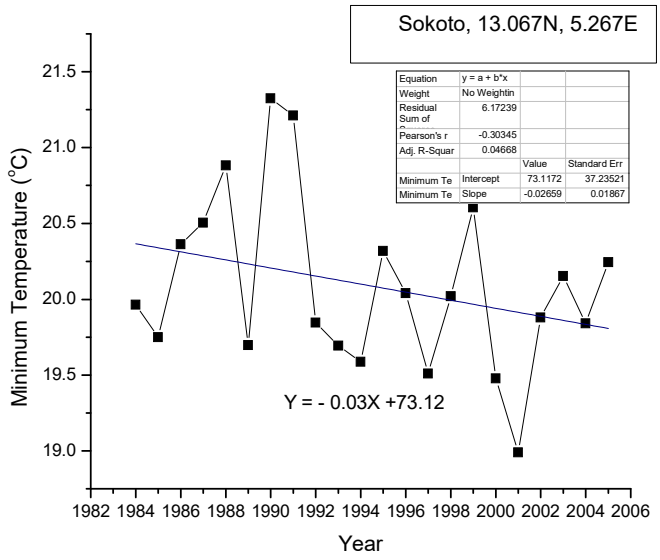

(b)

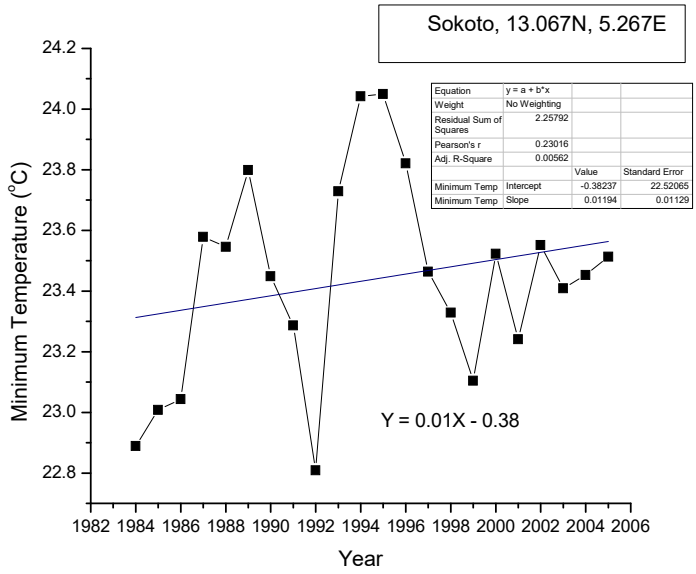

Fig 4.108: (a) Dry Season Trend of Minimum Temperature
(b)Rainy Season Trend of Minimum Temperature

(a)

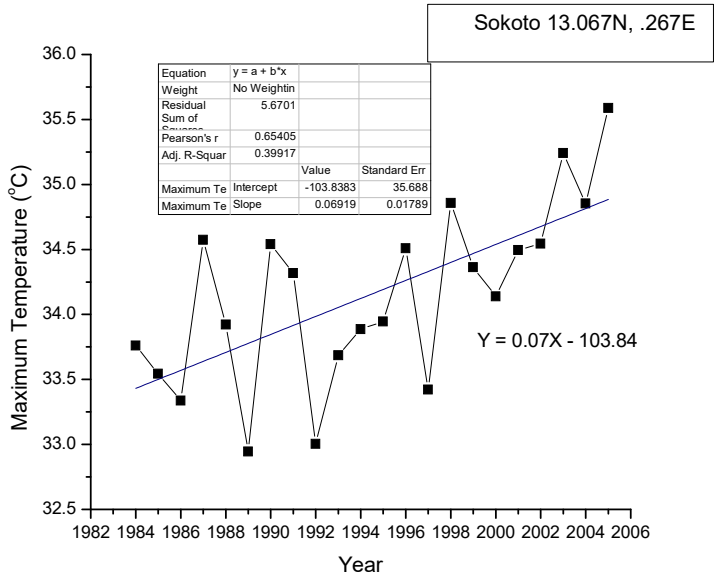

(b)

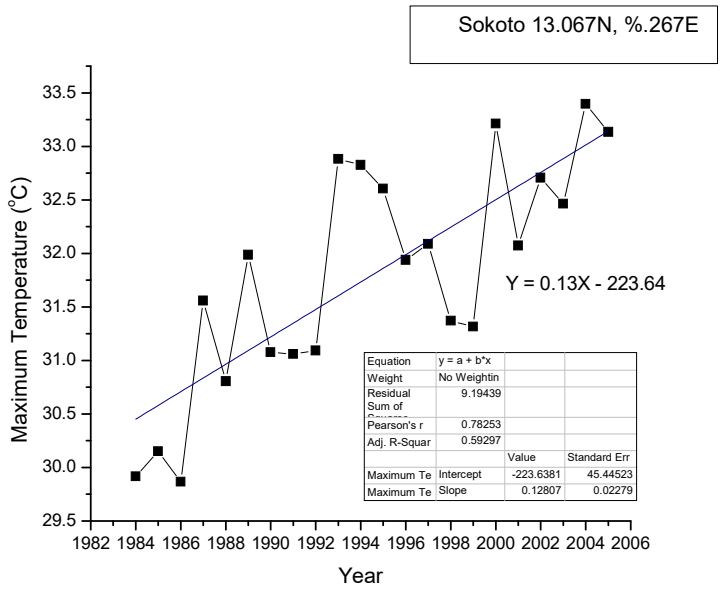

Fig 4.109: (a) Dry Season Trend of Maximum Temperature
(b)Rainy Season Trend of Maximum Temperature

Table 4.6: Summary of trend equations of Solar Radiation, Minimum and Maximum Temperatures during Dry and Rainy seasons

Location		Dry season Trend	Rainy season Trend
Port Harcourt	Solar radiation	Y = - 0.02X + 61.60	Y = -0.00X + 5.13
	Min Temp	Y = 0.01X + 12.19	Y = 0.01X + 6.17
	Max Temp	Y = -0.02X + 70.31	Y = -0.02X + 65.25
Calabar	Solar radiation	Y = - 0.03X + 70.68	Y = - 0.06X + 128.28
	Min Temp	Y = 0.02X - 11.60	Y = 0.03X - 26.57
	Max Temp	Y = 0.005X + 17.11	Y = -0.00001X + 25.66
Warri	Solar radiation	Y = - 0.03X + 70.32	Y = -0.04X + 88.91
	Min Temp	y = - 0.01X + 35.33	Y = 0.02X - 6.56
	Max Temp	Y = - 0.05X + 131.17	Y = - 0.02X + 63.94
Benin city	Solar radiation	Y = - 0.02X + 68.56	Y = 0.01X + 6.18
	Min Temp	Y = - 0.01X + 45.94	Y = 0.01X + 6.18
	Max Temp	Y = -0.07X + 166.67	Y = -0.03X + 92.02
Lagos	Solar radiation	Y = 0.01X - 9.79	Y = -0.03X + 82.93
	Min Temp	Y = -0.00X + 30.12	Y = 0.01X + 14.48
	Max Temp	Y = -0.044X + 115.77	Y = -0.03X + 79.20
Ibadan	Solar radiation	Y = - 0.03X + 70.45	Y = -0.08X + 177.14
	Min Temp	Y = - 0.01X + 40.36	Y = 0.00X + 13.77
	Max Temp	Y = -0.05X + 128.28	Y = -0.03X + 81.21
Ilorin	Solar radiation	Y = - 0.00X + 25.50	Y = -0.07X + 158.71
	Min Temp	Y = - 0.01X + 43.33	Y = 0.00X + 18.50
	Max Temp	Y = - 0.02X + 75.92	Y = -0.02X + 67.68
Abuja	Solar radiation	Y = 0.03X - 33.92	Y = -0.08X + 182.64
	Min Temp	Y = - 0.01X + 48.34	Y = - 0.00X + 27.13
	Max Temp	Y = - 0.01X + 46.80	Y = -0.00X + 26.26
Maiduguri	Solar radiation	Y = -0.06X + 136.35	Y = -0.10X + 212.60
	Min Temp	Y = -0.03X + 76.98	Y = 0.01X + 11.50
	Max Temp	Y = 0.03X - 33.29	Y = 0.06X - 88.90
Kano	Solar radiation	Y = - 0.04X + 102.95	Y = -0.10X + 221.46
	Min Temp	Y = - 0.01X + 43.77	Y = -0.00X + 27.52
	Max Temp	Y = 0.06X - 78.01	Y = 0.06X - 88.81
Sokoto	Solar radiation	Y = -0.05X + 124.79	Y = - 0.09X +204.42
	Min Temp	Y = - 0.03X +73.12	Y = 0.01X - 0.38
	Max Temp	Y = 0.07X - 103.84	Y = 0.13X - 223.64

4.6. Validation with Solar Radiation, Minimum Temperature and Maximum Temperature data obtained from Nigeria Meteorological Agency (NIMET)

The Nigeria Meteorological Agency (NIMET) provides a reliable source for ground basedatmospheric science data for a large part of the country. Subsequently, solar radiation data (global), minimum temperature and maximum temperature data for some of the locations were obtained from the Nigeria Meteorological Agency, Oshodi. This provides a valuable data set for the validation of the National Aeronautics and Space Administration, (NASA) atmospheric science data centre (ASDC) data set used in this work.

Table 4.8contains the different parameters and the locations for which they are available.

For each of these stations, the monthly average of each of the parameters was determined over 22-years (making 264 data points). The data was then smoothened by computing the 6-months moving average for each set. Thereafter, a comparison was made between the ground measured data and NASA (ASDC) satellite measured data by plotting the time series for each of the parameters. These, along with their respective linear regression fits are presented in Figures 4:110 to figs 4:115 for incident solar radiation, Figs 4:116 to fig 4:122 for minimum temperature and Fig 4:123 to Fig 4:130 for maximum temperature. The correlation coefficient, r, as obtained for the different parameters at the various locations is seen to range from a moderate value of 0.55 (incident solar radiation) for Sokoto to 0.96 (minimum temperature) for Maiduguri. Overall, there is a reasonable and acceptable level of agreement between the two data sets (Tables 4.9 and 4.10).

This shows that meteorological data measured through remote satellite sources can be considered as reliable and be used for scientific purposes.

Table 4.7:The available ground data and the locations.

S/No	Parameter	Location
1.	Incident Solar Radiation	Port Harcourt, Lagos, Ibadan, Ilorin, Abuja, Sokoto
2.	Minimum Temperature	Port Harcourt, Lagos, Ibadan, Abuja, Maiduguri, Kano, Sokoto
3.	Maximum Temperature	Port Harcourt, Benin, Lagos, Ibadan, Ilorin, Abuja, Maiduguri, Sokoto

(a)

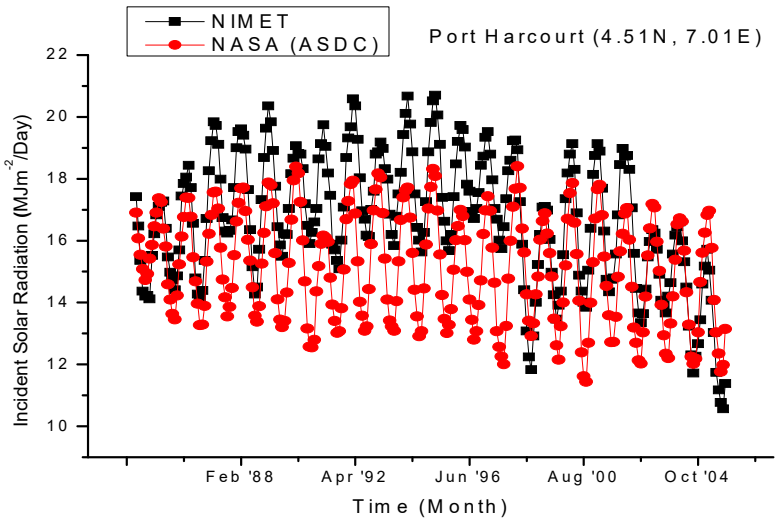

(b)

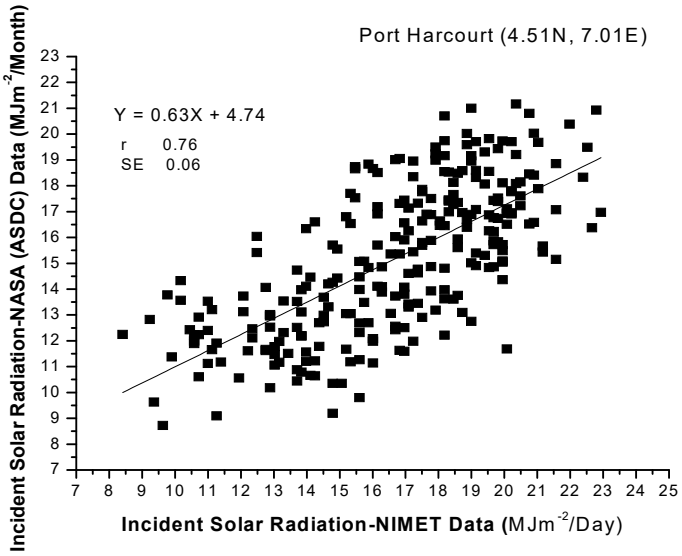

Fig 4.110: (a) Comparison of 6-Month Moving Average of Incident Solar Radiation from NIMET and NASA (ASDC) for Port Harcourt.

(b)Correlation of NIMET and NASA (ASDC) Mean Monthly values of Incident Solar Radiation for Port Harcourt

(a)

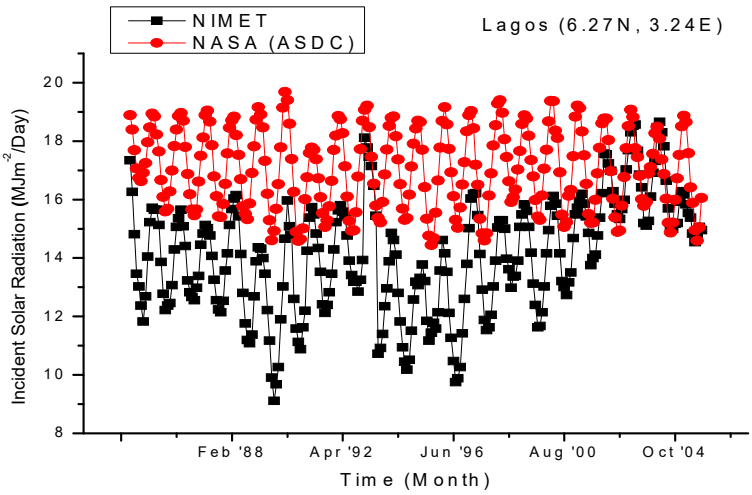

(b)

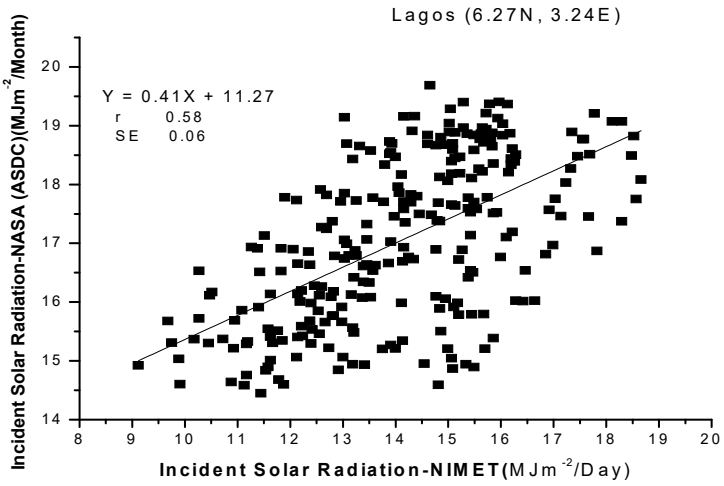

Fig 4.111: (a) Comparison of 6-Month Moving Average of Incident Solar Radiation from NIMET and NASA (ASDC) for Lagos.

(b)Correlation of NIMET and NASA (ASDC) Mean Monthly values of Incident Solar Radiation for Lagos

(a)

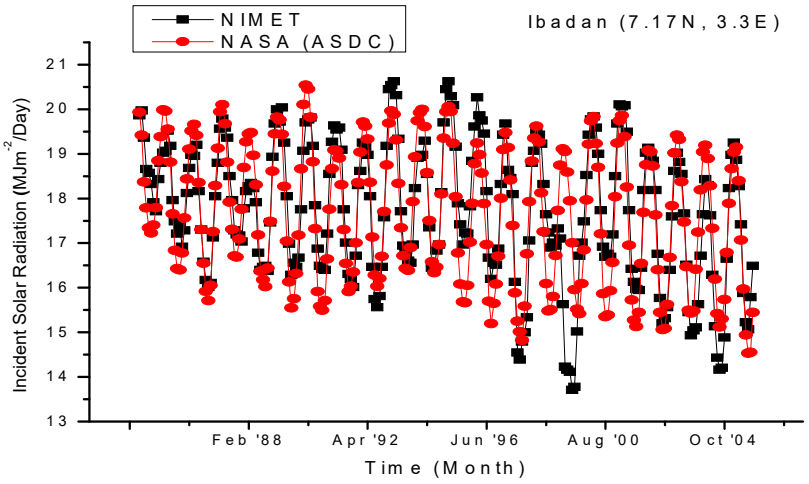

(b)

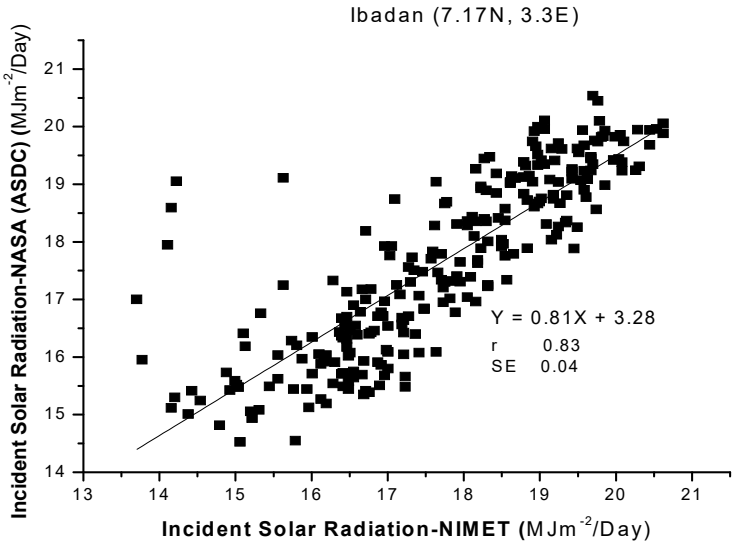

Fig 4.112: (a) Comparison of 6-Month Moving Average of Incident Solar Radiation from NIMET and NASA (ASDC) for Ibadan.

(b)Correlation of NIMET and NASA (ASDC) Mean Monthly values of Incident Solar Radiation for Ibadan

(a)

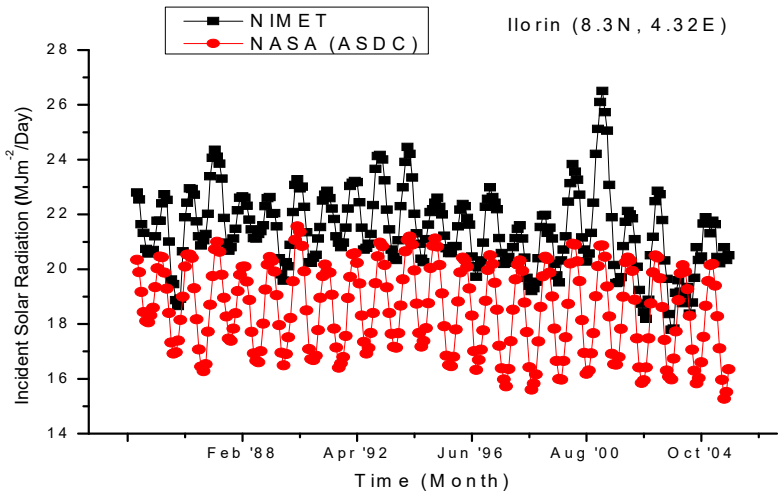

(b)

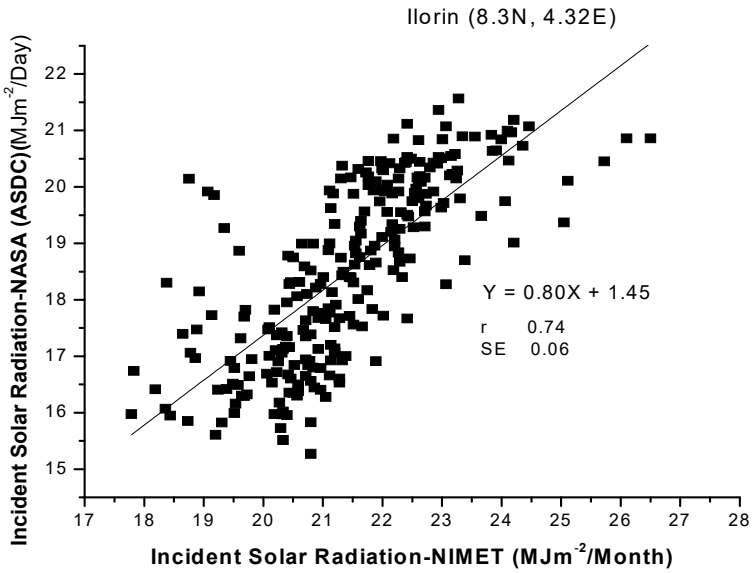

Fig 4.113: (a) Comparison of 6-Month Moving Average of Incident Solar Radiation from NIMET and NASA (ASDC) for Ilorin.

(b)Correlation of NIMET and NASA (ASDC) Mean Monthly values of Incident Solar Radiation for Ilorin

(a)

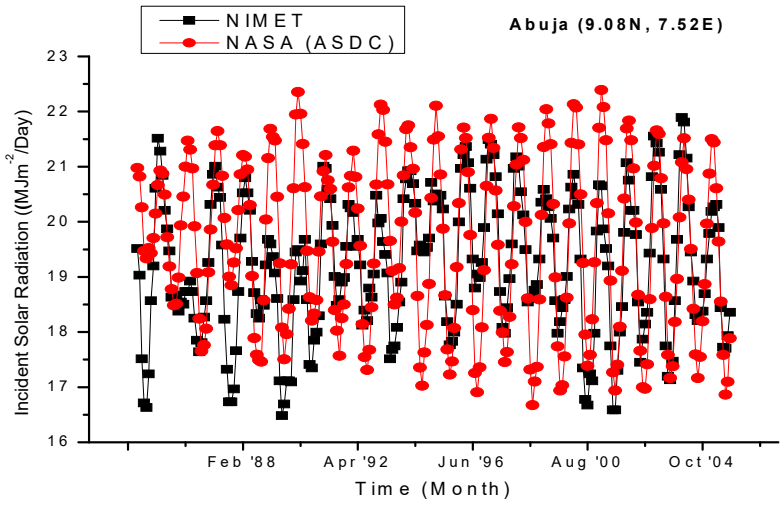

(b)

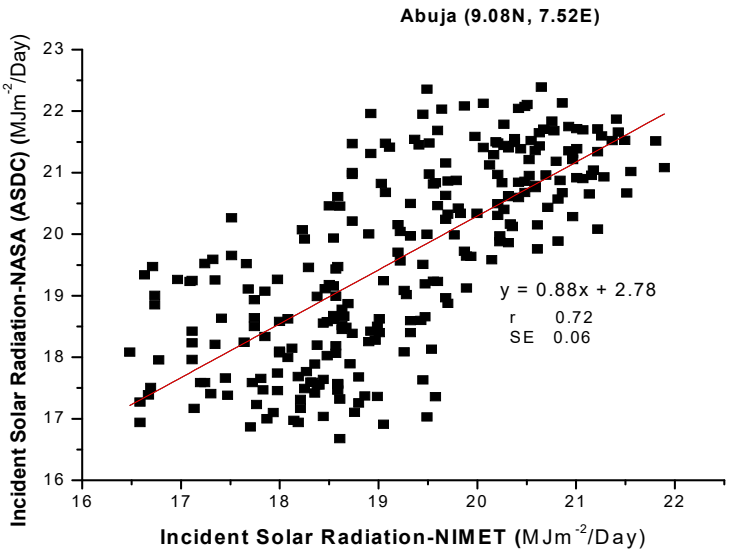

Fig 4.114: (a) Comparison of 6-Month Moving Average of Incident Solar Radiation from NIMET and NASA (ASDC) for Abuja.

(b)Correlation of NIMET and NASA (ASDC) Mean Monthly values of Incident Solar Radiation for Abuja

(a)

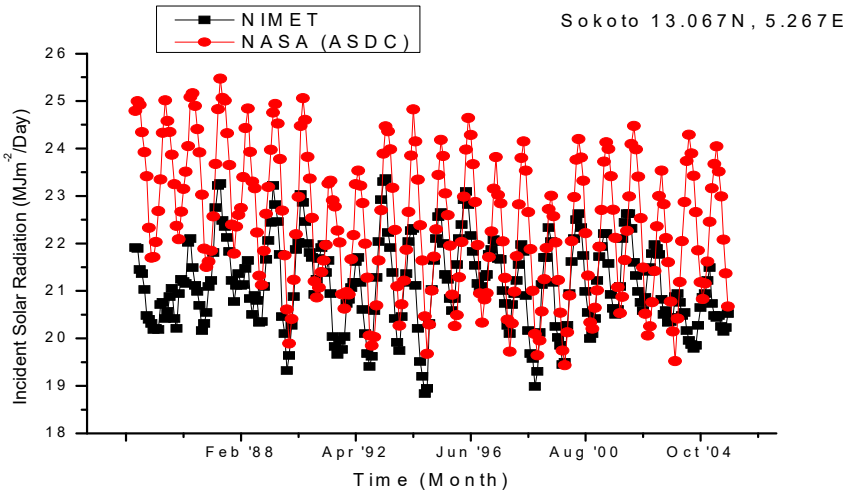

(b)

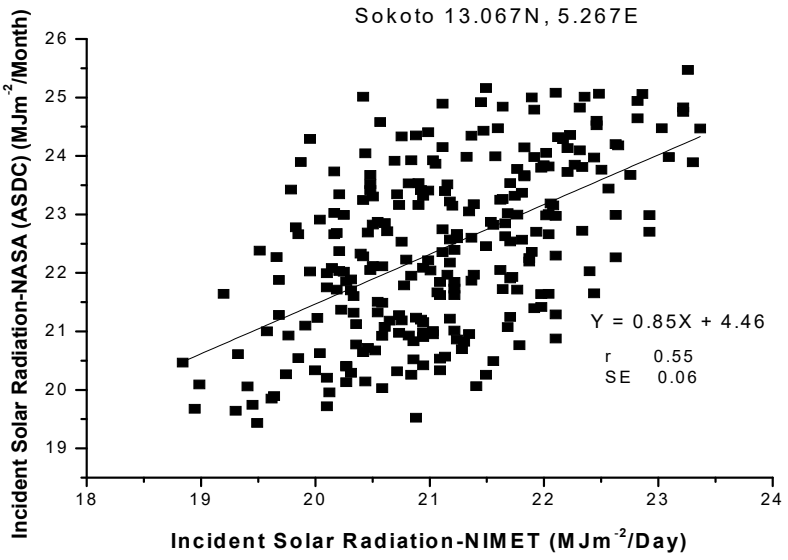

Fig 4.115: (a) Comparison of 6-Month Moving Average of Incident Solar Radiation from NIMET and NASA (ASDC) for Sokoto.

(b)Correlation of NIMET and NASA (ASDC) Mean Monthly values of Incident Solar Radiation for Sokoto

(a)

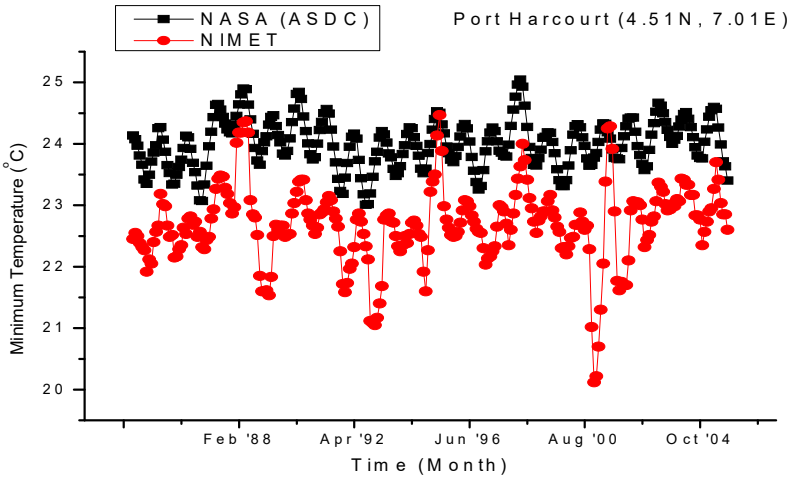

(b)

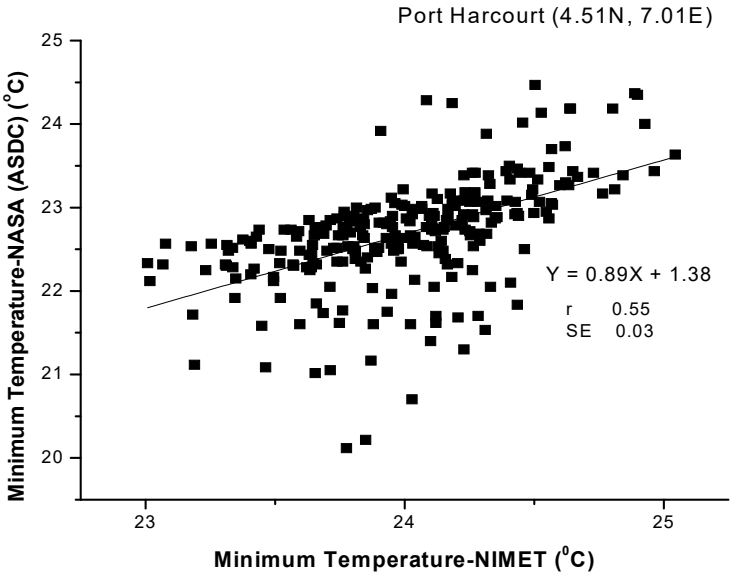

Fig 4.116: (a) Comparison of 6-Month Moving Average of Minimum Temperature from NIMET and NASA (ASDC) for Port Harcourt.

(b)Correlation of NIMET and NASA (ASDC) Mean Monthly values of Minimum Temperature for Port Harcourt

(a)

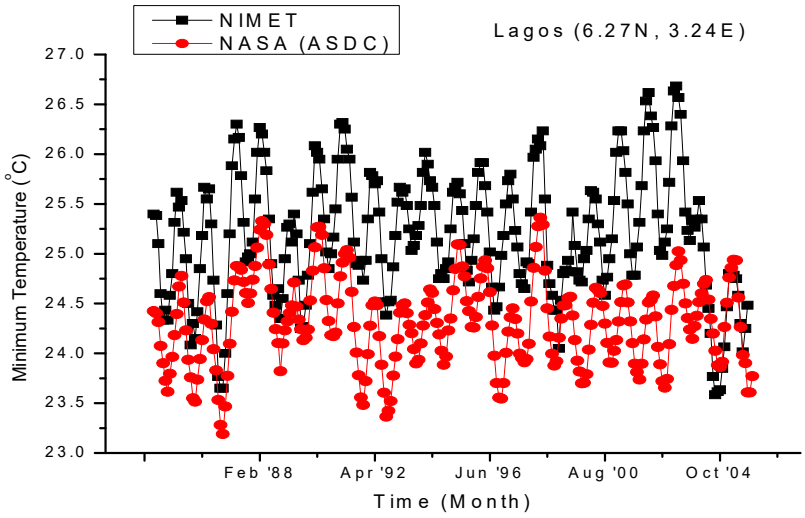

(b)

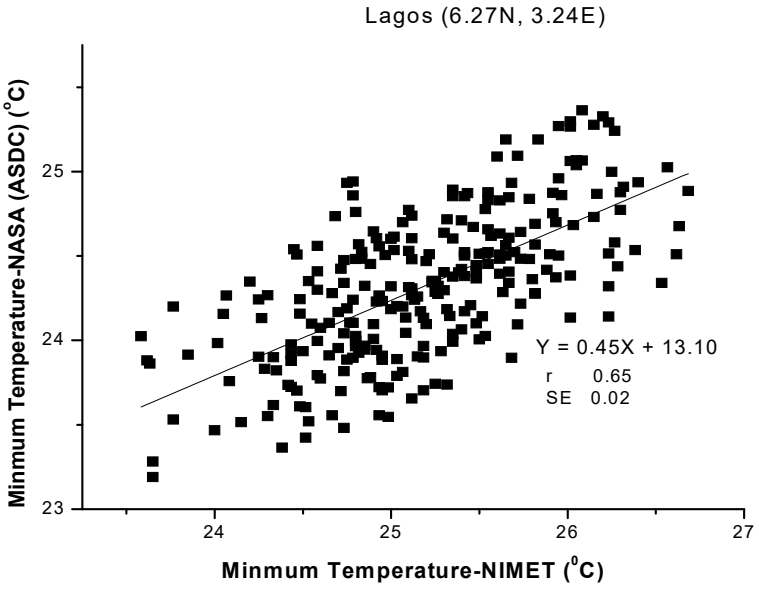

Fig 4.117: (a) Comparison of 6-Month Moving Average of Minimum Temperature from NIMET and NASA (ASDC) for Lagos.

(b)Correlation of NIMET and NASA (ASDC) Mean Monthly values of Minimum Temperature for Lagos

(a)

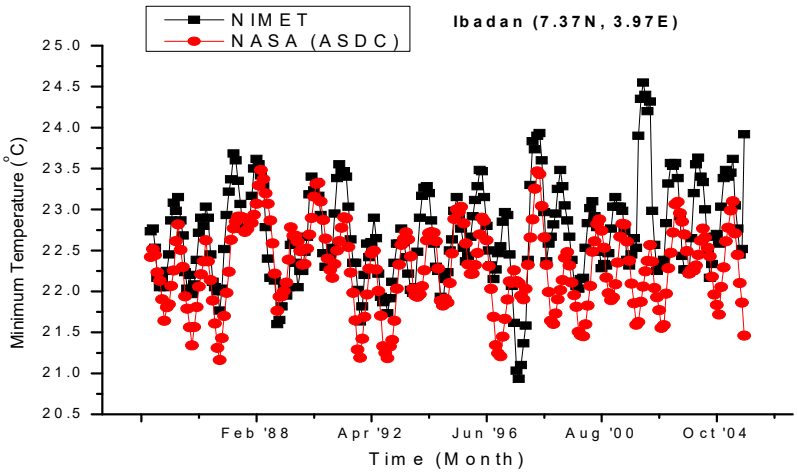

(b)

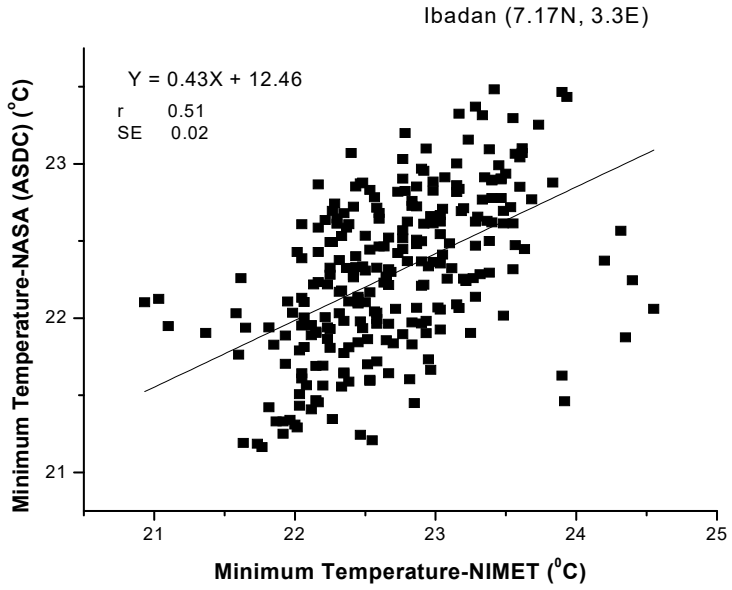

Fig 4.118: (a) Comparison of 6-Month Moving Average of Minimum Temperature from NIMET and NASA (ASDC) for Ibadan.

(b)Correlation of NIMET and NASA (ASDC) Mean Monthly values of Minimum Temperature for Ibadan

(a)

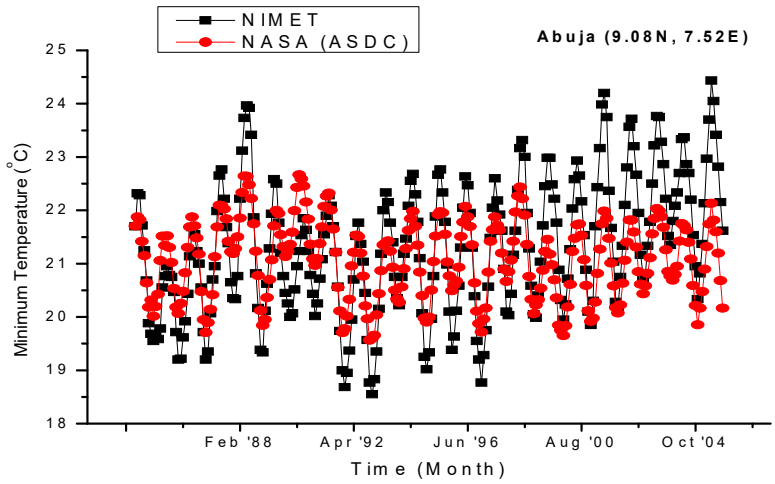

(b)

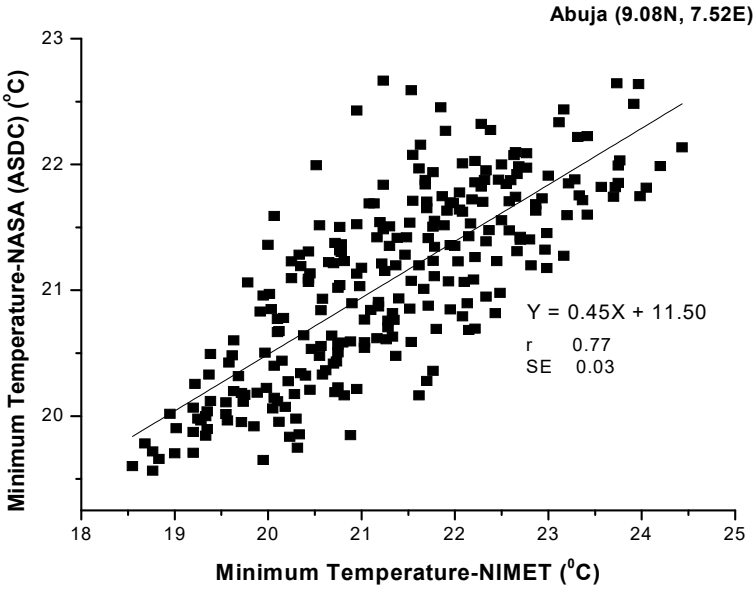

Fig 4.119: (a) Comparison of 6-Month Moving Average of Minimum Temperature from NIMET and NASA (ASDC) for Abuja.

(b)Correlation of NIMET and NASA (ASDC) Mean Monthly values of Minimum Temperature for Abuja

(a)

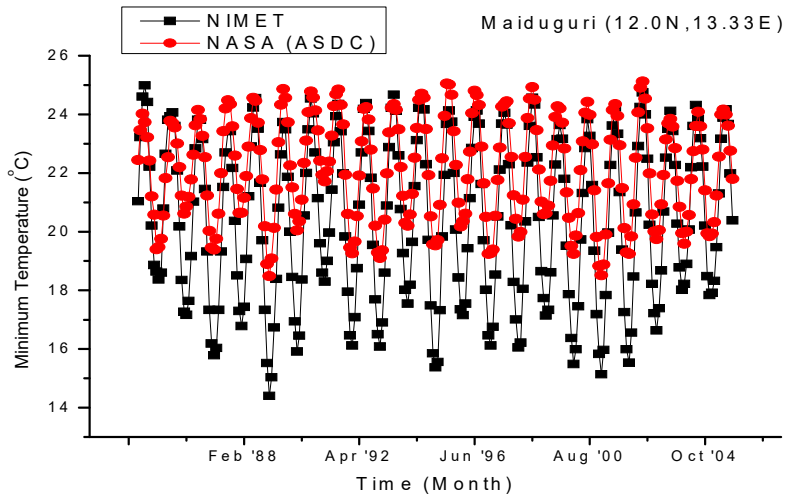

(b)

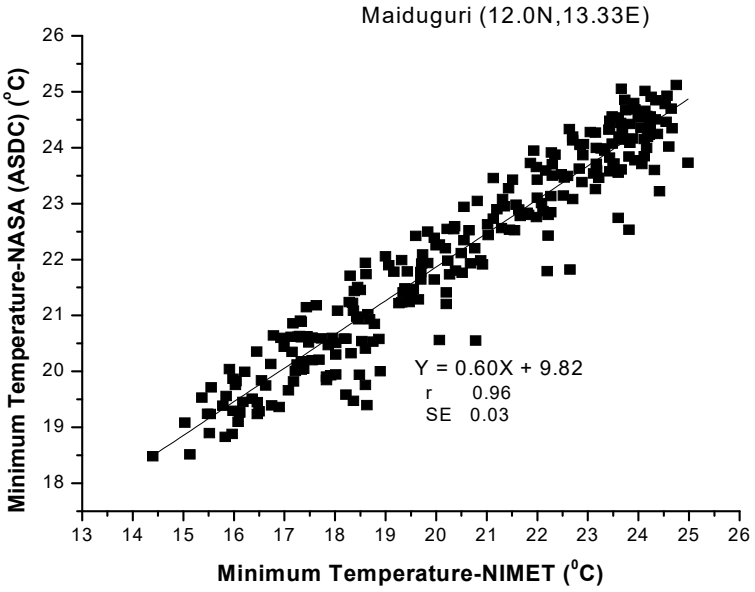

Fig 4.120: (a) Comparison of 6-Month Moving Average of Minimum Temperature from NIMET and NASA (ASDC) for Maiduguri.

(b)Correlation of NIMET and NASA (ASDC) Mean Monthly values of Minimum Temperature for Maiduguri

(a)

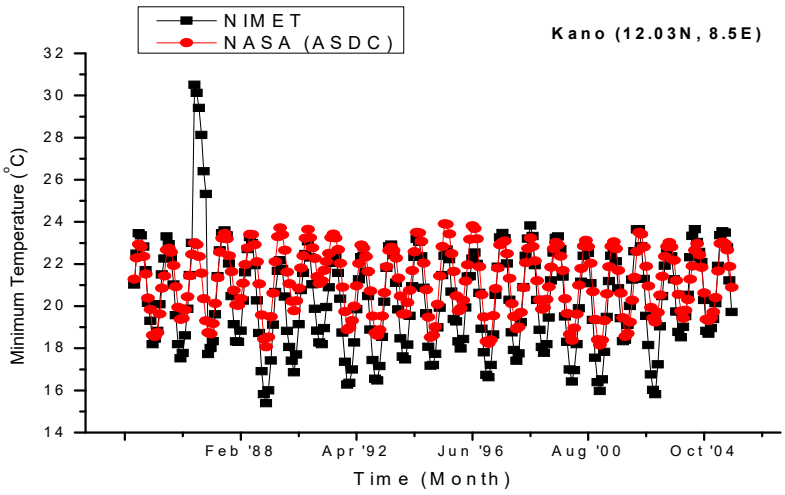

(b)

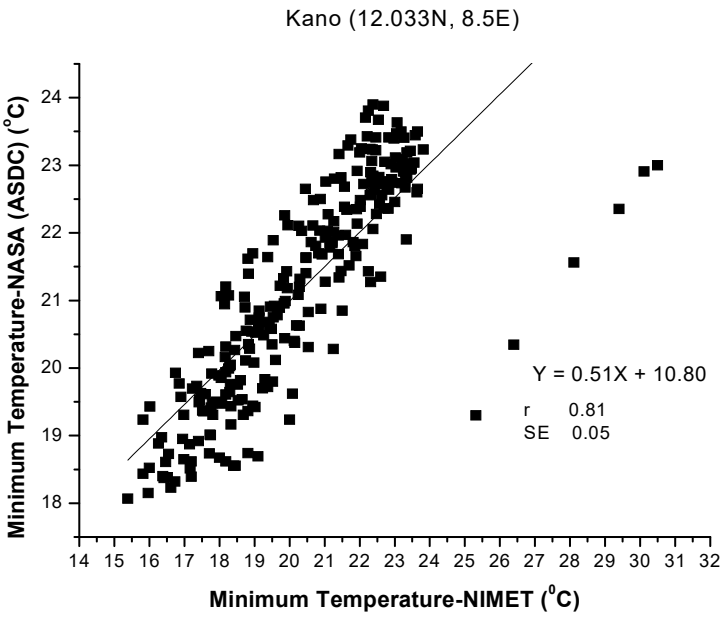

Fig 4.121: (a) Comparison of 6-Month Moving Average of Minimum Temperature from NIMET and NASA (ASDC) for Kano.

(b)Correlation of NIMET and NASA (ASDC) Mean Monthly values of Minimum Temperature for Kano

(a)

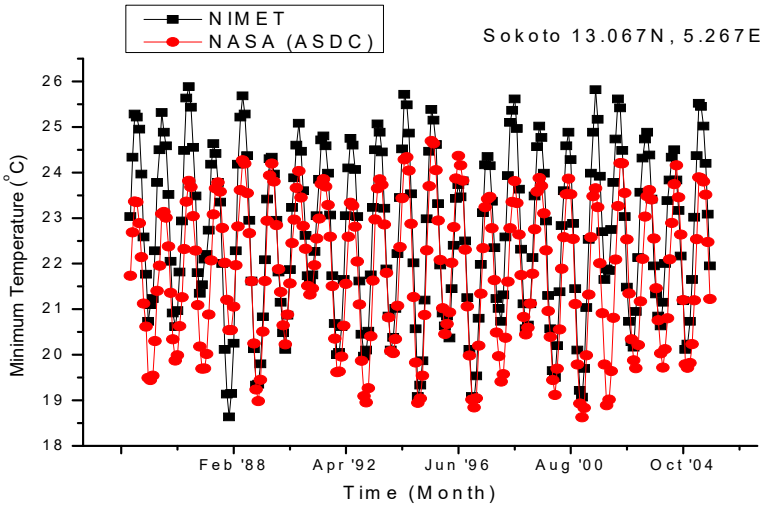

(b)

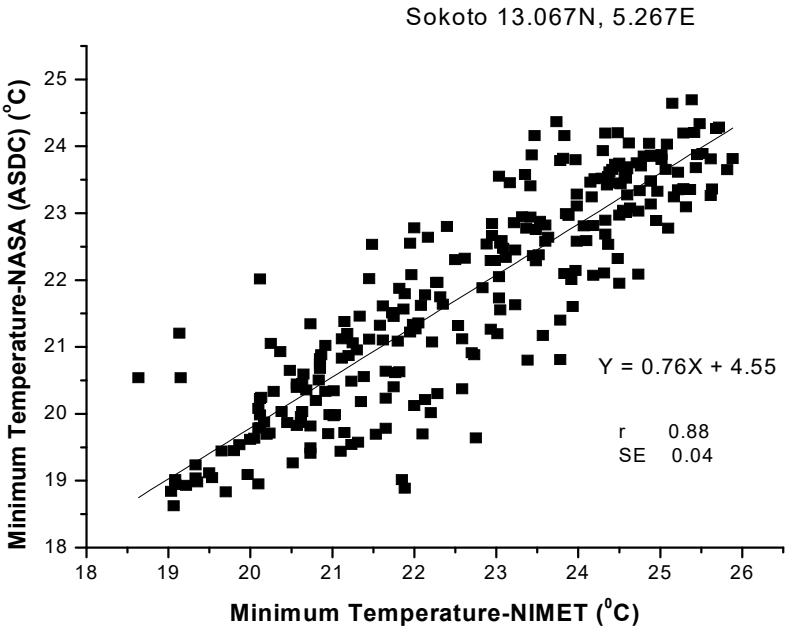

Fig 4.122: (a) Comparison of 6-Month Moving Average of Minimum Temperature from NIMET and NASA (ASDC) for Sokoto.

(b)Correlation of NIMET and NASA (ASDC) Mean Monthly values of Minimum Temperature for Sokoto

(a)

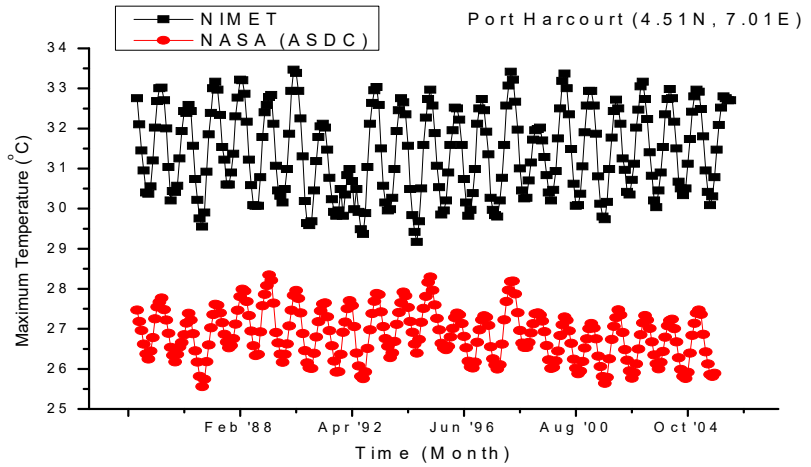

(b)

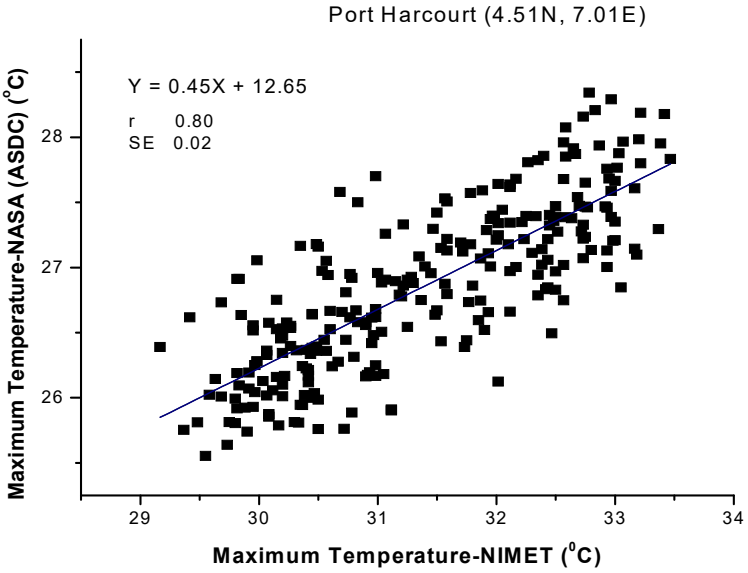

Fig 4.123: (a) Comparison of 6-Month Moving Average of Maximum Temperature from NIMET and NASA (ASDC) for Port Harcourt.

(b)Correlation of NIMET and NASA (ASDC) Mean Monthly values of Maximum Temperature for Port Harcourt

(a)

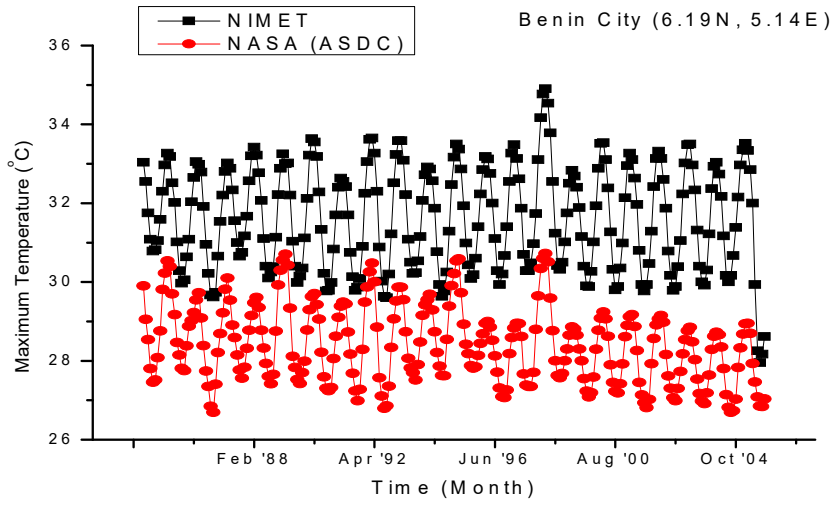

(b)

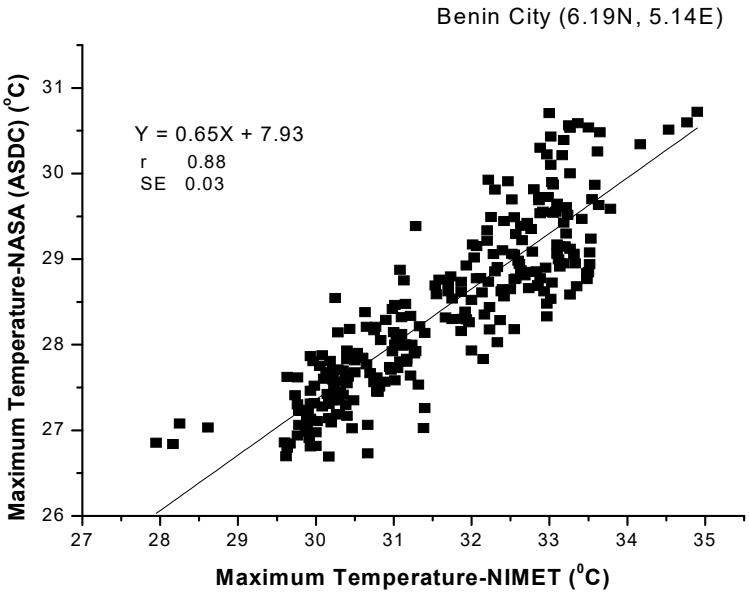

Fig 4.124: (a) Comparison of 6-Month Moving Average of Maximum Temperature from NIMET and NASA (ASDC) for Benin-City.

(b)Correlation of NIMET and NASA (ASDC) Mean Monthly values of Maximum Temperature for Benin City

(a)

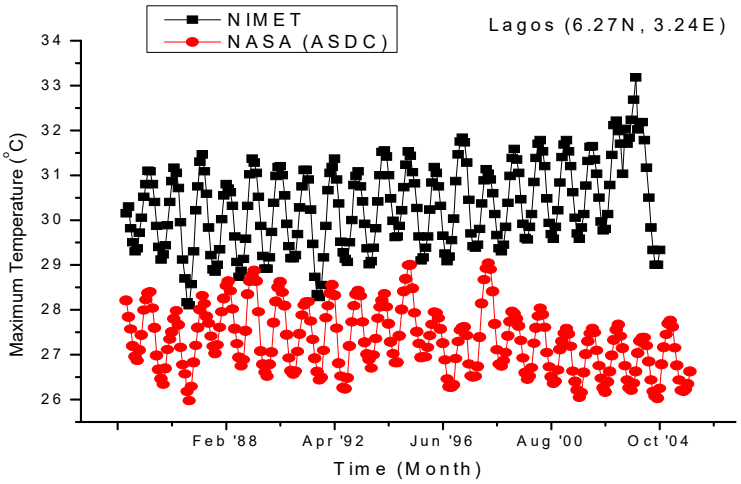

(b)

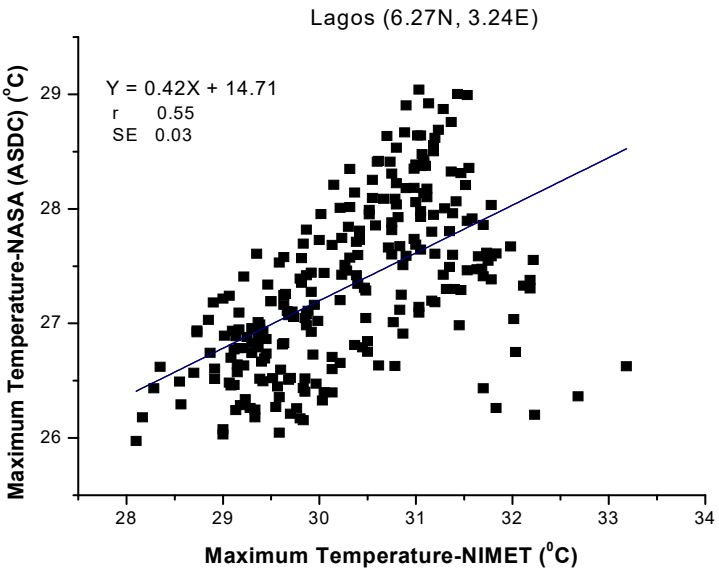

Fig 4.125: (a) Comparison of 6-Month Moving Average of Maximum Temperature from NIMET and NASA (ASDC) for Lagos.

(b)Correlation of NIMET and NASA (ASDC) Mean Monthly values of Maximum Temperature for Lagos

(a)

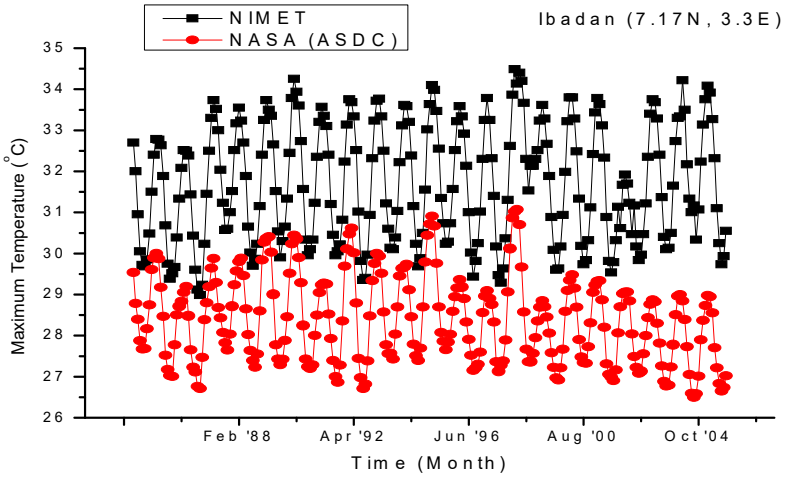

(b)

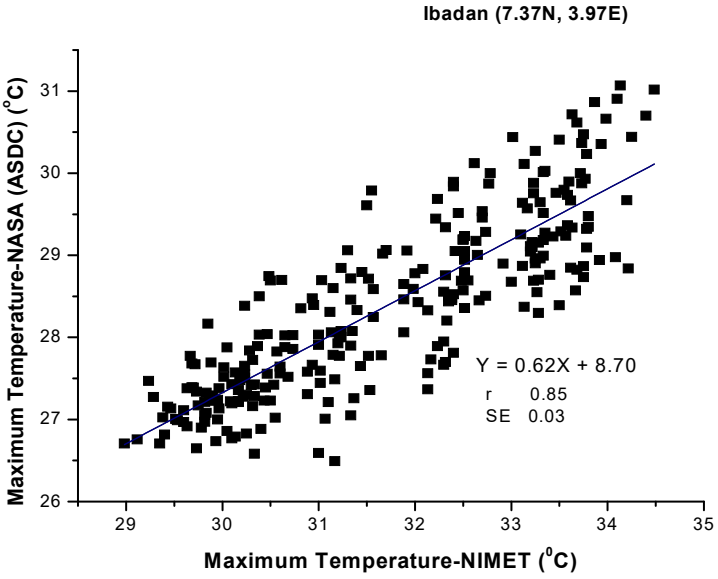

Fig 4.126: (a) Comparison of 6-Month Moving Average of Maximum Temperature from NIMET and NASA (ASDC) for Ibadan.

(b)Correlation of NIMET and NASA (ASDC) Mean Monthly values of Maximum Temperature for Ibadan

(a)

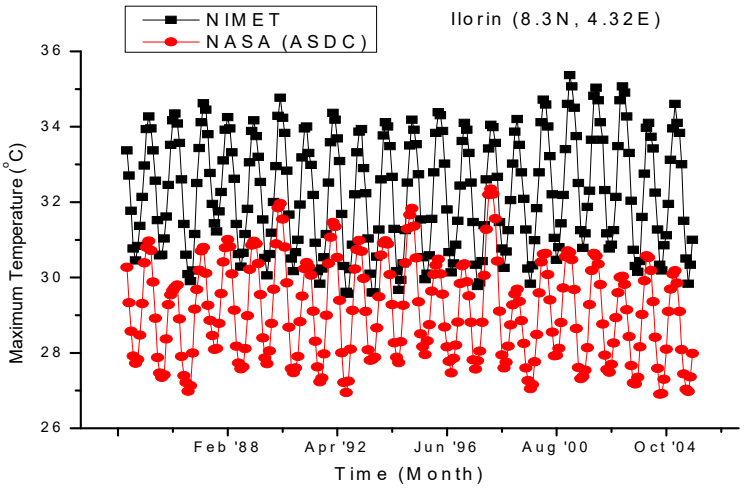

(b)

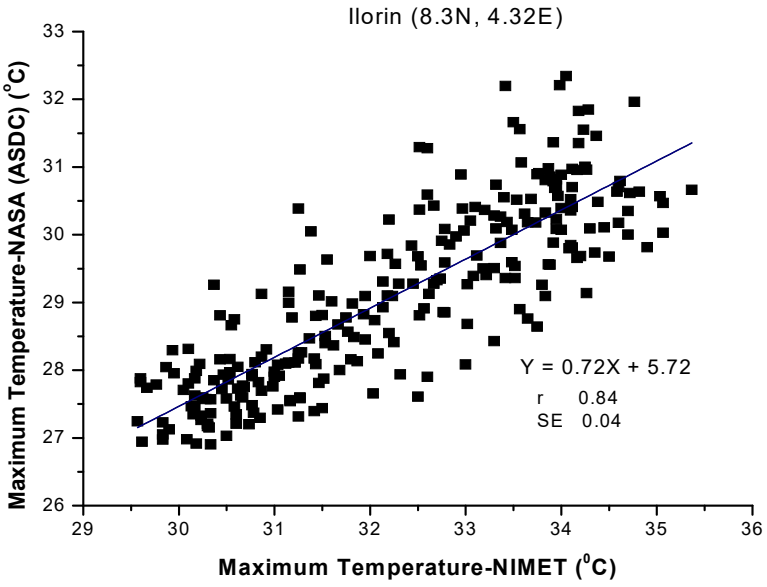

Fig 4.127: (a) Comparison of 6-Month Moving Average of Maximum Temperature from NIMET and NASA (ASDC) for Ilorin.

(b)Correlation of NIMET and NASA (ASDC) Mean Monthly values of Maximum Temperature for Ilorin

(a)

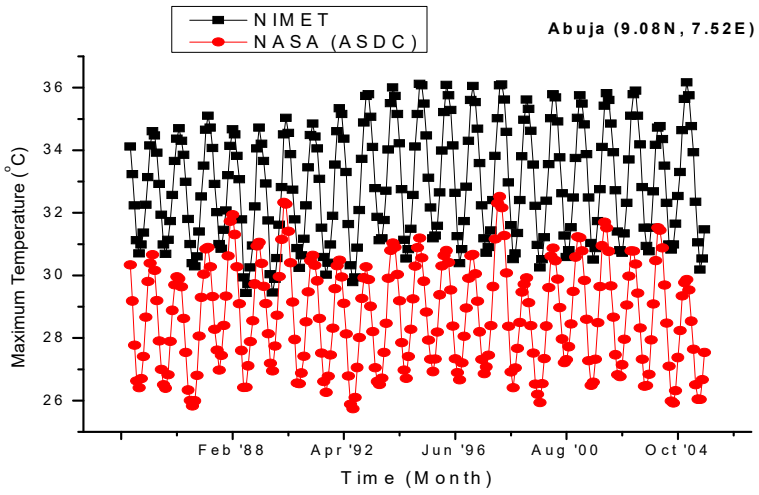

(b)

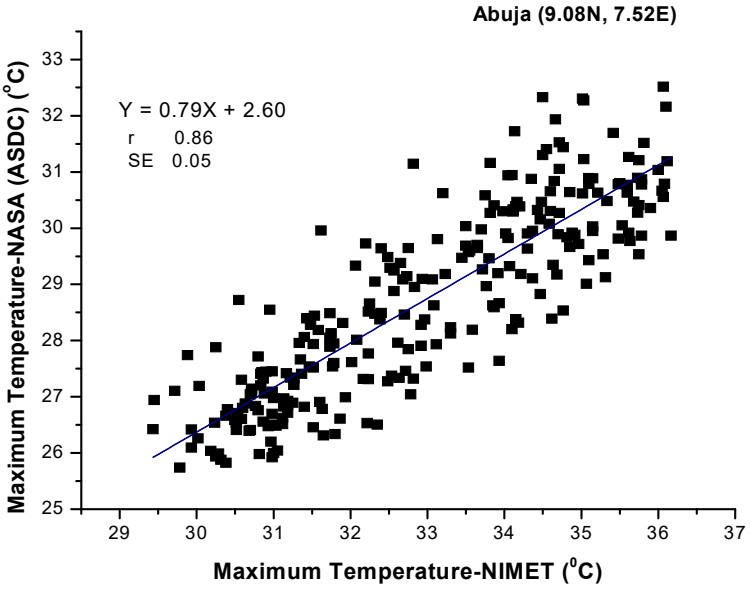

Fig 4.128: (a) Comparison of 6-Month Moving Average of Maximum Temperature from NIMET and NASA (ASDC) for Abuja.

(b)Correlation of NIMET and NASA (ASDC) Mean Monthly values of Maximum Temperature for Abuja

(a)

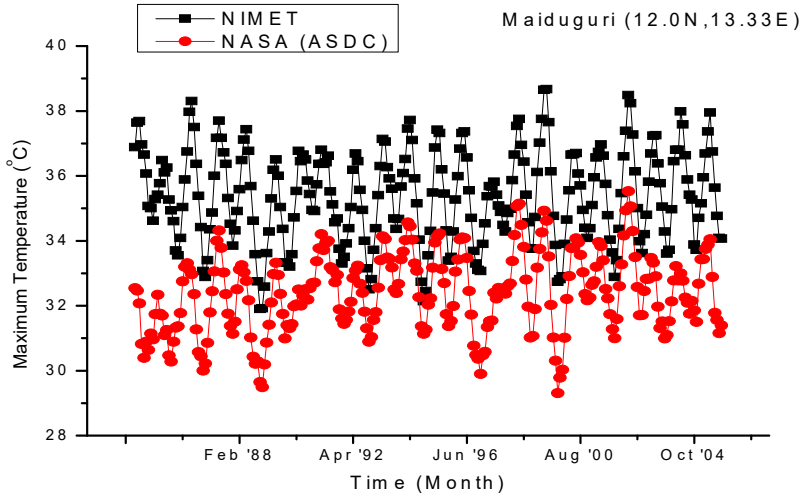

(b)

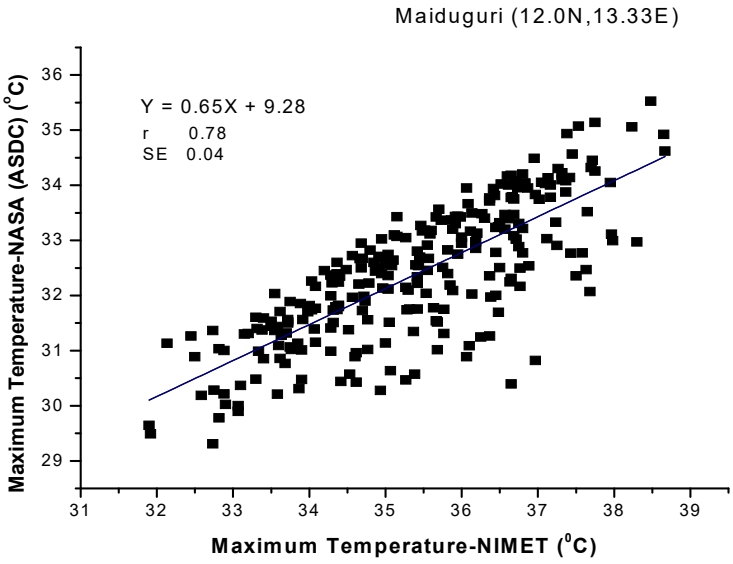

Fig 4.129: (a) Comparison of 6-Month Moving Average of Maximum Temperature from NIMET and NASA (ASDC) for Maiduguri.

(b)Correlation of NIMET and NASA (ASDC) Mean Monthly values of Maximum Temperature for Maiduguri

(a)

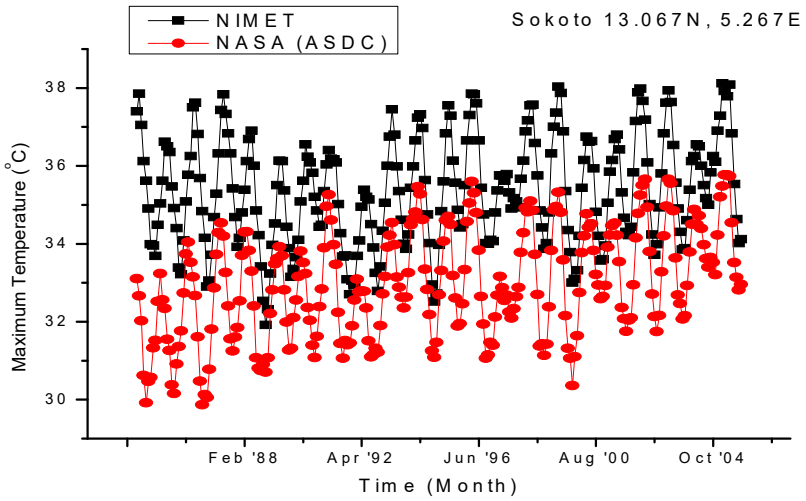

(b)

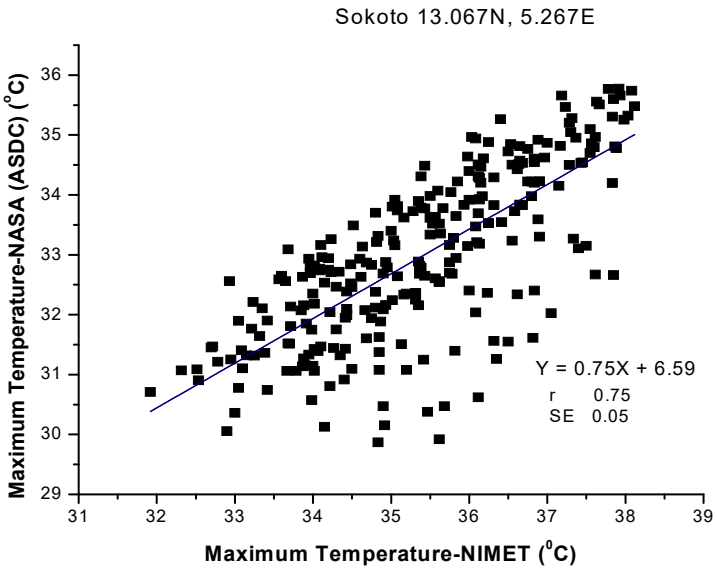

Fig 4.130: (a) Comparison of 6-Month Moving Average of Maximum Temperature from NIMET and NASA (ASDC) for Sokoto.

(b)Correlation of NIMET and NASA (ASDC) Mean Monthly values of Maximum Temperature for Sokoto

Table 4.8: Summary of correlation coefficients obtained for Solar Radiation

Location	Linear correlation coefficient, R	SE
Port Harcourt	0.76	0.06
Lagos	0.58	0.06
Ibadan	0.83	0.04
Ilorin	0.74	0.06
Abuja	0.72	0.06
Sokoto	0.55	0.06

Table 4.9: Summary of correlation coefficients of surface temperatures

Location	Minimum Temperature,		Maximum Temperature,	
	r	SE	r	SE
Port Harcourt	0.55	0.03	0.80	0.02
Lagos	0.65	0.02	0.55	0.03
Ibadan	0.51	0.02	0.85	0.03
Abuja	0.77	0.03	0.88	0.05
Maiduguri	0.960.78		0.04	
Kano	0.81	0.05		
Sokoto	0.88	0.04		
Benin-City			0.88	0.03
Ilorin			0.85	0.04

4.7 Development of Site-Independent Modified-Hay-Model (MHM)

4.7.1 Determination of the clear sky albedo ρ_a

Five of the locations which had complete and homogenousrecords from the ground observed data over 22-years were selected and used. The stations are Port-Harcourt, Lagos, Ilorin, Maiduguri and Sokoto. The clear sky albedo ρ_a was parameterized from physical principles (equation 3.53). The air mass at actual pressure (equation 3.45) was calculated as (Iqbal, 1983);

$$m_a = \frac{1.66}{P_0} \qquad (4.1)$$

where, P is the actual atmospheric pressure and P_0, the atmospheric pressure at sea level. The monthly mean values of P was obtained from the National Aeronautics and Space Administration (NASA) database and used in equation 4.1 to obtain m_a, the air mass at actual pressure at the locations. The monthly mean values of the aerosol optical thickness $k_a$at the wavelength of 380nm(τ_{380})was collected for Ilorin fromthe Aerosol Robotic Network's (AERONET) ground-based sun-photometer andfrom Total Ozone Mapping Spectrometer (TOMS) Satellite for the other four locations.Values of m_a and k_a weresubstituted in equation (3.43) to obtain the monthly mean values of the aerosol transmittance τ_a. This was further used in equation (3.53) to obtain the values of the clear sky albedo ρ_a for the locations The values of P, k_a, τ_a, and ρ_a for the five locations are presented in Tables 4.11 to 4.15. The value of the cloud base albedo ρ_c was taken as 0.6 (Hay, 1979; Iqbal, 1983) and monthly mean values of ground surface albedo, ρ_g, (Table 4.16) for the locations were obtained from the archives of the National Aeronautics and Space Administration (NASA).

Table 4.10. Monthly mean values of atmospheric pressure P, aerosol optical thickness k_a, aerosol transmittance τ_a and clear sky albedo $\rho_a$for Port Harcourt.

Month	P(kPa)	$\mathbf{k_a}$	$\boldsymbol{\tau_a}$	$\boldsymbol{\rho_a}$
January	99.7	0.42	0.51	0.12
February	99.6	0.49	0.47	0.12
March	99.6	0.46	0.48	0.12
April	99.6	0.43	0.51	0.12
May	99.7	0.36	0.56	0.11
June	99.9	0.31	0.60	0.11
July	100.0	0.16	0.74	0.09
August	100.0	0.10	0.83	0.09
September	99.9	0.11	0.82	0.09
October	99.8	0.16	0.74	0.09
November	99.7	0.23	0.67	0.10
December	99.7	0.27	0.63	0.10
Annual Average	99.8	0.29	0.61	0.11

Table 4.11. Monthly mean values of atmospheric pressure P, aerosol optical thickness k_a, aerosol transmittance τ_a and clear sky albedo $\rho_a$for Lagos.

Month	P (kPa)	$\mathbf{k_a}$	$\boldsymbol{\tau_a}$	$\boldsymbol{\rho_a}$
January	100.0	0.45	0.49	0.12
February	100.0	0.51	0.45	0.12
March	100.0	0.52	0.44	0.12
April	100.0	0.51	0.45	0.12
May	100.0	0.45	0.49	0.12
June	100.0	0.40	0.52	0.11
July	100.0	0.26	0.65	0.10
August	100.0	0.21	0.70	0.10
September	100.0	0.19	0.71	0.10
October	100.0	0.20	0.70	0.10
November	100.0	0.27	0.64	0.10
December	100.0	0.25	0.65	0.10
Annual Average	100.0	0.35	0.56	0.11

Table 4.12. Monthly mean values of atmospheric pressure P, aerosol optical thickness k_a, aerosol transmittance τ_a and clear sky albedo ρ_a for Ilorin.

Month	P (kPa)	$\mathbf{k_a}$	$\boldsymbol{\tau_a}$	$\boldsymbol{\rho_a}$
January	97.9	0.33	0.59	0.11
February	97.8	0.39	0.54	0.11
March	97.8	0.42	0.52	0.11
April	97.8	0.42	0.52	0.12
May	97.9	0.37	0.56	0.11
June	98.1	0.30	0.62	0.11
July	98.2	0.19	0.72	0.10
August	98.2	0.15	0.76	0.09
September	98.1	0.12	0.80	0.09
October	98.0	0.11	0.82	0.09
November	97.9	0.14	0.77	0.09
December	97.9	0.18	0.73	0.10
Annual Average	97.9	0.26	0.65	0.10

Table 4.13. Monthly mean values of atmospheric pressure P, aerosol optical thickness k_a, aerosol transmittance τ_a and clear sky albedo $\rho_a$for Maiduguri.

Month	P (kPa)	$\mathbf{k_a}$	$\boldsymbol{\tau_a}$	$\boldsymbol{\rho_a}$
January	97.7	0.21	0.69	0.10
February	97.6	0.25	0.66	0.10
March	97.3	0.28	0.63	0.10
April	97.1	0.33	0.59	0.11
May	97.2	0.37	0.56	0.11
June	97.4	0.34	0.58	0.11
July	97.5	0.30	0.62	0.11
August	97.5	0.26	0.66	0.10
September	97.4	0.21	0.70	0.10
October	97.4	0.17	0.74	0.09
November	97.5	0.13	0.79	0.09
December	97.7	0.14	0.78	0.09
Annual Average	97.4	0.25	0.66	0.10

Table 4.14. Monthly mean values of atmospheric pressure P, aerosol optical thickness k_a,aerosol transmittance $\tau_a$and clear sky albedoρ_a for Sokoto.

Month	P (kPa)	$\mathbf{k_a}$	$\boldsymbol{\tau_a}$	$\boldsymbol{\rho_a}$
January	97.4	0.19	0.72	0.10
February	97.3	0.24	0.67	0.10
March	97.1	0.28	0.63	0.10
April	96.9	0.33	0.59	0.11
May	97.0	0.36	0.57	0.11
June	97.2	0.37	0.56	0.11
July	97.3	0.34	0.58	0.11
August	97.3	0.30	0.61	0.11
September	97.3	0.26	0.65	0.10
October	97.2	0.22	0.69	0.10
November	97.3	0.17	0.75	0.09
December	97.4	0.14	0.77	0.09
Annual Average	97.2	0.27	0.64	0.10

Table 4.15. The monthly mean values of the ground surface albedo for the locations

	Locations				
Month	Port Harcourt	Lagos	Ilorin	Maiduguri	Sokoto
January	0.15	0.18	0.17	0.28	0.3
February	0.16	0.18	0.18	0.31	0.32
March	0.18	0.19	0.20	0.32	0.32
April	0.18	0.20	0.20	0.32	0.32
May	0.17	0.20	0.20	0.33	0.33
June	0.17	0.20	0.21	0.33	0.33
July	0.17	0.20	0.22	0.32	0.32
August	0.19	0.21	0.24	0.28	0.28
September	0.18	0.22	0.22	0.24	0.28
October	0.17	0.20	0.20	0.25	0.28
November	0.17	0.20	0.19	0.27	0.30
December	0.16	0.18	0.18	0.28	0.30
Annual Average	0.17	0.19	0.20	0.29	0.30

4.7.2. Estimation of Solar Radiation using the Modified-Hay model

The values of the various parameters for Ilorin were substituted into equation (3.38) and the regression coefficients a and b were obtained as 0.262 and 0.615 respectively. Five years data (22.72%) was used to calibrate and 17 years (77.27%) used to validate the model over Ilorin. The model was then tested over the other four locations of Port Harcourt, Lagos, Maiduguri and Sokoto.

Tables 4.17 to 4.21 displayed the monthly mean daily values of the estimated and the observed solar radiation while the trends of the models are shown in Fig. 4.131 to Fig. 4.135. The regression parameters and performance indicators of the models are presented in Tables 4.22 to 4.26.

Mean monthly values of the sunshine hours $\bar{n}$ and day length $\bar{N}$ obtained for five of the locations which are having complete and homogenous records from the observed data over 22-years, January 1984 to December 2005 were selected and substituted into the proposed model, equation (3.54) to estimate monthly average daily values of global radiation. Regression equations for the following existing models, Angstrom-Prescott, Almorox-Hontoria, Garcia and Chen-Li for each of the locations were developed from the dataset from which site-specific empirical coefficients were obtained. For the Bristow-Campbell model, the coefficients a_3 and c_3 (eq. 2.11) were used as recommended by the author while b_3 was calibrated using the stations dataset. The regression coefficients for the Hargreaves-Samani and Hay models were retained.

For the southernmost station Port Harcourt, the modified-Hay model have the best correlation coefficient, r = 0.906 with the second best, Hargreaves-Samani having $r = 0.888$. The performance indicators similarly showed the modified-Hay model had the best estimation with the lowest mean bias error (MBE) = - 0.991MJm^{-2}day^{-1}and root mean square error (RMSE) = 1.341MJm^{-2}day^{-1} respectively. For Lagos, the modified-Hay model has the correlation coefficient, $r = 0.964$, MBE = - 0.859 MJm^{-2}day^{-1} and RMSE = 1.034 MJm^{-2}day^{-1}. The closest in terms of$r = 0.916$ is the Hay model, but with poor performance indicators MBE = - 6.129MJm^{-2}day^{-1} and RMSE = 6.192MJm^{-2}day^{-1} respectively. Ilorin presented a slightly different scenario in terms of correlation coefficient r, with both Hay and modified-Hay models having very close $r = 0.927$ and $r = 0.929$ respectively. However, the Modified-Hay model provided a better estimation

performance indicators with MBE = - 0.014MJm^{-2}day^{-1} and RMSE = 0.785MJm^{-2}day^{-1} compared to Hay with MBE = - 4.440MJm^{-2}day^{-1} and RMSE = 4.514MJm^{-2}day^{-1}. In Maiduguri and Sokoto, the modified-Hay model had better correlation coefficients with $r = 0.910$ and $r = 0.901$ respectively. The Garcia model had a slightly better performance indicators for Maiduguri with MBE = 0.063MJm^{-2}day^{-1} and RMSE = 1.062MJm^{-2}day^{-1} compared to MBE = 0.989MJm^{-2}day^{-1} and RMSE=1.212MJm^{-2}day^{-1}for the modified-Hay. Similarly, Angstrom-Prescott model has a slightly lower MBE=0.010MJm^{-2}day^{-1} when compared to modified-Hay MBE=0.578MJm^{-2}day^{-1} for Sokoto. Overall, the modified-Hay model gave good estimation performances for the five locations where it was tested.It indicated a generally stable performance with a very low variation in all the five locations with the best $r = 0.964$ in Lagos and the lowest $r = 0.901$ in Sokoto.

The performance exhibited by the proposed model indicates that inclusion of the parameters, that is,the appropriate values of cloudless clear sky albedo (ρ_a) and the appropriate use of the modified day-length ($\overline{N}_m$)(Iqbal, 1983) in the model equation led to an improvement in the estimation accuracyof mean monthly daily values of global radiation over locations in Nigeria.

Table 4.16: Monthly mean daily values of Solar Radiation for Port Harcourt

Time (Month)	Incident Global Radiation ($\mathbf{MJm^{-2}/day}$)								
	Observed	Angstrom -Prescott	Almorox-Hontoria	Hargreaves-Samani	Bristow-Campbell	Garcia	Chen/Li	Hay	Modified -Hay
Jan	21.50	17.86	17.86	22.79	23.10	25.66	20.18	14.03	20.05
Feb	23.50	18.87	18.87	22.69	23.18	24.27	19.62	14.81	23.04
Mar	24.69	17.97	17.90	21.69	21.33	21.31	19.68	14.36	23.67
Apr	24.25	19.30	19.29	21.45	20.94	18.77	18.75	15.18	23.55
May	22.27	19.04	19.06	20.18	19.14	17.39	16.59	14.92	19.16
Jun	20.23	16.12	16.05	18.36	15.72	15.60	15.51	13.01	19.02
Jul	18.13	12.43	12.60	17.21	12.70	14.84	13.52	10.67	18.54
Aug	17.30	13.27	13.39	17.23	11.82	15.09	15.72	11.29	17.30
Sep	20.81	14.87	14.87	18.37	14.14	16.59	16.69	12.36	19.50
Oct	21.84	16.97	16.91	19.25	16.97	18.78	18.08	13.64	19.79
Nov	22.41	19.19	19.29	19.67	19.03	23.48	18.59	14.87	21.99
Dec	21.54	19.41	19.60	21.17	21.64	25.79	19.72	14.92	20.96

Table 4.17:Monthly mean daily values of Solar Radiation for Lagos

Time (Month)	Incident Global Radiation ($\mathbf{MJm^{-2}/day}$)								
	Observed	Angstrom-Prescott	Almorox-Hontoria	Hargreaves-Samani	Bristow-Campbell	Garcia	Chen/Li	Hay	Modified-Hay
Jan	21.50	13.59	13.52	15.33	11.42	22.24	19.08	14.93	20.97
Feb	23.50	15.72	15.73	16.42	12.56	21.01	16.71	16.97	21.37
Mar	24.69	15.01	14.92	15.95	10.10	19.74	18.64	16.50	23.98
Apr	24.25	16.33	16.32	15.91	9.85	18.61	15.94	17.69	24.30
May	22.27	15.56	15.52	15.55	9.70	15.25	13.87	16.93	21.40
Jun	20.23	11.91	11.89	15.25	9.60	15.35	12.05	13.59	19.70
Jul	18.13	10.67	10.78	13.97	6.66	14.19	11.84	12.47	17.51
Aug	17.30	10.73	10.87	13.74	5.74	17.19	17.62	12.59	16.71
Sep	20.81	12.38	12.35	14.56	7.17	18.58	14.43	14.12	19.38
Oct	21.84	14.80	14.74	14.99	8.90	20.40	15.11	16.19	21.53
Nov	22.41	15.52	15.60	14.41	8.95	15.87	13.05	16.64	20.88
Dec	21.54	15.23	15.34	15.13	11.56	18.99	13.04	16.29	20.41

Table 4.18:Monthly mean daily values of Solar Radiation for Ilorin

Time (Month)	Incident Global Radiation ($\mathbf{MJm^{-2}/day}$)								
	Observed	Angstrom-Prescott	Almorox-Hontoria	Hargreaves-Samani	Bristow-Campbell	Garcia	Chen/Li	Hay	Modified-Hay
Jan	21.50	19.69	19.60	19.39	22.36	17.49	21.58	16.65	20.80
Feb	23.50	21.68	21.60	20.83	23.95	17.85	23.18	18.83	23.38
Mar	24.68	21.72	21.64	20.63	24.34	17.71	23.46	18.92	23.63
Apr	24.25	21.55	21.54	19.70	22.99	17.25	20.66	18.92	23.68
May	22.27	22.58	22.49	18.20	20.22	16.72	19.17	18.64	23.33
Jun	20.23	21.65	21.61	17.08	17.93	15.99	18.37	17.26	21.75
Jul	18.13	20.31	20.42	16.07	15.04	15.80	16.92	14.30	18.53
Aug	17.30	19.48	19.74	16.18	14.86	16.01	17.10	13.34	17.54
Sep	20.81	20.91	20.90	17.47	18.53	16.32	19.29	15.20	19.55
Oct	21.84	21.70	21.60	17.75	20.19	16.37	19.90	17.24	21.65
Nov	22.41	21.38	21.40	19.08	22.29	16.98	21.59	18.30	22.67
Dec	21.54	20.40	20.41	19.21	21.90	17.23	21.34	17.58	21.77

Table 4.19:Monthly mean daily values of Global Radiation for Maiduguri

Time (Month)	Incident Global Radiation ($\mathbf{MJm^{-2}/day}$)								
	Observed	Angstrom-Prescott	Almorox-Hontoria	Hargreaves-Samani	Bristow-Campbell	Garcia	Chen/Li	Hay	Modified-Hay
Jan	20.18	19.69	19.60	21.59	21.72	20.72	19.40	18.66	20.23
Feb	22.57	21.68	21.60	23.11	23.60	22.84	19.98	20.56	22.56
Mar	24.45	21.72	21.64	25.07	25.53	24.40	20.03	20.48	25.68
Apr	24.39	21.55	21.54	24.45	26.47	23.76	19.78	20.21	25.51
May	22.78	22.58	22.49	22.57	25.98	23.016	19.41	21.28	23.70
Jun	21.13	21.65	21.61	20.66	24.39	21.40	18.65	20.34	22.62
Jul	18.86	20.31	20.42	18.61	20.91	20.46	18.32	18.92	20.06
Aug	21.63	19.48	19.74	17.86	19.07	19.69	18.33	18.03	23.07
Sep	20.12	20.91	20.89	19.10	22.24	21.28	18.41	19.61	22.75
Oct	21.60	21.70	21.60	21.47	23.85	20.77	18.23	20.56	22.60
Nov	20.80	21.38	21.40	22.24	22.05	20.74	18.81	20.35	21.15
Dec	21.55	20.40	20.41	20.96	21.03	19.98	19.05	19.41	21.99

Table 4.20:Monthly mean daily values of Global Radiation for Sokoto

Time (Month)	Incident Global Radiation ($\mathbf{MJm^{-2}/day}$)								
	Observed	Angstrom-Prescott	Almorox-Hontoria	Hargreaves-Samani	Bristow-Campbell	Garcia	Chen/Li	Hay	Modified-Hay
Jan	20.19	20.19	20.23	18.69	20.83	21.01	20.59	18.50	20.97
Feb	22.23	21.87	21.90	20.76	22.91	21.39	22.16	20.09	22.97
Mar	23.44	21.96	21.92	21.95	24.66	21.04	23.20	20.65	23.83
Apr	23.79	21.69	21.65	22.87	25.77	20.51	23.72	20.74	24.07
May	22.52	22.67	22.62	21.15	24.12	20.09	21.60	21.44	23.86
Jun	21.60	22.49	22.44	19.93	22.19	19.11	20.24	21.27	22.65
Jul	19.39	21.04	21.03	18.50	19.09	18.62	19.43	20.28	20.55
Aug	18.51	18.57	18.79	17.62	16.87	18.53	20.18	18.56	19.65
Sep	20.97	21.66	21.61	18.12	19.01	18.72	22.50	20.50	20.69
Oct	21.63	22.40	22.43	19.53	22.31	18.82	22.79	20.55	20.54
Nov	20.56	21.04	21.14	19.57	21.38	20.11	21.88	19.14	20.73
Dec	19.47	18.85	18.84	18.32	20.23	20.69	19.99	17.44	20.71

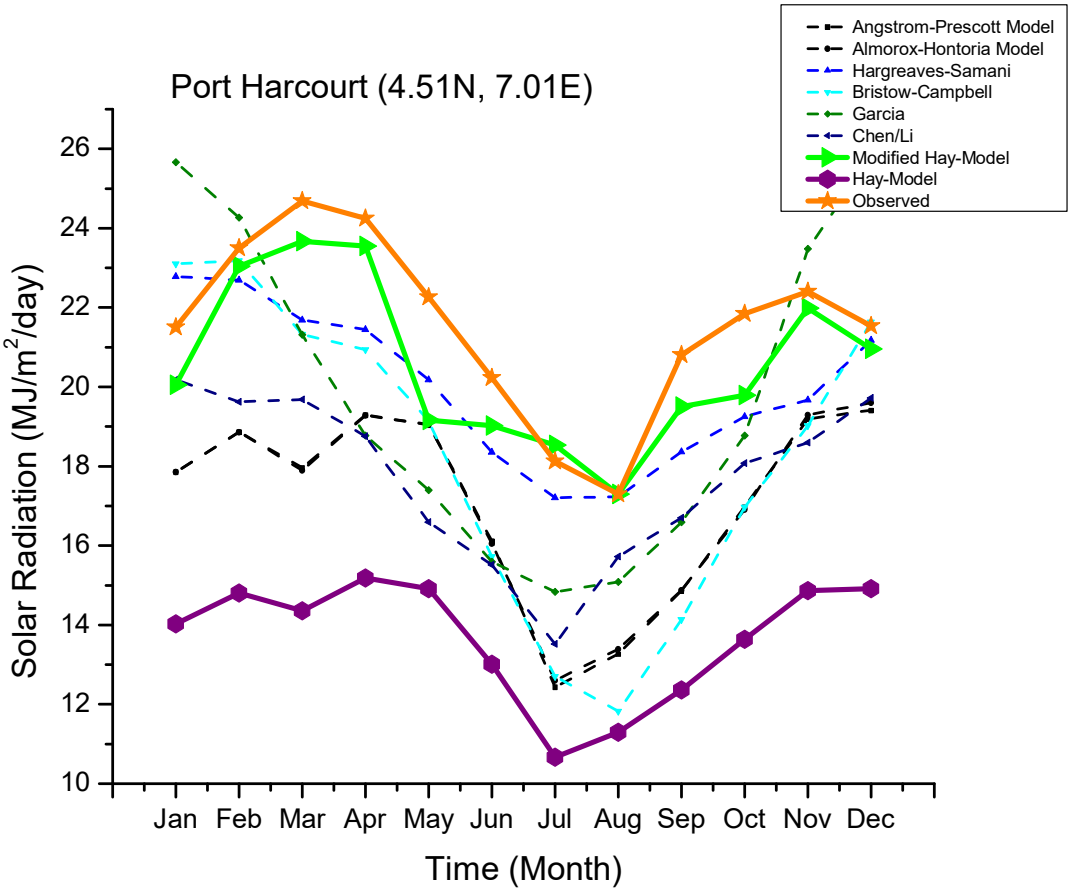

Fig 4.131: Comparison of the models with the ground observed values –Port Harcourt

Table 4.21: Regression parameters of models and corresponding values of Performanceindicators-Port-Harcourt

Model	Coefficients			r	MBE (MJm^{-2}/ day)	RMSE (MJm^{-2}/ day)
	a_i	b_i	c_i			
Angstrom-Prescott	0.178	0.912		0.847	-4.429	4.602
Almorox-Hontoria	0.165	0.390		0.834	-4.398	4.583
Hargreaves-Samani	0.190			0.888	-1.533	2.002
Bristow-Campbell	0.700	0.008	2.400	0.865	-3.229	4.021
Garcia	0.171	0.422		0.806	-1.740	3.726
Chen-Li	0.159	0.223	0.000	0.873	-3.816	4.075
Hay	0.1572	0.5566		0.874	-7.866	7.944
Modified-Hay	0.262	0.615		0.906	-0.991	1.341

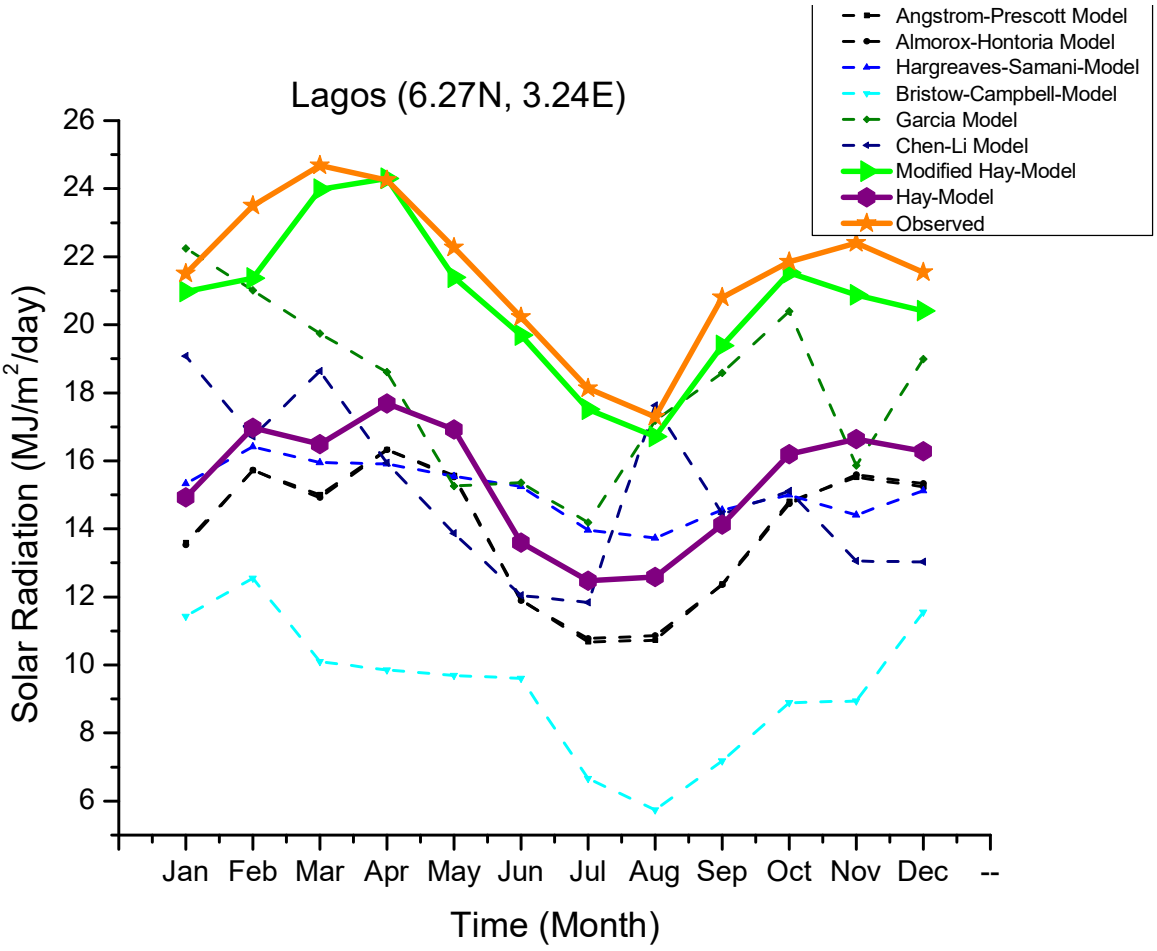

Fig.4.132. Comparison of the models with the ground observed values - Lagos

Table 4.22: Regression parameters of models and corresponding values of performance indicators-Lagos

Model	Coefficients			r	MBE (MJm^{-2}/ day)	RMSE (MJm^{-2}/ day)
	a_i	b_i	c_i			
Angstrom-Prescott	0.178	0.912		0.902	-7.581	7.636
Almorox-Hontoria	0.165	0.390		0.891	-7.573	7.635
Hargreaves-Samani	0.190			0.730	-0.891	1.690
Bristow-Campbell	0.700	0.008	2.400	0.603	-6.641	6.853
Garcia	0.019	0.897		0.362	2.132	3.422
Chen-Li	1.091	0.132	-0.012	0.370	-0.883	2.921
Hay	0.1572	0.5566		0.916	-6.129	6.192
Modified-Hay	0.262	0.615		0.964	-0.859	1.034

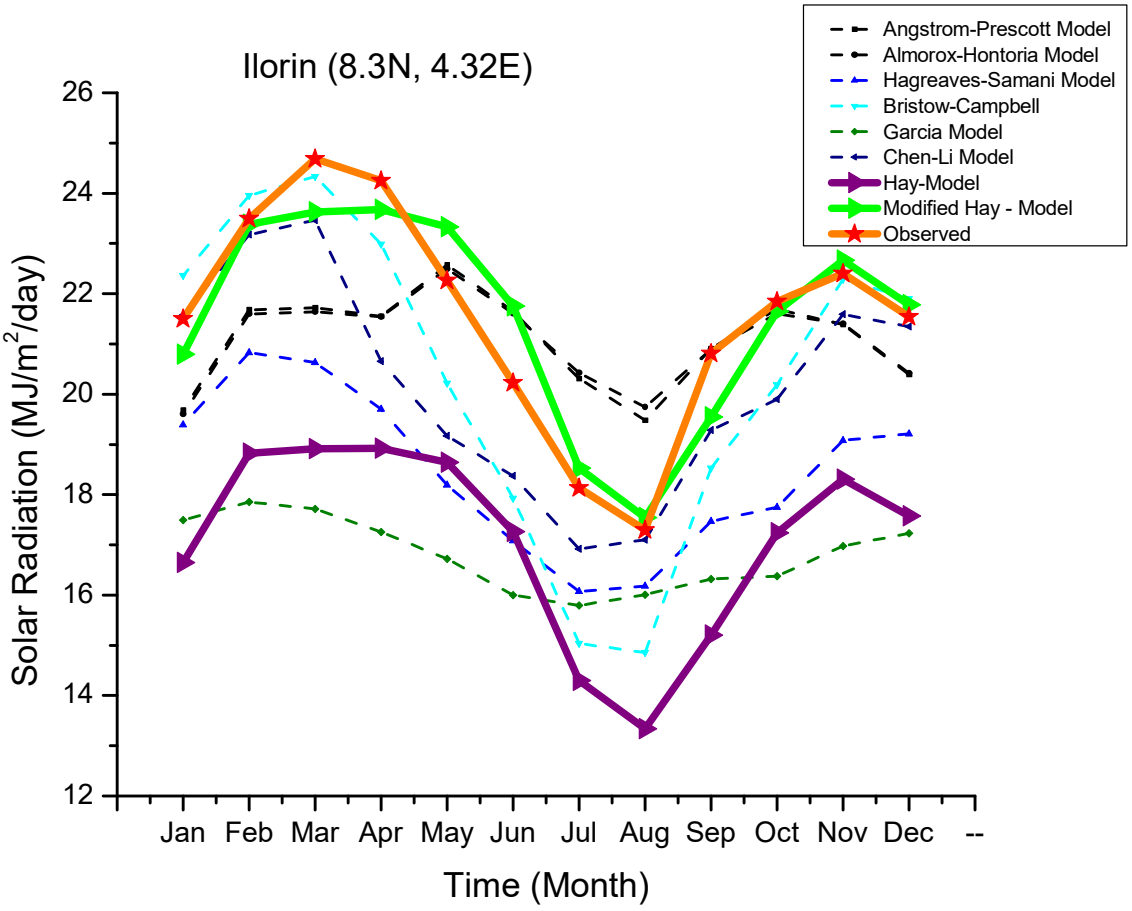

Fig.4.133.Comparison of the models with the ground observed values - Ilorin

Table 4.23: Regression parameters of models and corresponding values of performance indicators-Ilorin

Model	Coefficients			r	MBE (MJm^{-2}/ day)	RMSE (MJm^{-2}/ day)
	a_i	b_i	c_i			
Angstrom-Prescott	0.301	0.610		0.650	-0.450	1.748
Almorox-Hontoria	-0.024	0.379		0.607	-0.458	1.811
Hargreaves-Samani		0.160		0.522	-1.022	1.941
Bristow-Campbell	0.700	0.007	2.400	0.500	0.901	2.820
Garcia	0.357	0.283		0.597	2.681	3.048
Chen-Li	-0.696	0.301	0.004	0.530	0.723	2.011
Hay	0.1572	0.5566		0.927	-4.440	4.514
Modified-Hay	0.262	0.615		0.929	-0.014	0.785

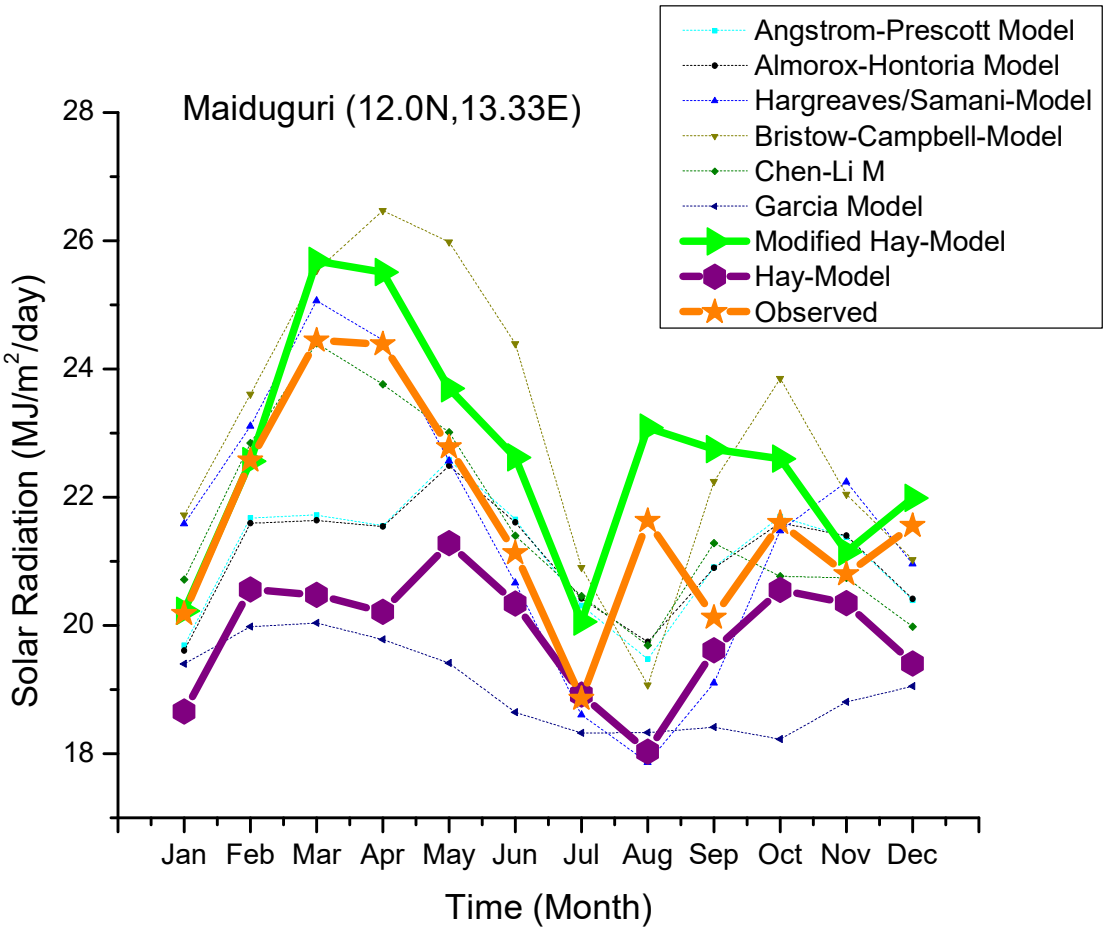

Fig.4.134. Comparison of the models with the ground observed values - Maiduguri

Table 4.24: Regression parameters of models and corresponding values of performance indicators-Maiduguri

Model	Coefficients			r	MBE (MJm^{-2}/ day)	RMSE (MJm^{-2}/ day)
	a_i	b_i	c_i			
Angstrom-Prescott	0.255	0.506		0.541	-0.584	1.468
Almorox-Hontoria	0.111	0.246		0.544	-0.592	1.469
Hargreaves-Samani	0.160			0.641	2.521	3.002
Bristow-Campbell	0.700	0.070	2.400	0.72	4.110	4.401
Garcia	0.395	0.163		0.472	0.063	1.062
Chen-Li	0.423	0.061	-0.001	0.750	2.640	2.811
Hay	0.1572	0.5566		0.520	-1.804	2.265
Modified-Hay	0.262	0.615		0.910	0.989	1.212

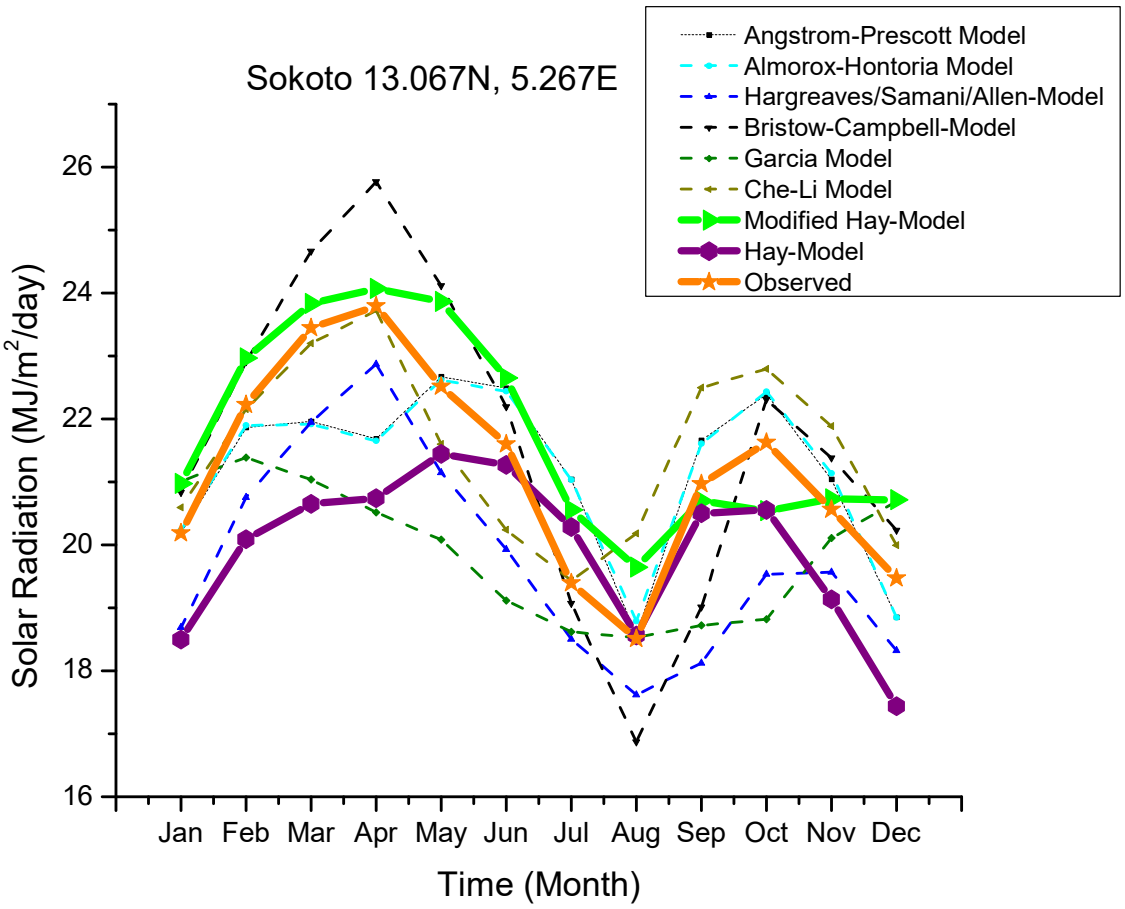

Fig.4.135. Comparison of the models with the ground observed values – Sokoto

Table 4.25: Regression parameters of models and corresponding values of Performanceindicators-Sokoto

Model	Coefficients			r	MBE ($\mathrm{MJm^{-2}/day}$)	RMSE ($M\mathrm{Jm^{-2}/day}$)
	a_i	b_i	c_i			
Angstrom-Prescott	0.088	0.762		0.776	0.010	1.000
Almorox-Hontoria	-0.165	0.390		0.768	0.025	1.012
Hargreaves-Samani	0.160			0.460	-1.15	1.87
Bristow-Campbell	0.700	0.070	2.400	0.450	0.710	2.320
Garcia	0.360	0.233		0.480	-1.010	1.540
Chen-Li	0.024	0.164	0.000072	0.840	0.620	0.962
Hay	0.1572	0.5566		0.706	-1.260	1.686
Modified-Hay	0.262	0.615		0.901	0.578	0.902

CHAPTER FIVE

5.1CONCLUSION

Incident solar radiation is unevenly distributed over the earth's surface. This is as a result of such variables like solar altitude, which is associated with latitude and seasons; and atmospheric conditions, which are determined by cloud coverage and level of atmospheric turbidity. This study examined the spatial and temporal nature of surface global horizontal solar radiation over eleven stations distributed within the different geographical parts of Nigeria using a 22-year satellite dataset (January 1984- December 2005) obtained from National Aeronautics and Space Agency (NASA) Atmospheric Science Data Centre and ground observed data obtained from Nigeria Meteorological agency, Lagos. The nature of the relationships that existed between incident solar radiation and atmospheric temperature (minimum and maximum) were also investigated. The time-series analysis of the 22-year dataset was made so as to have a better understanding of the temporal trends of the incident solar radiation.The major findings from this study are as follows:

1. The eleven locations were grouped into the four main climatic zones of Nigeria namely Mangrove swamp, Tropical rain forest, Guinea savannah and Sudan/Sahel savannah. The daily global solar irradiance was grouped into six classes using interval of 5. The result showed that the amount of global irradiance received on the surface has a zonal symmetry, increasing in the northward direction. This was shown to be in agreement with the observation of Persson (1999) in Sweden and was attributed to decreasing cloudiness in the northward direction.
2. The plots of the extra-terrestrial radiation, transmissivity and global solar radiation were respectively presented over the locations as a function of time and latitude. The contour lines showed that the amount of extra-terrestrial over a location at a particular time of the year is a function of the solar movement. Atmospheric transmissivity was seen to display both latitudinal and time dependence over the entire region, with its value increasing in the northward direction. A zonal symmetry was also observed in the spatial distribution of global solar radiation increasing in the northward direction. Comparing the spatial

distributions of the extra-terrestrial solar radiation, atmospheric transmissivity and global solar radiation, it was inferred that cloudiness is the major determinant factor in the distribution of surface global solar radiation over the region.

3. From the correlation coefficient obtained from the plot of surface temperatures (maximum and minimum) against incident solar radiation at different stations, the following results were evident;

i. A positive correlation exists between incident solar radiation and the maximum temperature.

ii. A poor correlation between incident solar radiation and minimum temperature. This is true in all locations examined except the northernmost station, Sokoto.

These results were given adequate explanations.

4. The time series of global solar radiation, atmospheric transmissivity and atmospheric temperatures between 1984 and 2005 were examined by determining the regression coefficient and plotting the fast Fourier transform to indicate the temporal trends. The decline in the amount of atmospheric transmissivity and incident global solar radiation noted over the entire region between 1984 and 1995 and a recovery thereafter were given comprehensive explanations. Also, the general decrease was noted in the temporal trends of the maximum temperatures and an increase in that of the minimum temperature over the locations below 9^0 latitude. This was adduced to increasing cloudiness over the locations during the years of investigation. The converse observations recorded on locations above 9^0were also adequately explained.

5. The satellite-derived datasets from NASA's Atmospheric Science Data Centre and ground measured data from Nigeria Meteorological Agency in Lagos showed acceptable level of correlation for incident solar radiation, minimum and maximum temperatures for all the stations. Finally, seven existing equation models werecalibrated and validated for five locations in the country and a new site-independent empirical model introduced.

5.2 Recommendation for further research

1. The quality of this work could be further enhanced if the period of data collection is increased from the 22 years used in this work to at least 30 yearswhich was not available at the moment.
2. The relationship between the temporal trends of the global radiation and that of the maximum temperature for the three locations above latitude 9°, that is Maiduguri, Kano and Sokoto need to be further investigated.

REFERENCES

Adeniyi, M. O., Nymphas, E. F. and Oladiran, E. O. 2012. Characteristics of total solar radiation in an urban tropical environment. *International Journal of the Physical Sciences* 7.30:5154-5161.

Adjepong, S. K. and Okujagu, C. 1987. Correlation between the time-series of air temperature and incident solar radiation at Port Harcourt, Nigeria. *Internal Report.ICTP, Trieste, Italy*339:127-131.

Akinoglu, B. G. and Ecevit, A. 1990. Construction of a quadratic model using modified Angstrom coefficients to estimate global solar radiation. *Solar Energy* 45:85-92.

Akpabio, L. E., Udo, S. O. and Etuk, S. E. 2005. Modeling Global Radiation for a Tropical Location: Onne, Nigeria. *Turkish Journal of Physics* 29:63-68.

Allen, R. G. 1995. Evaluation of Proceedures of estimating mean monthly Solar Radiation From air temperature. *Report submitted to the United Nation Food and Agricultural Organization, Rome.*

Allen, R. G. (1997). Self-calibrating method for estimating solar radiation from air temperature.*ASCE Journalof Hydrological Engineering*2:56-57.

Allen, R. G., Pereira, L. S., Raes, D. and Smith, M. 1998. Crop evapotranspiration guidelines for computing crop water requirements. *FAO Irrigation and drainage paper*56*:*214-221.

Almorox, J. and Hontoria, C. 2004. Global Solar Radiation estimation using sunshine duration in Spain. *Energy Conversion Management* 45.9-10:1529-35.

Almorox, J. 2011. Estimating global solar radiation from common meteorological data in Aranjuez, Spain. *Turkish Journal of Physics*35:53-64.

Amer E.H. and Younes M. A. 2006. Estimating the monthly discharge of aphotovoltaic Waterpumping system: model verification. *Energy Conversion and Management*47.15-16:2092-2102.

Angstrom, A. 1924. Solar and Terrestrial radiation.Report to the international

commission Forsolar research on actinometric investigations of solar and atmospheric radiation. *Quarterly Journal of Royal Meteorological Society* 50.210:121-126.

Annandale, J. G., Jovanovic, N. Z., Benade, N. and Allen, R. G. 2002.Software for Missingdata error analysis of Penman-Monteithreference evapotranspiration. *IrrigationScience* 21:57–67.

Areola, O., Ahmed, K., Leong, G. C., Irueghe, O. I., Ikwuyatum, G. O. and Adeleke, B. O. 2014. *Comprehensive Certificate Geography for senior secondary schools.* Revised ed. Ibadan: Longman press.

Babatunde, E. B. and Aro, T. O. 1995. Relation between Clearness Index and Cloudiness Index. *Renewable Energy*6.7:801-805.

Bamiro O. A. 1983. Empirical Relations for the Determination of SolarRadiation in Ibadan, Nigeria. *Solar Energy*31:85 – 94.

Besharat, F., Denghan, A. A. and Faghih, A. R. 2012. Empirical models for estimating global solar radiation in Yazd city, Iran. *Proceedings of the International Conference onSolarenergy for MENA region (INCOSOL).*22-23rd October 2012. Amman, Jordan, PpINOSOL, 2.

Bindi, M. And Miglietta, F. 1991. Estimating daily global radiation from air temperature andrainfall measurements. *Climate Research*1:117-124.

Binghao, J., Zhenghui, X., Aiguo, D., Chunxiang, S., and Feng, C. 2013. Evaluation of satellite and reanalysis products of downwardsurface solar radiation over East Asia: Spatial andseasonal variations. *Journal of Geophysical Research and Atmosphere*118:1–16.

Bonan, G. B. 2002. *Ecological Climatology: Concepts and Applications*. 3rd ed. London: Cambridge University Press.

Borzenkova, I. I. 1992. Energy balance and the roles of the sun, earth, oceans and atmosphere.*Encyclopedia of life support systems (EOLSS). Hydrological cycle*1.

Boyo, A. O. and Adeyemi, K. A. 2011. Analysis of solar radiation data from satellite and Nigeria meteorological station.*International Journal of Renewable Energy Research* 1.4:314-322.

Bristow, K. L. And Campbell, G. S. (1984). On the relationship between incoming solar radiation and daily maximum and minimum temperature.*Agriculturaland Forest Meteorolology* 31:59-166.

Brockwell, P. J. and Davis, R. A. 1991. *Time Series: Theory and Methods.* 2nd ed. New York:Springer-Verlag.

Budyko, M. I. 1969. The effect of solar radiation variations on the climate of the Earth. *Tellus XXI* 5:39-692891.

Burari, F. W. and Sambo, A. S. 2001. Models for the prediction of global solar radiation for Bauchi using meteorological data. *Nigeria Journal of Renewable Energy* 91:30-33.

Castellvi, F. 2008. Evaluation of three practical methods for estimating daily solar radiation indry climates. *The Open Atmospheric Science Journal*2:185-191.

Changnon, S.A. and Changnon, D. 2005. Importance of sky conditions on the record of 2004 mid-western crop yields. *Physical Geography* 26.2:99-111.

Chen, J. L. and Li, G. S. 2012. Estimation of monthly mean solar radiation from air temperature in combination with other routinely observed meteorological data inYangtze River Basin in China. *Meteorological Applications (wileyonlinelibrary.com)DOI:*10.1002/met.1306.

Cooley, J. W. and Tukey J. W. 1965. An algorithm for the machine calculation of complex Fourier series. *Mathematics of Computation*19:297–301.

Coops, N. C., Warring, R. J. and Moncrieff, J. B.(2000. Estimating mean monthly incident solar radiation on horizontal and inclined slopes from mean monthly temperatures extremes. *International Journal of Biometeorology*44:204-211.

Deneke, H., A. Feijt, A. van Lammeren, and C. Simmer(2005): Validation of a physical retrieval scheme of solar surface irradiances from narrowband satellite radiances.*Journalof Applied Meteorology* 44.9:1453-1466.

Dodge, Y. 2003. *The Oxford Dictionary of Statistical terms*. London: Oxford University Press.

Donald, C. A. 1982. *Meteorology Today: An Introduction to Weather, Climate and the Environment.*New York: West Publishing Co.

Drummond, A. J. and Thekaekara, M. P.1973.*The Extraterrestrial Solar Spectrum*. Institute of Environmental Science, Mount Prospect, Illinois.

Duffie, J. A. and Beckmann, W. A. 1980. *Solar Engineering of Thermal Processes*. New York: WileyInterscience Publications.

Ekpe, J. E. And Nnabuchi, M. N. 2012. Solar radiation in Onitsha: A correlation with average temperature. *Scholarly Journal of Biotechnology*1.5: 101-107.

El-Sebaii and Trabea A. A. 2005. Estimation of global solar radiation on horizontal surfaces over Egypt. *Egypt Journal of Solids* 28:1-8.

Everitt, B.S. 2003. The Cambridge Dictionary of Statistics, CUP. *ISBN 0-521-81099-X*

Falayi, E. O., Adepitan, J. O. and Rabiu, A. B. 2008. Empirical models for the correlation of global solar radiation with meteorological data for Iseyin, Nigeria. *International Journal of Physical Science* 3.9: 210-216.

Falodun, S. E. and Ogolo, E. O. 2007. Diurnal and Seasonal Variations of Global Solar Radiation at Akure, South – Western Nigeria.*Journal of Engineering and Applied Sciences* 2.1: 125-128

Folayan, C. O. 1988. Estimate of global solar radiation bound for some Nigerian cities. *Nigerian Journal of Solar Energy* 7:36-43.

Garcia, J. V. 1994. *Principios F'isicos de la Climatolog'ia Ediciones* .UNALM Universidad Nacional Agraria La Molina, Lima, Peru

Garg, H. P. and Garg, S. N. 1982. Prediction of global solar radiation from bright

sunshine and other meteorological parameters. *Solar India, proceedings of National Solar Energy Convention, Allied Publishers.*New Delhi *1004-1007.*

Garg, H. P. and Prakash, J. 2000. *Solar Energy: Fundamentals and Applications.* 2nd ed.New Delhi: Tata McGraw-Hill Education Pvt. Ltd.

Glover, J. and McCulloch, J. S. G. 1958. The empirical relation between solar radiation and hours of bright sunshine in the high altitude tropics. *Journal of Royal Meteorological Society 84.359: 56-60.*

Gregory, S. (1980). *Statistical methods and the Geographer*. 4th ed.London:Longman.

Gueymard, C.A. 2004. The sun's total spectral irradiance for solar energy applications and solar radiation models. *Solar Energy* 764: 423-453

Hand, I. F. 1939. Variation in solar radiation intensities at the surface of the earth in the United States.*Monthly Weather Review*September 1939: 338-340.

Hargreaves, G. H. 1981. Water requirements and man-induced climate change. *Journal of irrigation and Drainengineering ASCE* 107:247-255.

Hargreaves, G. H. and Samani, Z. A. 1982. Estimating Potential Evapo-transpiration. *Journal of irrigation and Drain engineering*108.3: 225-230.

Hargreaves, G. H. 1994. Simplified Coefficients for estimating monthly solar radiation in North America and Europe. *Departmental Paper, Department of Biology and Irrigation Engineering, Utah State Univ. Logan Utah*

Hay, J. E. 1970. Aspects of the heat and moisture balance of Canada.PhD. Thesis, Dept. of Geography. University of London.xxv + 322pp.

Hay, J. E. 1979. Calculation of monthly mean solar radiation for horizontal and inclined surfaces. *Solar Energy* 23.4: 301-307.

Hay, J. E. and Suckling, P.W. 1979. Networks for measuring and modeling solar Radiationin British Columbia and adjacent areas of Western Canada. *Canadian Geography*3:222-238.

Heidinger, A. K. 2003. Rapid daytime estimation of cloud properties over a large area

Fromradiance distributions. *Journal of Atmosphere and Oceanic Technology*20:1237-1250.

Hoyt, D. V. 1979. The Smithsonian Astrophysical Observatory Solar Constant Program. *Review of Geophysics and Space physics* 17:3-8.

Hunt, L. A., Kuchar, L., and Swanton, C. J. 1998. Estimation of solar radiation for use in Cropmodeling. *Agricultural and Forest Meteorology*91.3-4:293-300.

Hussain, M. 1984. Estimation of global and diffuse irradiation from sunshine duration and atmospheric water vapour content. *Solar Energy* 33:217-220.

Iloeje, N. P. 1980. *A new Geography of West Africa*. New revised ed. Essex. Longman press.

Iloeje, N. P. 1981. *A new Geography of Nigeria*. New revised ed. Ikeja. Longman press

Iqbal, M. 1983.*An introduction to Solar Radiation*. Don Mills, Ontario Canada: Academic Press.

Jauregui, E. and Luyando, E. 1999. Global Radiation attenuation by air pollution and its Effectson the thermal climate in Mexico City. *International journal of Climatology*19:683-694.

Journee, M. and Bertrand, C. 2010. Improving the spatio-temporal distribution of surface Solarradiation data by merging ground and satellite measurements. *Remote SensingEnvironment*114:2692-2704.

Kane, R. P. 1997. Interannual Variability of global radiation at Wageningen. *Internationaljournal of climatology*17:1487-1493.

Kasten, F. and Young, A. T. 1989.Revised optical air mass tables and approximation formula.*Applied Optics* 28:4735–4738

Kemp, M. U. 2007.Spatial and Temporal Distribution of Solar Radiation in Louisiana M.S. Thesis. Dept. of Geography and Anthropology. Louisiana State University. xix+101pp.

Kimothi, S., Bhattacharya,B.K., Semalty, P. D., Pandey,V. K. and Dadhwal, V. K. 2004.

Estimation of ground insolation using METEOSAT data over India. *Current Science*86.9:1308-1312.

Kolebaje, O. T. and Mustapha, L. O. 2012. On the performance of some predictive models Forglobal solar radiation estimate in tropical stations: Port Harcourt and Lokoja.*The African Review of Physics* 7.0015:145-163.

Kondratyev, K. Y. 1972.*Radiation Processes in the Atmosphere*. World Meteorological Organisation, W. M. O. No 309.

Korachagaon, I. and Bapat, V. N. 2012. Development of a Site-Independent mathematical model for the estimation of global solar radiation on earth surface around the globe. *International Journal of energy and environment* 3.2:295-304.

Kyle, T. G. 1991.*Atmospheric transmission, emission and scattering*. Oxford: Pergamon Press.

Lazlo, I., Ciren, P., Liu, H., Kondragunta, S., Tarpley, J. D. and Goldberg, M. D. 2008. Remotesensing of aerosol and radiation from geostationary satellites. *Advanced.Space Research*41:1882-1893.

Liepert, B. G. 2002. Observed reductions of surface solar radiation at sites in the United Statesand worldwide from 1961 to 1990.*Geophysical Research Letters* 29.10:61-1–61-4.

Liou, K. N. 2002. *An introduction to Atmospheric radiation*. *2nd ed.* New York: Academic Press.

Lunde, P. J. 1980. *Solar Thermal Engineering*. New York:Wiley.

Makowski, K. 2009. The daily temperature amplitude and surface solar radiation.*D.Sc.* Thesis, Institute for Atmospheric and Climate Science, ETH, Zurich, Switzerland.

Malinovic, S., Mihailovic, D. T., Kapor, D., Mijatovic, Z. and Arsenic, I. D. 2006. NEOPLANTA: A short description of the first Serbian UV index model. *Journal of Applied Meteorologyand Climatology* 45.8:1171-1177.

Nigeria Latitude and Longitude. 2018. In: *Maps of world.* Retrieved 16:08, June 22, 2018, fromhttps://www.mapsofworld.com/lat_long/nigeria-lat-long.html

Mavi, H. S. and Tuper, G. J. 2004. *Principles and Application of Climate Studies in Agriculture*. New York: Haworth Press.

Meza, F. and Varas E. 2000. Estimation of mean monthly solar global radiation as a function of temperature. *Agricultural and Forest Meteorol*ogy 100.231:241.

Michalsky, J. J., Anderson, G. P., Barnard, J., Delamere, J., Gueymard, C., Kato, S., Kiedron, P.,McComiskey, A. and Ricchiazzi, P. 2006. Shortwave radiative closure studies for clearskies during the atmospheric radiation measurement 2003 aerosol intensive observationperiod. *Journal of Geophysical Research-Atmospheres11.D14:D14S90. 85.*

Miglietta, F. 1991. Simulation of wheat ontogenesis. Appearance of main stem leaves in the field. *Climate Research 1:145-150.*

Moller, F. 1965. On the backscattering of global radiation by the sky. *Tellus 17:350-355.*

Muzathik, A. M. Nik, W. B., Ibrahim, M. Z. Samo, K. B. Sopian, K. and Alghoul, M. A.2011. Daily global solar radiation estimate based on sunshine hours. *International Journal of Mechanicaland Materials Engineering*6.1:75-80.

Neuwirth, F. 1980.The estimation of global and sky radiation in Austria.*Solar Energy* 24: 421-426

Newland, F. J. 1988. A study of solar radiation models for the coastal region of South China. *Solar Energy* 31:227-235.

Ododo J. C., Agbakwuru J. A. and Ogbu F. A. 1995. Correlation of Solar Radiation with Cloud Cover and relative Sunshine duration.*Energy Conversion and Management*37.10: 1555-1559

Ogolo, E. O. 2010. Evaluating the performance of some predictive models for estimating global solar radiation across varying climatic conditions in Nigeria. *Indian Journal of Radio and Space Physics* 39:121-131.

Okogbue, E.C. and Adedokun, J. A. 2002. Characterization of sky conditions over Ile-Ife, Nigeria, based on 1992-1998 solar radiation observations. *Meteoroligische Zeitschrift* II.6:419-423.

Okogbue, E. C.and Adedokun, J. A. 2009. Estimating Global Solar Irradiance from Air Temperature in a Humid Tropical station, Ondo, Nigeria.*Journal of Meteorologyand Climate Science*7:34-42.

Olatona, I. O. 2009.Analysis and Characterization of Aerosol optical thickness over the West African sub-region.Ph.D. Thesis. Dept. of Physics. University of Ibadan.xix+240

Otkin, J.A., Anderson, M.C. Mecikalski, J.R. and Diak, G.R. 2005. Validation of GOES Basedinsolation estimates using data from the U.S. Climate Reference Network. *Journalof Hydrometeorology* 6:4.460-475.

Panday, C. K. and Katiyar, A. K. 2010. Temperature base correlation for the estimation of global solar radiation on horizontal surface. *International Journal of Energy and Environment*1.4:737 – 744.

Pavolonis, M., Heidinger, A. K., and Uttal, T. 2005. Daytime global cloud typing from AVHRR and VIIRS: Algorithm description, validation and comparisons. *Journal of Applied Meteorology*44:804-826.

Perez, R., Ineichen, P., Moore, K., Kmiecik, M., Chain, C., George, R., and Vignola, F. 2002. A new operational model for satellite-derived irradiances: description and validation.*Solar Energy*73:307-393.

Perrin de Brichambaut, C.1975. Cahiers A.F.D.E.S. *Supplemment au. No.1, Eds, Europeenness Thermique et Industrie, Paris.*

Persson T. 1999. Solar Radiation Climate in Sweden. *Physical Chemistry of Earth (B)* 24.3:275-279.

Pinker, R. T. and Laszlo, I. 2002. Modeling surface solar irradiance for satellite applications on a global scale. *Journal of Applied Meteorology*31:194-211.

Prescott, J. A. 1940. Evaporation from a water surface in relation to solar radiation. *Trans*

RoyalSociety of Science, Australia, 64:114-125.

Radosavljevic, J. and Dordevic, A. 2001. Defining of the intensity of solar radiation on horizontal and oblique surfaces on earth. *FACTA UNIVERSITATIS, Working and Living Environmental Protection*2.1:77-86.

Rietveld, M. R. 1978. A new method for estimating the regression coefficients in the formularelating solar radiation to sunshine. *Agricultural Meteorology*9:243-252.

Rivington, M., Matthews, K. B., Bellocchi, G., and Buchan, K. 2006. Evaluating uncertainty introduced to process-based simulation model estimates by alternative sources of meteological data. *Agricultural Systems*88.2-3:451-471.

Saha, K. 2008. The Earth's Atmosphere. *Springer – Verlag Berlin Heidelberg 79 – 127*

Saha, M. N. and Srivastava, B. N. 1931.*A Treatise on Heat*. revised reprinted ed. Allahabad, India:The Indian Press Pvt. (Ltd) 969.

Safari, B. and Gasore, J. 2009.Estimation of global solar radiation in Rwanda. *Asian Journalof Scientific Research*2.2:68-75.

Samuel, T. D. M. A. 1991. Estimation of global solar radiation for Sri Lanka. *Solar Energy*47: 333-337.

Sanusi, Y. K. and Abisoye, S. G. 2011.Estimation of solar radiation at Ibadan, *Nigeria Journal of Emerging Trends in Engineering and Applied Science*2.4: 701-705.

Sengupta, M. 2010. A Physical method to compute surface radiation from geostationary satellites. *IV confrencia Latino Americana de Energia Solar y XVII Simposio Peruano deEnergia Solar, Cusco, 1-5, Nov. 2010.*

Shannon, C. E. 1949. Communication in the presence of noise. *Proceedings of the IRE, 37:10–21 January, 1949.*

Stine,W. B. and Geyer, M. 2001. In: *Power from the sun.* Retrieved 12.34, October 14, 2015, from *http://www.powerfromthesun.net/book.html*

Stowe, L. L., Davis, P. A., and McClain, E. P. 1999. Scientific basis and initial evaluation of the CLAVR-1 global clear cloud classification algorithm for the Advanced VeryHighResolution Radiometer.*Journal of Atmosphere and Oceanic Technology*16:656-681.

Tamm, E. and Thormalla, E. 1992. Handbook of Helionda: a program to simulate the effects of Meteorology, Place and Time. *Julich: BMFT – Forschungsprojekt* 0328932A.

Thekaekara, M. P. 1976. Solar Radiation Measurement: Techniques and Instrumentation*Solar Energy* 18.4:309.

Tompkins, A. 2010.*Introduction to Atmospheric Physics(Basic Physics Diploma)*. Course note. ICTP, Trieste, Italy. Version release date: May 11, 2010.

Trabea, A. A., and Shaltout, M. A. M. 2000. Correlation of global solar radiation with meteorological parameters over Egypt. *Renewable Energy* 21:297-308.

Tselioudis, G. and Rossow, W. B. 1994. Global, multiyear variations of optical thickness Withtemperature in low and cirrus clouds. *Geophysical Research. Letters 21:2211-2214.*

Venäläinen, A. and Heikinheimo, M. 1997. The spatial variation of long-term mean Globalradiation in Finland, 1997. *International Journal of Climatology* 17:415-426.

Vignola, F., Harlan, P., Perez, R., and Kmiecik, M. 2007. Analysis of satellite derived beam and global solar radiation data. *Solar Energy*81:768-772.

Wiin-Nielsen A. 1967. On the annual variation and spectral distribution of atmospheric energy.*Tellus* 19:540–558.

Wild, M., Folini, D., Schar, C., Loeb, N., Dutton, E. G. and Konig-Langlo, G. 2013. The global energy balance from a surface perspective. *Climate Dynamics* 40.11-12:3107-3134.

Wilks, D. 2006. *Statistical Methods in the Atmospheric Sciences*. New York: Academic Press.

Wong, L. T. and Chow, W. K. 2001. Solar Radiation Model. *Applied Energy* 69:191-224.

Yang, Z., Li, X.H. and HuY. F. 2006. Study on solar radiation and energy efficiency of building glass system. *Applied Thermal Engineering* 26.8-9: 956-961.

Ye, L. 1996. An Evaluation of Solar Radiation Variability in Louisiana.M.S. Thesis. Dept. of Geography and Anthropology.Louisiana State University.

Yucel, I., Shuttleworth, W. J., Pinker, R. T., Lu, L. And Sorooshian, S. 2002. Impact of ingesting Satellite-Derived Cloud Cover into the Regional Atmospheric Modelling System.*Monthly Weather Review*130:610-628.

Zekai, S. 2008.*Solar Energy fundamentals and modeling techniques: atmosphere, environment, climate change and renewable energy.*1st ed.London:Springer.

Zelenka, A., Perez, R., Seals, R. and Renne, D. 1999. Effective accuracy of satellite-derived hourly irradiances. *Theoretical and Applied Climatology* 62:199-207.

Zurich, ETH. 2009. Role of Solar Radiation in climate change.*Science Daily*.*Retrieved January 20, 2010.*

APPENDICES

APPENDIX I

1. Data used to determine the frequency distribution of the climatic regions

i) Mangrove Swamp Forest

Daily Global Insolation	Frequency of Occurrence % Warri	Frequency of Occurrence % Calabar	Frequency of Occurrence % Port Harcourt
0-5	4.99	5.31	4.57
5-10	9.96	15.3	14.51
10-15	16.95	22.11	22.76
15-20	40.29	30.54	40.49
20-25	27.69	25.86	17.61
25-30	0.11	0.88	0.06
30-35			

ii) Tropical Rain Forest

Daily Global Insolation	Frequency of Occurrence % Benin – City	Frequency of Occurrence % Lagos	Frequency of Occurrence % Ibadan
0-5	2.23	2.13	0.63
5-10	7.88	6.81	5.04
10-15	17.76	16.42	16.40
15-20	49.87	47.43	47.24
20-25	21.95	27.02	30.03
25-30	0.31	0.20	0.65
30-35			

iii) Guinea Savannah

Daily Global Insolation	Frequency of Occurrence %	Frequency of Occurrence %

	Ilorin	Abuja
0-5	0.41	0.45
5-10	3.41	2.85
10-15	14.2	9.88
15-20	38.97	31.55
20-25	41.61	52.17
25-30	1.41	3.11
30-35		

iv) Sudan/Sahel Savannah

Daily Global Insolation	Frequency of Occurrence % Benin - City	Frequency of Occurrence % Lagos	Frequency of Occurrence % Ibadan
0-5	0.35	0.09	0.11
5-10	1.18	1.18	0.96
10-15	2.9	3.04	2.78
15-20	28.19	24.39	21.18
20-25	49.56	53.14	46.06
25-30	17.82	18.08	28.8
30-35		0.07	0.11

APPENDIX II

2. Mean values of solar radiation used in plotting the contour maps

Location	Jan	Feb	Mar	Apr	May	Jun	Jul	Aug	Sept	Oct	Nov	Dec
Port Harcourt	18.81	18.94	17.34	16.71	15.39	13.16	11.82	12.43	12.31	13.28	15.28	18.01
Calabar	19.17	19.18	18.72	18.24	16.41	13.48	11.89	13.76	13.23	15.28	17.91	18.43
Warri	19.73	19.92	19.34	18.25	17.24	15.69	12.33	12.52	13.53	15.53	18.14	19.02
Benin City	20.21	20.55	19.90	18.79	18.29	16.90	12.94	12.39	13.88	16.23	18.72	19.54
Lagos	19.89	20.89	21.33	20.38	19.03	17.08	15.92	14.93	15.53	17.17	18.47	19.17
Ibadan	20.93	21.59	22.08	21.33	19.96	18.12	15.65	14.76	16.46	18.78	21.39	21.19
Ilorin	22.17	23.48	25.60	23.32	19.77	18.52	16.88	16.44	17.42	16.73	17.66	17.10
Abuja	22.94	24.98	30.32	24.29	18.46	18.67	17.99	18.01	16.34	10.73	9.22	10.35
Maiduguri	22.15	24.88	30.61	24.73	19.60	20.21	19.42	19.14	16.78	10.82	8.45	9.79
Kano	19.12	22.14	22.34	25.27	25.90	24.27	21.45	19.62	21.68	24.83	24.81	21.96
Sokoto	19.78	23.15	24.67	25.80	25.31	25.11	22.52	20.64	21.58	21.69	20.81	18.75